CANCER PREVENTION: TARGETING PREMALIGNANT EPITHELIAL NEOPLASMS IN THE ERA OF CANCER IMMUNOTHERAPY AND VACCINES

EDITED BY: Nicolas Cuburu, Olivera J. Finn and Sjoerd H. Van Der Burg
PUBLISHED IN: Frontiers in Immunology and Frontiers in Oncology

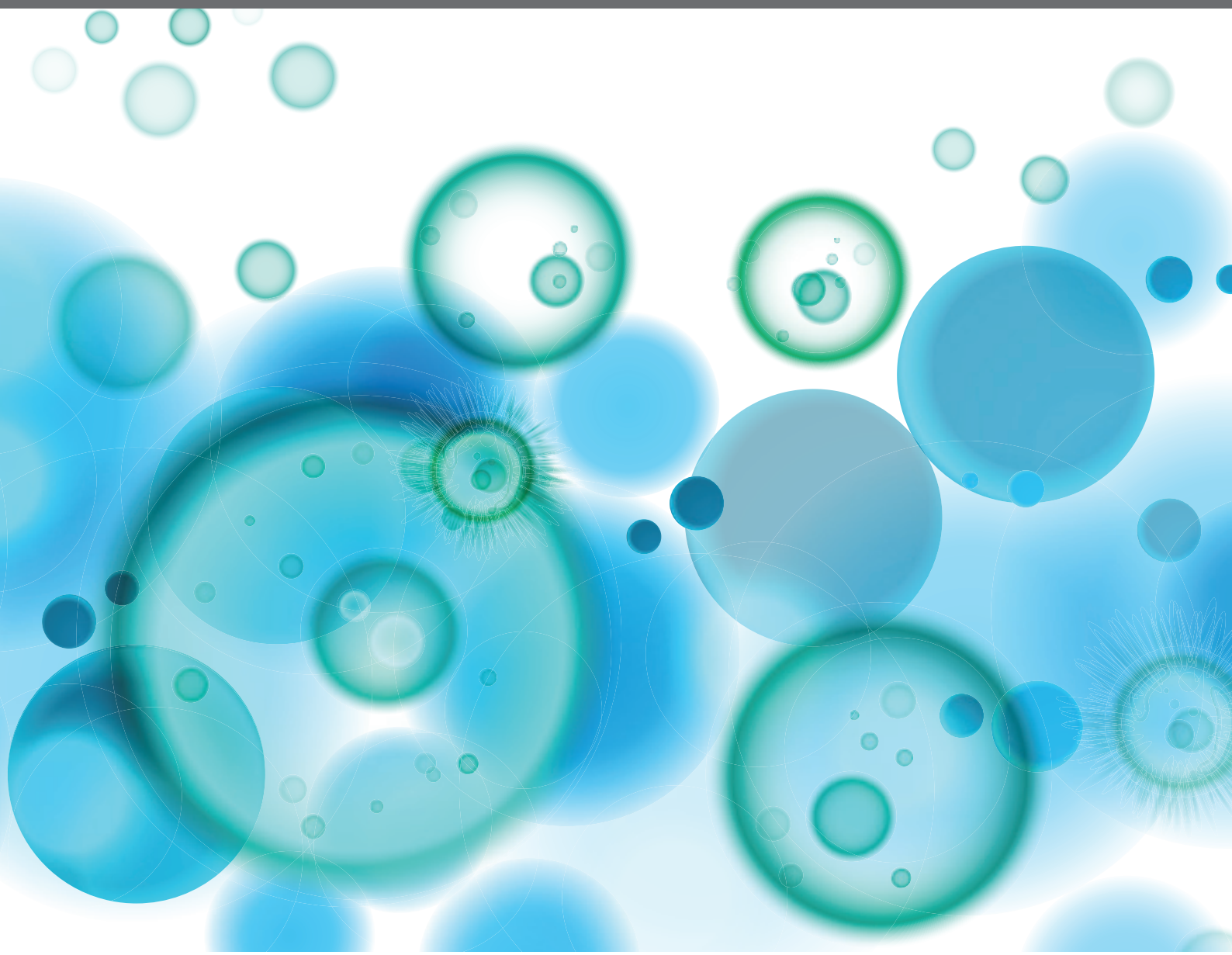

frontiers Research Topics

frontiers

ISSN 1664-8714
ISBN 978-2-88976-356-6
DOI 10.3389/978-2-88976-356-6

About Frontiers

Frontiers is more than just an open-access publisher of scholarly articles: it is a pioneering approach to the world of academia, radically improving the way scholarly research is managed. The grand vision of Frontiers is a world where all people have an equal opportunity to seek, share and generate knowledge. Frontiers provides immediate and permanent online open access to all its publications, but this alone is not enough to realize our grand goals.

Frontiers Journal Series

The Frontiers Journal Series is a multi-tier and interdisciplinary set of open-access, online journals, promising a paradigm shift from the current review, selection and dissemination processes in academic publishing. All Frontiers journals are driven by researchers for researchers; therefore, they constitute a service to the scholarly community. At the same time, the Frontiers Journal Series operates on a revolutionary invention, the tiered publishing system, initially addressing specific communities of scholars, and gradually climbing up to broader public understanding, thus serving the interests of the lay society, too.

Dedication to Quality

Each Frontiers article is a landmark of the highest quality, thanks to genuinely collaborative interactions between authors and review editors, who include some of the world's best academicians. Research must be certified by peers before entering a stream of knowledge that may eventually reach the public - and shape society; therefore, Frontiers only applies the most rigorous and unbiased reviews.
Frontiers revolutionizes research publishing by freely delivering the most outstanding research, evaluated with no bias from both the academic and social point of view. By applying the most advanced information technologies, Frontiers is catapulting scholarly publishing into a new generation.

What are Frontiers Research Topics?

Frontiers Research Topics are very popular trademarks of the Frontiers Journals Series: they are collections of at least ten articles, all centered on a particular subject. With their unique mix of varied contributions from Original Research to Review Articles, Frontiers Research Topics unify the most influential researchers, the latest key findings and historical advances in a hot research area! Find out more on how to host your own Frontiers Research Topic or contribute to one as an author by contacting the Frontiers Editorial Office: frontiersin.org/about/contact

CANCER PREVENTION: TARGETING PREMALIGNANT EPITHELIAL NEOPLASMS IN THE ERA OF CANCER IMMUNOTHERAPY AND VACCINES

Topic Editors:
Nicolas Cuburu, National Cancer Institute (NIH), United States
Olivera J. Finn, University of Pittsburgh, United States
Sjoerd H. Van Der Burg, Leiden University, Netherlands

Citation: Cuburu, N., Finn, O. J., Van Der Burg, S. H., eds. (2022). Cancer Prevention: Targeting Premalignant Epithelial Neoplasms in the Era of Cancer Immunotherapy and Vaccines. Lausanne: Frontiers Media SA.
doi: 10.3389/978-2-88976-356-6

Table of Contents

frontiers | Frontiers in Immunology

EDITORIAL
published: 24 May 2022
doi: 10.3389/fimmu.2022.924099

Editorial: Cancer Prevention: Targeting Premalignant Epithelial Neoplasms in the Era of Cancer Immunotherapy and Vaccines

Nicolas Çuburu[1], Olivera J. Finn[2]* and Sjoerd H. Van Der Burg[3]**

[1] Laboratory of Cellular Oncology, Center for Cancer Research, National Cancer Institute (NIH), Bethesda, MA, United States,
[2] Department of Immunology, School of Medicine, University of Pittsburgh, Pittsburgh, PA, United States,
[3] Department of Medical Oncology, Leiden University Medical Center, Leiden, Netherlands

Keywords: vaccine, immunotherapy, antigen discovery, animal model, premalignant lesion, tumor microenvironment

Editorial on the Research Topic

Cancer Prevention: Targeting Premalignant Epithelial Neoplasms in the Era of Cancer Immunotherapy and Vaccines

OPEN ACCESS

Edited and reviewed by:
Denise L. Doolan,
James Cook University, Australia

****Correspondence:***
Nicolas Çuburu
cuburun@mail.nih.gov
Olivera J. Finn
ojfinn@pitt.edu
Sjoerd H. Van Der Burg
S.H.van_der_Burg@lumc.nl

Specialty section:
This article was submitted to Vaccines and Molecular Therapeutics, a section of the journal Frontiers in Immunology

Received: *20 April 2022*
Accepted: *11 May 2022*
Published: *24 May 2022*

Citation:
Çuburu N, Finn OJ and Van Der Burg SH (2022) Editorial: Cancer Prevention: Targeting Premalignant Epithelial Neoplasms in the Era of Cancer Immunotherapy and Vaccines. Front. Immunol. 13:924099. doi: 10.3389/fimmu.2022.924099

Prevention of cancer is an essential intervention to reduce the cancer burden globally and public health measures targeting etiological factors such as tobacco consumption or oncogenic viruses as well as screening of early lesions have been extremely successful. Indeed, prophylactic vaccination against oncogenic human papillomavirus and hepatitis B virus have paved the way for immune-based interventions for the prevention of cancer (1).

Cancer immunotherapy was named the breakthrough of the year 2013 by Science Magazine; a decade later it has truly revolutionized the field of oncology (2). Advances in immuno-oncology are focused on late-stage metastatic cancers with the most urgent needs and highest potential to improve patients' immediate health. Remarkably, cancer immunotherapies such as immune checkpoint blockade or adoptive cell transfer have been associated with complete and durable cures, likely a consequence of the induction of long-lived anti-cancer immune responses. However, treatments of advanced cancers must also overcome powerful mechanisms of immune resistance in tumors and severe systemic adverse events, thereby preventing a higher therapeutic index.

Inspired by these successes, harnessing the immune system for the prevention and treatment of cancer could have a tremendous impact on cancer burden at a population level as well as providing immediate benefit to patients at high risk of developing cancer. To unleash this potential, the development of new diagnostics and immune interventions requires a deep understanding of the continuum of cellular and molecular modifications that often accumulate through many decades of cancer progression (3). The key factors could now begin to be identified at the early premalignant stages of cancer. This collection of original research and review articles covers emerging concepts in the field of premalignant lesions biology and offers a glimpse at possible immune-based interventions, including vaccines and combination therewith, to prevent their progression to cancer.

Initiatives to categorize systematically the immune and genetic landscapes of benign lesions such as the precancer genome atlas could provide a rationale for new interventions (4). A recent analysis of the progression of lung squamous cell carcinoma (SCC) showed that local immune activation and immune suppression occur in premalignant lesions but is limited compared to immune modulation in high grade

lesions and SCC (5). In this issue, Rangel et al. provide a comprehensive overview of HPV-negative head and cancer progression and how genetic alterations, notably TP53, CDKN2A and NOTCH1, lead to accumulation of macrophages, MDSCs and Treg in the microenvironment of developing lesions. Chadwick et al. provide evidence of the early contribution of TNF-α in the recruitment of inflammatory cells and progression of oropharyngeal squamous cell carcinoma (OPSCC) in a small cohort of patients. Using a chemically induced (4-NQO) OPSCC animal model they further demonstrate that targeting TNF-α could indeed prevent the progression of OPSCC in mice. Roudko et al. provide a very informative review on the genetic basis of Lynch syndrome caused by mutations in DNA mismatch repair (dMMR) resulting in genome instability. In addition, they discuss the status of current vaccines targeting neoepitopes associated with genome instability in microsatellite coding regions. Zachariah et al. provide a comprehensive review on the various types of premalignant breast cancer lesions and discuss the integration and advantages of targeted vaccines, notably HER2, in the context of standard of care and chemoprevention. Jacqueline et al. investigated the interaction between breast cancer cell lines that recapitulate the continuum of cancer progression, with macrophages *in vitro*. These elegant coculture experiments indicate that cell lines corresponding to normal epithelia or early premalignant phenotypes are not recognized by macrophages, but those corresponding to late premalignancy or advanced cancer phenotype cause pronounced activation of macrophages. They further identify surface markers, Annexin-A1 and CEACAM1, that are responsible for the interaction between breast premalignant and tumor cells and macrophages.

Transplantable syngeneic tumor models have been instrumental to establish proof of principle for therapeutic interventions against advanced cancer and to understand mechanisms of immune control and resistance to therapies. However, due extremely fast growth and profound genomic alterations, these models cannot fully recapitulate the slow development of cancer in situ. This collection offers excellent examples of animal models that can be leveraged for better understanding of premalignant lesions and cancer progression and to evaluate novel candidate vaccines or therapeutic interventions. Neckerman et al developed an adenoviral vector vaccine platform to be evaluated in a non-human primate model of persistent papillomavirus infection. Rangel at al. and Chadwick et al. used a chemically induced mouse model to study early immune modulation in OPSCC. Finally, Corulli et al. report two chemically induced (AOM) and transgenic APCmin transgenic colorectal cancer models for the evaluation of therapeutic vaccination against TAA. All these are models of spontaneous development of cancers and therefore are technically more challenging than classic syngeneic transplantable models as they require longer time to develop and have a variable penetrance.

The identification of protective antigens is critical to the development of vaccines for the treatment of premalignant neoplasia and to prevent cancer progression, Corulli et al. demonstrate by serology and T cell IFN-γ assays, that in colorectal cancer and adenomatous polyps overexpressed proteins CDC25B, COX2, RCAS1, and FASCIN1 are *bona fide* tumor associated antigens. In murine models of colorectal cancer, they demonstrate proof of principle of cancer prevention after vaccination by showing that CDC25B, COX2 and RCAS1 immunization leads to reduced tumor formation. These results provide a rationale for the identification, development, and use of TAA-based vaccines against colorectal cancer and its premalignant precursors. Understanding the genomic instability in microsatellite coding regions led to the identification of recurrent frameshift mutations encoding potentially protective neoantigens. Notably, preclinical studies in murine model of Lynch syndrome have shown improved survival and reduced tumor burden and a frame shift vaccine based on long peptide and CpG as adjuvant (6). Such vaccine could be the first off-the-shelf cancer vaccine to intercept colorectal cancer and other epithelial cancers at early stages before extensive immune suppression is established as an extrinsic resistance mechanism and before the acquisition of driver mutations in APC, BRAF and TP53. Zachariah et al. provide an exhaustive review on breast cancer precursor lesions and an update on current targeted therapies driver antigens such as HER-2 and breast antigens such as MUC-1, Lactaglobin and mammaglobin. Accumulating evidence of a good safety profile of dendritic cells vaccines targeting HER2 compared to chemoprevention offers an opportunity to intercept the development of invasive breast cancer at the early stages before immunoediting occurs and durable benefit may be obtained. Such approach if successful could provide safer alternative to chemoprevention at the DCIS or premalignant stages.

Cancers caused by infections contribute to 15% of the global cancer burden. The foreign nature of oncogenic viruses has allowed the development of powerful prevention tools to reduce the burden of virus-related cancers. For instance, HPV is a family of epitheliotropic virus with circular double stranded DNA and the main causative agent of cervical cancer and other epithelial cancers. Antibodies against the L1 capsid protein of HPV can effectively prevent infection and subsequent epithelial cell transformation driven by the viral oncogenes E6 and E7 which is at the basis of the current HPV VLP prophylactic vaccines. Huang et al. report a new humanized monoclonal antibody targeting the major capsid protein L1 of the oncogenic HPV type 18 which they propose constitute a novel type of microbicide. The implementation of such approach remains to be defined in the context of a widespread availability of highly efficacious prophylactic HPV vaccines as it is likely that such antibodies would be limited to prophylactic usage as HPV remains impervious to antibody neutralization once infection is established. In contrast, nonstructural E6 and E7 HPV oncogenes whose primary functions cause the degradation of p53 and Rb are required for cancer progression and persistence. These viral oncogenes represent ideal targets of therapeutic cancer vaccines as they are drivers of cancer progression. Several clinical trials including E6 and E7 antigens as synthetic long peptides or nucleic acid platform against cervical and vulvar intraepithelial neoplasia have shown therapeutic benefit and regression of premalignant lesions (7, 8). Most genital HPV infection, however, are naturally

cleared, and only persistent infection can lead to the development of premalignant lesions. Neckermann et al. propose a vaccine targeting nonstructural viral antigens E1 and E2 that are highly expressed during persistent HPV infection but lost as the lesions progress. They designed a vaccine candidate targeting the E1/E2 viral antigens to be evaluated in a Macaca fascicularis papillomavirus, a model of persistent natural infection that leads to the development of local lesions.

The recent successes of SARS COV2 mRNA vaccine showed that disruptive technologies can have a tremendous impact on public health. Beyond antigen characterization, this issue offers a glimpse at potential cancer vaccine candidates in terms of platforms, modalities, and adjuvants. Nekerman et al. report an adenoviral vector that can be delivered systemically or mucosally to target specifically mucoepithelial premalignant lesions. Corulli et al. report a vaccine platform based on selected MHC class 2 peptides given with water-in-oil-in-water adjuvant (CFA/IFA). In this model, vaccine efficacy relies on CD8+ T cells suggesting epitope spreading against antigens that were not included in the vaccine (9). Roudko et al. offers an overview of current vaccines against frame shift mutations in Lynch syndrome which include synthetic long peptides with a water-in-oil-in-water adjuvant (Montanide) or viral vectors (MVA, adenoviral vectors). Zacharia et al. offers a thorough overview of vaccine platforms targeting breast cancer with the potential to be repurposed against early lesions. Of note dendritic cells pulsed with HER2 showed excellent safety profile and efficacy, akin to the Sipuleucel-T vaccine, which is the first approved cancer for castrate resistant metastatic prostate cancers. Finally, in addition to HPV and HBV, vaccines against EBV and hepatitis C could have a profound impact in the prevention of nasopharyngeal carcinoma, Non-Hodgkins lymphoma and hepatocellular carcinoma. In addition, a Merkel cell polyomavirus vaccine targeting viral oncogenes is being evaluated for advanced Merkel cell carcinoma, but it could also prevent recurrence and metastasis if used in combination with surgical removal of early lesions.

With the increasing number of cancer epitopes that are validated experimentally, it becomes important to catalogue and curate these large datasets in order to facilitate the dissemination of information to the scientific community. Building on the successes of Immune Epitope Database (IEDB) in the field of autoimmunity and infectious diseases, Kosaloglu-Yalçin et al. present Cancer Epitope Database and Analysis Resource (CEDAR), a new platform that will offer soon a curated dataset of cancer epitopes that can be used to assess and refine prediction algorithms relevant to cancer antigens. This new dataset together with machine learning algorithm has the potential to integrate new relevant parameters and to build more powerful algorithm to predict actionable tumor antigens (10).

To conclude, remarkable efforts have been made to identify tumor associated antigens, characterize the premalignant and tumor immune microenvironments, and to develop vaccine platforms and adjuvants. This Research Topic offers an updated perspective on how to effectively use these advances to target premalignant lesions as a way to cancer prevention. Targeting early-stage of cancer development presents the advantage of targeting lesions when they are most likely to regress. Albeit, even at this stage, differences in the immune landscape may affect clinical outcome of different forms of immunotherapy (3). Important questions will need to be answered in the near future. For instance, can we identify markers of early lesions for most cancers and what would be the protective antigens? Can we develop therapeutics that tip the risk/benefit ratio in favor of intervention? What will be the long-term efficacy and safety profiles of vaccines targeting tumor associated antigens in terms of autoimmunity? How to integrate such preventative vaccines into routine preventative cancer screening and treatment? Because screening offers opportunity to effectively treat some developing lesions by surgical excision, it is likely that the impact of vaccines targeting premalignant lesions will be maximal either as neoaduvant therapy to prevent or downscale the surgical procedure (and as such the complications associated with it) or as adjuvant therapy to prevent later recurrences. Finally, the reduced cost and ease to deploy vaccines could have a tremendous impact in low resource settings where access to surgical procedures can be limited.

AUTHOR CONTRIBUTIONS

All authors listed have made a substantial, direct, and intellectual contribution to the work and approved it for publication.

ACKNOWLEDGMENTS

We would like to thank all the authors who have participated in this Research Topic and the reviewers for their invaluable comments.

REFERENCES

1. Enokida T, Moreira A, Bhardwaj N. Vaccines for Immunoprevention of Cancer. *J Clin Invest* (2021) 131. doi: 10.1172/JCI146956
2. Couzin-Frankel J. Breakthrough of the Year 2013. *Cancer Immunother Sci* (2013) 342:1432–3. doi: 10.1126/science.342.6165.1432
3. Spira A, Disis ML, Schiller JT, Vilar E, Rebbeck TR, Bejar R, et al. Leveraging Premalignant Biology for Immune-Based Cancer Prevention. *Proc Natl Acad Sci USA* (2016) 113:10750–8. doi: 10.1073/pnas.1608077113
4. Srivastava S, Ghosh S, Kagan J, Mazurchuk R, National Cancer Institute's HI. The Making of a PreCancer Atlas: Promises, Challenges, and Opportunities. *Trends Cancer* (2018) 4:523–36. doi: 10.1016/j.trecan.2018.06.007
5. Mascaux C, Angelova M, Vasaturo A, Beane J, Hijazi K, Anthoine G, et al. Immune Evasion Before Tumour Invasion in Early Lung Squamous Carcinogenesis. *Nature* (2019) 571:570–5. doi: 10.1038/s41586-019-1330-0
6. Gebert J, Gelincik O, Oezcan-Wahlbrink M, Marshall JD, Hernandez-Sanchez A, Urban K, et al. Recurrent Frameshift Neoantigen Vaccine Elicits Protective Immunity With Reduced Tumor Burden and Improved Overall Survival in a Lynch Syndrome Mouse Model. *Gastroenterology* (2021) 161:1288–302.e13. doi: 10.1053/j.gastro.2021.06.073
7. Trimble CL, Morrow MP, Kraynyak KA, Shen X, Dallas M, Yan J, et al. Safety, Efficacy, and Immunogenicity of VGX-3100, a Therapeutic Synthetic DNA Vaccine Targeting Human Papillomavirus 16 and 18 E6 and E7 Proteins for Cervical Intraepithelial Neoplasia 2/3: A Randomised, Double-Blind, Placebo-

Controlled Phase 2b Trial. *Lancet* (2015) 386:2078–88. doi: 10.1016/S0140-6736(15)00239-1
8. Kenter GG, Welters MJ, Valentijn AR, Lowik MJ, Berends-van der Meer DM, Vloon AP, et al. Vaccination Against HPV-16 Oncoproteins for Vulvar Intraepithelial Neoplasia. *N Engl J Med* (2009) 361:1838–47. doi: 10.1056/NEJMoa0810097
9. Brossart P. The Role of Antigen Spreading in the Efficacy of Immunotherapies. *Clin Cancer Res* (2020) 26:4442–7. doi: 10.1158/1078-0432.CCR-20-0305
10. Ehx G, Perreault C. Discovery and Characterization of Actionable Tumor Antigens. *Genome Med* (2019) 11:29. doi: 10.1186/s13073-019-0642-x

Conflict of Interest: The authors declare that the research was conducted in the absence of any commercial or financial relationships that could be construed as a potential conflict of interest.

Publisher's Note: All claims expressed in this article are solely those of the authors and do not necessarily represent those of their affiliated organizations, or those of the publisher, the editors and the reviewers. Any product that may be evaluated in this article, or claim that may be made by its manufacturer, is not guaranteed or endorsed by the publisher.

frontiers in Immunology

ORIGINAL RESEARCH
published: 24 June 2021
doi: 10.3389/fimmu.2021.678318

Potent Neutralizing Humanized Antibody With Topical Therapeutic Potential Against HPV18-Related Cervical Cancer

Bilian Huang[1†], Linjing Zhu[2†], Hongxia Wei[3], Haixia Shi[4], Doudou Zhang[2], Huanyun Yuan[2], Linlin Luan[2], Nan Zheng[1], Shijie Xu[2], Waqas Nawaz[1], Ying Hong[5], Xilin Wu[1,2*] and Zhiwei Wu[1,6,7,8*]*

[1] Center for Public Health Research, Medical School, Nanjing University, Nanjing, China, [2] Department of Antibody, Abrev Biotechnology Co., Ltd., Nanjing, China, [3] Department of Infection, Nanjing Hospital Affiliated to Nanjing University of Chinese Medicine, Nanjing, China, [4] Department of Antibody, Y-Clone Medical Science Co. Ltd., Suzhou, China, [5] Obstetrics and Gynecology Department, Nanjing Drum Tower Hospital, Affiliated Hospital of Nanjing University Medical School, Nanjing, China, [6] School of Life Sciences, Ningxia University, Yinchuan, China, [7] Jiangsu Key Laboratory of Molecular Medicine, Medical School, Nanjing University, Nanjing, China, [8] State Key Laboratory of Analytical Chemistry for Life Science, Nanjing University, Nanjing, China

OPEN ACCESS

Edited by:
Olivera J. Finn,
University of Pittsburgh, United States

Reviewed by:
Ji Wang,
Sun Yat-Sen University, China
Rupsa Basu,
Helaina Inc., United States

***Correspondence:**
Zhiwei Wu
wzhw@nju.edu.cn
Xilin Wu
xilinwu@nju.edu.cn
Ying Hong
hongying@nju.edu.cn

†These authors have contributed equally to this work

Specialty section:
This article was submitted to Vaccines and Molecular Therapeutics, a section of the journal Frontiers in Immunology

Received: 09 March 2021
Accepted: 31 May 2021
Published: 24 June 2021

Citation:
Huang B, Zhu L, Wei H, Shi H, Zhang D, Yuan H, Luan L, Zheng N, Xu S, Nawaz W, Hong Y, Wu X and Wu Z (2021) Potent Neutralizing Humanized Antibody With Topical Therapeutic Potential Against HPV18-Related Cervical Cancer. Front. Immunol. 12:678318. doi: 10.3389/fimmu.2021.678318

Cervical cancer caused by human papillomavirus (HPV) infections is the fourth most common cancer in women worldwide. Current prophylactic HPV vaccines have achieved promising success in preventing HPV infection. However, still 570,000 new cases were reported in 2018. The current primary treatment for the patient with cervical cancer is either surgery or chemoradiotherapy. Cervical cancer still lacks standard medical therapy. HPV18 induced cervical cancer has the worst prognosis and high mortality compared to other HPV infections. The development of HPV18 related with cervical malignancy requires the persistent infection of cervical–vaginal epithelium by HPV18 subtype, which can take years to transform the epithelium. This period of repeated infection provides a window for therapeutic intervention. Neutralizing antibodies formulated as topical agents that inhibit HPV18 infection should reduce the chance of cervical malignancy. We previously demonstrated that potent neutralizing anti-sera against HPV18 infection were induced by HPV18 viral like particle (VLP) generated in mammalian cells. We, therefore, isolated two potent neutralizing antibodies, 2A12 and 8H4, from over 3,810 hybridomas prepared from mice immunized with HPV18 VLP. 2A12 and 8H4 exhibited excellent potency, with 50% virus-inhibitory concentrations (IC_{50}) of 0.4 and 0.9 ng/ml, respectively. Furthermore, 2A12 and 8H4 recognized distinct and non-overlapping quaternary epitopes and bound specifically with HPV18. Humanized 2A12 (Hu2A12) retained comparable neutralizing activity against HPV18 infection in various acidic pH settings and in hydrogel formulation with IC_{50} values of 0.04 to 0.77 ng/ml, indicating that Hu2A12 will be a promising candidate for clinical development as a topical vaginal biopharmaceutical agent against HPV18 infection.

Keywords: HPV18, cervical cancer, neutralizing antibodies, topical agents, humanized antibody

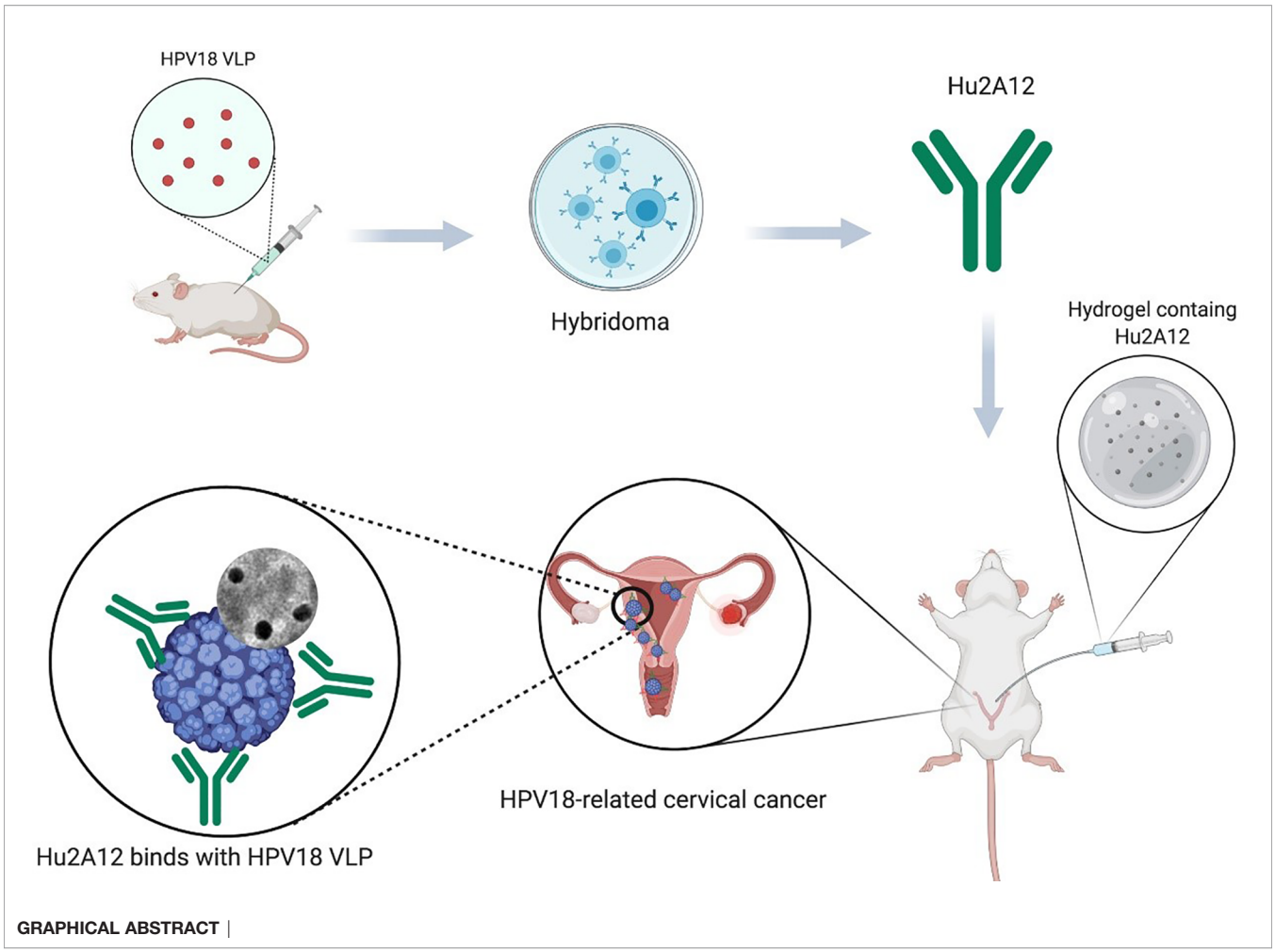

GRAPHICAL ABSTRACT |

HIGHLIGHTS

1. Two neutralizing antibodies against HPV18 with the highest potency were isolated from immunized mice.
2. The humanized antibody, Hu2A12, exhibits ultrahigh potency against HPV18 infection with IC_{50} value of 0.04 ng/ml.
3. Hu2A12 retains comparable neutralizing activity in various acidic pH settings and in hydrogel formulation.
4. Hu2A12 will be a promising candidate as a topical vaginal biopharmaceutical agent against HPV18 infection.

INTRODUCTION

Cervical cancer is the fourth most common tumor diagnosed in women worldwide (1). Persistent infections caused by high-risk Human papillomaviruses (HPV), such as 16, 18, 31, 33, 35, 39, 45, 51, 52, 56, 58, 59 and 68 are considered to be the main cause for the development of cervical cancer precursors, known as cervical intraepithelial neoplasia (CIN 1, 2, and 3), and invasive cervical cancer (2, 3).

Current prophylactic HPV vaccines have achieved remarkable success in preventing HPV infection (4, 5). However, a large number of women still failed to receive prophylactic HPV vaccines due to the high cost, failed to respond to the vaccination and other factors. In 2018, 570,000 new cases and 311,000 related deaths were reported globally, indicating effective treatment was urgently needed (6). Surgical or chemoradiotherapeutic regimens are the current primary treatment options for patients with cervical cancer. Specific medical treatment for HPV infection remains elusive (7).

Persistent HPV infection in the basal layer of the cervical epithelium is the main risk factor in the development of the premalignant conditions of cervical intraepithelial neoplasia or adenocarcinoma in situ. Without treatment, the transition from dysplasia to invasive carcinoma may take years to decades to develop in most women.

Current research on topical therapies for the treatment of HPV or CIN have promising results, signified by the randomized trials of immune-modulating (imiquimod), anti-proliferative (5-fluorouracil), and anti-viral (cidofovir) therapies (8–10). However, none of them has profound clinical evidence to be

recommended as a treatment for CIN 2–3 and surgery remains the standard of care (11). Cidofovir is an approved antiviral drug for the treatment of cytomegalovirus (CMV) retinitis in HIV patients. Clinical studies of cidofovir gel as a topical therapy had shown promising results for clearance of HPV or CIN. However, serious side effects were recently reported in the use of cidofovir in the treatment of HPV infection (12). All these indicate that topical anti-viral therapy is promising; however, antibody based topical therapy for HPV or CIN has not been reported yet.

The use of neutralizing antibodies with high potency and low toxicity have been widely applied to treat viral infections caused by a respiratory syncytial virus, cytomegalovirus, human immunodeficiency virus, Ebola virus and influenza virus (13, 14). The discovery and development of virus-neutralizing monoclonal antibodies can be a promising approach to eliminate HPV persistent infection and prevent the subsequent transition of invasive carcinoma.

After HPV16, HPV18 infection is the second most carcinogenic HPV genotype in a large percentage (approximately 10%), and highly enriched in adeno/adenosquamous and adenocarcinoma *in situ* compared to lower grades of diagnosis (2, 15, 16). HPV18 causes cervical cancer with the worst prognosis as compared with other types of HPV (17, 18). Two neutralizing antibodies against HPV18 were previously developed for diagnostic kit for HPV-18 (19). To our knowledge, no neutralizing antibodies with high potency have been developed for HPV18 treatment. We previously demonstrated that high potent neutralizing anti-sera against HPV18 infection could be induced by our HPV18 viral like particle (VLP) generated in the mammalian cell. In this study, two potent neutralizing antibodies, 2A12 and 8H4, were isolated from more than 3,810 hybridomas prepared from mice immunized with HPV18 VLP (20). 2A12 and 8H4 exhibited high potency, with IC_{50} of 0.4 and 0.9 ng/ml, respectively. Furthermore, 2A12 and 8H4 recognized distinct and non-overlapping quaternary epitopes and exhibited specific binding with HPV18. Humanized 2A12 (Hu2A12) retains comparable neutralizing activity against HPV18 infection in various acidic pH conditions and hydrogel with the IC_{50} of 0.04 to 0.7 ng/ml, indicating that Hu2A12 will be a promising candidate for clinical development as topical vaginal biopharmaceutical agents in hydrogel against HPV18 infection.

METHODS AND MATERIALS

Production of HPV18 VLP and HPV18 Pseudovirus

HPV18 VLP and pseudovirus were prepared using the plasmid of p18sheLL (Addgene, 37321) and the co-transfection of p18shell and pGMCMV-luc (Yeasen Biotech) as a reporter gene, respectively, as we previously described (20), with some modifications. In brief, the plasmids were mixed with PEI (Polysciences, MW25000, 23966-1) at a 1:3 ratio and then transfected into 293 TT cells. About 48 h post-transfection, cells were harvested and washed with DPBS twice. After centrifugation, the cell pellet was resuspended in 0.5% Triton X-100 and 25 mM ammonium sulfate. The cell lysate was then incubated at 37°C for 24 h. The matured lysate on ice was incubated for 15 min with the final concentration of 850 mM NaCl. After centrifugation, the supernatant was transferred for OptiPrep (D1156, Sigma-Aldrich, St. Louis, Missouri, USA) gradient purification at 40,000 rpm for 4.75 h. Different fractions were collected for verification.

Immunization of Mice

Five 8-week-old female Balb/c mice (M1~M5) were immunized by three subcutaneous injections, at two weeks interval, of 25–50 μg HPV18 VLP emulsified with Freund's adjuvant (Sigma, F5881 & F5506). Sera were collected one week after the third immunization and were used to further analysis. An intraperitoneal injection of HPV18 VLP without adjuvant was performed as the booster immunization before hybridoma.

Enzyme-Linked Immunosorbent Assay

To measure the serum titer or antibody against HPV18 VLP, ELISA plates (Corning, 9018) were coated with 0.5 μg/ml purified HPV18 VLP at 4°C overnight, then blocked in 2% bovine serum albumin-PBST. Sera were diluted in 2% bovine serum albumin-PBST. Diluted sera or hybridoma culture supernatant was added and then incubated at 37°C for 1.5 h. After a wash with PBST, anti-mouse IgG HRP conjugated antibodies (Jackson ImmunoResearch115-035-003) were added at 37°C for 60 min. For visualization, 100 μl 3,3′,5,5′-Tetramethylbenzidine (TMB, Sigma) substrate was added and incubated at room temperature for 10 min, and stopped with 50 μl 1 M HCl per well. Optical densities were determined at 450 nm using Infinite 200 (Tecan).

Preparation of Hybridomas and Identification of Candidate Clones

Mice were sacrificed 3 days after booster immunization. Splenocytes were isolated, fused with Sp2/0 cells (ATCC) in a 1:2 ratio using Electro Cell Manipulator (BTX Harvard Apparatus, ECM 2001) as described (21, 22). Fused cells were cultured in hypoxanthine aminopterin thymidine (HAT, Sigma, H0262) medium in multiple 96-well plates, and supernatants were tested after 7 days in culture. The supernatants of the individual hybridoma clones were screened for HPV18 VLP specific antibodies by ELISA. The selected positive hybridoma supernatants were further analyzed using neutralization assay. All the candidate clones were subcloned at least twice by limiting dilution.

HPV Neutralization Assay

The pseudovirus-based neutralization assay was performed to evaluate the activity of antibodies inhibiting HPV infection, following the previously reported method (20) with slight modifications. Briefly, 10,000 293TT cells were seeded per well overnight in a 96-well cell culture microplate in growth media. Serial dilutions of antibodies or anti-sera were incubated with HPV pseudovirus at 37°C for 1 h. Then, the mixture was transferred to the 96-well plates and incubated with cells at 37°C for 48 h. After that, the supernatant was removed, and

substrate (Promega Bright-Glo luciferase Assay System, E2650) was added to the samples to read Fluorescence intensity. The IC_{50} value was calculated based on the previously published standard algorithm (23).

Western Blot

About 200 ng HPV VLPs were mixed with 5× SDS-PAGE non-reduce sample buffer (250 mM Tris–HCl, pH 6.8, 10% SDS, 0.05% bromophenol blue, 20% glycerol) and boiled for 5 min. For reduced HPV18 VLP, 5x SDS-PAGE reduce sample buffer (250 mM Tris-HCl, pH 6.8, 500 mM DTT, 10% SDS, 0.05% bromophenol blue, 20% glycerol) was added. The proteins were separated by electrophoresis on 10% SDS-PAGE gels, and the gels were then transferred onto a 0.45-μm PVDF membrane. (Bio-Rad, 10485196). The membrane was soaked in blocking buffer (2% BSA in PBST) at room temperature for 1 h, and then incubated with hybridoma supernatant or anti-sera at room temperature for 2 h, followed by three times of washing. A secondary antibody of anti-mouse IgG with an IRDye 800CW (Li-COR, 925-32210) was used and the immunoblots were visualized using an Odyssey Infrared Imaging System (LI-COR).

Identification of Antibody Isotypes

Mouse antibody isotypes were determined using mouse monoclonal antibody subtype identification Kit (Cellway-Lab, C030215), following the manufacturer's protocol. In brief, a sample of evaluated antibody was added in the ELISA plate. After incubation and washing, the secondary antibodies specific for IgG1, IgG2a, IgG2b, IgG3, IgA and IgM were added. The high optical density (450 nm) suggests the right antibody isotype or subtype.

Flow Cytometric Analysis

293TT cells were transfected with the plasmid of p18sheLL to express VLP. Some 48 h later, cells were collected, fixed in formalin for 20 min, treated with 0.2% TritonX-100 for 10 min and then blocked in PBS with 1% FBS (PBSF) for 2 h. 2A12 and 8H4 were added and incubated for 1 h at room temperature. After washing twice with PBSF, binding antibodies were detected by an incubation at 4°C for 30 min with Alexa Fluor® 488-AffiniPure Goat Anti-Mouse IgG (H + L) (Jackson Immunoresearch, 115-545-146). After washing, the cells were resuspended in 500 μl PBSF and analyzed using ACEA NovoCyte TM (Agilent Biosciences) Nontransfected 293TT cells were served as a negative control.

Electron Microscopy and Immunogold Labeling

Immunoelectron microscopy (Immune-EM) of the HPV virion was performed as described previously (24). For staining, 10 μl HPV18 VLP was adsorbed on copper grids for 10 min. Afterward, the grids were blotted dry with filter paper and transferred facing down onto a drop of 2% BSA-PBS.10 min later, the grid floated on droplets including primary antibody for 1 h at room temperature, followed by the grids being rinsed on three drops of PBS in the same way. Then, an anti-mouse secondary antibody conjugated to 10 nm gold particles (Sigma G7652-.4ML) diluted 1:500 in 2% BSA-PBS was applied for 30 min. Following washing with PBS, the grid was negatively contrasted with 2% phosphotungstic acid (Macklin P829844-5g) by incubating at room temperature for 4 min. Finally, samples were dry and observed using transmission electron microscopy (JEM-2100).

Sequencing and Analysis of Mouse Ig Genes

Some $1 * 10^7$ hybridoma cells were collected and washed with PBS, then lysed with Trizol (Ambion, 15596018) to extract total RNA according to the manufacturer's instructions. RNA was reverse transcribed to cDNA using PrimeScript™II 1st Strand cDNA Synthesis Kit (Takara, 6210A). The resulting cDNA was used as the template for amplifying heavy and light-chain variable gene using the Mouse Ig-Primer Set (Merck Millipore, 6983). The gene was then sequenced, adopting standard methods (25). The International ImMunoGeneTics Information System (IMGT) (http://imgt.cines.fr) was used to analyze the variable domain VH/VL. To confirm the sequences, the vectors of pCDNA3.4-VH-CH and pCDNA3.4-VL-CL containing the gene of VH and VL were constructed and co-transfected 293TT cells. The cell supernatant was then detected by ELISA as described above.

Antibody Humanization

The mouse IgG humanization was achieved by complementarity determining regions (CDR) grafting (26, 27). The sequence of 2A12 VH/VL were blasted against human heavy and light variable chain by using searches of IMGT/Domain Gap Align comprehensive database of Ig. Combined with the sequence analysis of the Molecular Operating Environment (MOE) and its three-dimensional structure from molecular modeling, critical diversity residues in the framework of 2A12 were identified. Then CDR grafted with humanized heavy and light chain were constructed by partly replacing critical diversity residues with human original residues. The combined expression of diverse designed humanized heavy and light chains resulted in multiple different pairings of humanized antibodies molecules. Pairing with the highest affinity and neutralizing activity were selected.

Quantification of Mouse IgG

The mouse IgG in serum or in hybridoma supernatant was quantified using double antibody sandwich ELISA. Briefly, the anti-mouse IgG (Sigma, M0659, Fab specific, $F(ab')_2$ fragment antibody produced in goat) was coated. After blocking, series gradient diluted sample and mouse IgG standards (0–100 ng/ml) were added as primary antibodies, while anti-mouse IgG (Fc specific)–peroxidase antibody (Sigma, A2554) was used as a secondary antibody. The linear regression curve of the mouse IgG standards was drawn, and the OD_{450} value was brought into the equation to calculate the mouse IgG concentration of each sample.

Biolayer Interferometry

The affinity of HPV18 specific antibodies was determined using the Octet RED96 instrument (Sartorius). Amine reactive biosensor (AR2G, 18-5092) was used to immobilize the HPV18 VLP. AR2G biosensors were activated for 7 min with EDC

(400mM)/NHS (100 mM), and then immersed 15 min in HPV18 VLP which was diluted in pH 5.0 10 mM sodium acetate buffer. Transfer the sensor to ethanolamine for 7 min and then to 0.02% PBST for affinity assay. The kinetics assays were performed with a shaking speed of 1,000 rpm. Association with HPV18 VLP specific antibodies was measured for 4 min and dissociation in 0.02% PBST for 4 min. The affinity analysis was performed using a fast 1:1 binding model and the Data analysis software 8.0 (Sartorius).

The epitope-binding assay was performed with AR2G biosensor following the manufacturer's protocol 'in-tandem assay'. The immobilization of antigen was performed as above described, and then associated the first antibody (20 μg/ml) for 400 s following with the baseline step with 30s immersion in 0.02% PBST. Accordingly, the sensors were immersed for 400s with a second antibody at 20 μg/ml. Graph Pad was used to illustrate the time-response course of two antibodies binding to HPV18 VLP.

Preparation of Antibody Hydrogel and *In Vitro* Release Kinetics

To generate a hydrogel formulation contained antibodies, Hu2A12 was diluted in sterile ddH_2O at a final concentration of 1 mg/ml. Subsequently, 70 mg Hydroxyethyl cellulose (HEC, Macklin, H810926) was added to the 1 ml above antibody solution containing Hu2A12, which shook for 1 h at room temperature, accordingly, 7% (wt/vol) HEC hydrogel containing antibodies was prepared.

For drug release studies, 7% HEC containing Hu2A12 labeled with FITC (hu2A12-FITC) was prepared (28–30). Transwell (NEST, 725301) inserts perforated with ten 22-G needle were used as filters. About 300 μl hydrogel was applied onto the insert membrane, followed by a gentle addition of 0.5 ml PBS. Some 1.5 ml PBS was applied to the lower chamber. About 100 μl aliquots in the lower chamber were transferred to a black 96-well plate (Greiner, 655076) and made up by 100 μl fresh PBS at the indicated time. Hu2A12 labeled by FITC was quantified by fluorescence at 485 nm excitation wavelength and 525 nm emission wavelength using a fluorescence multi-well plate reader (Molecular Devices M3). *In vitro* cumulative percentage release was calculated using the formula as below:

$$\text{Relative amount of drug in released solution} = \text{OD}_{525} \text{ of sample withdrawn} * 20$$

$$\text{Cumulative percentage release (\%)} = \frac{\text{relative amount of drug in released solution at time t + cumulative drug withdrawn previous to t}}{\text{relative total amount of drug}}$$

Neutralization Activity Under Acidic Conditions

To apply the antibodies under acidic conditions, we firstly detected the neutralization activity of Hu2A12 in the media of pH 4, 5, 6, and 7. The complete DMEM media was adjusted with acidic acid to pH 4, 5, 6, and 7. The neutralization assay was similar to the 'HPV neutralization assay' as described above with some changes as follow. Both antibodies and pseudovirus were diluted in corresponding acidic media. Four hours after adding the mixture of antibodies and pseudovirus in the seeded cells, the acidic media was replaced with conventional media to avoid the cells from acid toxicity. Some 48 h later, neutralizing activity was measured.

The Hu2A12 released from vaginal hydrogel was evaluated for neutralization activity. Sodium acetate buffer (pH5.0) was applied as an antibody released buffer to mimic the acidic environment of the vagina. About 1.5 fold volume of acidic buffer was added to the antibody hydrogel, making the gel disintegrated completely in 37°C, which was maintained for 72 h. At 24 and 72 h, the released antibodies were sampled for neutralization assay.

In Vivo Retention of Antibody Hydrogel in a Mouse Model

Hu2A12 was labeled with far infrared dye YF®750 SE (US EVERBRIGHT INC, YS0056) (named Hu2A12-750). Nine female nude mice (18–22 g, Qing Long Shan Animal Breeding Grounds, Nanjing, China) were divided into three groups. Three mice in Group 1 were intra-vaginally treated with 50 μg Hu2A12-750 hydrogel, while three mice in Group 2 were injected with 50μg liquid Hu2A12-750 in the same way. The remaining three mice were used as negative control. Far infrared images were observed at 15 min, 4 h, 8 h, 24 h and 48 h with a small animal imaging system (NightOWL LB 983 NC100) at Ex: 740 nm/Em:780 nm. Images were captured by the CCD camera embedded in the imaging system and analyzed using Indigo imaging software Ver. A 01.19.01.

Statistics

Graphs were generated by GraphPad Prism 5.01 software or OriginPro 8.5 software (Origin-Lab). One- or 2-way ANOVA was performed for group comparisons. $P < 0.05$ was considered statistically significant with data shown as mean ± SEM or mean ± SD or median + range.

RESULTS

Generation of Anti-HPV18VLP mAbs

Balb/c mice were immunized with HPV18 VLP generated in 293TT cells as depicted in **Figure 1A**. High titer (ranging 1.0–9.8 × 10^6 dilution) anti-sera from five immunized mice specific for HPV18 VLP protein was achieved after the third immunization (**Figure 1B**). M1 mouse with the highest anti-serum titer was sacrificed for the hybridoma production. 1223 hybridoma supernatants, including 3,810 clones, were evaluated for the binding with HPV18 VLP protein, and, among them, 106 positive supernatants were scored as high positive (OD_{450} nm >1.0) for HPV18 VLP binding, yielding an overall hit rate of 8.7% (**Figure 1C**). Specially, hybridomas with high antigen binding were advanced for further subclone. Supernatants of seven mAbs were screened for preliminary neutralization assessment against HPV18 infection. Two monoclonal antibodies (named as 2A12 and 8H4) showed 100% inhibition against HPV18 infection

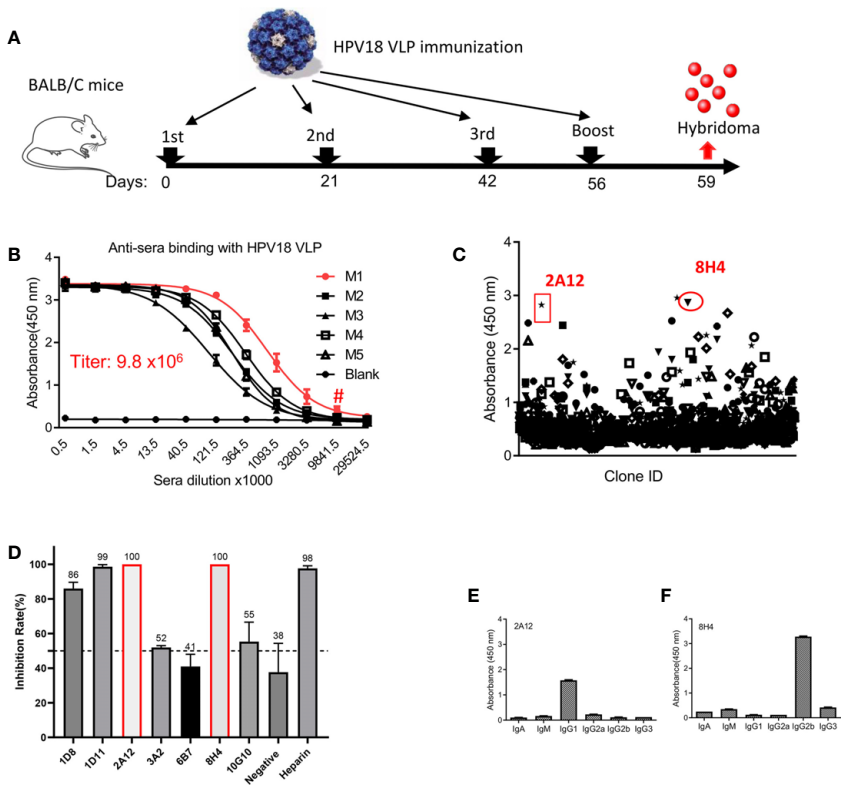

FIGURE 1 | Generation of mAbs against HPV18. **(A)** The experimental schedule of immunization. **(B)** The titer of anti-sera was evaluated after the 3rd immunization in mice receiving HPV18 VLP. Y-axis represents the absorbance at 450 nm, and X-axis is the anti-sera dilution fold. Anti-sera from five immunized mice labeled with M1-5 were tested, and serum from non-immunized mice (Blank) were taken as a negative control. M1 presents the best binding (red line), a titer of 9.8 × 10^6 dilution as indicated by #. **(C)** The summary of hybridoma supernatant binding with HPV18 VLP astested by ELISA. Each dot represents the binding of the supernatant from one culture well containing at least one hybridoma. Two dots, shown by red circle, indicate the parental clones of 2A12 and 8H14, respectively. **(D)** Top seven binders in **(C)** inhibiting HPV infection, each dot represents one hybridoma supernatant. Cell supernatant and heparin were taken as negative and positive controls, respectively. Two clones present complete inhibition were highlighted with red frame line. Subtype of 2A12 **(E)** and 8H4 **(F)** was tested by Subtype identification kit. Data of **(B, D–F)** represent mean ± SEM. All experiments of **(B–F)** were repeated twice.

(**Figure 1D**), and were selected for further characterization. 2A12 and 8H4 belong to IgG1 and IgG2b subtypes, respectively, as characterized by a subtyping kit (**Figures 1E, F**). Overall, Two mAbs with complete inhibition of HPV18 infection were isolated.

Binding Characterization of Downselected Antibodies

To further characterize the selected monoclonal antibodies, purified 2A12 and 8H4 were prepared and verified by SDS-PAGE (**Figure 2A**). ELISA results showed that 2A12 and 8H4 exhibited high binding with HPV18 VLP with EC_{50} values of 357 and 100 pM, respectively (**Figure 2B**). The binding of 2A12 and 8H4 to whole VLP was investigated by immune-electronic microscopy (Immune-EM). Dark dots of 10 nm colloidal gold particles conjugated with 2A12 or 8H4 but not the murine antibody (isotype control) surrounded the outer region of VLP, indicating that 2A12 and 8H4 recognized the HPV18 VLP (**Figure 2C**). 2A12 and 8H4 showed no reactivity with reduced HPV18 VLP as detected by Western-Blot (**Supplemental Figure 1**), suggesting that 2A12 and 8H4 epitopes are highly structure dependent. 2A12 and 8H4 were next evaluated for epitope specificity by bio-layer interferometry (BLI) using HPV18 VLP proteins as capture antigens. The antigens captured on AR2G biosensors were bound saturate concentrations (20 μg/ml) of 8H4 that were followed by 2A12 as the competing antibody at a concentration of 20 μg/ml. Only antibodies that bind to a non-competing site would be detected in the assay. The results revealed that 2A12 could still bind HPV 18 VLP even when HPV18 VLP was saturated by 8H4, suggesting that 2A12 and 8H4 react with distinct epitopes (**Figure 2D**). Purified 2A12 and 8H4 were further analyzed for HPV18 VLP binding kinetics by BLI. 2A12 and 8H4 bound HPV18 VLP with K_D values of 2.14 and 1.68 nM, respectively (**Figures 2E, F**). In summary, 2A12 and 8H4 recognize quaternary and non-overlapping epitopes with high affinity.

Binding Specificity of 2A12 and 8H4 With HPV VLPs

The cross-reactivity of 2A12 and 8H4 against VLPs from nine common types of HPV, including HPV6, 11, 16, 18, 31, 33, 45,

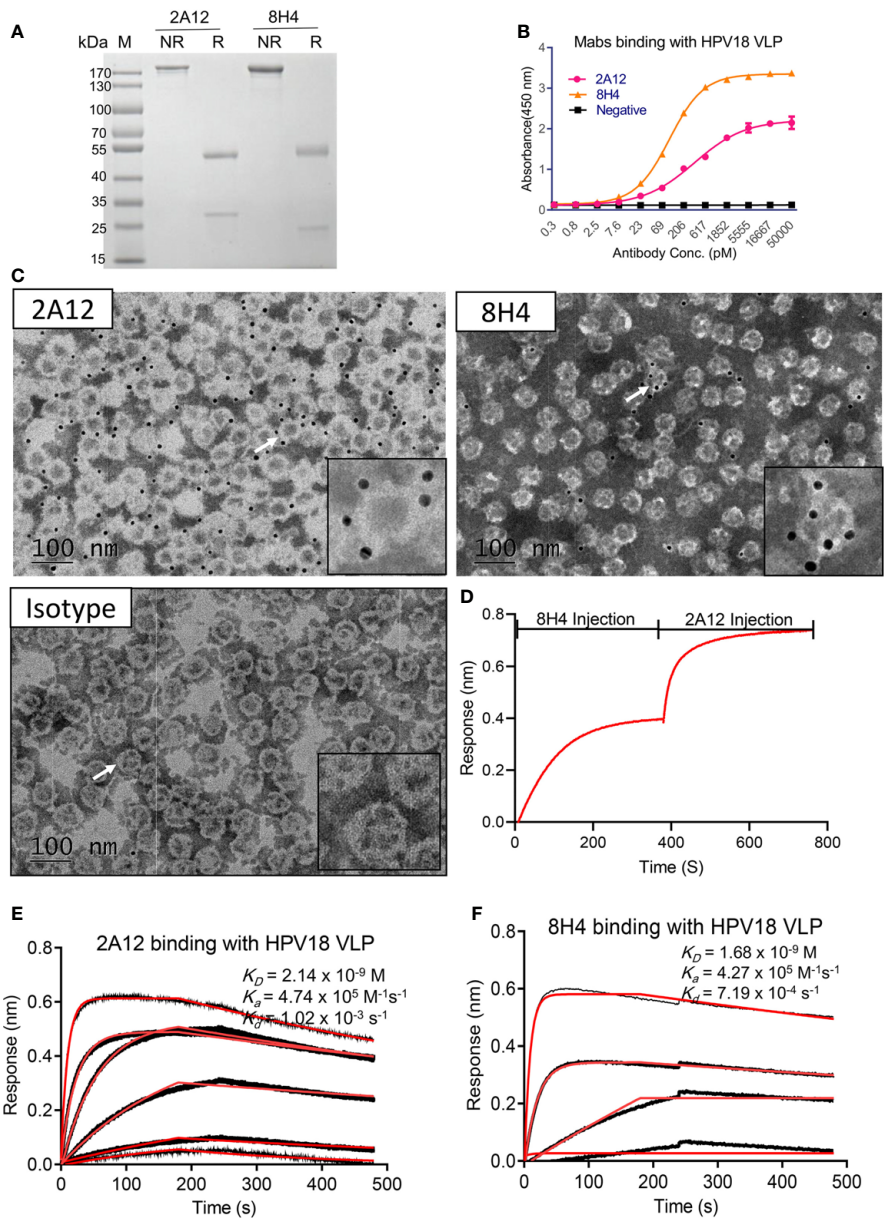

FIGURE 2 | Characterization of 2A12 and 8H14. **(A)** The purity of 2A12 and 8H4 was determined by SDS-PAGE under non-reducing (NR) or reducing condition (R). **(B)** Serially diluted 2A12 and 8H4 monoclonal antibody binding with HPV18 VLP was analyzed by ELISA. Data represent mean ± SEM. **(C)** Immune electronic microscopy negative staining image showing HPV 18 VLPs recognized by 2A12, 8H4 and isotype control as indicated. The insets are enlarged images of individual VLP as indicated by corresponding arrows. Black dots are antibody conjugated with 10 nm colloidal gold particles. Gray circles with the white ring are the VLPs. The bar indicates 100 nm. **(D)** Epitope specificity analysis of 8H4 and 2A12 by BLI. HPV18 VLP was coated on the sensor, 8H4 antibody was added to bind for 400 s, followed by the addition of 2A12 for another 400 s. Kinetic binding curve of 2A12 **(E)** and 8H4 **(F)** with HPV18 VLP. Binding curves are colored black, and fit of the data to a 1:1 binding model is colored red. All experiments were repeated twice.

52, and 58 was examined by ELISA, cell immunofluorescence and flow cytometry. ELISA showed that 2A12 and 8H4 reacted only with HPV18 VLP (**Figure 3A**). The specific binding was further validated by cell immunofluorescence and flow cytometry (**Figures 3B, C**). Altogether, these results indicate that 2A12 and 8H4 recognize respective epitopes that only present on HPV18 VLP.

2A12 and 8H4 Exhibited Excellent Neutralizing Potency Against HPV18

To examine the neutralizing activity of 2A12 and 8H4, HPV pseudovirus neutralization experiments were performed. 2A12 and 8H4 were able to completely neutralize HPV18 infection with high potency at IC_{50} of 0.44 and 0.86 ng/ml, respectively

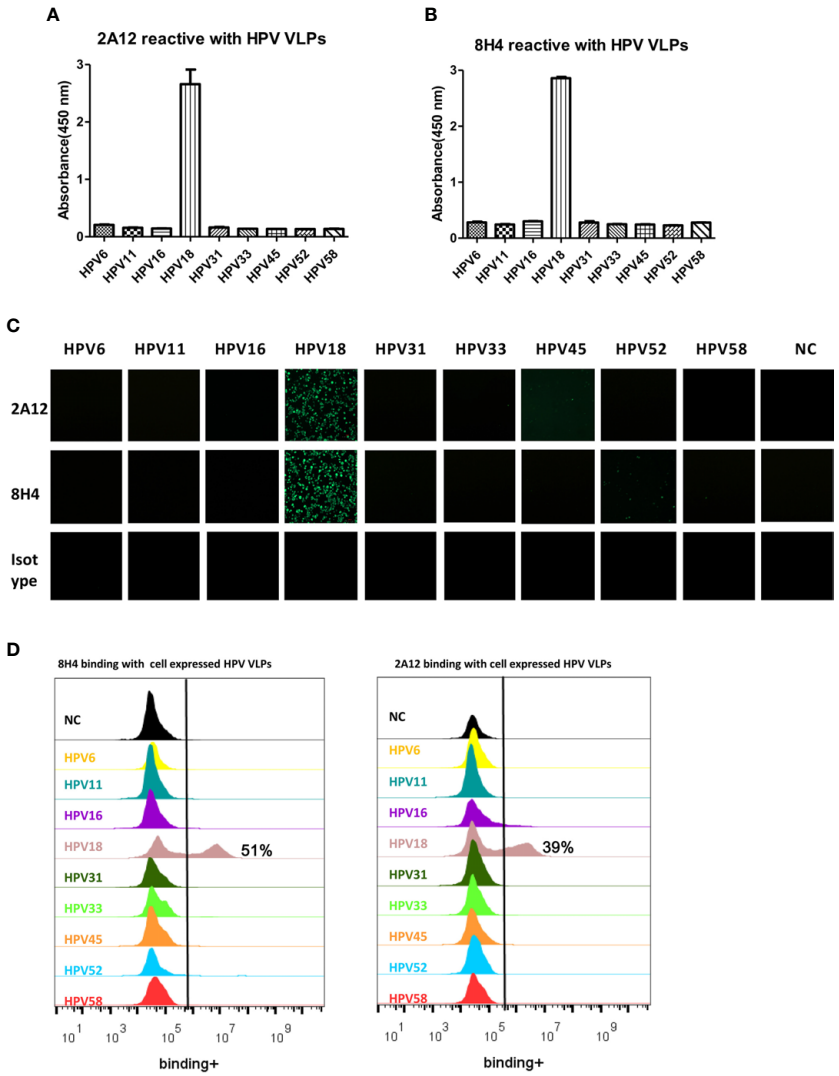

FIGURE 3 | Characterization of binding specificity of 2A12 and 8H4. Analysis of 2A12 **(A)** and 8H4 **(B)** binding with VLPs derived from various subtypes of HPV by ELISA. Data represent mean ± SEM. **(C)** 2A12 and 8H4 binding with various subtypes of HPV VLPs detected by immunofluorescence assay. Isotype control antibody (Isotype) was taken as a negative control. **(D)** 2A12 and 8H4 binding with various subtypes HPV VLPs detected by FACS. All experiments were repeated twice.

(**Figures 4A, B**). Expectedly, 2A12 and 8H4 failed to neutralize the infection of any other eight common HPV subtypes (**Figures 4C, D**), consistent with their binding specificities (**Figure 3**). Heparin (H4784, Sigma-Aldrich), a drug used in the treatment of HPV infection (31), was used as the positive control with an IC_{50} of heparin at 1.82×10^5 ng/ml. In other words, compared to the heparin control, 2A12 and 8H4 exhibited at least five orders of magnitude more potent neutralizing activity against HPV18 infection.

Functional Activity of Humanized 2A12

Given that 2A12 exhibited more potent neutralization against HPV18 infection with IC_{90} of 2.63 ng/ml compared to that conferred by 8H4 with IC_{90} of 35.78 ng/ml (**Figures 4A, B**). As a murine antibody, 2A12 will pose potential risk of immunogenicity when applied in human use and, therefore, needs to be humanized for clinical development. Surprisingly, humanized 2A12 (Hu2A12) exhibited improved binding with HPV18 VLP with an EC_{50} of 74.92 vs 492 pM for the parental 2A12 (**Figure 5A**). Consistently, Hu2A12 exhibited improved neutralization activity against HPV18 with an IC_{50} of 0.11ng/ml as compared to 2A12 with an IC_{50} of 0.44ng/ml (**Figure 5B**). The improved binding and neutralization activity were substantiated by the increased affinity of Hu2A12 to HPV18 VLP, with the K_D of 0.95 nM vs. 2.1 nM for 2A12 (**Figures 2D**, **5C**). Together, these results indicate that Hu2A12 has higher affinity and improved neutralization potency than the parental antibody (**Figures 5B**).

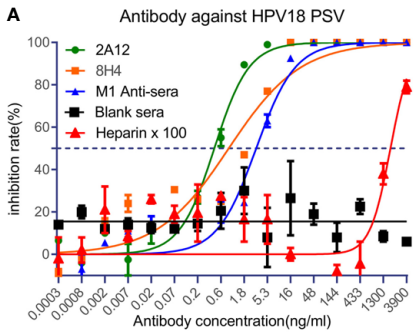

B

Reagents	IC_{50} (ng/ml)	IC_{80} (ng/ml)	IC_{90} (ng/ml)
2A12	0.44	1.35	2.63
8H4	0.86	9.05	35.78
M1 Anti-sera	3.16	11.31	23.85
Blank sera	/	/	/
Heparin	1.82E+05	3.59E+05	/

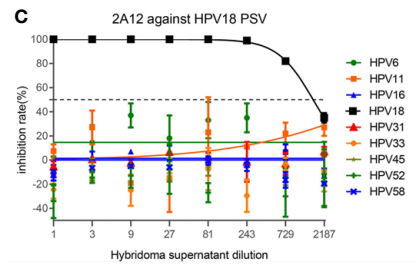

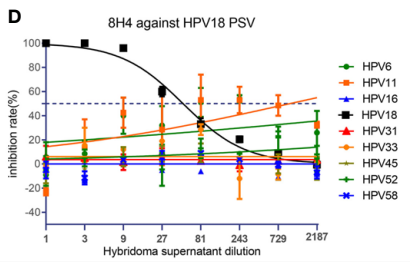

FIGURE 4 | Neutralization activity of 2A12 and 8H4. **(A)** Neutralization activity of mAbs and mouse sera against HPV18 pseudovirus infection. Heparin was taken as a positive control and heparin ×100 represents that the concentration of heparin in use is the indicated concentration at *X* axis multiply 100 fold. **(B)** Summary of the neutralization titers (IC_{50}, IC_{80} and IC_{90}) against HPV18 pseudovirus infection. Neutralization activity of 2A12 **(C)** and 8H4 **(D)** against the pseudovirus infection of various HPV subtypes. Data represent mean ± SEM. All experiments were repeated twice.

Given the fact that vaginal environment is acidic and HPV neutralizing antibodies topically applied must sustain the degradation, the potency of Hu2A12 against HPV18 in various acidic pH settings was evaluated. IC_{50} values in pH 4.0, 5.0, 6.0 and 7.0 were 0.77, 0.134, 0.08 and 0.04 ng/ml, respectively (**Figures 5D, E**), showing the decreasing trend as the pH dropped though still highly potent with an IC_{50} of 0.77 ng/ml at pH4.0 (**Figures 5D, E**). Given the pH values ranged from pH 4.0 to 6.0 in the vaginal cervix (32), such acidic environment may have a limited impact on the neutralizing activity of Hu2A12. Together, these data indicates that Hu2A12 could retain neutralizing activity as a topical agent for the treatment of HPV cervical infection.

In Vitro and *In Vivo* Characterization of Hu2A12-Hydrogel Formulation

Hu2A12 was formulated in hydrogel as a topical agent to increase vaginal retention and improve release. Hu2A12 in the hydrogel was completely released within 48 hours and the released Hu2A12 retained comparable neutralizing activity, indicating that Hu2A12-hydrogel could be applied to treat HPV18 infection as vaginal biopharmaceutical agent (**Figures 6A, B**). To measure the kinetics of Hu2A12 in the form of hydrogel, hydrogel containing 2A12 was applied to mouse vaginal and the release of Hu2A12 was monitored at various time points. Hu2A12 could be observed in mouse vaginal within 48 h (**Figures 6C, D**), consistent with the released results of *in vitro* experiment as shown in **Figure 6A**. H&E-stained vaginal tissues of the above mice showed that Hu2A12 in hydrogel did not induce infiltration of inflammatory cells in the vaginal sections compared to the Mock control (**Figure 6E**), suggesting that Hu2A12 in hydrogel induced no toxic to vaginal tissue as topical agents. Altogether, Hu2A12-hydrogel could be released and retained anti-viral activity against HPV infection in the vaginal cervix.

DISCUSSION

Current prophylactic HPV vaccines have achieved significant prevention against HPV infection. However, a large number of women still fail to receive prophylactic HPV vaccines due to various reasons, such as costs, availability, or nonresponding to vaccination. In 2018, there were 570,000 reported new cases and 311,000 related deaths, suggesting that effective medical treatment of HPV infection is urgently needed.

Persistent HPV infection is the main risk factor and a pre-requisite for the development of the premalignant conditions of cervical intraepithelial neoplasia or adenocarcinoma *in situ*. Therefore, neutralizing antibodies can be used to block the released virus from infecting nascent epithelial cells, thus inhibiting the malignant transformation of the cells. Neutralizing antibodies have been widely applied to treat viral infections caused by RSV, Ebola, HIV, SAR-CoV-2 etc. However, the development of HPV neutralizing antibodies is very rare.

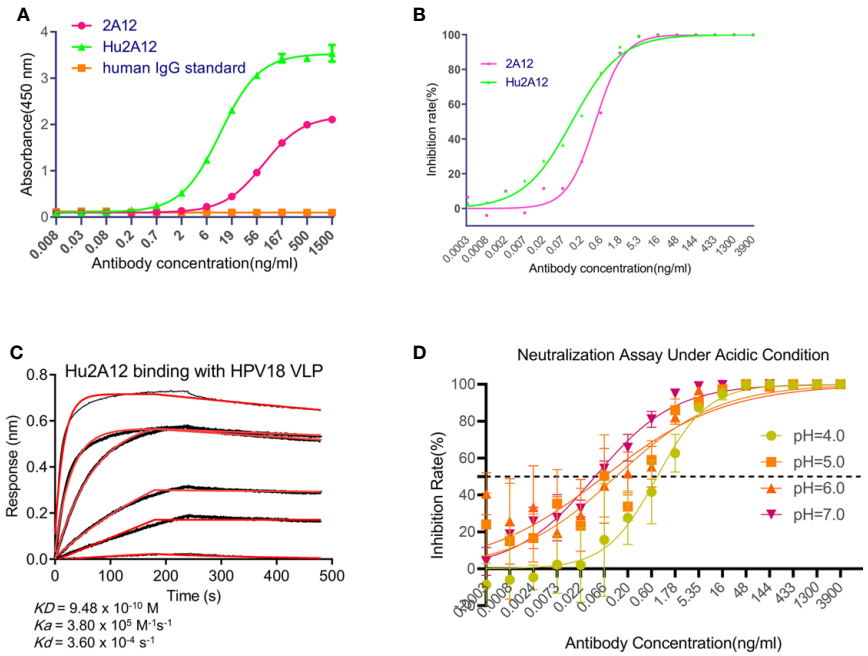

E

pH Values	IC_{50} (ng/ml)	IC_{80} (ng/ml)	IC_{90} (ng/ml)
7	0.0432	0.5582	2.5
6	0.087	2.615	19.13
5	0.1347	2.556	14.29
4	0.7732	3.998	10.45

FIGURE 5 | Characterization of humanized 2A12. **(A)** ELISA analysis of the reactivity of 2A12 and humanized 2A12 (Hu2A12) with HPV18 VLP. PBS binding with sGn served as a control (Blank). Data represent mean ± SEM **(B)** Neutralization activity of Hu2A12 against HPV18 pseudovirus infection. Data represent mean ± SEM. **(C)** Kinetic binding curve of Hu2A12 with HPV18 VLP. Binding curves are colored black, and fit of the data to a 1:1 binding model is colored red. **(D)** Neutralization activity of Hu2A12 against HPV18 pseudovirus infection under various pH. Different color curves represent different pH. **(E)** The summary of the neutralization titers (IC_{50}, IC_{80} and IC_{90}) against HPV18 pseudovirus infection in **(D)**. Data represent mean ± SEM. All experiments were repeated twice.

Thus our potent neutralizing antibody, Hu2A12, will be a potential candidate therapeutic agent for the topical treatment of HPV18 infection.

Considering the repeated cycles of HPV release and infection in the cervical basal epithelium, topical application of neutralizing antibodies will be a plausible approach to stop the HPV infection, thus preventing malignant transformation of the epithelium. Acid stable Hu2A12 will offer a valuable advantage for its application at the vaginal/cervical environment. In addition, the slow-release and the retention of bioactivity of Hu2A12 in hydrogel formulation offer additional benefits for using the antibody as a topical agent to treat HPV18 infection. Unlike vaccines, which usually take weeks to generate immune protection in vaccinated individuals, neutralizing mAbs as topical agents may provide immediate protection against viral infection, and are thus suitable for people at all ages and particularly suitable for high-risk populations and immunocompromised individuals who typically do not generate sufficient nAbs after vaccination. Furthermore, topical agents could release high concentration of potent neutralizing mAbs at the HPV infected sites compared to the systemic neutralizing mAbs elicited by HPV vaccine. In the developing world, even if the vaccines are available it would take many years to build up enough coverage of the populations under risk; therefore, in the foreseeable future women will continue to be infected and effective treatment drugs will be needed. Altogether, compared to the success in the prevention of HPV infection achieved by current licensed HPV vaccines, topical hydrogels containing anti-viral agents may provide immediate treatment for people without receiving HPV vaccines or who fail to mount antibody immunity after vaccination.

In this study, two potent neutralizing antibodies, 2A12 and 8H4 were isolated from hybridomas prepared from the mice immunized with HPV18 VLP. Both 2A12 and 8H4 could completely neutralize HPV18 infection with high potency with IC_{50} values of 0.44 to 0.86 ng/ml (**Figures 4A, B**). To our knowledge, these two antibodies are the most potent mAbs against HPV18 reported. Furthermore, 2A12 and 8H4 recognize

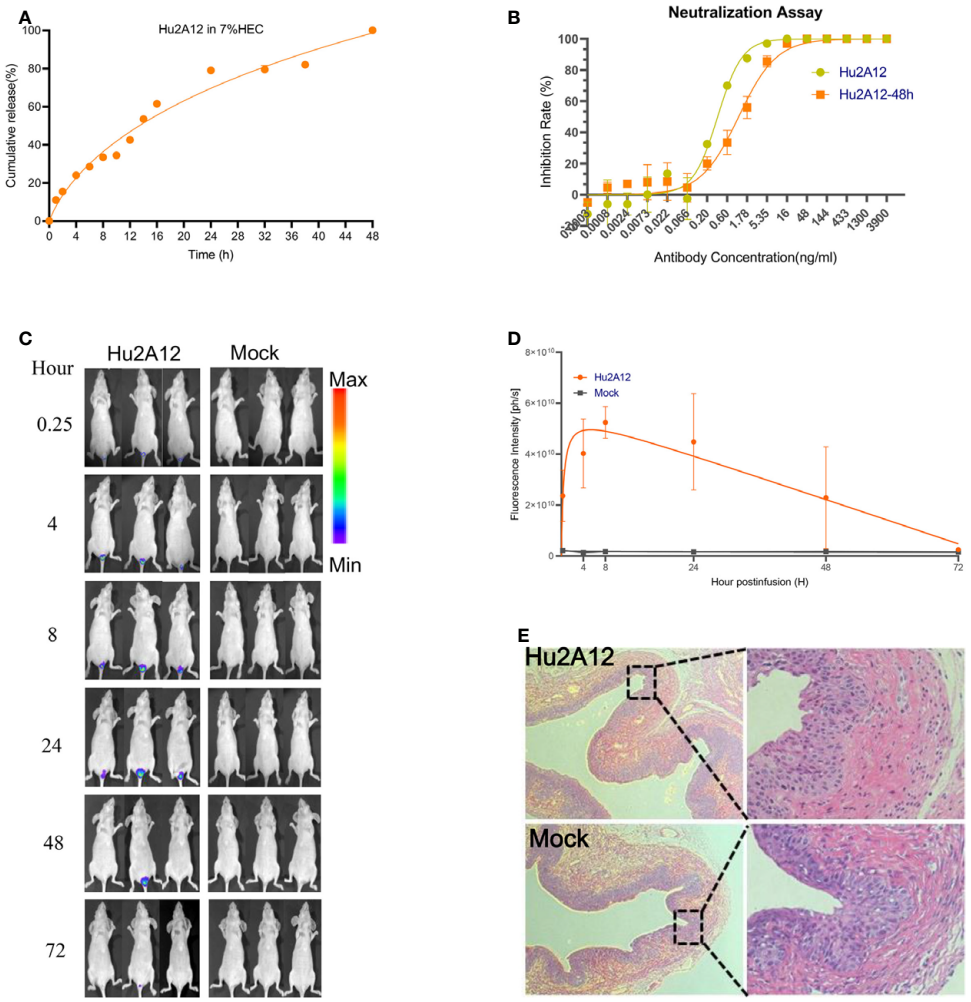

FIGURE 6 | Characterization of Hu2A12 in gel. **(A)** The release of Hu2A12 in gel was determined at the indicated time. Data represent mean ± SEM. **(B)** Neutralization activity of Hu2A12 and Hu2A12 released from the gel at 48 h (Hu2A12-48h). Data represent mean ± SEM. **(C)** Sequential *in vivo* imaging of Hu2A12-750 conjugated with dye YF750 injected into the vagina of nude mice. **(D)**. Fluorescence intensity (ph/s) of mice shown in **(C)**. Data represent mean ± SEM. **(E)** Representative vaginal sections of mice from Hu2A12 in hydrogel and Mock group in **(B)** were analyzed by H&E staining. The right panel is enlarged images as indicated by rectangle.Images were visualized under ×10 objective lens. All experiments of **(B, D, E)** were repeated twice.

distinct quaternary epitopes and exhibit highly specific binding with HPV18. Hu2A12 exhibited improved neutralizing activity against HPV18 infection and its neutralization activity was not affected in various acidic pH settings and in hydrogel (**Figures 5D, E**), suggesting that Hu2A12 can be a promising candidate for topical therapeutic agent against HPV18 infection.

Several topical therapies for HPV or CIN, including immune-modulators, anti-proliferative medications, antivirals, hormones, and herbal/alternative therapies are in various stages of clinical trial (11). Nevertheless, studies of antibodies as topical agents against HPV have been limited due to the difficulty in isolating antibodies with potent neutralizing activities, the challenge in delivering antibodies to the infection sites in the basal layer of the cervical epithelium and the efficacy of antibodies eliminating infected cells. The development of Hu2A12 will open a new therapeutic avenue for neutralizing antibodies as topical agents in treating other high-risk HPV infections such as HPV16, 31, 33, 45, 52, 58 etc.

The main limitation of this study is not evaluating the *in vivo* efficacy of Hu2A12-hydrogel in the treatment of HPV18 infection due to the lack of a suitable small animal model. Clinical trials demonstrated that robust neutralizing antibodies against HPV in serum and in cervicovaginal secretions were correlated to protection (33, 34), suggesting that human studies in the evaluating Hu2A12 as topical agents will be merited.

In summary, Hu2A12 with high neutralization potency against HPV18 was developed. The efficacy, delivery, safety, and accessibility of Hu2A12 were characterized, indicating that Hu2A12 will be promising as a topical agent to treat HPV18 infection.

DATA AVAILABILITY STATEMENT

The raw data supporting the conclusions of this article will be made available by the authors, without undue reservation.

ETHICS STATEMENT

The animal study was reviewed and approved by the Committee on the Use of Live Animals by the Ethics Committee of Nanjing Drum Tower Hospital.

AUTHOR CONTRIBUTIONS

All authors contributed to the work fulfilled the criteria adopted from ICMJE. BH, LZ, and XW conducted most experiments, analyzed the data, and wrote the draft manuscript. HW, HS, DZ, HY, NZ, SX, WN, and YH provided technical assistance and did animal experiments. XW and ZW designed the study, monitored and financially supported the study, and revised the manuscript. All authors contributed to the article and approved the submitted version.

FUNDING

This work was supported by The Major Research and Development Project (2018ZX10301406 to ZW), National Science Foundation of China (NSFC) (No. 81803414 to XW, 31970149 to ZW), Nanjing University-Ninxia University Collaborative Project (Grant# 2017BN04 to ZW), Research Foundation of JiangSu Commission Health project (Grant# ZDA2020014 to XW), and Jiangsu province "Innovative and Entrepreneurial talent" and Six Talent Peaks Project of Jiangsu Province.

SUPPLEMENTARY MATERIAL

The Supplementary Material for this article can be found online at: https://www.frontiersin.org/articles/10.3389/fimmu.2021.678318/full#supplementary-material

REFERENCES

1. Small W Jr, Bacon MA, Bajaj A, Chuang LT, Fisher BJ, Harkenrider MM, et al. Cervical Cancer: A Global Health Crisis. *Cancer* (2017) 123(13):2404–12. doi: 10.1002/cncr.30667
2. Doorbar J, Quint W, Banks L, Bravo IG, Stoler M, Broker TR, et al. The Biology and Life-Cycle of Human Papillomaviruses. *Vaccine* (2012) 30:F55–70. doi: 10.1016/j.vaccine.2012.06.083
3. Woodman CBJ, Collins SI, Young LS. The Natural History of Cervical HPV Infection: Unresolved Issues. *Nat Rev Cancer* (2007) 7(1):11–22. doi: 10.1038/nrc2050
4. Harper DM, DeMars LR. HPV Vaccines - A Review of the First Decade. *Gynecologic Oncol* (2017) 146(1):196–204. doi: 10.1016/j.ygyno.2017.04.004
5. Castle PE, Maza M. Prophylactic HPV Vaccination: Past, Present, and Future. *Epidemiol Infect* (2016) 144(3):449–68. doi: 10.1017/S0950268815002198
6. Arbyn M, Weiderpass E, Bruni L, de Sanjose S, Saraiya M, Ferlay J, et al. Estimates of Incidence and Mortality of Cervical Cancer in 2018: A Worldwide Analysis. *Lancet Glob Health* (2020) 8(2):E191–203. doi: 10.1016/S2214-109X(19)30482-6
7. Dadar M, Chakraborty S, Dhama K, Prasad M, Khandia R, Hassan S, et al. Advances in Designing and Developing Vaccines, Drugs and Therapeutic Approaches to Counter Human Papilloma Virus. *Front Immunol* (2018) 9:2478. doi: 10.3389/fimmu.2018.02478
8. Grimm C, Polterauer S, Natter C, Rahhal J, Hefler L, Tempfer CB, et al. Treatment of Cervical Intraepithelial Neoplasia With Topical Imiquimod a Randomized Controlled Trial. *Obstet Gynecol* (2012) 120(1):152–9. doi: 10.1097/AOG.0b013e31825bc6e8
9. Maiman M, Watts DH, Andersen J, Clax P, Merino M, Kendall MA. Vaginal 5-Fluorouracil for High-Grade Cervical Dysplasia in Human Immunodeficiency Virus Infection: A Randomized Trial. *Obstet Gynecol* (1999) 94(6):954–61. doi: 10.1016/S0029-7844(99)00407-X
10. Snoeck R, Noel JC, Muller C, De Clercq E, Bossens M. Cidofovir, a New Approach for the Treatment of Cervix Intraepithelial Neoplasia Grade III (CIN III). *J Med Virol* (2000) 60(2):205–9. doi: 10.1002/(SICI)1096-9071(200002)60:2<205::AID-JMV16>3.0.CO;2-8
11. Desravines N, Miele K, Carlson R, Chibwesha C, Rahangdale L. Topical Therapies for the Treatment of Cervical Intraepithelial Neoplasia (CIN) 2–3: A Narrative Review. *Gynecologic Oncol Rep* (2020) 33:100608. doi: 10.1016/j.gore.2020.100608
12. Stern PL, van der Burg SH, Hampson IN, Broker TR, Fiander A, Lacey CJ, et al. Therapy of Human Papillomavirus-Related Disease. *Vaccine* (2012) 30 (Suppl 5):F71–82. doi: 10.1016/j.vaccine.2012.05.091
13. Walker LM, Burton DR. Passive Immunotherapy of Viral Infections: 'Super-Antibodies' Enter the Fray. *Nat Rev Immunol* (2018) 18(5):297–308. doi: 10.1038/nri.2017.148
14. Kaplon H, Muralidharan M, Schneider Z, Reichert JM. Antibodies to Watch in 2020. *MAbs* (2020) 12(1):1703531. doi: 10.1080/19420862.2019.1703531
15. Guan P, Clifford GM, Franceschi S. Human Papillomavirus Types in Glandular Lesions of the Cervix: A Meta-Analysis of Published Studies. *Int J Cancer* (2013) 132(1):248–50. doi: 10.1002/ijc.27663
16. Li N, Franceschi S, Howell-Jones R, Snijders PJ, Clifford GM. Human Papillomavirus Type Distribution in 30,848 Invasive Cervical Cancers Worldwide: Variation by Geographical Region, Histological Type and Year of Publication. *Int J Cancer* (2011) 128(4):927–35. doi: 10.1002/ijc.25396
17. Gagliardi A, Porter VL, Zong Z, Bowlby R, Titmuss E, Namirembe C, et al. Analysis of Ugandan Cervical Carcinomas Identifies Human Papillomavirus Clade-Specific Epigenome and Transcriptome Landscapes. *Nat Genet* (2020) 52(8):800–10. doi: 10.1038/s41588-020-0673-7
18. Rader JS, Tsaih SW, Fullin D, Murray MW, Iden M, Zimmermann MT, et al. Genetic Variations in Human Papillomavirus and Cervical Cancer Outcomes. *Int J Cancer* (2019) 144(9):2206–14. doi: 10.1002/ijc.32038
19. Zhang Y, He Y, Li L, Liang ST, Yan M, Ren DY, et al. Development and Characterization of an HPV18 Detection Kit Using Two Novel HPV18 Type-Specific Monoclonal Antibodies. *Diagn Pathol* (2018) 13:55. doi: 10.1186/s13000-018-0727-7
20. Wu X, Ma X, Li Y, Xu Y, Zheng N, Xu S, et al. Induction of Neutralizing Antibodies by Human Papillomavirus Vaccine Generated in Mammalian Cells. *Antibody Ther* (2019) 2(2):45–53. doi: 10.1093/abt/tbz004
21. Greenfield EA. Electro Cell Fusion for Hybridoma Production. *Cold Spring Harb Protoc* (2019) 2019(10):684–88. doi: 10.1101/pdb.prot103184
22. Rems L, Usaj M, Kanduser M, Rebersek M, Miklavcic D, Pucihar G. Cell Electrofusion Using Nanosecond Electric Pulses. *Sci Rep* (2013) 3:3382. doi: 10.1038/srep03382

23. Buck CB, Pastrana DV, Lowy DR, Schiller JT. Generation of HPV Pseudovirions Using Transfection and Their Use in Neutralization Assays. *Methods Mol Med* (2005) 119:445–62. doi: 10.1385/1-59259-982-6:445
24. Guo X, Zhang L, Zhang W, Chi Y, Zeng X, Li X, et al. Human Antibody Neutralizes Severe Fever With Thrombocytopenia Syndrome Virus, an Emerging Hemorrhagic Fever Virus. *Clin Vaccine Immunol* (2013) 20 (9):1426–32. doi: 10.1128/CVI.00222-13
25. Johnston CM, Wood AL, Bolland DJ, Corcoran AE. Complete Sequence Assembly and Characterization of the C57BL/6 Mouse Ig Heavy Chain V Region. *J Immunol* (2006) 176(7):4221–34. doi: 10.4049/jimmunol.176.7.4221
26. Safdari Y, Farajnia S, Asgharzadeh M, Khalili M. Antibody Humanization Methods - A Review and Update. *Biotechnol Genet Eng Rev* (2013) 29:175–86. doi: 10.1080/02648725.2013.801235
27. Ahmadzadeh V, Farajnia S, Feizi MA, Nejad RA. Antibody Humanization Methods for Development of Therapeutic Applications. *Monoclon Antib Immunodiagn Immunother* (2014) 33(2):67–73. doi: 10.1089/mab.2013.0080
28. Zhai J, Mantaj J, Vllasaliu D. Ascorbyl Palmitate Hydrogel for Local, Intestinal Delivery of Macromolecules. *Pharmaceutics* (2018) 10(4):188. doi: 10.3390/pharmaceutics10040188
29. Aprodu A, Mantaj J, Raimi-Abraham B, Vllasaliu D. Evaluation of a Methylcellulose and Hyaluronic Acid Hydrogel as a Vehicle for Rectal Delivery of Biologics. *Pharmaceutics* (2019) 11(3):127. doi: 10.3390/pharmaceutics11030127
30. Epstein-Barash H, Stefanescu CF, Kohane DS. An *in Situ* Cross-Linking Hybrid Hydrogel for Controlled Release of Proteins. *Acta Biomater* (2012) 8 (5):1703–9. doi: 10.1016/j.actbio.2012.01.028
31. Giroglou T, Florin L, Schafer F, Streeck RE, Sapp M. Human Papillomavirus Infection Requires Cell Surface Heparan Sulfate. *J Virol* (2001) 75(3):1565–70. doi: 10.1128/JVI.75.3.1565-1570.2001
32. Laniewski P, Cui HY, Roe DJ, Barnes D, Goulder A, Monk BJ, et al. Features of the Cervicovaginal Microenvironment Drive Cancer Biomarker Signatures in Patients Across Cervical Carcinogenesis. *Sci Rep* (2019) 9:7333. doi: 10.1038/s41598-019-43849-5
33. Zhao H, Lin Z-J, Huang S-J, Li J, Liu X-H, Guo M, et al. Correlation Between ELISA and Pseudovirion-Based Neutralisation Assay for Detecting Antibodies Against Human Papillomavirus Acquired by Natural Infection or by Vaccination. *Hum Vaccines Immunotherapeutics* (2014) 10(3):740–6. doi: 10.4161/hv.27619
34. Huh WK, Joura EA, Giuliano AR, Iversen OE, de Andrade RP, Ault KA, et al. Final Efficacy, Immunogenicity, and Safety Analyses of a Nine-Valent Human Papillomavirus Vaccine in Women Aged 16-26 Years: A Randomised, Double-Blind Trial. *Lancet* (2017) 390(10108):2143–59. doi: 10.1016/S0140-6736(17)31821-4

Conflict of Interest: Author LZ was employed by the company Abrev Biotechnology Co., Ltd. Author HS was employed by Y-Clone Medical Science Co. Ltd. A patent application on 2A12 was submitted by Y-Clone Medical science Co. Ltd., under CN201911358261X.

The remaining authors declare that the research was conducted in the absence of any commercial or financial relationships that could be construed as a potential conflict of interest.

frontiers in Immunology

ORIGINAL RESEARCH
published: 24 August 2021
doi: 10.3389/fimmu.2021.735609

The Cancer Epitope Database and Analysis Resource: A Blueprint for the Establishment of a New Bioinformatics Resource for Use by the Cancer Immunology Community

*Zeynep Koşaloğlu-Yalçın[1], Nina Blazeska[1], Hannah Carter[2,3], Morten Nielsen[4,5], Ezra Cohen[3], Donald Kufe[6], Jose Conejo-Garcia[7,8], Paul Robbins[9], Stephen P. Schoenberger[10], Bjoern Peters[1,2] and Alessandro Sette[1,2]**

[1] Center for Infectious Disease and Vaccine Research, La Jolla Institute for Immunology, La Jolla, CA, United States, [2] Department of Medicine, University of California San Diego, La Jolla, CA, United States, [3] Moore's Cancer Center, University of California San Diego, La Jolla, CA, United States, [4] Department of Bio and Health Informatics, Technical University of Denmark, Lyngby, Denmark, [5] Instituto de Investigaciones Biotecnológicas, Universidad Nacional de San Martín, San Martín, Argentina, [6] Dana Farber Cancer Institute, Harvard Medical School, Boston, MA, United States, [7] Department of Gynecologic Oncology, H. Lee Moffitt Cancer Center and Research Institute, Tampa, FL, United States, [8] Department of Immunology, H. Lee Moffitt Cancer Center and Research Institute, Tampa, FL, United States, [9] National Cancer Institute, National Institutes of Health, Bethesda, MD, United States, [10] Laboratory of Cellular Immunology, La Jolla Institute for Immunology, La Jolla, CA, United States

OPEN ACCESS

Edited by:
Olivera J. Finn,
University of Pittsburgh, United States

Reviewed by:
Pramod Kumar Srivastava,
University of Connecticut, United States
Hans-Georg Rammensee,
University of Tübingen, Germany

***Correspondence:**
Alessandro Sette
alex@lji.org

Specialty section:
This article was submitted to Cancer Immunity and Immunotherapy, a section of the journal Frontiers in Immunology

Received: 02 July 2021
Accepted: 09 August 2021
Published: 24 August 2021

Citation:
Koşaloğlu-Yalçın Z, Blazeska N, Carter H, Nielsen M, Cohen E, Kufe D, Conejo-Garcia J, Robbins P, Schoenberger SP, Peters B and Sette A (2021) The Cancer Epitope Database and Analysis Resource: A Blueprint for the Establishment of a New Bioinformatics Resource for Use by the Cancer Immunology Community. Front. Immunol. 12:735609. doi: 10.3389/fimmu.2021.735609

Recent years have witnessed a dramatic rise in interest towards cancer epitopes in general and particularly neoepitopes, antigens that are encoded by somatic mutations that arise as a consequence of tumorigenesis. There is also an interest in the specific T cell and B cell receptors recognizing these epitopes, as they have therapeutic applications. They can also aid in basic studies to infer the specificity of T cells or B cells characterized in bulk and single-cell sequencing data. The resurgence of interest in T cell and B cell epitopes emphasizes the need to catalog all cancer epitope-related data linked to the biological, immunological, and clinical contexts, and most importantly, making this information freely available to the scientific community in a user-friendly format. In parallel, there is also a need to develop resources for epitope prediction and analysis tools that provide researchers access to predictive strategies and provide objective evaluations of their performance. For example, such tools should enable researchers to identify epitopes that can be effectively used for immunotherapy or in defining biomarkers to predict the outcome of checkpoint blockade therapies. We present here a detailed vision, blueprint, and work plan for the development of a new resource, the **C**ancer **E**pitope **D**atabase and **A**nalysis **R**esource (CEDAR). CEDAR will provide a freely accessible, comprehensive collection of cancer epitope and receptor data curated from the literature and provide easily accessible epitope and T cell/B cell target prediction and analysis tools. The curated cancer epitope data will provide a transparent benchmark

dataset that can be used to assess how well prediction tools perform and to develop new prediction tools relevant to the cancer research community.

Keywords: cancer, epitope analysis, database (all types), neoantigen, bioinformatics

INTRODUCTION

Recent years have witnessed a dramatic rise in interest towards cancer epitopes, studies that have been greatly facilitated by the dramatic decrease in the cost of whole-exome and transcriptome sequencing, as well as advances in mass spectrometry that has resulted in the generation of large datasets of candidate T cell epitopes that are naturally processed and presented (1). This resurgence of interest is linked to the exceptional success of immune checkpoint blockade therapies that disengage immune suppressive mechanisms and enable cancer antigen-specific T cells to recognize and attack tumor cells expressing those antigens (2–4). Additionally, current research suggests that combining checkpoint blockade treatment and neoantigen-directed therapies, such as vaccines or adoptive T cell transfer, can enhance treatment efficacy (5). More recently, checkpoint blockade therapies have been expanded to the neoadjuvant pre-surgical setting, where the aim is to enhance systemic immunity against a broader set of tumor antigens to eliminate micro-metastatic tumors that would otherwise be the source of a relapse (6). Despite these advances, only a subset of patients benefits from these immunotherapies.

Comprehensively cataloging all cancer epitope-related data linked to the biological, immunological, and clinical contexts will aid in understanding the biological mechanisms associated with efficacy and developing more effective therapeutic approaches. In parallel, researchers need access to computational epitope prediction and analysis tools but also need resources to aid in objective evaluation of the performance of different predictive strategies.

There have been several recent efforts to address these needs. The TANTIGEN 2.0 database (7) contains curated epitope and ligand elution data for many different cancer antigens, such as neoantigens and differentiation antigens. However, TANTIGEN does not include peptides that were shown to be ineffective and also lacks any association with clinical data. Similarly, The Cancer Antigenic Peptide Database (https://caped.icp.ucl.ac.be) also only includes curated epitope data for several different cancer antigens. NEPdb (8) contains curated neoantigens but lacks any other types of cancer antigens. For cataloged neoepitopes, associated receptor information and clinical data are also provided if available. It is possible to query NEPdb for an epitope sequence of interest, but there is no option to search for receptors. dbPepNeo (9) only contains curated HLA class I restricted neoantigens and ligand elution data. Importantly, while all resources provide some basic tools to query the databases for cancer types and peptide sequences, it is not possible to perform specific and granular queries. These resources do also not allow the user to perform any predictions for peptides of interest.

To fill these gaps, we here describe the plans and blueprint to develop a new resource, the Cancer Epitope Database and Analysis Resource (CEDAR). CEDAR is envisioned as a comprehensive bioinformatics resource, which will provide access to curated cancer epitope data, including mutated and non-mutated cancer epitopes, and bioinformatics tools for epitope and receptor analysis and prediction. The work proposed here will build on the Immune Epitope Database (IEDB), in existence since 2003, fully operational and independently funded until at least 2025 by the National Institute of Allergy and Infectious Diseases (NIAID) (10). The IEDB's focus is on allergy, infectious disease, transplantation, and autoimmunity but does not include cancer. Analogous to the IEDB, CEDAR will include all cancer-specific epitope data from various T cell and B cell experiments, MHC binding assays, and MHC ligandomics by mass-spectrometry. CEDAR will also include results from *in vivo* experiments such as tumor rejection and/or tumor control data. The granular curation of the data and the flexible query structure of CEDAR will allow the user to perform detailed queries to retrieve epitopes supported by different experimental data.

We believe that CEDAR will address an existing need because there is currently no comprehensive informatics resource available to the scientific community that stores data on cancer epitopes, the receptors that recognize them, and the immunological, clinical, and biological context in which they are recognized. In addition to a database of cancer epitopes, CEDAR will provide a set of analysis and prediction tools that will enable cancer researchers to predict putative epitope targets in a tumor sample of interest and also predict the likely specificity of T cell receptors (TCR) or B cell receptors (BCR) identified in single-cell sequencing data. CEDAR will also include benchmarking of existing epitope prediction tools and provide side-by-side comparisons of performance. The significance of these features lies in their utility for the broader community of cancer researchers. Currently, many cancer researchers are using the IEDB and its related tools to attempt to answer questions like this, which is suboptimal given that the IEDB was designed for applications outside of cancer (11).

RESULTS

A Plan to Define the CEDAR Database Scope Based on the Salient Characteristics of Cancer Epitope Data and Metadata

Following initial interviews with cancer experts, we identified the elements relating to an epitope that should be captured in CEDAR (**Figure 1**), including seven main "field groups", namely (1) related to the structure of the epitope, (2) the protein/antigen source from which the epitope is derived, (3) the host associated with the identified epitope responses, (4) the features of the tumor sample, isolate or model, (5) the effectors of the immune responses (both B

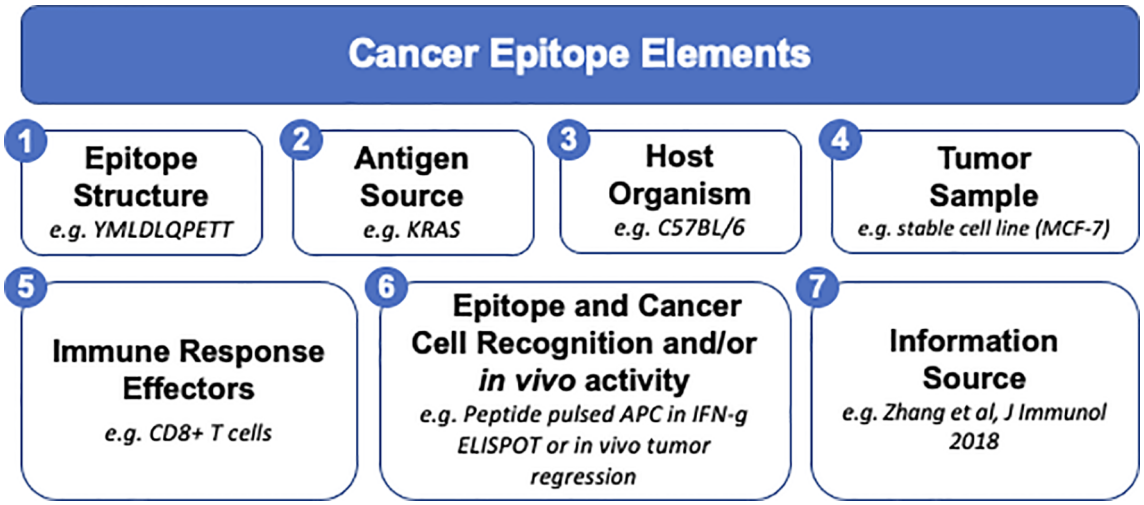

FIGURE 1 | Summary of salient characteristics of cancer epitope data and metadata for CEDAR.

and T cell responses), (6) the ability and modality of the effector responses to recognize the epitope and cancer cells, and (7) the source of the information that is captured. CEDAR will also identify whether the information captured is derived from a scientific publication, through a direct submission to CEDAR, or gathered from other online resources, and in each case, clearly state the provenance information.

Structure and Antigen Source of the Epitope and Type of Cancer Mutations

Different fields and subfields were defined to enable capturing information in a granular yet searchable and accurate fashion. First, we designated fields to capture the amino-acid sequence of the epitope together with associated post-translational modifications such as phosphorylation and glycosylation. In the case of non-peptidic epitopes, such as, for example, CHO epitopes recognized by antibody responses or ceramides used to expand natural killer (NK) T cells, the structures are captured following the format of ChEBI (12) and PubChem (13) resources.

We next defined a set of fields to indicate the general characteristics of the antigen. Specific fields distinguish and classify mutated epitopes (neoepitopes), tumor-associated antigens (TAA) such as differentiation or tissue-specific antigens (e.g., Melan-A, PSA), overexpressed antigens (e.g., HER-2, Muc-1), or cancer-germline antigens (e.g., MAGE, NY-ESO1). For peptidic antigens encoded in the host genome, we defined subfields to capture the gene and protein names of the unmodified antigen, the type [e.g., a self-protein or endogenous retroelement antigens such as long terminal repeats (LTR) or endogenous retroviruses (ERVs) (14)], and its frequency and magnitude of expression in healthy tissues for different tissue and cell types, as well as developmental stages (15). For non-peptidic self-antigens such as carbohydrates or gangliosides, we defined fields to record their presence in different tissues. Similarly, for epitopes derived from non-self-tumor-associated antigens, specific antigens are captured (e.g., protein from HPV). We designated a final set of fields to capture normal properties associated with the antigen, such as subcellular location and involvement in biological functions based on GeneOntology (16, 17), and whether the antigen is a driver gene, known to be causally linked to cancer progression (i.e., oncogene, tumor suppressor gene). A set of subfields also captures expression in pre-malignancies and the frequency and magnitude of expression in various tumor types (18, 19) and cancer cell lines (20).

We designated a distinct but equally important set of fields to capture the type of cancer mutations in the source antigen and their impact on the antigen, including the mutation type, such as single or multi nucleotide variants, frameshift, or non-frameshift indels and chromosomal rearrangements. The effect of the mutation (coding: missense or premature stop codon, frameshift, synonymous; non-coding: splice sites, UTR or other), and the outcome of the mutation on the antigen, distinguishing dysregulated expression, functional impact of the mutation on source antigen (21, 22), structural localization of mutation impact (23), localization in functional domains (21, 24), and known or predicted surface accessibility (23) are captured in additional subfields.

Fields Related to the Host Organism

We designated a set of fields and subfields to capture the organism associated with the epitope response in terms of species (most references will either be related to human responses or tumor animal models, primarily mice or rats), age, sex, strain or ethnicity, and the major histocompatibility complex (MHC). A separate set of fields was defined to capture the general feature of the cancer, such as natural occurrence and known associated risk factors *versus* induced cancers (genetically engineered organism with spontaneous tumor, xenograft, cancerogenic treatment induced). Cancer classification and diagnosis are captured in designated subfields as well, including anatomical site, histology, tumor stage,

and any type of pre-treatment. Additional subfields capture relevant characteristics of the host, such as microsatellite instability (MSI) and HPV status. If the subject from which the responses were derived was vaccinated, the specifics of such treatment are captured in terms of the vaccine antigen delivery format (synthetic peptide, mRNA, DNA plasmid, viral vector, and so on), adjuvant used, administration specifics, and formulation details. Additional fields were designated to capture other types of immunotherapies such as adoptive cell therapy (tumor-infiltrating lymphocytes (TIL) therapy, engineered TCR therapy, chimeric antigen receptor (CAR) T cell therapy, natural killer (NK) cell therapy), and checkpoint blockade therapy (e.g., anti-PD-1, anti-CTLA-4 therapy). If available, doses and dose sizes, information about targeted antigens, corresponding TCR sequences, 3D structures, and therapeutic interventions such as treatments with chemotherapy, radiation, surgery, or oncolytic viruses can be captured as well. Defined subfields will also capture clinical outcome, such as complete response, partial response, or cancer progression, and overall or progression-free survival, as well as reduction of tumor burden, change in tumor markers, and any adverse events of therapy, including autoimmune reactions.

We also designated fields to document the sample, isolate, or model associated with the source antigen of the epitope. Specifically, the sample nature (primary sample/short-term line vs. stable cell line), its occurrence (primary, metastasis, recurring), and whether the sample was obtained pre- or post-treatment. If available, tumor sample purity is also captured (from histology or predicted from sequencing data), as well as the overall mutational burden of the sample. Any available evidence for epitope/antigen expression in terms of frequency and magnitude of epitope/antigen expression in the sample is also documented. Importantly, CEDAR has designated fields to capture the evidence type for the epitope/antigen as detected in whole-genome, whole-exome, transcriptome, or targeted gene panel sequencing, together with the depth and coverage at the epitope site. In the event of a mutated antigen, details related to the mutation are stored, such as its origin (somatic/germline), tools that reported the mutation, read depth at the mutation site, and variant allele frequencies in the tumor DNA sample and RNA sample, if available. Supporting mass-spectrometry elution data are also be captured if available. A separate set of fields was defined to document features related to the tumor environment, including the presence of T cells and characterized subsets.

CEDAR will also include results from *in vivo* experiments such as tumor rejection and/or tumor control data. In such cases, details about the used mouse models or the patients from clinical trials will also be captured.

Fields Related to Capturing Immune Responses

CEDAR aims to capture the general features of the effector material, including the source of effector cells or antibodies, whether they were (*ex vivo*) T cells, short-term cultured or stable cell lines that were isolated from a tumor-affected host, or whether they were induced/engineered cell lines. Information related to antibody class and subclass and cell phenotypes, including CD4/CD8/NKT subset data and expression of phenotypic markers, is also captured. If available, corresponding TCR and antibody sequences, as well as 3D structures, will also be documented, considering the different levels of resolution associated with various techniques such as targeted sequencing of CDR3 regions and full-length TCR sequencing. We also designated subfields for possible synonymous TCR or BCR sequences encoded by different V(D)J sequences, with the opportunity to capture evidence of immunoediting or antigen loss, if available.

In addition to this, CEDAR also documents the specific assays performed to measure recognition. Examples include ELISPOT, intracellular cytokine staining (ICS) or tetramer assays for T cells, ELISA, antibody-dependent cell-mediated cytotoxicity (ADCC), and fluorescence assays for antibodies. A separate series of fields were defined to capture the effector mode of recognition, namely the capacity to recognize tumor cells directly, cell lines transfected with RNA, or cell lines pulsed with peptides. Particularly relevant for MHC class II-restricted responses is the curation of the type of antigen-presenting cell (APC) involved in the assay determination. A final and most crucial set of fields was defined to capture the results of the assessment, as available in qualitative (positive/negative) and quantitative (magnitude) terms. Importantly, the quality of negative controls associated with the assay, such as data related to MHC and antigen expression, will be carefully curated because a negative result is not valid if the MHC or antigen is not expressed. CEDAR will also capture the number of subjects tested/responded, the type of tested 'target', and in the case of mutated epitopes, whether both mutated and wildtype peptides were tested, and the associated outcomes.

Mapping Database Fields to Community-Supported Standards/Ontologies

In our planning and blueprint development for CEDAR, we have drawn on our experience operating the Immune Epitope Database (IEDB). Our extensive experience with the IEDB, which we initiated in 2003 and have been maintaining and enhancing over the past 18 years, has provided us with important lessons on what to do and, more importantly, what not to do when designing and maintaining an epitope database and analysis resource. By multiple metrics, the IEDB is a success, with >4,000,000 experiments characterizing >1,300,000 epitopes from >22,000 references curated; a monthly rate of >30,000 unique visitors, and over >3,900 citations per year (based on 2020 data). Importantly, even though the IEDB is currently not funded to respond to the needs of the cancer community, up to one-third of current IEDB users are applying its functionality in a cancer research setting. As part of our outreach activities, we have gathered requests from these users on how the IEDB could be improved for cancer researchers.

To accurately represent epitope information, the IEDB has developed a semantically well-defined data structure, which utilizes community-supported ontologies for most of its specific fields (**Figure 2**). The core of this data structure has proven to be remarkably flexible and robust, as it has been used to capture over

4 million assay records to date, enabling powerful aggregate queries on epitope information gathered in diverse settings. For example, for epitopes derived from viruses, the NCBI taxonomy is used to capture the particular virus that the epitope is known to originate from. This enables us to capture all synonymous names used to refer to that particular entity ("Human Papillomavirus 16" or "HPV16" or "Human Papillomavirus type 16"). It also allows storing and querying for information at different levels of granularity, such as obtaining all epitopes derived from viruses in the genus "Alphapapillomavirus" or specifying that an epitope was found in a particular isolate of HPV16. As other knowledge resources use the same NCBI taxonomic framework to represent organisms, it makes our data FAIR (findable, accessible, interoperable, and reusable) (25), which is particularly important for the (re-)use of IEDB data by the broader science community (26).

We plan to follow the same paradigm in CEDAR and will ensure that each database field can be mapped to an accessible, community-supported ontology. For fields where the scope overlaps with the IEDB, the same standards can simply be re-used. For database fields that are specific to cancer, standards/ontologies will need to be identified to curate them accurately. We have already identified the need for additional cancer-specific disease terms, including disease states and stages. Disease states will continue to be described using Disease Ontology (DO) (27) terms, which will be expanded and refined to include all cancer terms. Additionally, all cancer-related disease terms will be grouped under the parent term 'neoplasm', which aligns with the classification of cancers in the National Cancer Institute Thesaurus (NCIT) (28). Similarly, the NCIT terms will be used to specify cancer stages and link these terms to their official NCIT definitions and identifiers. Our team is proficient in working with vocabulary providers and standardization efforts, and we will enthusiastically embrace recommendations and/or participate in efforts to develop data standards within the ITCR and general cancer research community.

Development and Implementation of a Web-Enabled Query and Reporting Interface

One of the challenges for biomedical community databases is to ensure that the query interfaces are intuitive and that the generated reports provide understandable and scientifically accurate results. An initial design for the CEDAR web query

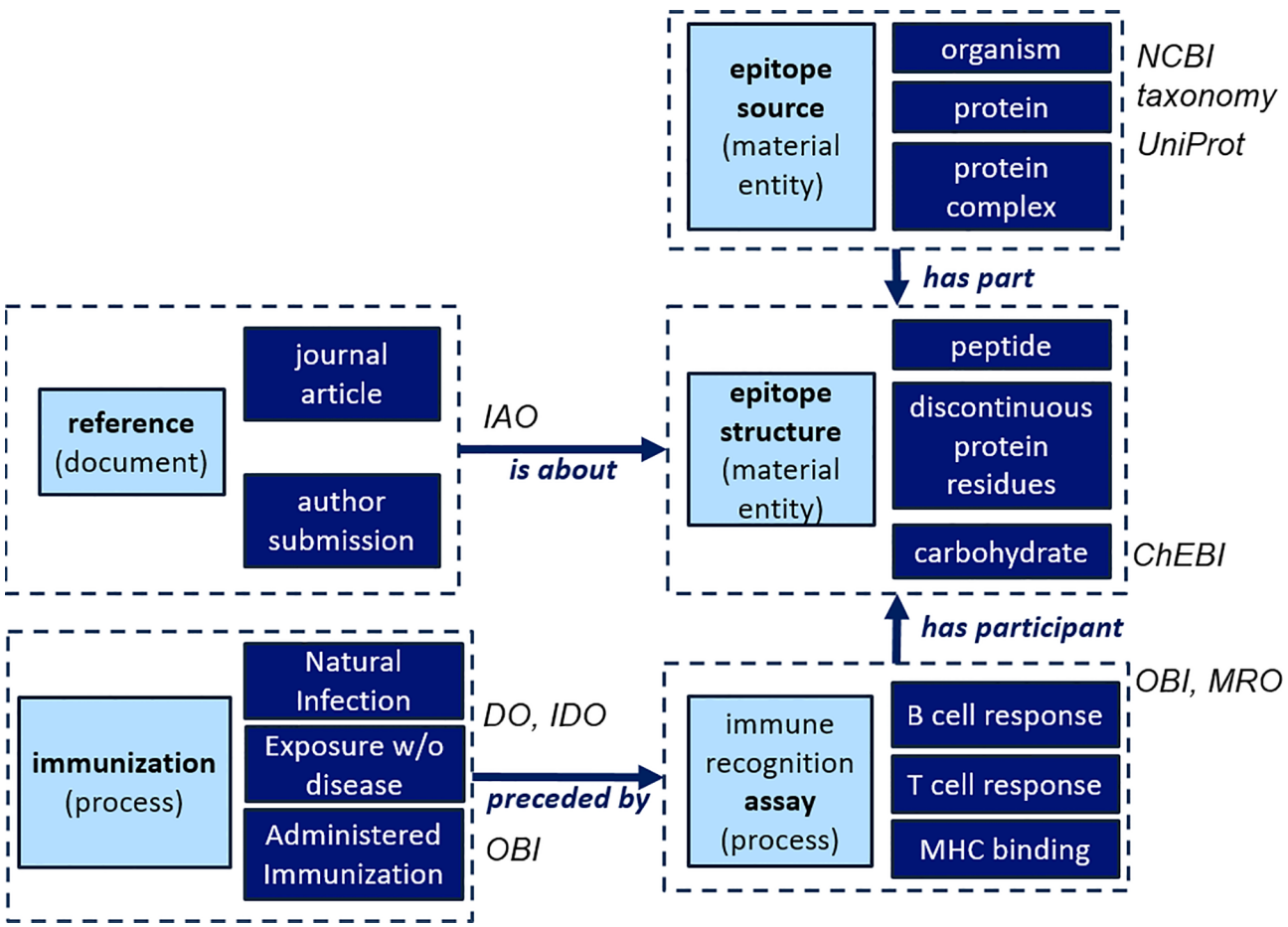

FIGURE 2 | IEDB high-level structure and ontological backbone.

interface (**Figure 3**) focuses on making the most requested pieces of information immediately accessible. This query interface shares fields with those present in the IEDB for epitope structure, host, assays used to characterize the response, and MHC-restriction. At the same time, it enables the direct query for the source of the epitope as it is relevant to cancer, namely source antigen, neoplasm, immune response induction, and treatment. We anticipate adding antigen subtypes, a characterization of the neoplasm/tumor, the ability to select methods used to induce immune responses, and information on the treatment a host was undergoing. It will, for example, be possible to search for all epitopes in a given cancer type or epitopes associated with a specific mutation or gene of interest. The granular curation of the data and the flexible query structure of CEDAR will allow for example to retrieve data related to either natural presentation, recognition of synthetic antigens or both. More detailed searches will also be possible, such as searching for a specific type of assay or for instances where a specific type of treatment occurred.

Background on the IEDB Curation Process

To identify and curate relevant publications that contain experimental cancer epitope data, CEDAR will utilize the validated curation approach established and optimized for the IEDB and modify specific steps where required. Over the last 18 years, we have developed, implemented, and continuously optimized the process to identify relevant journal articles for the IEDB and extract information from them, as outlined in **Figure 4**. Scientific literature is constantly monitored by querying the PubMed database on a biweekly basis with broad keyword queries, purposely designed to be comprehensive, in order to retrieve a broad universe of papers that should include all references describing immune epitopes. Over time, these specialized, broad queries have selected over 244,000 references from over 32 million papers available in PubMed.

Based on the abstract, automated text classifier tools and human experts then narrow these references down to those with likely relevance (29–31). The criteria for passing this initial selection require that the reference is within the scope of the database, provide novel data (for example, review papers and use of epitopes as a mere marker or tag are excluded), and describe the epitope molecular structure in sufficient detail and granularity (reports of simple reactivity against whole proteins or undefined structures are excluded). Following these determinations, the reference is classified as "relevant", and further subdivided into a specific disease category. The full text of relevant articles is then retrieved and assigned to a doctoral-level curator who extracts the data and enters it into the IEDB database curation system. The curated records are peer-reviewed, and once accepted, become visible to the public. The general curation processes are described in detail in previous publications (30, 32–34) and have been continuously adapted as new assay types are established, as has been done to capture receptor data from high throughput sequencing (35).

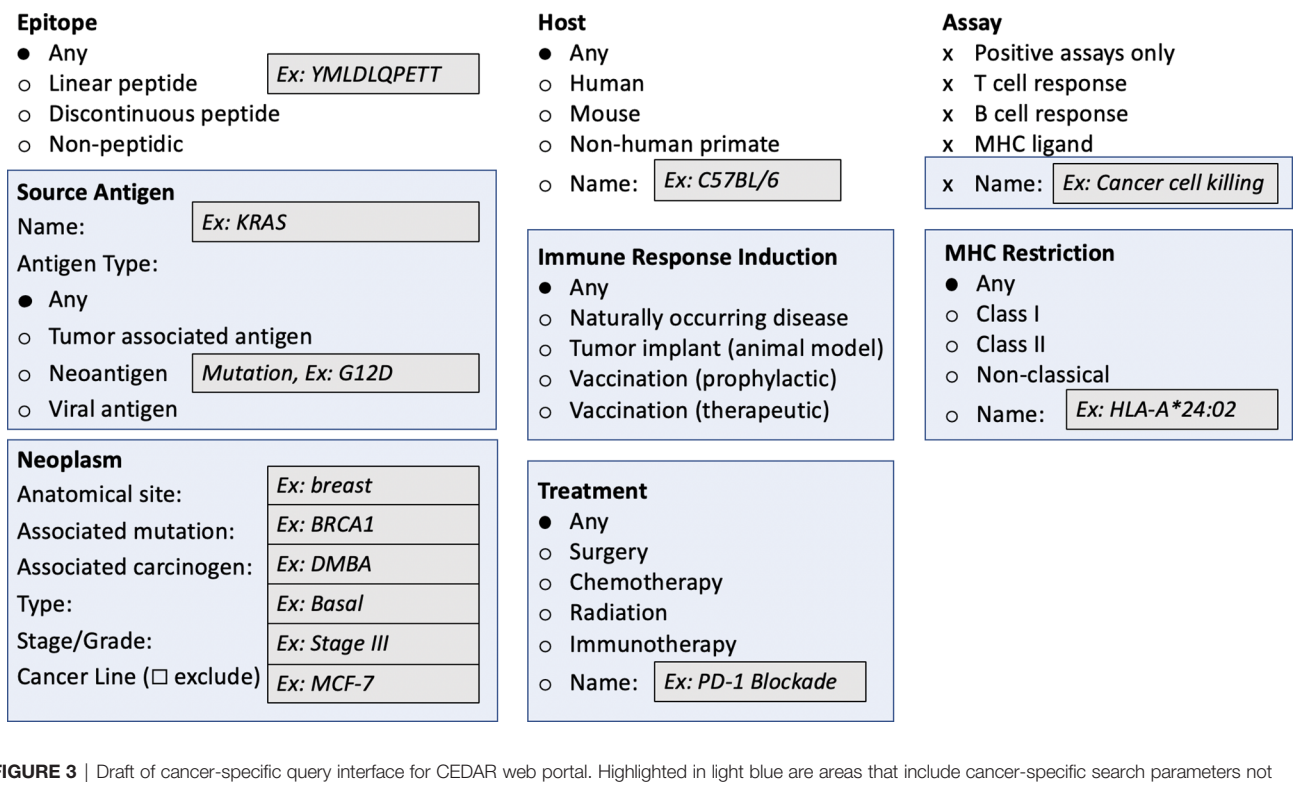

FIGURE 3 | Draft of cancer-specific query interface for CEDAR web portal. Highlighted in light blue are areas that include cancer-specific search parameters not present in the current IEDB interface.

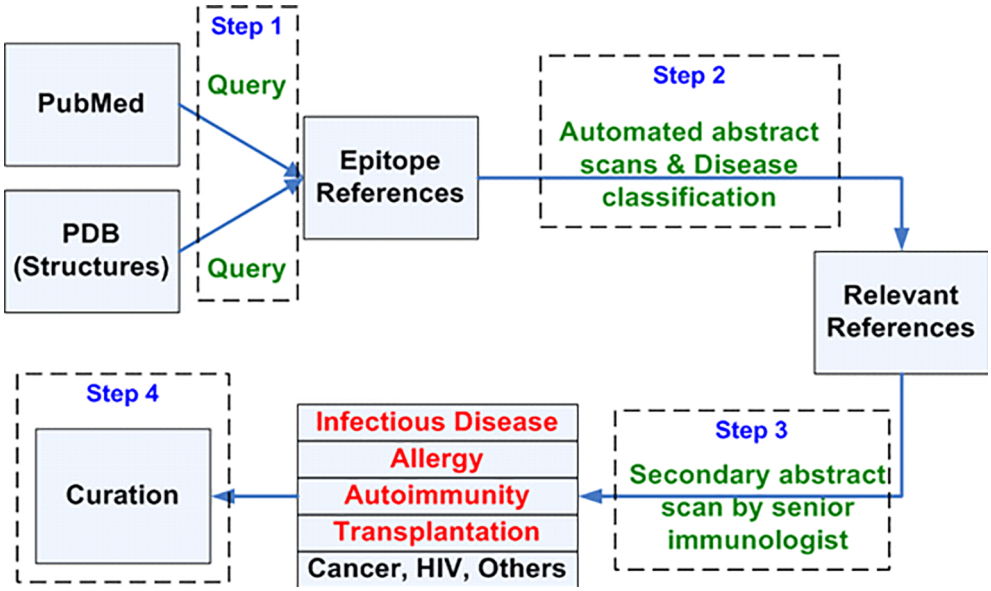

FIGURE 4 | Workflow for identifying curatable journal articles.

Development of a Prioritized Queue of Cancer-Related Articles for Curation

In preparation for cancer curation, papers that contain curatable epitope information as part of the IEDB curation workflow were further categorized by the use of automated text classifiers (29–31, 36) and manual inspection, in broad primary classes (Cancer, Infectious Diseases (excluding HIV which is curated by the Los Alamos database), Allergy, Autoimmunity, Transplantation and "Other". The percentage of references classified in each of these broad categories is shown in **Figure 5**. Cancer references account for 10.6% of all identified and curatable epitope references. These references were further subdivided into a set of 20 subcategories, grouped as a function of similar antigens and/or cancer types. The most frequent category is melanoma antigens (MAA, 20%), reflecting the prominence of these antigen types in immunological investigations. Other frequent categories are carbohydrate antigens such as Lewis and related antigens (LEWIS, 3.3%), and popular antigens such as mucin (5.5%), Her2 and associated antigens (6.4%), MAGE and associated antigens (4.8%), prostate associated antigens (PROS, 4.0%), p53 (2.6%), antigens associated with lymphoid cancers (LEU, 5.6%), and CEA (2.1%). Neoepitope references were classified separately and presently account for only 5.0%; however, the number of papers in this category has been rapidly rising in recent years.

In addition to this, we plan to inspect and broaden the initial PubMed query by adding keywords to ensure we capture all cancer epitope-specific articles. Our automated document classifier will be re-trained to specifically identify articles that contain cancer epitope-specific information, as we have done for

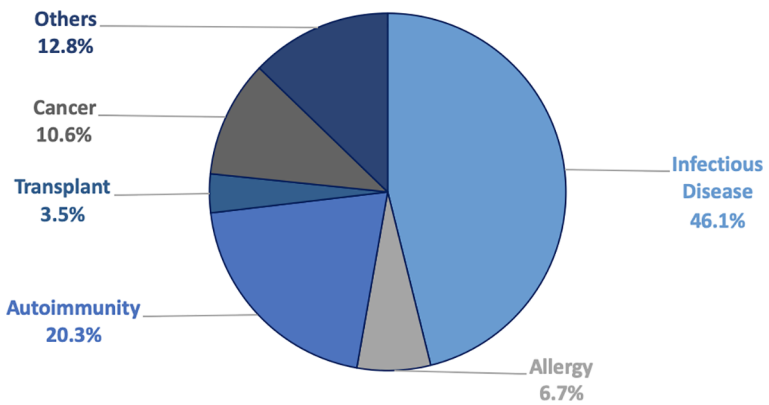

FIGURE 5 | Breakdown of classified and curatable references.

other categories before. Different categories will be addressed in a sequential fashion. Our current first priority for curation includes neoepitopes and T cell epitopes associated with melanoma, breast, and prostate cancers, as these are among the most frequently studied in basic investigations and clinical trial settings.

Curating Previously Identified Relevant Cancer Articles With Immune Epitope Data

To begin curation of cancer epitope literature, curators will follow the curation rules encoded in the IEDB curation manual, a living document (37), which will be expanded and customized for CEDAR. In brief, for each epitope entered into the database, the structure of the epitope, i.e., an amino acid sequence for peptidic epitopes and a chemical structure for non-peptidic epitopes, is described. If the epitope is naturally occurring, the protein and organism from which the epitope was derived are also entered; for example, the human melanoma antigen recognized by T cells 1 (MART-1) protein. Additionally, all experimental assays in which the epitope was studied are added as T cell, B cell, or MHC ligand assays. The details of each assay include information such as the host, whose immune response was studied, the disease state and stage of the individual, the type of effector cells (CD8+ T cells) or antibodies (monoclonal IgG1) being studied, and the assay method (ELISA, flow cytometry, etc.) that was utilized. Curation also captures the sequences of the epitope-specific TCRs and BCRs.

Curators capture data by entering it into dynamic and interactive web forms designed to optimize productivity and to ensure accurate and consistent data entry. This curation interface enforces curation rules as the curator enters the data, which takes advantage of the ontology-based data structure on a per-field basis. Once the curator has completed entering the data, additional validation rules that cross-compare the content of different fields are checked by the system prior to allowing the curation to be submitted. Just as development will be required on front-end user interfaces to support cancer-specific query and reporting better, the back-end curation system will also require development to allow for appropriate data entry. This system will be updated in coordination with the query and reporting interface development described above and based on the outreach feedback described below.

Curated Cancer Epitope Datasets for Benchmarking Epitope Prediction Tools

The following sections describe the benchmarking, improvement and development of epitope prediction methods. The results epitope predictions will lead to validation experiments determining which epitopes are actually of biological significance, which is arguably the ultimate goal. These results will, in a recursive modality, be fed back into training of epitope predictions, leading to increased prediction accuracy and significance.

Multiple computational tools and pipelines have been developed to predict cancer epitopes in the scientific community (38). The comprehensive sets of epitopes curated in CEDAR can be used to evaluate the performance of these tools. These benchmarking results will inform tool developers on the most valuable prediction approaches and tool users on which tools they can most rely on. Moreover, the epitope datasets created in this process will be valuable for the broader community in developing new tools. Since many of the tools evaluated will have been trained on subsets of existing data, 'live benchmarks' will also be implemented, which consist of automated pipelines that run predictions on epitope datasets just before they are released in CEDAR. We have previously implemented such 'live-benchmarks' for MHC class I (39) and MHC class II (40) binding predictions in the IEDB, and the framework established for these is easily expandable for CEDAR.

We previously performed a small benchmark on the predictability of cancer T cell epitopes with different prediction approaches (41). More comprehensive studies can be performed by taking advantage of the curation activities described above, which will already have translated the free text information from journal articles into a structured format. The granular curation in CEDAR will allow to distinguish different datasets, such as peptides shown to *i)* bind MHC, *ii)* be naturally processed and presented by MHC, *iii)* be recognized by T cells when provided as a synthetic antigen, and *iv)* be recognized by T cells as part of a tumor cell. Providing separate datasets for separate biological questions makes it easier for tool developers and users to communicate what a specific algorithm was trained and evaluated on.

We plan to extract these datasets focusing on high-quality experimental records and will make them accessible in formats that can be easily parsed with commonly utilized machine learning algorithms and data analysis packages. We plan to add columns containing additional factors that can help in the predictions. For example, based on the tumor type, the expression level of different source antigens can be estimated using National Cancer Institute (NCI) databases such as cBioPortal (19, 42) and the GDC Data Portal (43), even if that expression data is not specifically measured in the original experiments.

Development of Novel Tools to Predict Cancer Epitopes

While most methods for predicting cancer T cell epitopes evolve around MHC binding prediction, which is a necessary step for an epitope to be recognized by T cells, other factors, such as the abundance of the epitope (or its precursors) in the tumor and the availability of a TCR repertoire capable of recognizing the epitope, influence T cell recognition. A thorough assessment of the importance of these different features is required, and CEDAR will provide independent datasets continuously acquired over time through the above-described curation process. Here we describe features that have been considered by multiple investigators as drivers of differential immune recognition (11, 44–49).

We and others have performed analyses correlating measures of the abundance of an MHC ligand with its likelihood to be recognized by T cells (11, 46–48, 50). For cancer epitopes that

arise from a mutation (neoepitopes), the abundance is expected to correlate with the frequency of the mutation in the tumor DNA, as well as with the RNA expression level. Our preliminary analysis of in-house data, as well as data recently published from the NCI (46), showed that the variant allele frequency in the RNA is significantly correlated with neoantigen recognition (**Figure 6**). Thus, including a measure of epitope abundance into machine learning methods is expected to improve cancer epitope prediction. Accordingly, for non-mutated cancer epitopes, the abundance of the associated source antigen, for example as measured by RNA-Seq or proteomic analysis, might improve epitope prediction and will be analyzed in detail.

The TCR repertoire is shaped by both central and peripheral tolerance. Specifically, T cells with receptors binding to self-peptides are expected to undergo apoptosis or adopt a regulatory phenotype. Thus, we and others have hypothesized that peptides with high similarity to host peptides have a lower likelihood to be recognized by T cells (44, 49, 51, 52). For cancer epitopes, the similarity to self-peptides is expected to be of particular relevance, given that - by definition - cancer epitopes are highly similar to host peptides. It will be important to develop metrics of peptide similarity that correlate best with peptide immunogenicity in a cancer epitope setting and determine if they improve the performance of epitope immunogenicity predictions (53). Furthermore, it has been hypothesized that, as TCRs have evolved to be cross-reactive for similar epitopes in order to provide protection from rapidly evolving pathogens (54, 55), cancer epitopes with similarity to pathogen sequences may be more immunogenic, and this similarity may correlate with clinical outcome (56). It was also suggested that neoantigens from driver genes are more likely to be recognized by T cells (46).

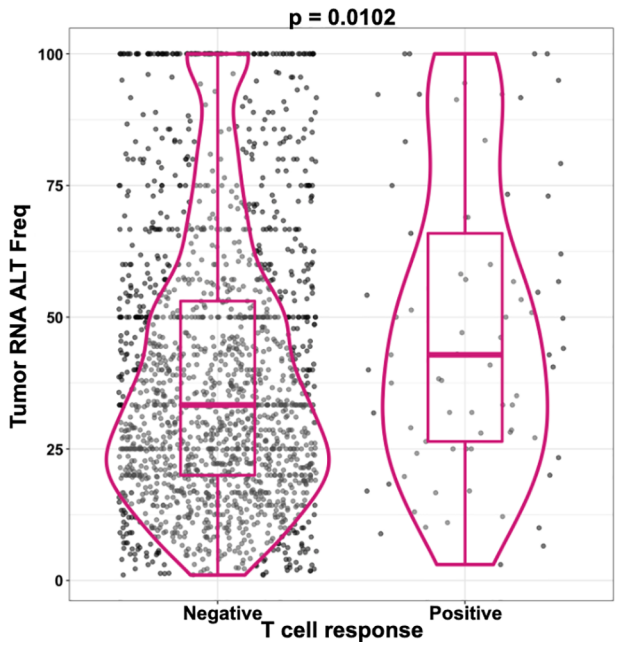

FIGURE 6 | RNA correlation with neoantigen recognition.

As entries in CEDAR will be linked to specialized databases that host such information, we will be able to easily access all information and include it in the training of machine learning methods. The Cancer Genome Atlas (TCGA), the Catalogue Of Somatic Mutations In Cancer (COSMIC) (57), and the Cancer Gene Census (CGC) (57) are all examples of databases that can be utilized to retrieve information about recurrent cancer mutations and whether a mutation is affecting a driver gene or not. Newly generated sets of experimentally validated T cell epitopes that will become available in CEDAR will allow users to assess specific hypotheses, such as mentioned above and *in silico* prediction pipelines in general, that were created and tested on limited datasets.

Using the newly curated datasets from CEDAR, different combinations of features can be included in training machine learning methods to optimize the prediction of epitope recognition (**Figure 7**). The model can be trained to predict any cancer-epitope related outcome, such as cancer epitope recognition *in vitro* or *in vivo activity* (such as tumor regression or experimental model outcomes). With more epitope data becoming available, we will regularly update classifiers and assess whether the data contains additional features (including specificity to TCRs) that might be of relevance for predicting cancer epitopes. We estimate that the size of the training data set made available through the CEDAR curation of approximately 1,770 references will equal at least 50,000 epitopes, based on a comparison of the current epitope count in the IEDB. This data set should be sufficiently large to explore multiple training strategies and features for consideration.

Development of Cancer Epitope Analysis Tools

In our interactions with cancer immunologists and clinicians, it was pointed out that immunoinformatics tools to predict MHC binding and antigen-processing are not user-friendly, as they often require elaborate pre- and post-processing of input and output data to make them applicable in the cancer setting. We identified several recurrent operations involved in analyzing cancer epitopes, and we plan to create analysis tools that allow automation and integration into cancer epitope-specific pipelines.

Determining what neo-peptides are generated by a given mutation, for example, is non-trivial when complex mutations such as frameshifts or splicing variants are involved. We plan to provide tools to generate lists of overlapping n-mers to be included in experiments, given a mutation of interest (e.g., KRAS G12V or chr:12 341234 A<T).

It is also of interest to identify if a given mutation or peptide has already been tested for immunogenicity, and if so, in what context. CEDAR will be interlinked with specialized databases such as TCGA, COSMIC, the CGC, and dbSNP, as mentioned above. We plan to develop tools to retrieve all available information for a given mutation, including if a given peptide has already been described in CEDAR (as a cancer epitope) or the IEDB (e.g., for pathogen-derived epitopes) and whether it is found elsewhere in the host proteome. Another important analysis tool will provide MHC binding predictions for a set of

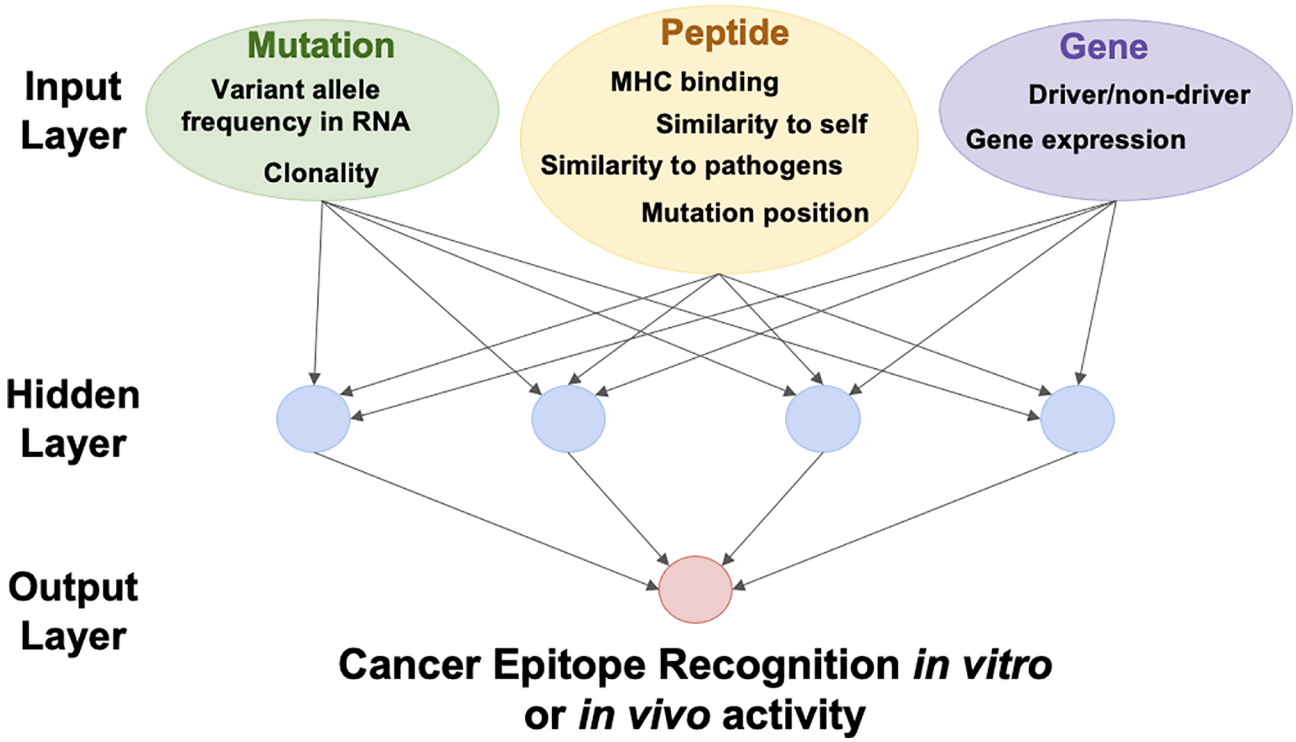

FIGURE 7 | Schematic of an Artificial Neural Network we could implement to learn determinants of Cancer Epitope Recognition.

mutated and associated wildtype sequences in the context of a set of MHC alleles.

Likewise, it is of interest to determine if TCR or BCR sequences have been described before. For CEDAR, all published cancer-specific receptor sequences and their recognized cancer epitopes will be curated. This combined database will provide a comprehensive list of receptor sequences and the epitopes they recognize. We have developed a 'receptor lookup' tool (58), which accepts the TCR β chain CDR3 sequence as an input, and identifies if TCRs with that exact sequence (or a highly similar one) have been previously characterized, and if so, what the previously identified epitope specificity is. This tool was designed to handle large input datasets, such as those generated by TCR repertoire sequencing experiments, and will annotate for each receptor if it has been found before and what epitopes it was previously reported to recognize in both cancer and other disease settings.

DISCUSSION

Here we present our vision and "blueprint" to design and implement the Cancer Epitope Database and Analysis Resource (CEDAR), which will provide a comprehensive collection of cancer epitopes curated from the literature, as well as cancer epitope prediction and analysis tools. CEDAR will leverage our decades of experience from the development of the IEDB, which is fully operational and has been funded since 2003 through a contract from NIAID, with an extension to 2025. The IEDB focuses on allergy, infectious disease, transplantation, and autoimmunity but excludes cancer. Of note, the current **Figures 1–3** reflect the initial prototype based on the direct result of the input received in the initial planning stages by our panel of experts. We however expect that these will evolve over time as the prototypes are implemented and additional feedback is received.

It is now well recognized that understanding the nature of cancer epitopes and their cognate receptors enables us to answer important scientific questions. For example, researchers are examining how the mutation and epitope load in a given tumor relate to the success of checkpoint blockade treatments (4). In addition to this, current research explores epitope-based vaccines and the transfer of epitope-specific T cells and TCRs for use in personalized therapies (4, 5, 59, 60). Epitopes recognized across different individuals provide ideal targets for more cost-effective, off-the-shelf immunotherapies, re-igniting interest in tumor-associated antigens. While mutation-based neoantigens have received considerable attention in recent years, the CEDAR initiative will also curate all data related to cancer-specific but non-mutated antigens, e.g. based on cancer-specific protein expression and processing variations, or cryptic antigens.

This interest is not limited to T cells, as several therapies also take advantage of defined antibodies and BCRs. Moreover, the ability to readily sequence TCRs and BCRs through single-cell sequencing studies of tumor tissues has provided an impetus to

develop tools that facilitate the identification of tumor-specific T cells and B cells in these samples. To address these needs, CEDAR will provide a central, freely accessible catalog of cancer epitope and receptor data linked to the biological, immunological, and clinical contexts in which they were described. The ultimate goal is to come "full circle" and link epitope recognition and immunological readouts to outcomes of disease, treatment, and vaccination. We also aim to use these data to develop and evaluate machine learning-based epitope and TCR/BCR specificity prediction tools for the analysis resource component of CEDAR.

The CEDAR website will initially be developed based on our experience in translational cancer research, as well as feedback obtained from a diverse set of cancer experts. The website will enable intuitive and scientifically accurate cancer-specific queries and reports. This will be implemented by leveraging the existing IEDB database, curation, and query and reporting infrastructure, and expanding it to represent clinical and disease phenotypes beyond what is currently in the IEDB. Additional fields relevant to cancer will be accurately captured, such as different forms and histologies of cancer and associated immunological, biological, and clinical information. Based on our preliminary data, the modifications required in the IEDB infrastructure to enable CEDAR can be implemented in a period of 12 months. Once established, subsequent modifications to CEDAR will be driven by broader community feedback.

Curation of immune epitope data from literature, relevant to cancer immunology, will include B and T cell epitopes associated with cancer antigens, and in particular, naturally processed and presented epitopes recognized in the context of a tumor, such as the ones recognized by tumor-infiltrating lymphocytes. Epitope data gathered in immunotherapy studies, in human clinical trials and animal models, will also be captured along with the sequences of both naturally occurring and engineered cancer epitope-specific TCRs and BCRs.

Data related to cancer-specific HLA ligandomics analysis by mass spectrometry will also be prominently curated and displayed, as well as data demonstrating epitopes' natural presentation on tumor cells. Currently, natural ligand data is already curated in the IEDB, and more than 872,001 eluted ligands are curated and accessible through the IEDB website. These data together with any cancer-specific data will be accessible through both the IEDB and CEDAR webpages.

The granular curation of the data and the flexible query structure of CEDAR will allow the user to extract the data most relevant for different queries. For example data related to natural presentation or recognition of tumor targets is arguably the most important whenever available, whereas recognition of synthetic antigens by T cells has frequently led to false positive results. The flexible query structure of CEDAR will allow to retrieve data related to either natural presentation, recognition of synthetic antigens or both.

CEDAR will curate all cancer epitope data obtained either *in vivo* or *in vitro*. Tumor rejection or tumor control data is one of the measures of activity of cancer epitopes and will be curated as such where available. Indeed, several studies have published data in mouse models and human clinical trials where the ability of individual cancer epitopes has been tested *in vivo* (61–65). Arguably, this is the most significant activity of a cancer epitope. A number of studies also previously reported T cell responses against cancer epitopes *in vitro*, which however did not result in clinical activity when tested *in vivo* (66–68). Furthermore, human studies (69, 70) and mouse studies (71, 72) have highlighted contradictions in the data on neoepitope recognition. As CEDAR will include data from both, *in vitro* and *in vivo* experiments, it will be possible to analyze any correlations between T and B cell responses *in vitro* and associated antitumor efficacy *in vivo*.

To the best of our knowledge, CEDAR would provide the first comprehensive and curated cancer epitope database in which the biological, immunological, and clinical context is captured with high granularity and is retrievable for analysis with ease and accuracy. Currently, none of the available repositories capture comprehensive cancer epitope information with the necessary granularity. CEDAR will provide query and reporting strategies specifically designed to meet the needs of cancer researchers to make cancer epitope data and metadata accessible. These strategies are designed specifically for CEDAR and will be developed in a timely and cost-effective manner, relying on the existing IEDB infrastructure, which is based on over 18 years of work experience and development.

Large efforts have been dedicated to developing novel approaches for improved prediction and/or identification of cancer neoepitopes (1, 41, 52, 56, 73–77). Each of these efforts proposed different features to complement HLA binding prediction to improve the ability of identifying cancer neoepitopes. However, these studies are highly heterogeneous in terms of data generation, validation techniques, and the generality of the obtained conclusions, further challenged by an often very limited sample size. The Tumor Neoantigen Selection Alliance (TESLA) has provided an attempt to address these issues by generating uniform data sets to be used by the community for prediction of neoepitope candidates with subsequent experimental validation (49). The main conclusion from this work was that immunogenic tumor epitopes 'are those tumor peptides that have strong MHC binding affinity and long half-life, are expressed highly and have either low agretopicity or high foreignness' (49).

CEDAR will further this kind of analysis and provide a validated set of cancer epitope prediction and analysis tools. Users will have access to implementations for published tools that currently have no web-accessible versions and, objective and transparent benchmarks of all tools will be performed using literature data that becomes available in CEDAR through ongoing curation efforts. In line with what has been the case for general T cell epitope prediction tools, the availability of comprehensive datasets within the IEDB and benchmarking has been pivotal for the identification of well-performing tools, excluding anecdotal results. Similarly, we expect that these properties of CEDAR will allow users to identify none-dataset specific properties and help move the field of cancer neoepitope prediction forward. Finally, new tools will be developed

based on lessons learned from the benchmarks that include cancer-specific considerations, such as gene expression. Additionally, we aim to provide a tool that will compare the mutant and wildtype sequences in terms of their ability to bind cognate HLA molecules and trigger T cell responses when evaluating immunogenicity.

We will greatly expand the development, hosting, and availability of different strategies to predict the immunogenicity and clinical efficacy of cancer epitopes, as well as their potential as a surrogate marker of positive clinical evolution following cancer treatments. The availability of large, curated cancer epitope datasets, reference implementations of prediction approaches, and clear metrics of success is necessary to inform both the community of tool developers on what makes a tool useful and the community of tool users on which tool to use for their application. Users will be provided with unbiased, objective, and transparent evaluations of different epitope prediction tools side-by-side, with the code being made publicly available. Cross-comparison of prediction approaches on epitope datasets derived from cancer *versus* other diseases (infection, allergy, autoimmunity) will determine if there are predictable features of cancer epitopes that differentiate them from other epitopes.

As the CEDAR data will be hosted side-by-side with IEDB data, the resulting combined dataset will encompass all known epitopes and their TCRs and BCRs, regardless of disease context. This dataset will enable highly innovative analyses, namely the ability to identify TCR and BCR sequences with known (or inferred) epitope specificity from repertoire sequencing data. With the increasing ease of isolating and sequencing TCRs, the identified repertoire can be compared to the continuously growing database of known TCR:epitope:MHC interactions. This will allow identification of TCRs in tumor-associated T cells targeting known neoepitopes or tumor-associated antigens, as well as TCRs targeting viral epitopes (60, 78, 79). Some studies have reported enrichment of TCRs that recognize viral epitopes in TIL that could be cross-reactive, as well as TCRs capable of recognizing unmutated self-peptides expressed in normal tissue (80, 81), which could result in autoimmune side-effects of checkpoint blockade treatments. Ultimately, CEDAR will prove to be a powerful resource for the cancer community and will help advance cancer research and the development of effective cancer therapies.

DATA AVAILABILITY STATEMENT

The original contributions presented in the study are included in the article/supplementary material. Further inquiries can be directed to the corresponding author.

AUTHOR CONTRIBUTIONS

ZK-Y, NB, AS, and BP prepared the manuscript. HC, MN, EZ, DK, JC-G, PR, and SPS reviewed and edited the manuscript. All authors contributed to the article and approved the submitted version.

FUNDING

Research reported in this publication was supported by the National Cancer Institute of the National Institutes of Health under award numbers U24CA248138 and U01DE028227.

REFERENCES

1. Abelin JG, Keskin DB, Sarkizova S, Hartigan CR, Zhang W, Sidney J, et al. Mass Spectrometry Profiling of HLA-Associated Peptidomes in Mono-Allelic Cells Enables More Accurate Epitope Prediction. *Immunity* (2017) 46:315–26. doi: 10.1016/j.immuni.2017.02.007
2. Zamora AE, Crawford JC, Thomas PG. Hitting the Target: How T Cells Detect and Eliminate Tumors. *J Immunol* (2018) 200:392–9. doi: 10.4049/jimmunol.1701413
3. Topalian SL, Drake CG, Pardoll DM. Immune Checkpoint Blockade: A Common Denominator Approach to Cancer Therapy. *Cancer Cell* (2015) 27:450–61. doi: 10.1016/j.ccell.2015.03.001
4. Schumacher TN, Scheper W, Kvistborg P. Cancer Neoantigens. *Annu Rev Immunol* (2019) 37:173–200. doi: 10.1146/annurev-immunol-042617-053402
5. Curran MA, Glisson BS. New Hope for Therapeutic Cancer Vaccines in the Era of Immune Checkpoint Modulation. *Annu Rev Med* (2019) 70:409–24. doi: 10.1146/annurev-med-050217-121900
6. Topalian SL, Taube JM, Pardoll DM. Neoadjuvant Checkpoint Blockade for Cancer Immunotherapy. *Science* (2020) 367(6477):eaax0182. doi: 10.1126/science.aax0182
7. Zhang G, Chitkushev L, Olsen LR, Keskin DB, Brusic V. TANTIGEN 2.0: A Knowledge Base of Tumor T Cell Antigens and Epitopes. *BMC Bioinf* (2021) 22:40. doi: 10.1186/s12859-021-03962-7
8. Xia J, Bai P, Fan W, Li Q, Li Y, Wang D, et al. NEPdb: A Database of T-Cell Experimentally-Validated Neoantigens and Pan-Cancer Predicted Neoepitopes for Cancer Immunotherapy. *Front Immunol* (2021) 12:644637. doi: 10.3389/fimmu.2021.644637
9. Tan X, Li D, Huang P, Jian X, Wan H, Wang G, et al. Dbpepneo: A Manually Curated Database for Human Tumor Neoantigen Peptides. *Database (Oxf)* (2020) 2020:1–8. doi: 10.1093/database/baaa004
10. Vita R, Mahajan S, Overton JA, Dhanda SK, Martini S, Cantrell JR, et al. The Immune Epitope Database (IEDB): 2018 Update. *Nucleic Acids Res* (2019) 47:D339–43. doi: 10.1093/nar/gky1006
11. Gartner JJ, Parkhurst MR, Gros A, Tran E, Jafferji MS, Copeland A, et al. A Machine Learning Model for Ranking Candidate HLA Class I Neoantigens Based on Known Neoepitopes From Multiple Human Tumor Types. *Nat Cancer* (2021) 2:1–12. doi: 10.1038/s43018-021-00197-6
12. Hastings J, Owen G, Dekker A, Ennis M, Kale N, Muthukrishnan V, et al. ChEBI in 2016: Improved Services and an Expanding Collection of Metabolites. *Nucleic Acids Res* (2016) 44:D1214–9. doi: 10.1093/nar/gkv1031
13. Kim S, Chen J, Cheng T, Gindulyte A, He J, He S, et al. PubChem 2019 Update: Improved Access to Chemical Data. *Nucleic Acids Res* (2019) 47:D1102–9. doi: 10.1093/nar/gky1033
14. Smith CC, Selitsky SR, Chai S, Armistead PM, Vincent BG, Serody JS. Alternative Tumour-Specific Antigens. *Nat Rev Cancer* (2019) 19:465–78. doi: 10.1038/s41568-019-0162-4
15. Uhlen M, Fagerberg L, Hallstrom BM, Lindskog C, Oksvold P, Mardinoglu A, et al. Proteomics. Tissue-Based Map of the Human Proteome. *Science* (2015) 347:1260419. doi: 10.1126/science.1260419

16. The Gene Ontology C. The Gene Ontology Resource: 20 Years and Still GOing Strong. *Nucleic Acids Res* (2019) 47:D330–8. doi: 10.1093/nar/gky1055
17. Ashburner M, Ball CA, Blake JA, Botstein D, Butler H, Cherry JM, et al. Gene Ontology: Tool for the Unification of Biology. The Gene Ontology Consortium. *Nat Genet* (2000) 25:25–9. doi: 10.1038/75556
18. Cancer Genome Atlas Research N, Weinstein JN, Collisson EA, Mills GB, Shaw KR, Ozenberger BA, et al. The Cancer Genome Atlas Pan-Cancer Analysis Project. *Nat Genet* (2013) 45:1113–20. doi: 10.1038/ng.2764
19. Cerami E, Gao J, Dogrusoz U, Gross BE, Sumer SO, Aksoy BA, et al. The Cbio Cancer Genomics Portal: An Open Platform for Exploring Multidimensional Cancer Genomics Data. *Cancer Discov* (2012) 2:401–4. doi: 10.1158/2159-8290.CD-12-0095
20. Ghandi M, Huang FW, Jane-Valbuena J, Kryukov GV, Lo CC, McDonald ER3rd, et al. Next-Generation Characterization of the Cancer Cell Line Encyclopedia. *Nature* (2019) 569:503–8. doi: 10.1038/s41586-019-1186-3
21. Reva B, Antipin Y, Sander C. Predicting the Functional Impact of Protein Mutations: Application to Cancer Genomics. *Nucleic Acids Res* (2011) 39: e118. doi: 10.1093/nar/gkr407
22. Tokheim C, Karchin R. CHASMplus Reveals the Scope of Somatic Missense Mutations Driving Human Cancers. *Cell Syst* (2019) 9:9–23.e8. doi: 10.1016/j.cels.2019.05.005
23. Klausen MS, Jespersen MC, Nielsen H, Jensen KK, Jurtz VI, Sonderby CK, et al. NetSurfP-2.0: Improved Prediction of Protein Structural Features by Integrated Deep Learning. *Proteins* (2019) 87:520–7. doi: 10.1002/prot.25674
24. Sigrist CJ, de Castro E, Cerutti L, Cuche BA, Hulo N, Bridge A, et al. New and Continuing Developments at PROSITE. *Nucleic Acids Res* (2013) 41:D344–7. doi: 10.1093/nar/gks1067
25. Wilkinson MD, Dumontier M, Aalbersberg IJ, Appleton G, Axton M, Baak A, et al. The FAIR Guiding Principles for Scientific Data Management and Stewardship. *Sci Data* (2016) 3:160018. doi: 10.1038/sdata.2016.18
26. Vita R, Overton JA, Mungall CJ, Sette A, Peters B. FAIR Principles and the IEDB: Short-Term Improvements and a Long-Term Vision of OBO-Foundry Mediated Machine-Actionable Interoperability. *Database (Oxford)* (2018) 2018. doi: 10.1093/database/bax105
27. Schriml LM, Mitraka E, Munro J, Tauber B, Schor M, Nickle L, et al. Human Disease Ontology 2018 Update: Classification, Content and Workflow Expansion. *Nucleic Acids Res* (2019) 47:D955–62. doi: 10.1093/nar/gky1032
28. Fragoso G, de Coronado S, Haber M, Hartel F, Wright L. Overview and Utilization of the NCI Thesaurus. *Comp Funct Genomics* (2004) 5:648–54. doi: 10.1002/cfg.445
29. Wang P, Morgan AA, Zhang Q, Sette A, Peters B. Automating Document Classification for the Immune Epitope Database. *BMC Bioinf* (2007) 8:269. doi: 10.1186/1471-2105-8-269
30. Vita R, Peters B, Sette A. The Curation Guidelines of the Immune Epitope Database and Analysis Resource. *Cytometry A* (2008) 73:1066–70. doi: 10.1002/cyto.a.20585
31. Davies V, Vaughan K, Damle R, Peters B, Sette A. Classification of the Universe of Immune Epitope Literature: Representation and Knowledge Gaps. *PloS One* (2009) 4:e6948. doi: 10.1371/journal.pone.0006948
32. Vita R, Vaughan K, Zarebski L, Salimi N, Fleri W, Grey H, et al. Curation of Complex, Context-Dependent Immunological Data. *BMC Bioinf* (2006) 7:341. doi: 10.1186/1471-2105-7-341
33. Salimi N, Vita R. The Biocurator: Connecting and Enhancing Scientific Data. *PloS Comput Biol* (2006) 2:e125. doi: 10.1371/journal.pcbi.0020125
34. Fleri W, Vaughan K, Salimi N, Vita R, Peters B, Sette A. The Immune Epitope Database: How Data Are Entered and Retrieved. *J Immunol Res* (2017) 2017:5974574. doi: 10.1155/2017/5974574
35. Mahajan S, Vita R, Shackelford D, Lane J, Schulten V, Zarebski L, et al. Epitope Specific Antibodies and T Cell Receptors in the Immune Epitope Database. *Front Immunol* (2018) 9:2688. doi: 10.3389/fimmu.2018.02688
36. Seymour E, Damle R, Sette A, Peters B. Cost Sensitive Hierarchical Document Classification to Triage PubMed Abstracts for Manual Curation. *BMC Bioinf* (2011) 12:482. doi: 10.1186/1471-2105-12-482
37. IEDB. *Curation Manual 2.0*. (2007). Available at: http://curationwiki.iedb.org/wiki/index.php/Curation_Manual2.0
38. Richters MM, Xia H, Campbell KM, Gillanders WE, Griffith OL, Griffith M. Best Practices for Bioinformatic Characterization of Neoantigens for Clinical Utility. *Genome Med* (2019) 11:56. doi: 10.1186/s13073-019-0666-2
39. Trolle T, Metushi IG, Greenbaum JA, Kim Y, Sidney J, Lund O, et al. Automated Benchmarking of Peptide-MHC Class I Binding Predictions. *Bioinformatics* (2015) 31:2174–81. doi: 10.1093/bioinformatics/btv123
40. Andreatta M, Trolle T, Yan Z, Greenbaum JA, Peters B, Nielsen M. An Automated Benchmarking Platform for MHC Class II Binding Prediction Methods. *Bioinformatics* (2018) 34:1522–8. doi: 10.1093/bioinformatics/btx820
41. Kosaloglu-Yalcin Z, Lanka M, Frentzen A, Logandha Ramamoorthy Premlal A, Sidney J, Vaughan K, et al. Predicting T Cell Recognition of MHC Class I Restricted Neoepitopes. *Oncoimmunology* (2018) 7:e1492508. doi: 10.1080/2162402X.2018.1492508
42. Gao J, Aksoy BA, Dogrusoz U, Dresdner G, Gross B, Sumer SO, et al. Integrative Analysis of Complex Cancer Genomics and Clinical Profiles Using the Cbioportal. *Sci Signal* (2013) 6:pl1. doi: 10.1126/scisignal.2004088
43. Grossman RL, Heath AP, Ferretti V, Varmus HE, Lowy DR, Kibbe WA, et al. Toward a Shared Vision for Cancer Genomic Data. *N Engl J Med* (2016) 375:1109–12. doi: 10.1056/NEJMp1607591
44. Richman LP, Vonderheide RH, Rech AJ. Neoantigen Dissimilarity to the Self-Proteome Predicts Immunogenicity and Response to Immune Checkpoint Blockade. *Cell Syst* (2019) 9:375–82.e4. doi: 10.1016/j.cels.2019.08.009
45. Kim S, Kim HS, Kim E, Lee MG, Shin EC, Paik S, et al. Neopepsee: Accurate Genome-Level Prediction of Neoantigens by Harnessing Sequence and Amino Acid Immunogenicity Information. *Ann Oncol* (2018) 29:1030–6. doi: 10.1093/annonc/mdy022
46. Parkhurst MR, Robbins PF, Tran E, Prickett TD, Gartner JJ, Jia L, et al. Unique Neoantigens Arise From Somatic Mutations in Patients With Gastrointestinal Cancers. *Cancer Discov* (2019) 9:1022–35. doi: 10.1158/2159-8290.CD-18-1494
47. Kreiter S, Vormehr M, van de Roemer N, Diken M, Lower M, Diekmann J, et al. Erratum: Mutant MHC Class II Epitopes Drive Therapeutic Immune Responses to Cancer. *Nature* (2015) 523:370. doi: 10.1038/nature14567
48. Granados DP, Yahyaoui W, Laumont CM, Daouda T, Muratore-Schroeder TL, Cote C, et al. MHC I-Associated Peptides Preferentially Derive From Transcripts Bearing miRNA Response Elements. *Blood* (2012) 119:e181–91. doi: 10.1182/blood-2012-02-412593
49. Wells DK, van Buuren MM, Dang KK, Hubbard-Lucey VM, Sheehan KCF, Campbell KM, et al. Key Parameters of Tumor Epitope Immunogenicity Revealed Through a Consortium Approach Improve Neoantigen Prediction. *Cell* (2020) 183:818–34.e13. doi: 10.1016/j.cell.2020.09.015
50. Sarkizova S, Klaeger S, Le PM, Li LW, Oliveira G, Keshishian H, et al. A Large Peptidome Dataset Improves HLA Class I Epitope Prediction Across Most of the Human Population. *Nat Biotechnol* (2020) 38:199–209. doi: 10.1038/s41587-019-0322-9
51. Bresciani A, Paul S, Schommer N, Dillon MB, Bancroft T, Greenbaum J, et al. T-Cell Recognition Is Shaped by Epitope Sequence Conservation in the Host Proteome and Microbiome. *Immunology* (2016) 148:34–9. doi: 10.1111/imm.12585
52. Bjerregaard AM, Nielsen M, Jurtz V, Barra CM, Hadrup SR, Szallasi Z, et al. An Analysis of Natural T Cell Responses to Predicted Tumor Neoepitopes. *Front Immunol* (2017) 8:1566. doi: 10.3389/fimmu.2017.01566
53. Kim Y, Sidney J, Pinilla C, Sette A, Peters B. Derivation of an Amino Acid Similarity Matrix for Peptide: MHC Binding and Its Application as a Bayesian Prior. *BMC Bioinf* (2009) 10:394. doi: 10.1186/1471-2105-10-394
54. Mason D. A Very High Level of Crossreactivity Is an Essential Feature of the T-Cell Receptor. *Immunol Today* (1998) 19:395–404. doi: 10.1016/S0167-5699(98)01299-7
55. Sioud M. T-Cell Cross-Reactivity may Explain the Large Variation in How Cancer Patients Respond to Checkpoint Inhibitors. *Scand J Immunol* (2018) 87:e12643. doi: 10.1111/sji.12643
56. Luksza M, Riaz N, Makarov V, Balachandran VP, Hellmann MD, Solovyov A, et al. A Neoantigen Fitness Model Predicts Tumour Response to Checkpoint Blockade Immunotherapy. *Nature* (2017) 551:517–20. doi: 10.1038/nature24473

57. Sondka Z, Bamford S, Cole CG, Ward SA, Dunham I, Forbes SA. The COSMIC Cancer Gene Census: Describing Genetic Dysfunction Across All Human Cancers. *Nat Rev Cancer* (2018) 18:696–705. doi: 10.1038/s41568-018-0060-1
58. Chronister WD, Crinklaw A, Mahajan S, Vita R, Kosaloglu-Yalcin Z, Yan Z, et al. TCRMatch: Predicting T-Cell Receptor Specificity Based on Sequence Similarity to Previously Characterized Receptors. *Front Immunol* (2021) 12:640725. doi: 10.3389/fimmu.2021.640725
59. Vormehr M, Tureci O, Sahin U. Harnessing Tumor Mutations for Truly Individualized Cancer Vaccines. *Annu Rev Med* (2019) 70:395–407. doi: 10.1146/annurev-med-042617-101816
60. Guedan S, Ruella M, June CH. Emerging Cellular Therapies for Cancer. *Annu Rev Immunol* (2019) 37:145–71. doi: 10.1146/annurev-immunol-042718-041407
61. Tran E, Turcotte S, Gros A, Robbins PF, Lu YC, Dudley ME, et al. Cancer Immunotherapy Based on Mutation-Specific CD4+ T Cells in a Patient With Epithelial Cancer. *Science* (2014) 344:641–5. doi: 10.1126/science.1251102
62. Carreno BM, Magrini V, Becker-Hapak M, Kaabinejadian S, Hundal J, Petti AA, et al. Cancer Immunotherapy. A Dendritic Cell Vaccine Increases the Breadth and Diversity of Melanoma Neoantigen-Specific T Cells. *Science* (2015) 348:803–8. doi: 10.1126/science.aaa3828
63. Gubin MM, Zhang X, Schuster H, Caron E, Ward JP, Noguchi T, et al. Checkpoint Blockade Cancer Immunotherapy Targets Tumour-Specific Mutant Antigens. *Nature* (2014) 515:577–81. doi: 10.1038/nature13988
64. Hinrichs CS, Rosenberg SA. Exploiting the Curative Potential of Adoptive T-Cell Therapy for Cancer. *Immunol Rev* (2014) 257:56–71. doi: 10.1111/imr.12132
65. Castle JC, Kreiter S, Diekmann J, Lower M, van de Roemer N, de Graaf J, et al. Exploiting the Mutanome for Tumor Vaccination. *Cancer Res* (2012) 72:1081–91. doi: 10.1158/0008-5472.CAN-11-3722
66. Rosenberg SA, Yang JC, Schwartzentruber DJ, Hwu P, Marincola FM, Topalian SL, et al. Immunologic and Therapeutic Evaluation of a Synthetic Peptide Vaccine for the Treatment of Patients With Metastatic Melanoma. *Nat Med* (1998) 4:321–7. doi: 10.1038/nm0398-321
67. Rosato A, Zoso A, Milan G, Macino B, Dalla Santa S, Tosello V, et al. Individual Analysis of Mice Vaccinated Against a Weakly Immunogenic Self Tumor-Specific Antigen Reveals a Correlation Between CD8 T Cell Response and Antitumor Efficacy. *J Immunol* (2003) 171:5172–9. doi: 10.4049/jimmunol.171.10.5172
68. Anichini A, Molla A, Mortarini R, Tragni G, Bersani I, Di Nicola M, et al. An Expanded Peripheral T Cell Population to a Cytotoxic T Lymphocyte (CTL)-Defined, Melanocyte-Specific Antigen in Metastatic Melanoma Patients Impacts on Generation of Peptide-Specific CTLs But Does Not Overcome Tumor Escape From Immune Surveillance in Metastatic Lesions. *J Exp Med* (1999) 190:651–67. doi: 10.1084/jem.190.5.651
69. Ghorani E, Rosenthal R, McGranahan N, Reading JL, Lynch M, Peggs KS, et al. Differential Binding Affinity of Mutated Peptides for MHC Class I Is a Predictor of Survival in Advanced Lung Cancer and Melanoma. *Ann Oncol* (2018) 29:271–9. doi: 10.1093/annonc/mdx687
70. Rech AJ, Balli D, Mantero A, Ishwaran H, Nathanson KL, Stanger BZ, et al. Tumor Immunity and Survival as a Function of Alternative Neopeptides in Human Cancer. *Cancer Immunol Res* (2018) 6:276–87. doi: 10.1158/2326-6066.CIR-17-0559
71. Brennick CA, George MM, Moussa MM, Hagymasi AT, Seesi SA, Shcheglova TV, et al. An Unbiased Approach to Defining Bona Fide Cancer Neoepitopes That Elicit Immune-Mediated Cancer Rejection. *J Clin Invest* (2021) 131(3): e142823. doi: 10.1172/JCI142823
72. Ebrahimi-Nik H, Michaux J, Corwin WL, Keller GL, Shcheglova T, Pak H, et al. Mass Spectrometry Driven Exploration Reveals Nuances of Neoepitope-Driven Tumor Rejection. *JCI Insight* (2019) 5(14):e129152. doi: 10.1172/jci.insight.129152
73. Chen B, Khodadoust MS, Olsson N, Wagar LE, Fast E, Liu CL, et al. Predicting HLA Class II Antigen Presentation Through Integrated Deep Learning. *Nat Biotechnol* (2019) 37:1332–43. doi: 10.1038/s41587-019-0280-2
74. Abelin JG, Harjanto D, Malloy M, Suri P, Colson T, Goulding SP, et al. Defining HLA-II Ligand Processing and Binding Rules With Mass Spectrometry Enhances Cancer Epitope Prediction. *Immunity* (2019) 51:766–79.e17. doi: 10.1016/j.immuni.2019.08.012
75. Bulik-Sullivan B, Busby J, Palmer CD, Davis MJ, Murphy T, Clark A, et al. Deep Learning Using Tumor HLA Peptide Mass Spectrometry Datasets Improves Neoantigen Identification. *Nat Biotechnol* (2018) 37:55–63. doi: 10.1038/nbt.4313
76. Muller M, Gfeller D, Coukos G , Bassani-Sternberg M. 'Hotspots' of Antigen Presentation Revealed by Human Leukocyte Antigen Ligandomics for Neoantigen Prioritization. *Front Immunol* (2017) 8:1367. doi: 10.3389/fimmu.2017.01367
77. Bassani-Sternberg M, Chong C, Guillaume P, Solleder M, Pak H, Gannon PO, et al. Deciphering HLA-I Motifs Across HLA Peptidomes Improves Neo-Antigen Predictions and Identifies Allostery Regulating HLA Specificity. *PloS Comput Biol* (2017) 13:e1005725. doi: 10.1371/journal.pcbi.1005725
78. Cole DK, Bulek AM, Dolton G, Schauenberg AJ, Szomolay B, Rittase W, et al. Hotspot Autoimmune T Cell Receptor Binding Underlies Pathogen and Insulin Peptide Cross-Reactivity. *J Clin Invest* (2016) 126:3626. doi: 10.1172/JCI89919
79. Bethune MT, Joglekar AV. Personalized T Cell-Mediated Cancer Immunotherapy: Progress and Challenges. *Curr Opin Biotechnol* (2017) 48:142–52. doi: 10.1016/j.copbio.2017.03.024
80. Linette GP, Stadtmauer EA, Maus MV, Rapoport AP, Levine BL, Emery L, et al. Cardiovascular Toxicity and Titin Cross-Reactivity of Affinity-Enhanced T Cells in Myeloma and Melanoma. *Blood* (2013) 122:863–71. doi: 10.1182/blood-2013-03-490565
81. Cameron BJ, Gerry AB, Dukes J, Harper JV, Kannan V, Bianchi FC, et al. Identification of a Titin-Derived HLA-A1-Presented Peptide as a Cross-Reactive Target for Engineered MAGE A3-Directed T Cells. *Sci Transl Med* (2013) 5:197ra103. doi: 10.1126/scitranslmed.3006034

Author Disclaimer: The content is solely the responsibility of the authors and does not necessarily represent the official views of the National Institutes of Health.

Conflict of Interest: The authors declare that the research was conducted in the absence of any commercial or financial relationships that could be construed as a potential conflict of interest.

Publisher's Note: All claims expressed in this article are solely those of the authors and do not necessarily represent those of their affiliated organizations, or those of the publisher, the editors and the reviewers. Any product that may be evaluated in this article, or claim that may be made by its manufacturer, is not guaranteed or endorsed by the publisher.

frontiers in Immunology

ORIGINAL RESEARCH
published: 30 August 2021
doi: 10.3389/fimmu.2021.729809

Multi-Epitope-Based Vaccines for Colon Cancer Treatment and Prevention

*Lauren R. Corulli[1], Denise L. Cecil[1], Ekram Gad[1], Marlese Koehnlein[1], Andrew L. Coveler[1], Jennifer S. Childs[1], Ronald A. Lubet[2] and Mary L. Disis[1]**

[1] University of Washington (UW) Medicine, Cancer Vaccine Institute, University of Washington, Seattle, WA, United States, [2] Division of Cancer Prevention, National Cancer Institute, Bethesda, MD, United States

OPEN ACCESS

Edited by:
Olivera J. Finn, University of Pittsburgh, United States

Reviewed by:
Jeffrey Schlom, National Cancer Institute (NCI), United States
Yona Keisari, Tel Aviv University, Israel
Ronit Mazor, United States Food and Drug Administration, United States

***Correspondence:**
Mary L. Disis
ndisis@uw.edu

Specialty section:
This article was submitted to Cancer Immunity and Immunotherapy, a section of the journal Frontiers in Immunology

Received: *23 June 2021*
Accepted: *13 August 2021*
Published: *30 August 2021*

Citation:
Corulli LR, Cecil DL, Gad E, Koehnlein M, Coveler AL, Childs JS, Lubet RA and Disis ML (2021) Multi-Epitope-Based Vaccines for Colon Cancer Treatment and Prevention. Front. Immunol. 12:729809. doi: 10.3389/fimmu.2021.729809

Background: Overexpression of nonmutated proteins involved in oncogenesis is a mechanism by which such proteins become immunogenic. We questioned whether overexpressed colorectal cancer associated proteins found at higher incidence and associated with poor prognosis could be effective vaccine antigens. We explored whether vaccines targeting these proteins could inhibit the development of intestinal tumors in the azoxymethane (AOM)-induced colon model and APC Min mice.

Methods: Humoral immunity was evaluated by ELISA. Web-based algorithms identified putative Class II binding epitopes of the antigens. Peptide and protein specific T-cells were identified from human peripheral blood mononuclear cells using IFN-gamma ELISPOT. Peptides highly homologous between mouse and man were formulated into vaccines and tested for immunogenicity in mice and *in vivo* tumor challenge. Mice treated with AOM and APC Min transgenic mice were vaccinated and monitored for tumors.

Results: Serum IgG for CDC25B, COX2, RCAS1, and FASCIN1 was significantly elevated in colorectal cancer patient sera compared to volunteers (CDC25B p=0.002, COX-2 p=0.001, FASCIN1 and RCAS1 p<0.0001). Epitopes predicted to bind to human class II MHC were identified for each protein and T-cells specific for both the peptides and corresponding recombinant protein were generated from human lymphocytes validating these proteins as human antigens. Some peptides were highly homologous between mouse and humans and after immunization, mice developed both peptide and protein specific IFN-γ-secreting cell responses to CDC25B, COX2 and RCAS1, but not FASCIN1. FVB/nJ mice immunized with CDC25B or COX2 peptides showed significant inhibition of growth of the syngeneic MC38 tumor compared to control (p<0.0001). RCAS1 peptide vaccination showed no anti-tumor effect. In the prophylactic setting, after immunization with CDC25B or COX2 peptides mice treated with AOM developed significantly fewer tumors as compared to controls (p<0.0002) with 50% of mice remaining tumor free in each antigen group. APC Min mice immunized with CDC25B or COX2 peptides developed fewer small bowel tumors as compared to controls (p=0.01 and p=0.02 respectively).

Conclusions: Immunization with CDC25B and COX2 epitopes consistently suppressed tumor development in each model evaluated. These data lay the foundation for the development of multi-antigen vaccines for the treatment and prevention of colorectal cancer.

Keywords: immunotherapy, colon cancer, CDC25B, COX2, IFN-gamma

INTRODUCTION

Active immunization as a colorectal cancer treatment and prevention strategy offers several advantages to classic drug-based approaches. Vaccines are administered over a short period of time without the need for daily dosing. Vaccines that induce tumor trafficking Type I T-cells, including $CD8^+$ T-cells, could be used in combination with immune checkpoint inhibitor therapy to potentially increase clinical responses. Immunologic memory is generated ensuring an adaptive cellular immune response poised to eliminate aberrant cells at the time they arise for prevention of disease recurrence or even primary prevention. Once primed by a vaccine, T-memory cells, are active for years and can be boosted periodically with further vaccinations. In addition, vaccines have been shown to be non-toxic (1).

There have been numerous clinical studies immunizing patients against proteins expressed in the colon with limited to no adverse events. Indeed, a single antigen vaccine targeting MUC-1 has progressed to clinical evaluation in patients with previous high-risk adenomas as a first attempt in colorectal cancer immuno-prevention (2). The vaccine was immunogenic, generating high levels of MUC-1 specific antibodies, and was safe with few reported adverse effects. However, studies in transgenic mouse models have shown that multi-antigen vaccines are significantly more effective in inhibiting the progression of pre-invasive to invasive cancer and preventing clinical disease than single antigen vaccines alone (3).

Vaccines have had remarkable success in preventing cancers of viral origin such as hepatitis B and human papillomavirus, in part because the vaccines targeted proteins that drive oncogenesis. That success is extending to cancer treatment. A human papillomavirus vaccine as a treatment partner with an immune checkpoint inhibitor resulted in increased clinical responses as compared to what would be expected with an immune checkpoint inhibitor alone (4). In order to extrapolate similar success to the prevention of colorectal cancer, we need well-defined, biologically relevant, immunogenic proteins that are important to maintaining the malignant phenotype and can be targeted in a multi-antigen vaccine. To identify colorectal cancer associated antigens, we focused on two major characteristics of the protein candidates. The first was overexpression of the protein in cancer as compared to normal tissues. Aberrant overexpression of a protein in the malignant state is a major mechanism by which that protein becomes immunogenic (5). The second characteristic was the importance of the protein in colorectal cancer growth. This importance could be assessed by the expression of the protein negatively influencing prognosis or that protein having an essential biologic function in colorectal cancer pathogenesis. We identified four candidates based on these and other characteristics described below; CDC25B, COX2, FASCIN1 and RCAS1. CDC25B is overexpressed in over 40% of colorectal cancers and in multivariate analysis is an independent predictor of poor prognosis (risk ratio for death 3.7 as compared to non-expressers) (6). The CDC25B protein phosphatase regulates the cell cycle by activating cyclin-dependent protein kinases (7). In pre-clinical models CDC25 is essential to proliferation of intestinal epithelial stem cells and overexpression could be an early alteration in colorectal cancer pathogenesis (7). COX-2 is overexpressed in a majority of colon cancers and overexpression is also linked with a poor prognosis (8). In a study of over 660 colon cancer cases, COX-2-positive tumors were associated with an increased cancer-specific mortality (multivariate HR, 2.12; 95% CI, 1.23-3.65) (8). In addition, over 50% of adenomatous polyps overexpress the COX-2 protein as compared to adjacent normal tissues (9). Overexpression of COX-2 correlated with increasing adenoma size and an increasing degree of epithelial dysplasia (9). FASCIN1 and RCAS1 have been reported to be overexpressed in 26% of colon adenocarcinomas and 100% of metastatic lymph nodes from colorectal cancer patients respectively (10, 11). Strong diffuse expression of FASCIN1 is associated with a worse prognosis as compared to patients with FASCIN1 negative tumors, p=0.023 (10). RCAS1 expression imparts a poorer prognosis for colon cancer patients and protein expression has been reported to induce apoptosis in tumor infiltrating lymphocytes (12).

Here we describe the antigenicity of these colorectal cancer associated proteins, identify T-cell epitopes suitable for inclusion in a vaccine, and demonstrate how a vaccine with two of the antigens, CDC25B and COX2, consistently reduced tumor development in two mouse models.

MATERIAL AND METHODS

Human Subjects

The colorectal cancer patients (n=50) ranged in age from 31-89 (median age 61), and 50% were female. Stage I (12%), stage II (24%), stage III (24%) and stage V (40%) patient sera were evaluated (purchased from Innovative Research). Volunteer donors (n=50) ranged in age from 23-84 (median age 52.7), and 32% were female (Puget Sound Blood Bank). All donors met criteria for blood donation. Sera were aliquoted and stored

Abbreviations: AOM, Azoxymethane; cSPW, Corrected spots per well; IFN-γ, Interferon-gamma; PBMC, Peripheral blood mononuclear cells; SPW, Spots per well; SEM, Standard error of measurement.

at -80°C until use. For IFN-γ-secreting-cell studies, peripheral blood mononuclear cells (PBMC) were obtained from either a single blood draw of 10 patients with colorectal cancer in remission and at least 30 days from the end of chemotherapy or by leukapheresis from 10 volunteer donors, all after informed consent. Cells were cryopreserved as previously described (13).

Identification of Antigens

We performed a literature search in PubMed with search terms "protein overexpression" and "poor prognosis" and "colorectal cancer", using the following criteria to identify candidate vaccine antigens from the resultant proteins: (1) a greater than 20% incidence of overexpression in colon cancer, (2) a predictor of poor prognosis, and/or (3) a predictor of early disease recurrence, and (4) known biologic function in colon cancer pathogenesis. Four candidate antigens were selected for evaluation: CDC25B, COX2, FASCIN1 and RCAS1.

Evaluation of Antigen-Specific Humoral Immunity

Indirect ELISA was performed as previously described with the following modifications: recombinant proteins CDC25B, COX2, FASCIN1, and RCAS1 (Novus Biologicals) were diluted with carbonate buffer to a concentration of 1 μg/ml (14). Data are presented as antigen specific IgG in μg/ml. A sample was defined as positive when the serum IgG value was greater than the mean and two standard deviations of the control sera (n=50) evaluated for each protein. The cutoff was determined at 0.51 μg/ml for CDC25B, 0.63 μg/ml for COX2, 1.44 μg/ml for FASCIN1, and 2.12 μg/ml for RCAS1. ELISA results were validated by Western Blotting on individual strips of nitrocellulose as previously described with a sensitivity and specificity, respectively of 83% and 83% for CDC25B, 100% and 100% for COX2, 100% and 100% for FASCIN1, and 100% and 100% for RCAS1 (**Supplementary Figure 1**) (14).

Analysis of Peptide and Protein-Specific T-Cell Responses

Peptides predicted to promiscuously bind human MHC II were selected as previously described (15). Briefly, a combined scoring system using three widely available algorithms for predicting class II binding was used for the 15 most common MHC class II alleles (DRB1*0101, DRB1*1501, DRB1*0301, DRB1*0401, DRB1*0404, DRB1*0405, DRB1*0701, DRB1*0802, DRB1*0901, DRB1*1101, DRB1*1201, DRB1*1302, DRB3*0101, DRB4*0101, and DRB5*0101). For each available MHC class II allele, 20 peptide sequences (15-20mer) were initially selected solely based on the rank order of the predicted binding affinity. Scores (S) for each amino acid were summed up across the multiple MHC class II alleles from all three algorithms. The number (N) of MHC class II alleles for which each amino acid was predicted to have high affinity binding was counted. A rank score for each amino acid was defined as S x N. The following three algorithms were used for prediction of class II peptides derived from each protein sequence: SYFPEITHI (Institute for Cell Biology, Heidelberg, Germany), Propred (Institute of Microbial Technology, Chandigarh, India) and Rankpep (Harvard, Boston, MA).

Peptides chosen for evaluation encompassed at least 25% of the predicted high affinity binding regions of each protein and shared >75% homology with mouse (**Supplementary Table 1**). The peptides were synthesized and purified by high-performance liquid chromatography (>95% purity, Genemed Synthesis Inc). Human PBMC were evaluated by ELISPOT for antigen-specific IFN-gamma (γ) as previously described (16, 17). The ELISPOT used 10 μg/ml each of experimental peptide and the negative control peptide HIVp52 as well as 1 μg/ml of the corresponding recombinant protein (Novus Biologicals) and the positive controls of peptide pools for Cytomegalovirus, Epstein-Barr Virus and Influenza Virus (CEF; Anaspec) or tetanus toxoid (List Biological Laboratories). Human peptide T-cell lines were generated as previously described from volunteer donors demonstrating significant IFN-γ responses to the selected epitopes (18). The T-cell lines were assayed *via* IFN-γ ELISPOT using 1 μg/ml experimental recombinant protein (Novus Biologicals) and negative control recombinant protein Cyclin B (US Biologicals) and 10 μg/ml each of experimental peptides and the negative control peptide TRIP13-p104. Data for ELISPOTS are reported as corrected spots/well (cSPW) which is the mean number of spots for each experimental antigen minus the mean number of spots detected in no antigen control wells ± SEM.

Mouse splenic cells were evaluated by ELISPOT for antigen-specific IFN-γ secretion as published, except for the following modifications; splenic cells were incubated with antigens for 72 hours and spots were developed with the AEC substrate kit (BD Biosciences) (17). Data are reported as cSPW for individual antigens.

Animal Models and Cell Line

Animal care and use were in accordance with institutional guidelines. APC Min [Strain name: C57BL/6J-ApcMin/J] males, C57BL6/J females, and FVB/nJ mice were purchased from Jackson Laboratory and allowed to acclimate for one week before treatment. The offspring from mated APC Min males and C57BL6/J females were genotyped by PCR for the presence of the Min mutation using primers as follows: Wild-Type: 5'-GCCATCCCTTCACGTTAG-3', Common: 5'-TTCC ACTTTGGCATAAGGC-3', Mutant: 5'-TCCTGAGAAAG ACAGAAGTTA-3'. Both male and female mice testing positive for the Min mutation were included in the study and randomized into treatment groups. For the AOM model, FVB/nJ mice were treated with 10 mg/kg of AOM (Sigma-Aldrich) twice a week *via* intraperitoneal (ip) injection for six weeks (19). A power analysis determined that 4 to 8 mice/group would achieve a power of at least 93.8% to detect difference between groups. The mouse colon cancer cell line derived from an AOM induced tumor (kindly provided by Dr. David Threadgill), MC38, was validated by IDEXX testing.

Vaccination and Assessment of Tumor Growth

FVB/nJ, C57BL6/J or APC Min offspring were immunized subcutaneously at 6 ± 2 weeks of age with 50 μg each peptide in a pool per antigen with equal volume of adjuvant, PBS alone, or adjuvant alone. Complete Freund's Adjuvant was used in the first immunization, followed by Incomplete Freund's Adjuvant (Sigma-Aldrich) for subsequent immunizations for a total of three immunizations two weeks apart. Peptide vaccine boosters were given at 15-16 and 21-22 weeks of age. AOM treatments began two weeks after the final vaccine and mice were sacrificed at 26 weeks of age. APC Min mice were sacrificed at 16 ± 2 weeks. The entire colon from the AOM model or entire small intestine from APC Min mice were removed at sacrifice and cut longitudinally with dissection scissors. Fecal matter was washed off then tissues were fixed in formalin for a minimum of 24 hours. Intestinal tracts were removed from formalin and tumors were counted under a Nikon SMZ645 microscope by the same operator for each experiment.

For the tumor implant model, $4x10^4$ MC38 cells were implanted subcutaneously in C57BL6/J mice 2 weeks after the final vaccine. Mice were monitored for tumor growth every 2-3 days using Vernier calipers as previously described (20). Mice were sacrificed upon reaching a cumulative tumor volume of $1200mm^3$ or if tumors developed ulcers. Depletion of $CD4^+$ and $CD8^+$ T-cells was performed as published (15). Briefly, 100 μg anti-CD8 or 250 μg anti-CD4 monoclonal antibodies (UCSF) were injected i.p for 3 consecutive days before the first vaccine. The treatment was repeated twice weekly until termination of the study. This regimen resulted in >95% CD4+ or CD8+ T-cell depletion. Tumor growth for all experiments is reported as mean (± SEM) tumor volume (mm^3) (15).

Immunohistochemistry

Immunohistochemistry was performed on colon tumors from the AOM model as previously described (20). Briefly, the fixed sections cut from frozen blocks were blocked with 10% goat serum (Vector Labs) for 1 hour at room temperature then incubated overnight with rat-anti-mouse CD8 (clone KT15; 1:100; AbD Serotec) or rat-anti-mouse CD4 (clone 4SM95; 5 μg/ml; eBioscience). After extensive washing, the slides were incubated with Alexa Fluor 488 goat-anti-rat (Abcam; 1:500) for 1 hour at room temperature. Cover slips were mounted with Prolong Gold antifade with DAPI (Life technologies). Positive cells and DAPI stained nuclei were counted in three random high-powered fields per slide and expressed as a mean percent of positive stained cells of total cell counted.

Statistical Analysis

Model assumptions were checked using the Shapiro-Wilk normality test and by visual inspection of residual and fitted value plots. The unpaired, two-tailed Student's t-test and ANOVA test was used to evaluate differences when normality was confirmed. When normality of the data was not confirmed, the non-parametric Kruskal-Wallis and Man-Whitney tests were used. Differences in tumor volume was determined by two-way ANOVA with a Dunnett post-test for multiple comparisons. A p value of <0.05 was considered significant (GraphPad Software, Prism v.8).

RESULTS

CDC25B, COX2, FASCIN1, and RCAS1 Are Colon Cancer Antigens

To determine whether the chosen proteins were immunogenic, we evaluated whether a humoral immune response could be detected. IgG antibodies were detected at higher magnitude in colon cancer patients as compared to controls for all proteins. Significantly higher levels of CDC25B-specific IgG antibodies were observed in patients with colorectal cancer (median, 0.28 μg/ml; range, 0.01-3.34 μg/ml) as compared to volunteer donors (median, 0.20 μg/ml; range, 0.1-0.61 μg/ml; p=0.041; **Figure 1A**). Thirty-six percent of colorectal cancer patients and eight percent of volunteer donors were seropositive for this antigen. Serum COX2 IgG was significantly elevated in the patients (median, 0.447 μg/ml; range, 0-2.97 μg/ml) compared to the control (median, 0.21 μg/ml; range, 0.10-0.87 μg/ml p=0.023; **Figure 1B**). Forty-two percent of colorectal cancer patients and six percent of volunteer donors were seropositive for this antigen. FASCIN1-specific IgG levels were greater in colorectal cancer sera (median, 1.55μg/ml; range, 0-16.88 μg/ml) compared to control donor sera (median, 0.42μg/ml; range; 0.01-1.81 μg/ml; p=0.008; **Figure 1C**). Fifty percent of colorectal cancer patients and six percent of volunteer donors were seropositive for this antigen. Greater RCAS1-specific serum IgG was detected in patients (median, 3.11μg/ml; range, 0.03-13.07) as compared to the control (median, 0.39μg/ml; range, 0.01-2.03 μg/ml; p<0.001; **Figure 1D**). Sixty-two percent of colorectal cancer patients and no volunteer donors were seropositive for this antigen. Increased levels of IgG was positively correlated with increased stage of colorectal cancer for FASCIN1 (p=0.04) and RCAS1 (p=0.008) and no correlation was associated with CDC25B or COX2. Only increased FASCIN1-specific IgG levels in colorectal cancer was negatively correlated with the age of the donor (p=0.006). Both CDC25B-specific and COX2-specific IgG levels were higher in males than females (p=0.009 and p=0.010, respectively) whereas no difference between males and females were observed for FASCIN1 and RCAS.

IFN-γ-Secreting Cells Specific for Both Peptide and Protein Antigens Can Be Identified in the Peripheral Blood of Colorectal Cancer Patients

We evaluated 13 putative class II epitopes derived from CDC25B, COX2, FASCIN1, and RCAS1 and corresponding recombinant protein for IFN-γ secretion using PBMC derived from colorectal cancer patients and volunteer donors (**Supplementary Table 1**). Significant IFN-γ secretion was observed in colorectal cancer patients after stimulation with the majority of epitopes (**Figure 2A**). The CDC25B recombinant protein (mean, 138 ± 35 corrected spots

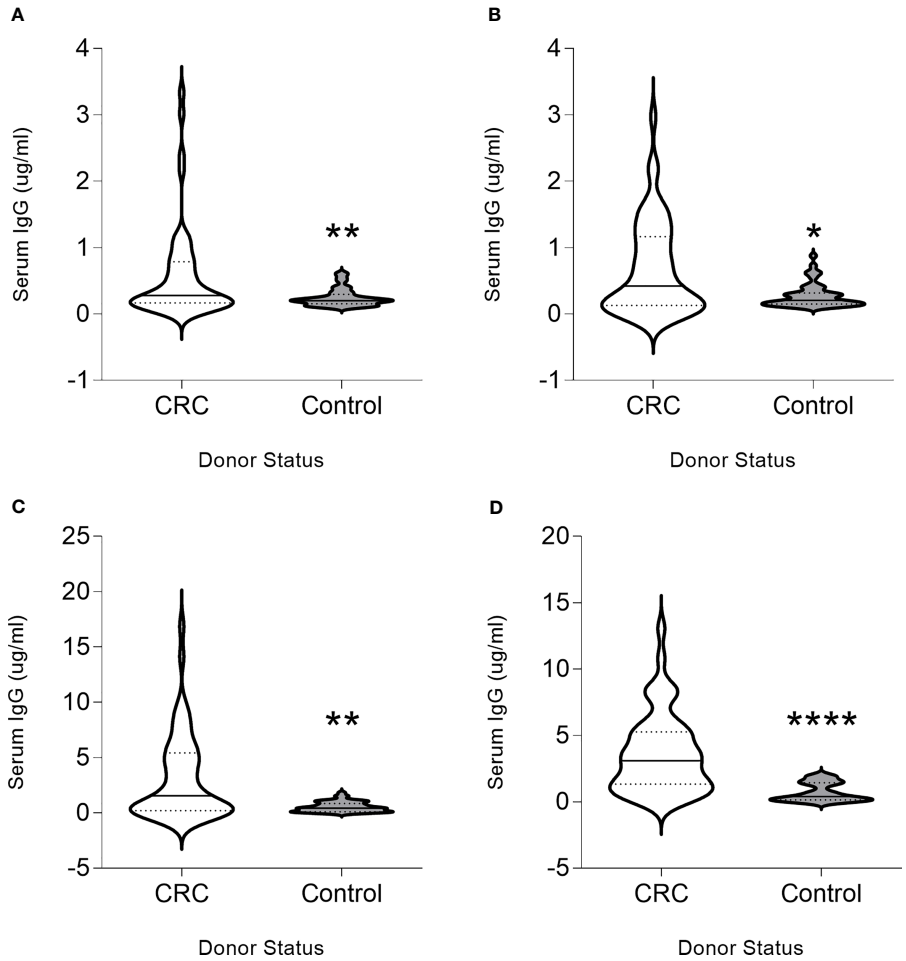

FIGURE 1 | CDC25B, COX2, FASCIN1 and RCAS1 are colon cancer antigens. Serum IgG (μg/ml) from donors with colorectal cancer (CRC) or volunteer controls (control) for **(A)** CDC25B, **(B)** COX2, **(C)** FASCIN1 and **(D)** RCAS1 presented as violin plots, solid line at median and dotted lines at quartiles. *p < 0.05, **p < 0.01, ****p < 0.0001.

per well (CSPW), p=0.042), and peptides CDC25B-p130 (median, 112 CSPW; range 10-278 CSPW, p=0.035) and CDC25B-p405 (mean, 152 ± 35 CSPW, p=0.021; **Figure 2A**) induced higher IFN-γ secretion as compared to an irrelevant peptide negative control (HIVp52). COX-2-derived epitopes p81 (mean, 150 ± 36 CSPW, p=0.026), p279 (mean, 135 ± 33 CSPW, p=0.040), and p538 (median, 114 CSPW; range 3-322 CSPW, p=0.019) as well as the recombinant protein (mean, 171 ± 44 CSPW, p=0.002; **Figure 2A**) induced a greater IFN-γ response than the negative control. Only recombinant FASCIN1 protein (mean, 144 ± 29 CSPW, p=0.018), FASCIN1-p21 (mean, 142 ± 35 CSPW, p=0.035) and FASCIN1-p374 (mean, 158 ± 44 CSPW, p=0.036; **Figure 2A**) induced significant IFN-γ secretion in colorectal cancer PBMC. IFN-γ secretion was significantly increased when PBMC were stimulated with the RCAS1 recombinant protein (mean, 277 ± 42 CSPW, p=0.005) and peptides RCAS1-p8 (mean, 184 ± 50 CSPW, p=0.022), RCAS1-p91 (median, 372; range, 5-458 CSPW, p<0.0001), RCAS1-p126 (mean, 172 ± 43 CSPW, p=0.019) and RCAS1-p161 (mean, 170 ± 46 CSPW, p=0.025; **Figure 2A**) as compared to the negative control.

There was no significant difference observed when the median response of the volunteer cohort for each peptide was compared to the median HIVp52 response, (p>0.05 for all epitopes and recombinant protein; **Figure 2B**). There were individual volunteer donors who demonstrated IFN-γ responses to some of the identified epitopes and proteins (**Figure 2B**) and those positive responses were no different from the responses observed in colorectal cancer patients (p>0.05 for all). Donor PBMC from volunteer donors found to demonstrate significant IFN-γ secretion to the antigens were used to generate peptide specific T-cell lines which also responded to the corresponding recombinant protein (**Supplementary Figure 2**).

IFN-γ Inducing Peptide-Based Vaccines Derived From CDC25B and COX2 Inhibit the Growth of MC38 *In Vivo*

The T-cell epitopes were highly homologous between mouse and human (median 96% (range 78-100); **Supplementary Table 1**). We immunized C57BL6/J mice with the identified epitopes to

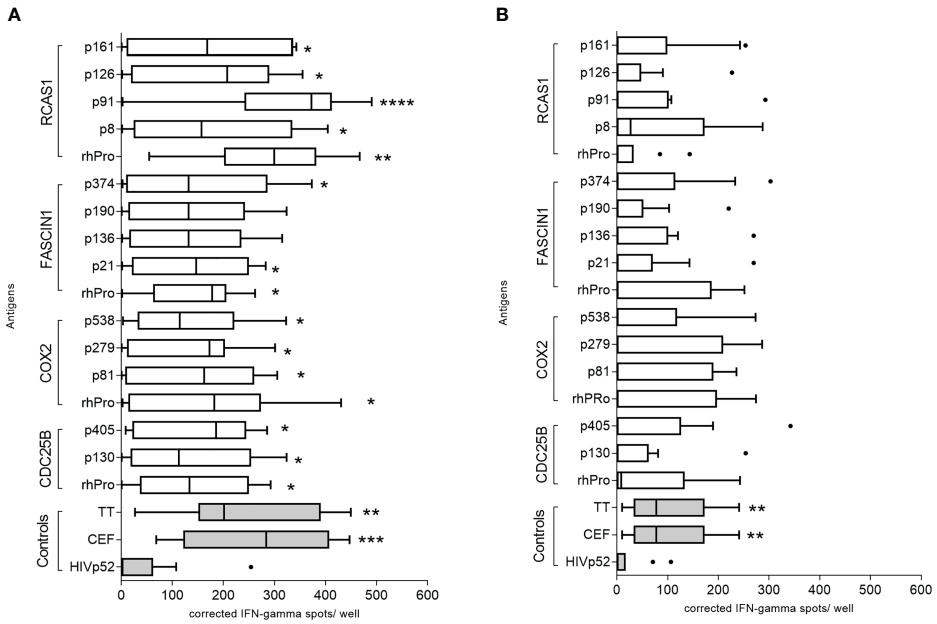

FIGURE 2 | IFN-γ-secreting cells specific for both peptide and protein antigens can be identified in the peripheral blood of colorectal cancer patients. Corrected spots per well for **(A)** colorectal cancer patient or **(B)** volunteer donor PBMC stimulated with recombinant protein and individual peptides, presented as a box and whisker plots, horizontal line at median and Tukey outliers (filled circles). Negative control: HIVp52-66 and positive controls: pool of overlapping viral epitopes (CEF) and tetanus toxoid (TT). rhPro: recombinant human protein for that antigen set. *p < 0.05, ***p < 0.001, ****p < 0.0001 compared to the negative control. n = 10 colorectal cancer patients and 10 volunteer donors.

determine whether we could generate peptide and protein specific T-cells in preparation for *in vivo* tumor challenge. Immunization induced a significant IFN-γ immune response for peptides derived from CDC25B, COX2, and RCAS1 and the corresponding protein (p<0.001 for all **Supplementary Figures 3A, B, D** respectively). However, neither the FASCIN1 peptide nor recombinant protein generated an IFN-γ response in FASCIN1 peptide-vaccinated mice, thus, FASCIN1 was not evaluated further for anti-tumor activity (**Supplementary Figure 3C**).

C57BL6/J mice were immunized with multi-peptide vaccines derived from each antigen; CDC25B, COX2, and RCAS1. Only the CDC25B and COX2 significantly inhibited tumor growth. The mean tumor volume at the termination of the study from mice receiving the CDC25B (365 ± 165 mm^3; **Figure 3A**) or COX2 multi-peptide vaccine (211 ± 106 mm^3; **Figure 3B**) was significantly reduced as compared to the control (883 ± 481 mm^3; p<0.001 for both). However, the mean tumor volume of mice receiving the RCAS1 multi-peptide vaccine (656 ± 189 mm^3) was no different than the volume observed in control mice (775 ± 214 mm^3; p=0.713; **Figure 3C**). Since the RCAS1 vaccine did not demonstrate anti-tumor activity the vaccine was not evaluated further in the experiments described below.

To determine which T-cell subset mediated the antitumor effect, we studied the *in vivo* response to the multi-peptide

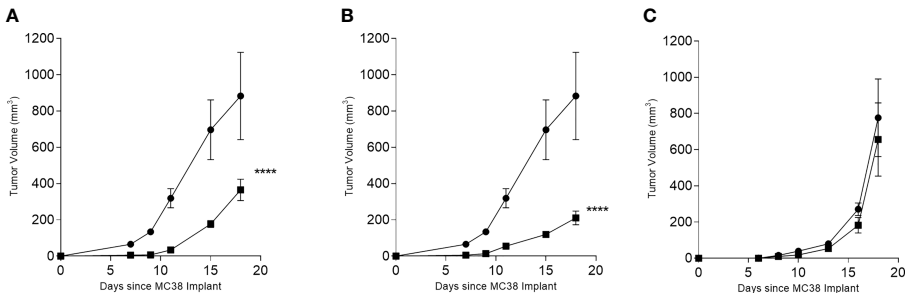

FIGURE 3 | INF-γ-inducing peptide-based vaccines derived from CDC25B or COX2 inhibit the growth of MC38 *in vivo*. Mean (± SEM) tumor volume (mm^3) in multi-peptide immunized mice (■) or PBS immunized mice (●) for **(A)** CDC25B peptide mix, **(B)** COX2 peptide mix and **(C)** RCAS1 peptide mix. ****p < 0.0001, n = 4-8 mice/group.

vaccines for COX2 and CDC25B in more detail. As expected, we observed significant MC38 tumor inhibition in mice immunized with the CDC25B ($p<0.001$; **Figure 4A**) or COX2 ($p=0.043$; **Figure 4B**) vaccine and treated with a control IgG. Treatment with anti-CD4 did not affect tumor inhibition and tumor volumes were similar to vaccine alone ($p>0.49$ for all). Depletion of $CD8^+$ T-cells, however, abrogated the anti-tumor effect of either vaccine and tumor growth was no different from controls ($p=0.858$ for CDC25B and $p=0.087$ for COX2).

Multi-Peptide Vaccination With Epitopes Derived From CDC25B or COX2 Prevents the Development of Tumors in Both the Colon And Small Intestine

We evaluated whether vaccination with epitopes from either CDC25B or COX2 could inhibit lesions in a spontaneous tumor model. As the vaccines had shown anti-tumor efficacy against MC38, we first evaluated efficacy in the AOM model. Mice immunized with CDC25B (mean, 1.1 ± 1.4 tumors) or COX2 peptides (mean, 1.4 ± 1.8 tumors) developed significantly fewer colon tumors as compared to the control (mean, 6.3 ± 2.8 tumors $p<0.0001$ for all; **Figure 5A**). Indeed, 50% of vaccinated mice in each group had no evidence of any lesions at the time of sacrifice.

We examined the phenotype of the tumor infiltrating T-cells in lesions that persisted after vaccination and observed that $CD8^+$ T-cell levels were increased by 10-fold in tumors when the mice were immunized with the CDC25B peptide vaccine and by 16-fold after immunization with the COX2 peptide vaccine as compared to the control ($p<0.001$; **Figure 5B** and **Supplementary Figure 4**). The levels of $CD4^+$ T-cells infiltrating the tumor were low and no different than levels observed in the control for mice immunized with CDC25B or COX2 peptides ($p>0.55$ for both; **Figure 5C** and **Supplementary Figure 4**).

We also examined whether the vaccine would inhibit the development of intestinal polyps in APC Min mice, which have a mutation in the APC gene. Mice immunized with CDC25B (mean, 53.4 ± 23.5 tumors) or COX2 peptides (50.3 ± 18.1 tumors) developed significantly fewer small bowel tumors as compared to control mice (mean, 87.5 ± 25.7 tumors; $p<0.021$ for all; **Figure 5D**).

DISCUSSION

Progress in the clinical translation of colon cancer vaccines would benefit from the identification of antigens suitable for immunization. Colorectal cancer is associated with a low mutation rate; therefore, neo-antigens do not play a major role in the immune modulation of most colorectal cancer subtypes (21). Many colorectal cancers associated immunogenic proteins are nonmutated and overexpressed in the tumor. Data presented here demonstrate that (1) patients with colorectal cancer can develop significant immune responses to nonmutated proteins that are important in driving the biology of the disease, (2) multi-epitope vaccines designed to elicit tumor specific $CD4^+$ T-cells have potent anti-tumor activity, and (3) vaccines targeting colon cancer associated antigens can have prophylactic efficacy in spontaneous intestinal tumor models.

Epitopes predicted to bind human class II molecules could be identified for each of the antigens and the peptide specific T-cells generated recognize and respond to protein presented by autologous antigen presenting cells. Vaccines designed to stimulate tumor antigen specific T-cells, particularly those which elicit IFN-γ, uniquely modulate the tumor microenvironment. Tumor trafficking IFN-γ-secreting T-cells activate local antigen presenting cells and enhance cross-priming of tumor proteins resulting in a broadening of the immune response to additional antigens in the lesion (22). Cytokines, such as IFN- γ, promote the proliferation and recruitment of $CD8^+$ T-cells into the tumor. IFN-γ can reverse functional defects in antigen presentation, including increasing upregulation of MHC I and allowing innate immune cells to more effectively present antigen to cytotoxic T-cells (23). The role of $CD8^+$ T-cells in tumor eradication has been reported for other epitope-based IFN-γ-stimulating vaccines. The anti-tumor effect of peptide immunization targeting IGFBP-2 in mice

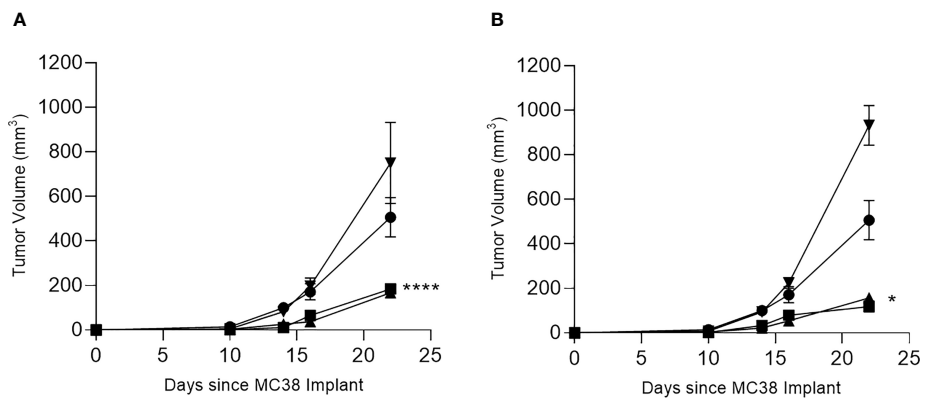

FIGURE 4 | The anti-tumor efficacy of vaccination is dependent on $CD8^+$ T cells. Mean (± SEM) tumor volume (mm^3) from mice immunized with PBS (●) or with **(A)** CDC25B peptides or **(B)** COX2 peptides and treated with control IgG (■), anti-CD8 (▼) or anti-CD4 (▲). *$p < 0.05$, ****$p < 0.0001$; n = 5 mice/group.

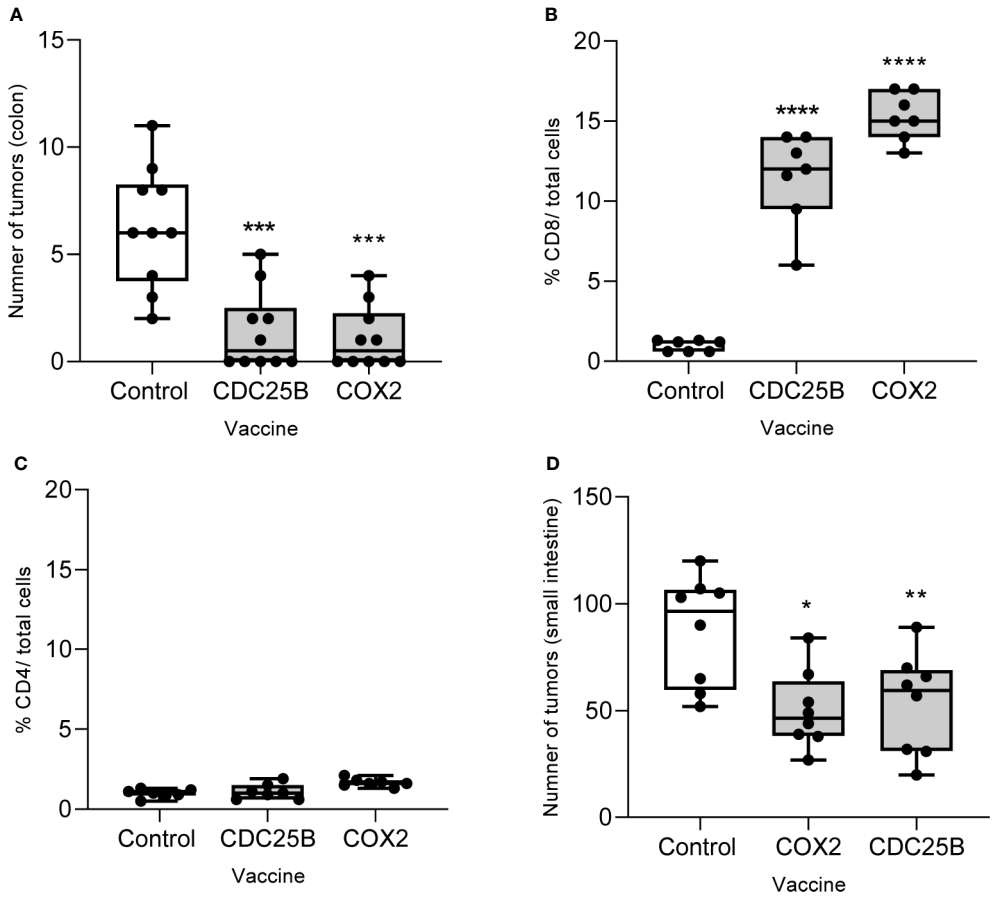

FIGURE 5 | Multi-peptide vaccination with epitopes derived from CDC25B or COX2 prevents the development of tumors in both the colon and small intestine. **(A)** The number of tumors in the colon from AOM-treated mice immunized with the indicated vaccine; n = 10/group. Percent of **(B)** $CD8^+$ or **(C)** $CD4^+$ T cells out of total cells quantified by immunohistochemistry on tumors collected from AOM-treated mice after immunization with the indicated vaccine. n = 7/group. **(D)** Number of tumors in the small bowel after APC-min mice were immunized with the indicated vaccine; n = 8/group. All data are presented as box and whisker plots, horizontal line at median and whiskers min to max; *p < 0.05, **p < 0.01, ***p < 0.001, ****p < 0.0001.

challenged with a mammary cancer cell line was also dependent on $CD8^+$ T-cells (15). These data underscore that vaccines designed to elicit IFN-γ-secreting T-cells have a broader immunologic impact than just increasing tumor-specific effector T-cells in the peripheral blood.

Both CDC25B and COX-2 can be expressed in high risk polyps that may progress to carcinomas, so we evaluated vaccination in two spontaneous tumor models for disease prophylaxis; AOM induced colon cancer and intestinal polyp formation in APC Min mice. Tumors caused by AOM are frequent in the distal part of the colon, resembling the location of spontaneous colorectal cancers in humans (24). The APC Min mouse has phenotypic and genetic similarities to human familial adenomatous polyposis although the numerous adenomas that develop in the animal are mainly located in the small intestine. The adaptive immune infiltrate in polyps consists of predominantly T-regulatory and Th17 cells (25). Immunization with either CDC25B or COX-2 epitopes could inhibit and even prevent tumor growth. Further, $CD8^+$ tumor infiltrating T-cells were significantly induced with vaccination. In a recent meta-analysis of tumors derived from over 20,000 colorectal cancer patients, an increased number of $CD8^+$ tumor infiltrating lymphocytes was associated with an improved cancer specific and overall survival (26). Vaccines, such as ours, that can elicit $CD8^+$ tumor infiltrating lymphocytes could potentially have clinical benefit for the treatment and prevention of colon cancer.

One concern in immunizing non-cancer bearing individuals with vaccines targeting non-mutated proteins is the potential for the development of autoimmune disease. There are many reports of T-cells directed against non-mutated tumor antigens being identified in the peripheral blood of not only cancer patients, but also non-cancer bearing individuals. Both $CD4^+$ and $CD8^+$ T-cells specific for PRAME, a melanoma antigen, could be expanded from the peripheral blood of healthy donors (27). The expanded T-cell lines demonstrated anti-tumor activity *in vitro*. T-cells specific for multiple cyclin B1 specific CD4 T-cell epitopes could be expanded from both cancer patients and volunteer donors (28). One study, using tetramers directed against class II epitopes, identified T-cells specific for

tyrosinase and NY-ESO in the peripheral blood of most healthy individuals evaluated (29). An investigation of multiple antigens in 114 blood donors found T-cells of both low and high avidity against WT-1 (15%), MUC1 (14%), PRAME (15%) and HER2 (5%) (30). Investigators hypothesized that the presence of these cells could be related to gonadal-testis expression and pregnancy. Several elegant studies have shown that clonal deletion in the thymus may eliminate some self-reactive T-cells, but many more remain in the periphery and are under the control of peripheral tolerance (31). These self-epitopes were not presented by thymic antigen presenting cells. Indeed, investigations have shown that self-peptide specific T-cells in the blood of healthy individuals are found at frequencies similar to non-self-peptides (32). Presumably, this large self-reactive T-cell pool would prevent holes in the T-cell repertoire that pathogens could exploit (32). The large self-reactive T-cell pool provides a memory population to exploit for cancer vaccines, albeit mechanisms of peripheral tolerance must be overcome.

There is a long history of immunizing cancer patients, in the therapeutic setting, with vaccines directed against such antigens. Investigators evaluated the toxicity profile of vaccines tested in over 200 phase I clinical trials. In the 4,942 patients assessed, the rate of greater than Grade 3 adverse events was 1.25 events per 100 patients (1). While the low adverse event rate associated with vaccines targeting non-mutated cancer related proteins is encouraging, as studies move into the prophylactic setting close monitoring for autoimmune symptomology must be considered.

Colorectal cancer is one of the most common solid tumors impacting patients and even those with early stage disease have a risk of relapse after optimal treatment. Vaccines directed against proteins maintaining the malignant phenotype have the potential to limit recurrence or even the development of disease. Studies in pre-clinical models have shown that multiple antigen cancer vaccines are more clinically effective than immunizing with a single antigens alone (3). Work described here provides proof of principle that multiple nonmutated tumor antigens can be identified for use in a vaccine for colorectal cancer therapy and prevention.

DATA AVAILABILITY STATEMENT

The raw data supporting the conclusions of this article will be made available by the authors, without undue reservation.

ETHICS STATEMENT

The studies involving human participants were reviewed and approved by University of Washington Human Subjects Division. The patients/participants provided their written informed consent to participate in this study. The animal study was reviewed and approved by University of Washington Animal Care and Use Committee.

AUTHOR CONTRIBUTIONS

MD and RL contributed to conception and design of the study. LC, EG, and MK performed the *in vivo* and *in vitro* experiments. LC performed the statistical analyses. DC wrote the first draft of the manuscript. All authors contributed to the article and approved the submitted version.

FUNDING

NCI contract HHSN261200433001C and the Fundación Lograng. MLD is supported by the Helen B. Slonaker Endowed Professor for Cancer Research and an American Cancer Society Clinical Professorship (CRP-15-106-01-LIB).

ACKNOWLEDGMENTS

We respectfully acknowledge Dr. Elizabeth Broussard and the late Dr. Juan Pablo Marquez for significant work contributed to this manuscript.

SUPPLEMENTARY MATERIAL

The Supplementary Material for this article can be found online at: https://www.frontiersin.org/articles/10.3389/fimmu.2021.729809/full#supplementary-material

Supplementary Table 1 | Predicted MHC Class II binding epitopes. Orange highlighted epitopes were validated as responding to protein.

Supplementary Figure 1 | Example Western blot validation of IgG antibody response to colorectal cancer antigens. **(A)** CDC25B; 62kD **(B)** COX2; 115kD **(C)** FASCIN1; 60 kD and **(D)** RCAS1; 50kD. (I) polyclonal antibody specific for the antigen, (II) a representative ELISA positive patient sample, (III) an ELISA negative subject sample. Molecular weight protein marker (far left).

Supplementary Figure 2 | Epitope-specific cells respond to naturally processed protein. IFN-γ ELISPOT cSPW (corrected spots per well) for **(A)** CDC25B-p130-specific T-cells, **(B)** CDC25B-p405specific T-cells, **(C)** COX2-p81-specific T-cells, **(D)** COX2-p279-specific T-cells, **(E)** COX2-p538-specific T-cells, **(F)** Fascin-p384 specific T-cells, **(G)** RCAS1-p8-specific T-cells and **(H)** RCAS1-p91-specific T-cells stimulated with the expansion peptide or corresponding recombinant protein. TRIP13-p141 and recombinant Cyclin B are used as negative peptide and protein controls, respectively; ****$p < 0.0001$, ***$p < 0.001$, **$p < 0.01$, *$p < 0.05$.

Supplementary Figure 3 | CDC25B, COX2, RCAS1, but not FASCIN1 peptides and protein elicit an IFN-γ response in mice. Mean (±SEM) IFN-γ corrected spots per well (cSPW) when splenocytes were stimulated with the indicated antigen after vaccination with peptides derived from **(A)** CDC25B, **(B)** COX2 **(C)** FASCIN1, and **(D)** RCAS1. *$p < 0.05$, ***$p < 0.001$ as compared to the negative control HIVp52 peptide.

Supplementary Figure 4 | Representative immunohistochemistry for CD8 and CD4 on tumors collected from the colon after immunization with the indicated vaccine. Positive T-cells are stained green and all cells are stained blue.

REFERENCES

1. Rahma OE, Gammoh E, Simon R, Khleif SN. Is the "3+3" Dose Escalation Phase 1 Clinical Trial Design Suitable for Therapeutic Cancer Vaccine Development? A Recommendation for Alternative Design. *Clin Cancer Res* (2014) 20(18):4758–67. doi: 10.1158/1078-0432.CCR-13-2671
2. Kimura T, McKolanis JR, Dzubinski LA, Islam K, Potter DM, Salazar AM, et al. MUC1 Vaccine for Individuals With Advanced Adenoma of the Colon: A Cancer Immunoprevention Feasibility Study. *Cancer Prev Res (Phila)* (2013) 6:18–26. doi: 10.1158/1940-6207.CAPR-12-0275
3. Disis ML, Gad E, Herendeen DR, Lai VP, Park KH, Cecil DL, et al. A Multiantigen Vaccine Targeting Neu, IGFBP-2, and IGF-IR Prevents Tumor Progression in Mice With Preinvasive Breast Disease. *Cancer Prev Res (Phila)* (2013) 6:1273–82. doi: 10.1158/1940-6207.CAPR-13-0182
4. Youn JW, Hur SY, Woo JW, Kim YM, Lim MC, Park SY, et al. Pembrolizumab Plus GX-188E Therapeutic DNA Vaccine in Patients With HPV-16-Positive or HPV-18-Positive Advanced Cervical Cancer: Interim Results of a Single-Arm, Phase 2 Trial. *Lancet Oncol* (2020) 21:1653–60. doi: 10.1016/S1470-2045(20)30486-1
5. Goodell V, Waisman J, Salazar LG, de la Rosa C, Link J, Coveler AL, et al. Level of HER-2/Neu Protein Expression in Breast Cancer may Affect the Development of Endogenous HER-2/Neu-Specific Immunity. *Mol Cancer Ther* (2008) 7:449–54. doi: 10.1158/1535-7163.MCT-07-0386
6. Takemasa I, Yamamoto H, Sekimoto M, Ohue M, Noura S, Miyake Y, et al. Overexpression of CDC25B Phosphatase as a Novel Marker of Poor Prognosis of Human Colorectal Carcinoma. *Cancer Res* (2000) 60:3043–50.
7. Lee G, Origanti S, White LS, Sun J, Stappenbeck TS, Piwnica-Worms H. Contributions Made by CDC25 Phosphatases to Proliferation of Intestinal Epithelial Stem and Progenitor Cells. *PloS One* (2011) 6:e15561. doi: 10.1371/journal.pone.0015561
8. Ogino S, Kirkner GJ, Nosho K, Irahara N, Kure S, Shima K, et al. Cyclooxygenase-2 Expression Is an Independent Predictor of Poor Prognosis in Colon Cancer. *Clin Cancer Res* (2008) 14:8221–7. doi: 10.1158/1078-0432.CCR-08-1841
9. McLean MH, Murray GI, Fyfe N, Hold GL, Mowat NA, El-Omar EM. COX-2 Expression in Sporadic Colorectal Adenomatous Polyps Is Linked to Adenoma Characteristics. *Histopathology* (2008) 52:806–15. doi: 10.1111/j.1365-2559.2008.03038.x
10. Hashimoto Y, Skacel M, Lavery IC, Mukherjee AL, Casey G, Adams JC. Prognostic Significance of Fascin Expression in Advanced Colorectal Cancer: An Immunohistochemical Study of Colorectal Adenomas and Adenocarcinomas. *BMC Cancer* (2006) 6:241. doi: 10.1186/1471-2407-6-241
11. Leelawat K, Engprasert S, Tujinda S, Suthippintawong C, Enjoji M, Nakashima M, et al. Receptor-Binding Cancer Antigen Expressed on SiSo Cells can be Detected in Metastatic Lymph Nodes From Gastrointestinal Cancers. *World J Gastroenterol* (2005) 11:6014–7. doi: 10.3748/wjg.v11.i38.6014
12. Okada K, Nakashima M, Komuta K, Hashimoto S, Okudaira S, Baba N, et al. Expression of Tumor-Associated Membrane Antigen, RCAS1, in Human Colorectal Carcinomas and Possible Role in Apoptosis of Tumor-Infiltrating Lymphocytes. *Mod Pathol* (2003) 16:679–85. doi: 10.1097/01.MP.0000074732.17945.6C
13. Disis ML, dela Rosa C, Goodell V, Kuan LY, Chang JC, Kuus-Reichel K, et al. Maximizing the Retention of Antigen Specific Lymphocyte Function After Cryopreservation. *J Immunol Methods* (2006) 308:13–8. doi: 10.1016/j.jim.2005.09.011
14. Broussard EK, Kim R, Wiley JC, Marquez JP, Annis JE, Pritchard D, et al. Identification of Putative Immunologic Targets for Colon Cancer Prevention Based on Conserved Gene Upregulation From Preinvasive to Malignant Lesions. *Cancer Prev Res (Phila)* (2013) 6:666–74. doi: 10.1158/1940-6207.CAPR-12-0484
15. Park KH, Gad E, Goodell V, Dang Y, Wild T, Higgins D, et al. Insulin-Like Growth Factor-Binding Protein-2 Is a Target for the Immunomodulation of Breast Cancer. *Cancer Res* (2008) 68:8400–9. doi: 10.1158/0008-5472.CAN-07-5891
16. Cecil DL, Holt GE, Park KH, Gad E, Rastetter L, Childs J, et al. Elimination of IL-10-Inducing T-Helper Epitopes From an IGFBP-2 Vaccine Ensures Potent Antitumor Activity. *Cancer Res* (2014) 74:2710–8. doi: 10.1158/0008-5472.CAN-13-3286
17. Cecil DL, Slota M, O'Meara MM, Curtis BC, Gad E, Dang Y, et al. Immunization Against HIF-1alpha Inhibits the Growth of Basal Mammary Tumors and Targets Mammary Stem Cells *In Vivo*. *Clin Cancer Res* (2017) 23:3396–404. doi: 10.1158/1078-0432.CCR-16-1678
18. Cecil DL, Park KH, Gad E, Childs JS, Higgins DM, Plymate SR, et al. T-Helper I Immunity, Specific for the Breast Cancer Antigen Insulin-Like Growth Factor-I Receptor (IGF-IR), Is Associated With Increased Adiposity. *Breast Cancer Res Treat* (2013) 139:657–65. doi: 10.1007/s10549-013-2577-z
19. Biswas S, Chytil A, Washington K, Romero-Gallo J, Gorska AE, Wirth PS, et al. Transforming Growth Factor Beta Receptor Type II Inactivation Promotes the Establishment and Progression of Colon Cancer. *Cancer Res* (2004) 64:4687–92. doi: 10.1158/0008-5472.CAN-03-3255
20. Gad E, Rastetter L, Slota M, Koehnlein M, Treuting PM, Dang Y, et al. Natural History of Tumor Growth and Immune Modulation in Common Spontaneous Murine Mammary Tumor Models. *Breast Cancer Res Treat* (2014) 148:501–10. doi: 10.1007/s10549-014-3199-9
21. Muzny DM, Bainbridge MN, Chang K, Dinh HH, Drummond JA, Fowler G, et al. Comprehensive Molecular Characterization of Human Colon and Rectal Cancer. *Nature* (2012) 487:330–7. doi: 10.1038/nature11252
22. Tatsumi T, Gambotto A, Robbins PD, Storkus WJ. Interleukin 18 Gene Transfer Expands the Repertoire of Antitumor Th1-Type Immunity Elicited by Dendritic Cell-Based Vaccines in Association With Enhanced Therapeutic Efficacy. *Cancer Res* (2002) 62:5853–8.
23. Fruh K, Yang Y. Antigen Presentation by MHC Class I and its Regulation by Interferon Gamma. *Curr Opin Immunol* (1999) 11:76–81. doi: 10.1016/S0952-7915(99)80014-4
24. Rosenberg DW, Giardina C, Tanaka T. Mouse Models for the Study of Colon Carcinogenesis. *Carcinogenesis* (2009) 30:183–96. doi: 10.1093/carcin/bgn267
25. Chae WJ, Bothwell AL. Spontaneous Intestinal Tumorigenesis in Apc (/Min+) Mice Requires Altered T Cell Development With IL-17a. *J Immunol Res* (2015) 2015:860106. doi: 10.1155/2015/860106
26. Idos GE, Kwok J, Bonthala N, Kysh L, Gruber SB, Qu C. The Prognostic Implications of Tumor Infiltrating Lymphocytes in Colorectal Cancer: A Systematic Review and Meta-Analysis. *Sci Rep* (2020) 10:3360. doi: 10.1038/s41598-020-60255-4
27. Stanojevic M, Hont AB, Geiger A, O'Brien S, Ulrey R, Grant M, et al. Identification of Novel HLA-Restricted Preferentially Expressed Antigen in Melanoma Peptides to Facilitate Off-the-Shelf Tumor-Associated Antigen-Specific T-Cell Therapies. *Cytotherapy* (2021) 23:694–703. doi: 10.1016/j.jcyt.2021.03.001
28. Chevaleyre C, Benhamouda N, Favry E, Fabre E, Mhoumadi A, Nozach H, et al. The Tumor Antigen Cyclin B1 Hosts Multiple CD4 T Cell Epitopes Differently Recognized by Pre-Existing Naive and Memory Cells in Both Healthy and Cancer Donors. *J Immunol* (2015) 195:1891–901. doi: 10.4049/jimmunol.1402548
29. Danke NA, Koelle DM, Yee C, Beheray S, Kwok WW. Autoreactive T Cells in Healthy Individuals. *J Immunol* (2004) 172:5967–72. doi: 10.4049/jimmunol.172.10.5967
30. Lutz M, Worschech A, Alb M, Gahn S, Bernhard L, Schwab M, et al. Boost and Loss of Immune Responses Against Tumor-Associated Antigens in the Course of Pregnancy as a Model for Allogeneic Immunotherapy. *Blood* (2015) 125:261–72. doi: 10.1182/blood-2014-09-601302
31. Malhotra D, Linehan JL, Dileepan T, Lee YJ, Purtha WE, Lu JV, et al. Tolerance Is Established in Polyclonal CD4(+) T Cells by Distinct Mechanisms, According to Self-Peptide Expression Patterns. *Nat Immunol* (2016) 17:187–95. doi: 10.1038/ni.3327
32. Yu W, Jiang N, Ebert PJ, Kidd BA, Muller S, Lund PJ, et al. Clonal Deletion Prunes But Does Not Eliminate Self-Specific Alphabeta CD8(+) T Lymphocytes. *Immunity* (2015) 42:929–41. doi: 10.1016/j.immuni.2015.05.001

Conflict of Interest: MD is a stockholder in EpiThany and receives grant support from Celgene, EMD Serono, Pfizer, Janssen, and Precigen.

The remaining authors declare that the research was conducted in the absence of any commercial or financial relationships that could be construed as a potential conflict of interest.

this article, or claim that may be made by its manufacturer, is not guaranteed or endorsed by the publisher.

frontiers in Immunology

MINI REVIEW
published: 24 September 2021
doi: 10.3389/fimmu.2021.757804

Lynch Syndrome and MSI-H Cancers: From Mechanisms to "Off-The-Shelf" Cancer Vaccines

Vladimir Roudko[1,2,3], *Cansu Cimen Bozkus*[3,4], *Benjamin Greenbaum*[5,6], *Aimee Lucas*[7], *Robert Samstein*[2,3,8] *and Nina Bhardwaj*[3,4]*

[1] Department of Oncological Sciences, Icahn School of Medicine at Mount Sinai, New York, NY, United States, [2] Precision Immunology Institute, Icahn School of Medicine at Mount Sinai, New York, NY, United States, [3] Tisch Cancer Institute, Icahn School of Medicine at Mount Sinai, New York, NY, United States, [4] Division of Hematology and Medical Oncology, Icahn School of Medicine at Mount Sinai, New York, NY, United States, [5] Epidemiology and Biostatistics, Computational Oncology program, Memorial Sloan Kettering Cancer Center, New York, NY, United States, [6] Physiology, Biophysics & Systems Biology, Weill Cornell Medical College, New York, NY, United States, [7] Henry D. Janowitz Division of Gastroenterology, Samuel D. Bronfman Department of Medicine, Icahn School of Medicine at Mount Sinai, New York, NY, United States, [8] Department of Radiation Oncology, Mount Sinai Hospital, New York, NY, United States

OPEN ACCESS

Edited by:
Olivera J. Finn, University of Pittsburgh, United States

Reviewed by:
Arya Biragyn, National Institute on Aging (NIH), United States
Kevin Van der Jeught, Indiana University School of Medicine, United States

***Correspondence:**
Nina Bhardwaj
nina.bhardwaj@mssm.edu

Specialty section:
This article was submitted to Cancer Immunity and Immunotherapy, a section of the journal Frontiers in Immunology

Received: *12 August 2021*
Accepted: *08 September 2021*
Published: *24 September 2021*

Citation:
Roudko V, Cimen Bozkus C, Greenbaum B, Lucas A, Samstein R and Bhardwaj N (2021) Lynch Syndrome and MSI-H Cancers: From Mechanisms to "Off-The-Shelf" Cancer Vaccines. Front. Immunol. 12:757804. doi: 10.3389/fimmu.2021.757804

Defective DNA mismatch repair (dMMR) is associated with many cancer types including colon, gastric, endometrial, ovarian, hepatobiliary tract, urinary tract, brain and skin cancers. Lynch syndrome – a hereditary cause of dMMR – confers increased lifetime risk of malignancy in different organs and tissues. These Lynch syndrome pathogenic alleles are widely present in humans at a 1:320 population frequency of a single allele and associated with an up to 80% risk of developing microsatellite unstable cancer (microsatellite instability – high, or MSI-H). Advanced MSI-H tumors can be effectively treated with checkpoint inhibitors (CPI), however, that has led to response rates of only 30-60% despite their high tumor mutational burden and favorable immune gene signatures in the tumor microenvironment (TME). We and others have characterized a subset of MSI-H associated highly recurrent frameshift mutations that yield shared immunogenic neoantigens. These frameshifts might serve as targets for off-the-shelf cancer vaccine designs. In this review we discuss the current state of research around MSI-H cancer vaccine development, its application to MSI-H and Lynch syndrome cancer patients and the utility of MSI-H as a biomarker for CPI therapy. We also summarize the tumor intrinsic mechanisms underlying the high occurrence rates of certain frameshifts in MSI-H. Finally, we provide an overview of pivotal clinical trials investigating MSI-H as a biomarker for CPI therapy and MSI-H vaccines. Overall, this review aims to inform the development of novel research paradigms and therapeutics.

Keywords: Lynch syndrome, MSI-H, dMMR, immunotherapy, cancer vaccine

INTRODUCTION

In the United States, an individual's lifetime risk for developing cancer is estimated to be as high as 40% (www.cancer.org, "Lifetime Risk of Developing or Dying From Cancer"). Cancer is a genetic disorder in which somatic mutations in specific genes confer a selective growth advantage for tumors. Such mutations can be inherited through the germline, which results in a hereditary predisposition to an early-onset cancer, or can occur sporadically in non-germline carriers. One example is the hereditary nonpolyposis colorectal cancer syndrome known as Lynch syndrome. Defining the genetic causes for Lynch syndrome has uncovered a connection between the cellular machinery that regulates DNA repair, cancer formation and informed clinical approaches to manage the disease.

Lynch syndrome or hereditary non-polyposis colorectal cancer (HNPCC) is characterized by germline inactivation of one allele of genes involved in the mismatch repair system, namely *MLH1*, *MSH2*, *MSH6*, *PMS2 or EPCAM* and have received prominent clinical and research attention and since 1985 (1, 2). More than 1500 variants of Lynch syndrome alleles have been identified including: retrotransposition and Alu-like element insertion events (3–5), splice site mutations and large exonic deletions (6–8). However, inactivation of *MLH1* or *PMS2* alleles are the most frequent ones and are associated with approximately 80% of Lynch syndrome cases (9, 10). Lynch-associated genetic abnormalities frequently lead to cancer at ages of 30–40-years and in a broad range of tissues (**Figure 1A**), including: colon, stomach, brain, pancreas, small intestine, endometrial and urothelial tracts (12–18).

Colorectal, stomach and endometrial cancers cumulatively account for the second most common cancer types and one of the leading causes of cancer deaths in developed countries (19). The majority of the solid tumor cases are proficient in mismatch

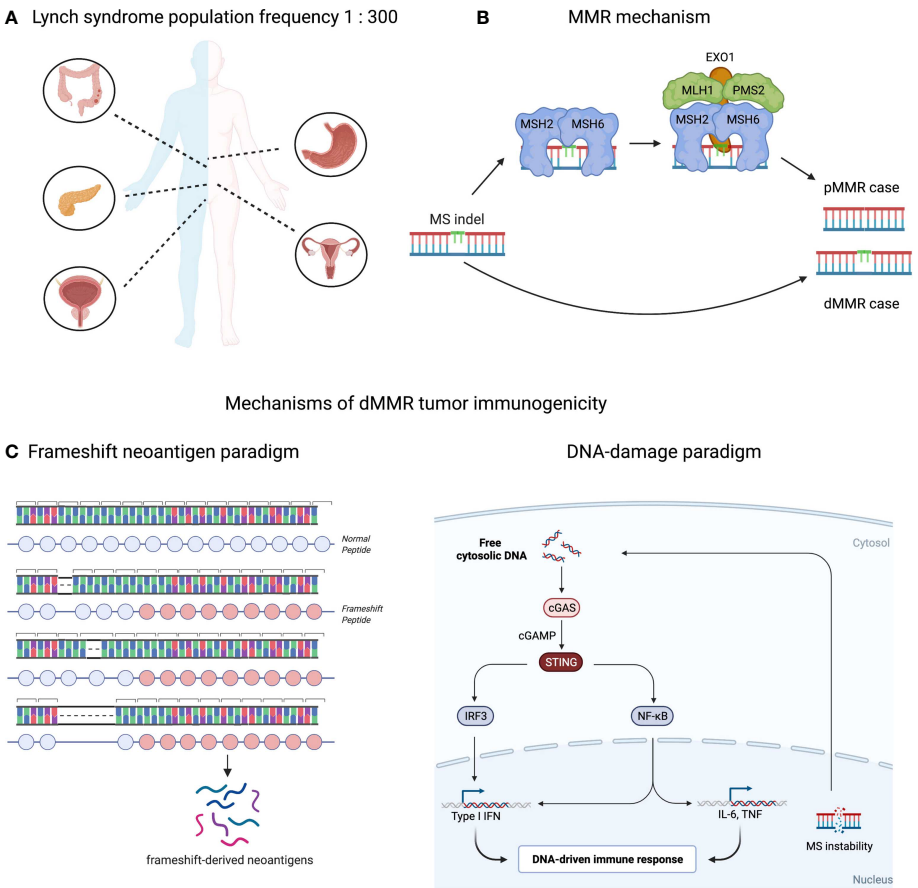

FIGURE 1 | Population, molecular and immunological aspects of mismatch-repair deficient (dMMR) tumors. **(A)** Predispositions to different cancers conferred by Lynch syndrome condition. Approximately 1 in 300 people in the U.S. has the Lynch Syndrome associated alleles. Carriers have 80% lifetime risk developing cancer including: colorectal, stomach, pancreas, urinary track and prostate for males and urinary, ovary or uterus tracks for females. In total, Lynch syndrome accounts for 2-3% solid tumor cases (11). **(B)** Mismatch repair (MMR) mechanism. MS indels occurring during DNA replication are repaired by MMR system (proficient MMR). *MSH2-MSH3* or *MSH2-MSH6* complexes, called MutSα or MutSβ, detect the error and recruit the *MLH1-PMS1*, *MLH1-PMS2* or *MLH1-MLH3* (MutLα/β/γ complexes respectively) to bind to the DNA and bring DNA exonuclease with PCNA to the mutation site. The mismatch is then excised and repaired following by DNA resynthesis and re-ligation. These aberrations are left unrepaired in case of MMR deficiency. **(C)** Two complementary paradigms explaining immune responses in dMMR tumors: neoantigen-driven (left part), and innate immune driven (right part).

repair (pMMR), however an estimated 14% (95% CI: 10%-19%) of cases are dMMR (20–23). These dMMR cases arise mainly from sporadic, tumor-specific inactivation of MMR pathway (24, 25) however a few cases – 2-3% of all colorectal and endometrial cancer cases (11) – have germline Lynch syndrome alleles as the ones described above (26). In the latter case, cancer onset transpires upon genetic inactivation of the second allele (in the case of the *PMS2* allele) or epigenetic silencing of gene expression (in the case of the *MLH1* allele) and subsequent acquisition of driver mutations in genes such as *APC*, *KRAS*, *PI3K*, *PTEN*, *BRAF* and/or *p53* (13, 27–32). Though pMMR and dMMR share similar profiles of tumor drivers, their genomic makeups are different. One of the molecular feature of dMMR tumors is high tumor mutation burden over-represented by somatic indel mutations within short tandem repeats – microsatellites – a molecular signature termed as a high microsatellite instability, or MSI-H (27, 33–35).

MMR MOLECULAR MECHANISM AND BIOMARKER STRATEGIES

Microsatellite extension or shortening in MSI-H tumors happens upon breaking down of the MMR molecular mechanism that controls microsatellite loci length (18, 36). During replication DNA polymerases incorporate deoxyribonucleotides into the growing chain of DNA using one of the paternal DNA strands as a template, thus copying genetic information with high fidelity. However, at microsatellite repeats DNA polymerases can slip from the template upon replication resulting in insertion or deletion of microsatellite units that structurally resembles a "bulge" of non-complemented DNA nucleotides within the parent/daughter DNA double strand helix. The MMR system guards against this type of mutagenesis by detecting and eliminating these bulges. First, *MSH2-MSH3* or *MSH2-MSH6* complexes, called MutSα or MutSβ, detect the error and recruit the *MLH1-PMS1*, *MLH1-PMS2* or *MLH1-MLH3* (MutLα/β/γ complexes respectively) to bind to the DNA and bring DNA exonuclease with *PCNA* to the mutation site (**Figure 1B**). The mismatch is then excised and repaired following by DNA resynthesis and re-ligation (33, 37). Since MSI-H cancers are defective in one of the MMR factors, mismatches in malignant cells remain unrepaired and accumulate indel mutations at high rates (18). Depending on where the microsatellite (MS) loci is located in the human genome, the effect of indel mutations differ: if it occurs within a non-coding segment of the genome, the indel mutation may have limited-to-no effect on overall gene expression or function; if it happens in a regulatory or splicing-required segment, the indel might affect linked gene expression; if it occurs within a protein-coding region the indel may result in expression of a truncated protein with novel peptide extension at the C-terminus (38). These cancer-specific peptide extensions called frameshifts can be exploited clinically in a variety of immunotherapy strategies which will be reviewed later.

Multiple biomarker strategies have been developed to detect either Lynch syndrome in the germline or assess penetration of MSI-H phenotype in tumors. Amsterdam II criteria and the Bethesda criteria are two clinically approved methods to diagnose Lynch syndrome in patients, and include a range of molecular tests with familial analysis of disease allele penetration (39). Several protocols exist to characterize MSI-H tumors: immunohistochemistry assay to quantify loss of MMR proteins such as *MLH1*, *MSH2*, *PMS2* and *MSH6*, genomic PCR tests to measure MS length variability at the various MS loci and quantification of somatic MS variation from WES/WGS data acquired from matched tumor/normal DNA samples using next generation sequencing and computational tools to calculate standardized MSI-H metrics like the "MSI score" (40–45). The strategies vary widely in terms of recall, sensitivity and specificity; thus, combining multiple protocols may increase the precision of the overall diagnosis (39, 46–48).

MSI-H CANCER AND CLINICAL MANAGEMENT

The standard of care for MSI-H cancer patients has changed from primarily chemotherapy to include immune checkpoint inhibitors. Approved for pMMR colorectal tumors, standard of care 5-fluorouracil (5-FU)-based regiments turned out to be ineffective in dMMR cases due to the lack of enzymes recognizing DNA damage inflicted by the drug (45, 49). Moreover, dMMR is turned out to be a negative prognostic biomarker for the objective response to 5-FU therapy and overall survival (49). Despite a setback in targeted therapy modalities for dMMR cancers, synthetic lethal interactions hold promise to improve the outcomes. dMMR tumors represent a good example of a system, where simultaneous co-inhibition of two factors may lead to cancer cell apoptosis and death. It has been found, that inhibition of Werner helicase is synthetically lethal with inactive *MSH2* or *PMS1* – the causative mutations of dMMR cancers. Mechanistically, the helicase is critical to unwind aberrantly replicated DNA and to maintain genome integrity of MSI-H tumors (50, 51). Pharmacological targeting of Werner helicase in dMMR cases still awaits its clinical application.

High tumor mutation burden (TMB) and comparatively strong immune cell infiltration of dMMR tumors sparked interest in applying checkpoint inhibitor (CPI) and other immunotherapy approaches (38, 52–54). Many studies confirmed a strong correlation between objective response rates to CPI and TMB in multiple cancers (55–58). A recent stage II multicohort clinical trial KEYNOTE-158 showed that TMB score is predictive for overall and progression free survival in the adjuvant CPI setting (59). Similarly, a range of clinical studies led by Dr. Diaz Jr. confirmed the strong association between responses to CPI and dMMR tumor status in a tissue-agnostic fashion (60, 61). Further investigation suggested dMMR status or MSI-H score to being predictive to CPI responses in solid tumors (62–64). These results led to the fast-track approval of dMMR as a biomarker for CPI by FDA and initiation of prospective stage II/III clinical trials, e.g., NCT02563002 or NCT04008030, to evaluate dMMR as a predictive biomarker. An interesting observation has arisen suggesting dMMR might

be a confounding parameter for TMB biomarker in colorectal cancer patients treated with CPI: dMMR patients, which are often TMB-high due to intrinsic mechanisms of efficient somatic mutagenesis, clinically do better than "TMB-high but pMMR" patients (65). This clinical observation suggests the importance of the biological mechanism generating high somatic mutation load in tumor responsiveness to CPI. For instance, several hypotheses have been suggested to explain high CPI response rates in dMMR mechanistically. One of them is the "frameshift neoantigen" paradigm. Neoantigens are cancer-specific peptides that are usually derived from somatic mutations and presented on MHC-I or MHC-II complexes (66). dMMR tumors are enriched in frameshifts and neoantigens derived from these peptide extensions might confer tumor immunogenicity (67–70). Theoretically, one frameshift mutation may encode a peptide yielding multiple neoantigens with broad MHC-I/II specificities, thereby increasing the probability of (a) epitope presentation, (b) cancer antigen sampling by dendritic cells, (c) T cell recognition and (d) T cell-mediated tumor killing. We and others have shown exceptional immune responses against these frameshift peptides expressed in dMMR tumors, thus supporting the "frameshift neoantigen" paradigm (71–73). Another hypothesis is built around innate immune signaling driven by DNA instability. The aberrant DNA fragments are spilled over from the nucleus during DNA replication and recognized by *cGAS-STING* as "non-self" inducing Type I interferon and inflammatory NFkB responses (74, 75). In agreement with this hypothesis, recent study by Mowat et al. showed that *cGAS-STING* driven type I interferon signaling is required for *CXCL10*/*CCL5*-dependent T cell recruitment to dMMR tumor site (76). Both "frameshift-neoantigen" and "DNA instability" models are instructive and complementary in explaining the origins of the dMMR tumor immunogenicity (**Figure 1C**).

LYNCH SYNDROME/MSI-H CANCER AND "OFF-THE-SHELF" VACCINES

dMMR immunotherapies also include the implementation of cancer vaccine strategies in therapeutic and prospective settings (77). Several reasons suggest that such strategies might become successful. First, many dMMR associated somatic mutations are non-random across the genome. Known tumor drivers such as mutations in *APC*, *TP53* or *BRAF* genes are clonal, positively selected by the developing tumor and overrepresented within dMMR patient samples. Similarly, certain frameshift mutations are found to be under positive selection despite encoding immunogenic neoantigens (78, 79). From a tumor evolution perspective, such "cost" of an immunogenic frameshift can be accepted only if loss-of-function mutation confers a tumor growth advantage. Adaptive resistance against emerged neoantigens can be acquired later through general immune suppression mechanisms like *PDL-1* upregulation, infiltration of the TME by myeloid-derived suppressor cells or T regulatory cells, *TGF-β* expression or other genomically encoded immune-escape mechanisms (80). However, the positively selected frameshifts can be harnessed clinically as shared cancer vaccines (81, 82). Several targets including *RNF43*^{fs}, *TGFBR2*^{fs}, *ASTE1*^{fs}, *AIM2*^{fs}, have been extensively validated in numerous immunological assays: priming and boosting naïve T cell populations in healthy donors, confirming cytotoxic capacity of CD8+ T cell responses in tumor killing assays and detecting frameshift-specific memory responses within blood and tumor T cell compartments in dMMR cancer patients and Lynch syndrome populations (71, 83–85). The latter is particularly interesting because it suggests that immunological responses against frameshifts are observed in the absence of detectable cancer. In line with these results, a study lead by Dr. Kloor has documented dMMR mutations in crypts and polyps of Lynch syndrome patients which are not cancerous (86). These findings confirm that cancer development and loss of the mismatch repair system are two independent genomic events decoupled in time and may follow each other in any order (32). It also indicates that MS instability can happen early and progress without being recognized by the host immune system, likely because the majority of MS loci – targets of MS instability – are non-coding and spread over the human genome in a random fashion. Alternatively, instability of a protein coding MS locus does not necessarily lead to tumor transformation and might reflect a frequent, hotspot somatic passenger mutation such as those occurring in a healthy dividing cells (87, 88). It might take several cellular divisions and multiple MS instability events to develop a genetic background with an invasive tumor phenotype. Although, complete removal of dMMR cell populations might not be achieved due to the immune "invisibility" of such MS unstable clones, prospective vaccination against frequently observed and/or early detected frameshifts in dMMR cancer or dMMR Lynch syndrome patients is likely to increase the efficiency of immune surveillance of pro-tumorigenic cell populations and potentially delay tumor progression in the at-risk populations. Multiple vaccine formulations including different combinations of shared dMMR-associated frameshifts are currently undergoing safety and immunogenicity tests in clinical trials involving dMMR cancer and Lynch syndrome patients with established tumors (**Table 1**) (89, 90). It will be exciting to evaluate the clinical outcomes and cancer protection of Lynch syndrome patients in the prospective vaccine setting, similarly to the recently published antigen-agnostic immunomodulatory strategy involving naproxen – inhibitor of prostaglandin signaling (54). Recently published a proof-of-concept study confirmed therapeutic efficiency of a shared frameshift vaccine to delay tumor progression in mouse models of Lynch syndrome (91).

Several considerations have to be taken during the development and application of a shared dMMR vaccine. General factors, including the platform selection (DNA, RNA, peptide), adjuvant, routes of administration and etc. – have been extensively reviewed elsewhere (92), but here we will discuss tumor intrinsic and potential acquired resistance mechanisms (93). As it has been mentioned above, dMMR tumors have enormous potential to develop somatic mutations through loss of DNA replication fidelity. dMMR tumors can be perceived as a

TABLE 1 | List of registered clinical trials of cancer vaccines and/or CPI in dMMR/Lynch syndrome patients.

Study ID	Title	Status	Locations
CPI and other immunotherapy clinical trials in dMMR cancers			
NCT04612309	Retrospective Study on the Use of Immunotherapy in Patients With MSI-H Metastatic Colorectal Cancer	Recruiting	Italy
NCT04795661	Immunotherapy in MSI/dMMR Tumors in Perioperative Setting.	Not yet recruiting	France
NCT03827044	Avelumab Plus 5-FU Based Chemotherapy as Adjuvant Treatment for Stage 3 MSI-High or POLE Mutant Colon Cancer	Active, not recruiting	UK
NCT03206073	A Phase I/II Study of Pexa-Vec Oncolytic Virus in Combination With Immune Checkpoint Inhibition in Refractory Colorectal Cancer	Active, not recruiting	USA
NCT03150706	Avelumab for MSI-H or POLE Mutated Metastatic Colorectal Cancer	Active, not recruiting	South Korea
NCT03435107	Durvalumab for MSI-H or POLE Mutated Metastatic Colorectal Cancer	Active, not recruiting	South Korea
NCT04019964	Nivolumab in Biochemically Recurrent dMMR Prostate Cancer	Recruiting	USA
NCT02052908	Naproxen in Preventing DNA Mismatch Repair Deficient Colorectal Cancer in Patients with Lynch Syndrome	Completed	USA
Clinical trials involving off-the-shelf cancer vaccines			
NCT04799431	Neoantigen-Targeted Vaccine Combined With Anti-PD-1 Antibody for Patients With Stage IV MMR-p Colon and Pancreatic Ductal Cancer	Not yet recruiting	USA
NCT04117087	Pooled Mutant KRAS-Targeted Long Peptide Vaccine Combined With Nivolumab and Ipilimumab for Patients With Resected MMR-p Colorectal and Pancreatic Cancer	Recruiting	USA
NCT01885702	Dendritic Cell Vaccination in Patients With Lynch Syndrome or Colorectal Cancer With MSI	Active, not recruiting	Netherlands
NCT03152565	Avelumab Plus Autologous Dendritic Cell Vaccine in Pre-treated Metastatic Colorectal Cancer Patients	Completed	Spain
NCT04041310	Nous-209 Genetic Vaccine for the Treatment of Microsatellite Unstable Solid Tumors	Recruiting	USA
NCT01461148	Vaccination Against MSI Colorectal Cancer	Completed	Germany

"mutator" machine: cell population with an intrinsic mechanism to sample many different genotypes in a very rapid manner. Administration of external pressure such as through the vaccine-mediated expansion of tumor-specific T cell clones, may promote the development of tumor resistance against the host immune system. Several studies have reported up to 30% frequency of loss-of-function mutations in β-2-microglobulin (*B2M*) – a gene required for MHC-I antigen presentation and processing; up to 70% frequency of mutations in *TGFBR2* – cytokine receptor, rendering tumors non-responsive to *TGF-β* mediated suppression; up to 80% cumulative frequency of mutations in other genes related to innate and adaptive immune signaling pathways, namely *IFN-γ* response (*JAK1, JAK2*) and inflammasome activation (*CASP5*, *AIM2*). Other genomic mechanisms include loss of heterozygosity in *HLA-I* loci which drives tumor escape from CD8+ T cell cytotoxicity (94). Additionally, nonsense-mediated decay of the frameshifted messenger RNA can decrease immunogenicity against frameshift-derived neoantigens due to altered stability of the mutated RNA (95, 96). Non-genetic mechanisms of acquired resistance also can be found in the TME of the dMMR tumors, including: increased *Wnt*/β-catenin signaling in tumor associated fibroblasts; increased infiltration of *Foxp3*+ T regs; upregulated expression of immune checkpoints *PDL-1* and *CTLA-4*; as well as *CD47* "don't eat me" signals for macrophages and dendritic cells (93, 97, 98). Interestingly, a retrospective analysis of *B2M* expression and mutation status in colorectal dMMR cancer patients showed favorable clinical outcomes in patient cohorts despite *B2M* loss-of-function mutations, counterintuitive to the mechanisms of MHC-I dependance of immune-mediated tumor rejection (99, 100). A recent study by Germano et al. addressed this question and found CD4+ T cells being responsible for tumor rejection and the development of strong immune responses in *B2M*-null dMMR tumors (101). These and many other disparities between assumed inhibitory mechanisms and clinical outcomes in patients will inform many other mechanisms of therapy response and resistance which might exist in the dMMR cancer setting.

CONCLUSIONS AND PERSPECTIVES

Understanding the trajectories of dMMR tumor genome evolution at the single cell level with and without applied immune pressure will help to describe the landscape of acquired and intrinsic tumor resistance. Knowledge of these mechanisms might inform additional interventions important to include in the shared vaccine formulations such as MHC-II epitopes and/or NK cell engagers or myeloid cell modulation (38). CPI clinical trials conducted in dMMR patients can provide useful insights to address these questions. Discussed previously disparities between observed genomic alterations and immunotherapy clinical outcomes may inform novel mechanisms of immune resistance and response in dMMR tumors. Exploratory genetic and expression analysis of non-responder dMMR patient tumor samples from large-scale phase III CPI clinical trials will be highly informative to address these questions (60). Similarly, large scale sequencing and imaging data mining will be crucial to understand the mechanisms of dMMR tumor and immune cell dynamics. The majority of the detected frameshifts and MS loci indels are subclonal with relatively stable chromosomal copy number. If one specific mutation provides an immune resistance and doing so – growth advantage – why does not it become clonal during tumor evolution? A potential explanation is the uneven spatial

tumor clone distribution and cooperativity between different tumor clones which might provide tumor benefit (102). Indeed, one can imagine the tumor surface lined up by clones governing immune resistance protecting other clones growing in the tumor core from infiltrating immune cells. In this "mutual dependency" scenario subclonal protective mutation will be sufficient to gain tumor growth advantage as a whole tumor cell community. Thus, spatially-resolved genomic studies combined with single-cell studies will be extremely informative to gain insight on spatial biomarkers associated with resistance and response to CPI and improve cancer vaccines designs by informing the inclusion of as many frameshifts derived from different tumor clones as possible (103).

In conclusion, we highlight several questions which remain important to address regarding treatment and prevention of MSI tumor in the near future. How many novel MS indels appear per each genome replication in dMMR lesions and/or dMMR Lynch syndrome crypts? What is the probability of acquiring a frameshift expressed at the protein level? Can sequence-based motifs predict the earliest frameshift to appear during dMMR development? Computational modelling leveraging whole genome MSI-H samples will be informative to answer these questions. Which frameshifts generate the most frequent immune responses *in vitro* and in dMMR cancer/Lynch syndrome patients? Which frameshift combination confers the best protective and cytotoxic potential in different cellular models of dMMR cancer progression? Extensive immunological studies will be very informative to address these points. Finally, characterizing and quantifying tumor intrinsic and acquired mechanisms of resistance from either clinical CPI trials or tumor model studies will be important to find alternative ways of improving therapeutic responses in patients' populations. Overall, immunotherapeutic development to treat or protect against dMMR tumorigenesis experiences a new spiral of fruitful and exciting research.

AUTHOR CONTRIBUTIONS

VR wrote the manuscript. VR, CC, BG, AL, RS, and NB revised the manuscript. All authors contributed to the article and approved the submitted version.

FUNDING

Support is provided by seed fund from Tisch Cancer Institute at Mount Sinai Hospital.

REFERENCES

1. Lynch H, Schuelke G, Kimberling W, Albano W, Lynch J, Biscone K, et al. Hereditary Nonpolyposis Colorectal Cancer (Lynch Syndromes I and II). Biomarker Studies. *Cancer* (1985) 56:939–51. doi: 10.1002/1097-0142(19850815)56:4<939::AID-CNCR2820560440>3.0.CO;2-T
2. Lynch HT, Kimberling W, Albano W, Lynch JF, Schuelke G, Sandberg AA, et al. Hereditary Nonpolyposis Colorectal Cancer (Lynch Syndromes I and II). Clinical Description of Resource. *Cancer* (1985) 56:934–8. doi: 10.1002/1097-0142(19850815)56:4<934::AID-CNCR2820560439>3.0.CO;2-I
3. Yamamoto G, Miyabe I, Tanaka K, Kakuta M, Watanabe M. SVA Retrotransposon Insertion in Exon of MMR Genes Results in Aberrant RNA Splicing and Causes Lynch Syndrome. *Eur J Hum Genet* (2021) 1:680–6. doi: 10.1038/s41431-020-00779-5
4. Salo-mullen YLE, Zhang L. Insertion of an Alu-Like Element in MLH1 Intron 7 as a Novel Cause of Lynch Syndrome. *Mol Genet Genomics Med* (2020) 8(15):1–7. doi: 10.1002/mgg3.1523
5. Yang C, Li Y, Trottier M, Farrell MP, David EES, Zsofia JG, et al. Insertion of an SVA Element in MSH2 as a Novel Cause of Lynch Syndrome. *Genes Chromosomes Cancer* (2021) 60(8):1–6. doi: 10.1002/gcc.22950
6. Cui S, Zhang X, Zou R, Ye F, Wang Y, Sun J. MLH1 Exon 12 Gene Deletion Leading to Lynch Syndrome: A Case Report. *Oncol Res Treat* (2021) 44:414–20. doi: 10.1159/000516659
7. Stella A, Wagner A, Shito K, Lipkin SM, Watson P, Guanti G, et al. A Nonsense Mutation in MLH1 Causes Exon Skipping in Three Unrelated HNPCC Families. *Cancer Res* (2001) 61:7020–4.
8. Yang C, Sheehan M, Borras E, Cadoo K, Offit K, Zhang L. Characterization of a Germline Splice Site Variant MLH1 C. 678 − 3T > A in a Lynch Syndrome Family. *Familial Cancer* (2020) 19(4):315–22. doi: 10.1007/s10689-020-00180-7
9. Dong L, Zou S, Jin X, Lu H, Zhang Y, Guo L, et al. Cytoplasmic MSH2 Related to Genomic Deletions in the MSH2/EPCAM Genes in Colorectal Cancer Patients With Suspected Lynch Syndrome. *Front Oncol* (2021) 11:627460. doi: 10.3389/fonc.2021.627460
10. Chung DC, Rustgi AK. The Hereditary Nonpolyposis Colorectal Cancer Syndrome: Genetics and Clinical Implications. *Ann Internal Med* (2019) 138 (7):560–70. doi: 10.7326/0003-4819-138-7-200304010-00012
11. Boland P, Yurgelun M, Boland R. Recent Progress in Lynch Syndrome and Other Familial Colorectal Cancer Syndromes. *CA: A Cancer J Clin Cancer J* (2019) 68(3):217–31. doi: 10.3322/caac.21448.Recent
12. Lindner AK, Schachtner G, Tulchiner G, Thurnher M, Untergasser G, Obrist P, et al. Lynch Syndrome: Its Impact on Urothelial Carcinoma. *Int J Mol Sci* (2021) 22:531. doi: 10.3390/ijms22020531
13. Power DG, Gloglowski E, Lipkin SM. Clinical Genetics of Hereditary Colorectal Cancer. *Hematol Oncol Clin* (2010) 24:837–59. doi: 10.1016/j.hoc.2010.06.006
14. Carethers JM, Stoffel EM, Carethers JM, Stoffel EM, Gastroenterology D, States U. Advances in Colorectal Cancer Lynch Syndrome and Lynch Syndrome Mimics: The Growing Complex Landscape of Hereditary Colon Cancer. *World J Gastroenterol* (2015) 21(31):9253–61. doi: 10.3748/wjg.v21.i31.9253
15. Ryan NAJ, Blake D, Cabrera-dandy M, Glaire MA, Evans DG, Crosbie EJ. The Prevalence of Lynch Syndrome in Women With Endometrial Cancer: A Systematic Review Protocol. *Systematic Rev* (2018) 121:1–6. doi: 10.1186/s13643-018-0792-8
16. Evrard C, Alexandre J. Predictive and Prognostic Value of Microsatellite Instability in Gynecologic Cancer (Endometrial and Ovarian). *Cancers* (2021) 13:(10)1–15. doi: 10.3390/cancers13102434
17. Sekine M, Enomoto T. Precision Medicine for Hereditary Tumors in Gynecologic Malignancies. *J Obstetrics Gynaecol Res* (2021) 47:2597–606. doi: 10.1111/jog.14861
18. Salem ME, Bodor JN, Puccini A, Xiu J, Goldberg RM, Grothey A, et al. Relationship Between MLH1, PMS2, MSH2 and MSH6 Gene-Specific Alterations and Tumor Mutational Burden in 1057 Microsatellite Instability-High Solid Tumors. *Int J Cancer* (2020) 147:2948–56. doi: 10.1002/ijc.33115
19. Sung H, Ferlay J, Siegel RL, Laversanne M, Soerjomataram I, Jemal A, et al. Global Cancer Statistics 2020: GLOBOCAN Estimates of Incidence and Mortality Worldwide for 36 Cancers in 185 Countries. *A Cancer J Clin* (2021) 71(3):209–49. doi: 10.3322/caac.21660
20. Kim TM, Laird PW, Park PJ. The Landscape of Microsatellite Instability in Colorectal and Endometrial Cancer Genomes. *Cell* (2013) 58(15):3455–60. doi: 10.1016/j.cell.2013.10.015

21. Zhang B, Wang J, Wang X, Zhu J, Liu Q, Shi Z, et al. Proteogenomic Characterization of Human Colon and Rectal Cancer. *Nature* (2014) 513 (7518):382–7. doi: 10.1038/nature13438
22. Dou Y, Kawaler EA, Cui Zhou D, Gritsenko MA, Huang C, Blumenberg L. Clinical Proteomic Tumor Analysis Consortium. Proteogenomic Characterization of Endometrial Carcinoma. *Cell* (2020) 180(4):729–48. doi: 10.1016/j.cell.2020.01.026
23. Lorenzi M, Amonkar M, Zhang J, Mehta S, Liaw K. Epidemiology of Microsatellite Instability High (MSI-H) and Deficient Mismatch Repair (dMMR) in Solid Tumors: A Structured Literature Review. *Hindawi J Oncol* (2020) 2020:1807929. doi: 10.1155/2020/1807929
24. Cortes-Ciriano I, Lee S, Park WY, Kim TM, Park PJ. A Molecular Portrait of Microsatellite Instability Across Multiple Cancers. *Nat Commun* (2017) 8:1–12. doi: 10.1038/ncomms15180
25. Cunningham JM, Christensen ER, Tester DJ, Burgart LJ, Thibodeau SN. Hypermethylation of the hMLHl Promoter in Colon Cancer With Microsatellite Instability. *Cancer Res* (1998) 58:3455–60.
26. Latham A, Srinivasan P, Kemel Y, Shia J, Bandlamudi C. Microsatellite Instability Is Associated With the Presence of Lynch Syndrome Pan-Cancer. *J Clin Oncol* (2021) 37(4):286–95. doi: 10.1200/JCO.18.00283
27. Veigl M, Kastury L, Olechnowicz J, Ma A, Markowitz S. Biallelic Inactivation of hMLH 1 by Epigenetic Gene Silencing, a Novel Mechanism Causing Human MSI Cancers. *PNAS* (1998) 95:8698–702. doi: 10.1073/pnas.95.15.8698
28. Ellenson LH. Hmlh1 Promoter Hypermethylation in Microsatellite Instability-Positive Endometrial Carcinoma. *Am J Pathol* (1999) 155 (5):1399–402. doi: 10.1016/S0002-9440(10)65451-X
29. Cunningham JM, Christensen ER, Tester DJ, Burgart LJ, Thibodeau SN, Roche PC. Hypermethylation of the hMLHl Promoter in Colon Cancer With Microsatellite Instability. *Cancer Res* (1998) 58(15):3455–60.
30. Marchiò C, De Filippo MR, Ng CKY, Piscuoglio S, Soslow RA, Reis-Filho JS, et al. PIKing the Type and Pattern of PI3K Pathway Mutations in Endometrioid Endometrial Carcinomas. *Gynecol Oncol* (2015) 137(2):321–8. doi: 10.1016/j.ygyno.2015.02.010
31. Getz G, Gabriel SB, Cibulskis K, Lander E, Sivachenko A, Sougnez C, et al. Integrated Genomic Characterization of Endometrial Carcinoma. *Nature* (2013) 497(7447):67–73. doi: 10.1038/nature12113
32. Ahadova A, Gallon R, Gebert J, Ballhausen A, Endris V, Kirchner M. Three Molecular Pathways Model Colorectal Carcinogenesis in Lynch Syndrome. *Int J Cancer* (2018) 143:139–50. doi: 10.1002/ijc.31300
33. Sinicrope FA, Sargent DJ. Molecular Pathways: Microsatellite Instability in Colorectal Cancer: Prognostic, Predictive, and Therapeutic Implications. *Clin Cancer Res* (2012) 18(6):1506–12. doi: 10.1158/1078-0432.CCR-11-1469
34. Vasaikar S, Huang C, Wang X, Petyuk VA, Savage SR, Wen B, et al. Proteogenomic Analysis of Human Colon Cancer Reveals New Therapeutic Opportunities. *Cell* (2019) 177(4):1035–1049.e19. doi: 10.1016/j.cell.2019.03.030
35. Arzimanoglou II, Lallas T, Osborne M, Barber H, Gilbert F. Microsatellite Instability Differences Between Familial and Sporadic Ovarian Cancers. *Carcinogenesis* (1996) 17(9):1799–804. doi: 10.1093/carcin/17.9.1799
36. Lipkin SM, Wang V, Jacoby R, Banerjee-basu S, Baxevanis AD, Lynch HT, et al. MLH3: A DNA Mismatch Repair Gene Associated With Mammalian Microsatellite Instability. *Nat Genet* (2000) 24:27–35. doi: 10.1038/71643
37. Zhao P, Li L, Jiang X, Li Q. Mismatch Repair Deficiency/Microsatellite Instability-High as a Predictor for Anti-PD-1/PD-L1 Immunotherapy Efficacy. *J Hematol Oncol* (2019) 12(1):1–14. doi: 10.1186/s13045-019-0738-1
38. Kloor M, Von Knebel Doeberitz M. The Immune Biology of Microsatellite-Unstable Cancer. *Trends Cancer* (2016) 2(3):121–33. doi: 10.1016/j.trecan.2016.02.004
39. Cohen SA, Pritchard CC, Jarvik GP. Lynch Syndrome: From Screening to Diagnosis to Treatment in the Era of Modern Molecular Oncology. *Annu Revew Genomics Hum Genet* (2019) 20(4):1–15. doi: 10.1146/annurev-genom-083118-015406
40. Delhomme N, Mähler N, Schiffthaler B, Sundell D. Guidelines for RNA-Seq Data Analysis. *Epigenesys Protocol* (2014), 1–24.
41. Hempelmann JA, Lockwood CM, Konnick EQ, Schweizer MT, Antonarakis ES, Lotan TL, et al. Microsatellite Instability in Prostate Cancer by PCR or Next-Generation Sequencing. *J ImmunoTher Cancer* (2018) 6(29):1–7. doi: 10.1186/s40425-018-0341-y
42. Yamaguchi K, Kasajima R, Takane K, Hatakeyama S, Shimizu E. Application of Targeted Nanopore Sequencing for the Screening and Determination of Structural Variants in Patients With Lynch Syndrome. *J Hum Genet* (2021). doi: 10.1038/s10038-021-00927-9
43. Ratovomanana T, Cohen R, Svrcek M, Renaud F, Siret A, Letourneur Q, et al. Performance of Next Generation Sequencing for the Detection of Microsatellite Instability in Colorectal Cancer With Deficient DNA Mismatch Repair. *Gastroenterology* (2021) 161(3):814–26. doi: 10.1053/j.gastro.2021.05.007
44. Niu B, Ye K, Zhang Q, Lu C, Xie M, Mclellan MD, et al. MSIsensor: Microsatellite Instability Detection Using Paired Tumor-Normal Sequence Data. *Bioinformatics* (2014) 30(7):1015–6. doi: 10.1093/bioinformatics/btt755
45. Diao Z, Han Y, Chen Y, Zhang R, Li J. The Clinical Utility of Microsatellite Instability in Colorectal Cancer. *Crit Rev Oncol/Hematol* (2021) 157:103171. doi: 10.1016/j.critrevonc.2020.103171
46. Kurnit KC. Microsatellite Instability in Endometrial Cancer: New Purpose for an Old Test. *Cancer* (2019) 125(13):1–10. doi: 10.1002/cncr.32058
47. Lu Y, Soong TD, Elemento O. A Novel Approach for Characterizing Microsatellite Instability in Cancer Cells. *PloS One* (2013) 8(5):1–10. doi: 10.1371/journal.pone.0063056
48. Acosta M–, Marín F, Puliafito B, Bonifaci N, Fernández A, Navarro M, et al. High-Sensitivity Microsatellite Instability Assessment for the Detection of Mismatch Repair Defects in Normal Tissue of Biallelic Germline Mismatch Repair Mutation Carriers. *J Med Genet* (2020) 57(4):269–73. doi: 10.1136/jmedgenet-2019-106272
49. Hewish M, Lord CJ, Martin SA, Cunningham D, Ashworth A. Mismatch Repair Deficient Colorectal Cancer in the Era of Personalized Treatment. *Nat Rev Clin Oncol* (2010) 7(4):197–208. doi: 10.1038/nrclinonc.2010.18
50. Picco G, Cattaneo C, van Vliet E, Crisafulli G, Rospo G, Consonni S, et al. Werner Helicase Is a Synthetic-Lethal Vulnerability in Mismatch Repair – Deficient Colorectal Cancer Refractory to Targeted Therapies, Chemotherapy and Immunotherapy. *Cancer Discov* (2021) 11(8):1923–37. doi: 10.1158/2159-8290.CD-20-1508
51. Chan EM, Shibue T, Mcfarland JM, Gaeta B, Ghandi M, Dumont N, et al. WRN Helicase Is a Synthetic Lethal Target in Microsatellite Unstable Cancers. *Nature* (2019) 568:551–6. doi: 10.1038/s41586-019-1102-x
52. Gatalica Z, Vranic S, Xiu J, Swensen J. High Microsatellite Instability (MSI-H) Colorectal Carcinoma: A Brief Review of Predictive Biomarkers in the Era of Personalized Medicine. *Familial Cancer* (2016) 15(3):405–12. doi: 10.1007/s10689-016-9884-6
53. Chalabi M, Fanchi LF, Dijkstra KK, Van Den Berg JG, Snaebjornsson P, Maas M, et al. Neoadjuvant Immunotherapy Leads to Pathological Responses in MMR-Proficient and MMR-Deficient Early-Stage Colon Cancers. *Nat Med* (2020) 26:566–76. doi: 10.1038/s41591-020-0805-8
54. Reyes-Uribe L, Wu W, Gelincik O, Bommi PV, Francisco-Cruz A, Solis LM, et al. Naproxen Chemoprevention Promotes Immune Activation in Lynch Syndrome Colorectal Mucosa. *Gut* (2021) 70:555–66. doi: 10.1136/gutjnl-2020-320946
55. Snyder A, Makarov V, Merghoub T, Yuan J, Zaretsky JM, Desrichard A, et al. Genetic Basis for Clinical Response to CTLA-4 Blockade in Melanoma. *New Engl J Med* (2014) 371(23):2189–99. doi: 10.1056/NEJMoa1406498
56. Rizvi NA, Hellmann MD, Snyder A, Kvistborg P, Makarov V, Havel JJ, et al. Mutational Landscape Determines Sensitivity to PD-1 Blockade in Non-Small Cell Lung Cancer. *Science* (2015) 348(6230):124–8. doi: 10.1126/science.aaa1348
57. Van Allen EM, Miao D, Schilling B, Shukla SA, Blank C, Zimmer L, et al. Genomic Correlates of Response to CTLA-4 Blockade in Metastatic Melanoma. *Science* (2015) 350(6257):207–11. doi: 10.1126/science.aad0095
58. Cristescu R, Mogg R, Ayers M, Albright A, Murphy E, Yearley J, et al. Pan-Tumor Genomic Biomarkers for PD-1 Checkpoint Blockade – Based Immunotherapy. *Science* (2018) 3593:eaar3593. doi: 10.1126/science.aar3593
59. Marabelle A, Fakih M, Lopez J, Shah M, Shapira-frommer R, Nakagawa K, et al. Association of Tumour Mutational Burden With Outcomes in Patients With Advanced Solid Tumours Treated With Pembrolizumab: Prospective Biomarker Analysis of the Multicohort, Open-Label, Phase 2 KEYNOTE-158 Study. *Lancet Oncol* (2020) 21:1353–65. doi: 10.1016/S1470-2045(20)30445-9

60. Andre T, Shiu K-K, Kim T, Jensen B, Jensen L, Punt C, et al. Pembrolizumab in Microsatellite-Instability–High Advanced Colorectal Cancer. *New Engl J Med* (2020) 383(23):2207–18. doi: 10.1056/NEJMoa2017699
61. Le DT, Uram JN, Wang H, Bartlett BR, Kemberling H, Eyring AD, et al. PD-1 Blockade in Tumors With Mismatch-Repair Deficiency. *New Engl J Med* (2015) 372(26):2509–20. doi: 10.1056/NEJMoa1500596
62. Dudley JC, Lin MT, Le DT, Eshleman JR. Microsatellite Instability as a Biomarker for PD-1 Blockade. *Clin Cancer Res* (2016) 22(4):813–20. doi: 10.1158/1078-0432.CCR-15-1678
63. Le DT, Durham JN, Smith KN, Wang H, Bjarne R, Aulakh LK, et al. Mismatch-Repair Deficiency Predicts Response of Solid Tumors to PD-1 Blockade. *Science* (2017) 357(6349):409–13. doi: 10.1126/science.aan6733.Mismatch-repair
64. Danley K, Schmitz K, Ghai R, Sclamberg J, Buckingham L, Burgess K, et al. A Durable Response to Pembrolizumab in a Patient With Uterine Serous Carcinoma and Lynch Syndrome Due to the MSH6 Germline Mutation. *Oncol* (2021) 312. doi: 10.1002/onco.13832
65. Rousseau B, Foote M, Maron S, Diplas B, Lu S, Argiles G, et al. The Spectrum of Benefit From Checkpoint Blockade in Hypermutated Tumors. *New Engl J Med* (2021) 384(12):1168–70. doi: 10.1056/NEJMc2031965
66. Roudko V, Greenbaum B, Bhardwaj N. Computational Prediction and Validation of Tumor-Associated Neoantigens. *Front Immunol* (2020) 11:27. doi: 10.3389/fimmu.2020.00027
67. Wagner S, Mullins S C, Linnebacher M. Colorectal Cancer Vaccines: Tumor-Associated Antigens vs Neoantigens. *World J Gastroenterol* (2018) 24 (48):5418–32. doi: 10.1007/s12519-013-0433-1
68. Speetjens FM, Lauwen MM, Franken KL, Rhijn CMJ, Duikeren S, Bres SA, et al. Prediction of the Immunogenic Potential of Frameshift-Mutated Antigens in Microsatellite Instable Cancer. *Int J Cancer* (2008) 845:838–45. doi: 10.1002/ijc.23570
69. Maletzki C, Schmidt F, Dirks WG, Schmitt M, Linnebacher M. Frameshift-Derived Neoantigens Constitute Immunotherapeutic Targets for Patients With Microsatellite-Instable Haematological Malignancies: Frameshift Peptides for Treating MSI+ Blood Cancers. *Eur J Cancer* (2013) 49 (11):2587–95. doi: 10.1016/j.ejca.2013.02.035
70. Turajlic S, Litchfield K, Xu H, Rosenthal R, McGranahan N, Reading JL, et al. Insertion-And-Deletion-Derived Tumour-Specific Neoantigens and the Immunogenic Phenotype: A Pan-Cancer Analysis. *Lancet Oncol* (2017) 18 (8):1009–21. doi: 10.1016/S1470-2045(17)30516-8
71. Roudko V, Bozkus CC, Orfanelli T, McClain C, Carr C, O'Donnel T, et al. Shared Immunogenic Poly-Epitope Frameshift Mutations in Microsatellite Unstable Tumors. *Cell* (2020) 183(6):1634–49. doi: 10.1016/j.cell.2020.11.004
72. Ballhausen A, Przybilla MJ, Jendrusch M, Haupt S, Pfaffendorf E, Seidler F, et al. The Shared Frameshift Mutation Landscape of Microsatellite-Unstable Cancers Suggests Immunoediting During Tumor Evolution. *Nat Commun* (2020) 11:1–13. doi: 10.1038/s41467-020-18514-5
73. Mandal R, Samstein RM, Lee K, Havel JJ, Wang H, Krishna C, et al. Genetic Diversity of Tumors With Mismatch Repair Deficiency Influences Anti – PD-1 Immunotherapy Response. *Science* (2019) 491:485–91. doi: 10.1126/science.aau0447
74. Guan J, Lu C, Jin Q, Fu Y-X, Li G-M. MLH1 Deficiency-Triggered DNA Hyperexcision by Exonuclease 1 Activates the cGAS-STING Pathway. *Cancer Cell* (2021) 39:109–21. doi: 10.1016/j.ccell.2020.11.004
75. Lu C, Guan J, Lu S, Jin Q, Rousseau B, Lu T, et al. DNA Sensing in Mismatch Repair-Deficient Tumor Cells Is Essential for Anti-Tumor Immunity. *Cancer Cell* (2021) 39:96–108. doi: 10.1016/j.ccell.2020.11.006
76. Mowat C, Mosley SR, Namdar A, Schiller D, Baker K. Anti-Tumor Immunity in Mismatch Repair-Deficient Colorectal Cancers Requires Type I IFN – Driven CCL5 and CXCL10. *J Exp Med* (2021) 218(9). doi: 10.1084/jem.20210108
77. Magnus Von Knebel D, Matthias K. Towards a Vaccine to Prevent Cancer in Lynch Syndrome Patients. *Familial Cancer* (2013) 12:307–12. doi: 10.1007/s10689-013-9662-7
78. Maruvka YE, Mouw KW, Karlic R, Parasuraman P, Kamburov A, Polak P, et al. Analysis of Somatic Microsatellite Indels Identifies Driver Events in Human Tumors. *Nat Biotechnol* (2017) 35(10):951–9. doi: 10.1038/nbt.3966
79. Haasl R, Payseur B. Remarkable Selective Constraints on Exonic Dinucleotide Repeats. *Evolution* (2014) 68(9):2737–44. doi: 10.1111/evo.12460.REMARKABLE
80. Catalano I, Grassi E, Bertotti A, Trusolino L. Immunogenomics of Colorectal Tumors: Facts and Hypotheses on an Evolving Saga. *Trends Cancer* (2019) 80(18):1–10. doi: 10.1016/J.TRECAN.2019.10.006
81. Leoni G, Alise AMD, Cotugno G, Langone F, Garzia I, De Lucia M, et al. A Genetic Vaccine Encoding Shared Cancer Neoantigens to Treat Tumors With Microsatellite Instability. *Cancer Res* (2020) 80:3972–82. doi: 10.1158/0008-5472.CAN-20-1072
82. Kloor M, Reuschenbach M, Pauligk C, Karbach J, Rafiyan M-R, Al-Batran S-E, et al. A Frameshift Peptide Neoantigen-Based Vaccine for Mismatch Repair-Deficient Cancers: A Phase I/IIa Clinical Trial. *Clin Cancer Res* (2020) 1(603):1–31. doi: 10.1158/1078-0432.CCR-19-2706
83. Saterdal I, Gjertsen M, Straten P, Gaudernack G. A TGFbRII Frameshift-Mutation-Derived CTL Epitope Recognised by HLA-A2-Restricted CD8 + T Cells. *Cancer Immunol Res* (2001) 50:469–76. doi: 10.1007/s002620100222
84. Sæterdal I, Bjørheim J, Lislerud K, Gjertsen MK, Bukholm IK, Olsen OC, et al. Frameshift-Mutation-Derived Peptides as Tumor-Specific Antigens in Inherited and Spontaneous Colorectal Cancer. *PNAS* (2001) 98(23):13255–60. doi: 10.1073/pnas.231326898
85. Garbe Y, Maletzki C, Linnebacher M. An MSI Tumor Specific Frameshift Mutation in a Coding Microsatellite of MSH3 Encodes for HLA-A0201-Restricted CD8+ Cytotoxic T Cell Epitopes. *PloS One* (2011) 6(11):2–9. doi: 10.1371/journal.pone.0026517
86. Kloor M, Huth C, Voigt AY, Benner A, Schirmacher P, Doeberitz MVK, et al. Prevalence of Mismatch Repair-Defi Cient Crypt Foci in Lynch Syndrome: A Pathological Study. *Lancet Oncol* (2012) 13(6):598–606. doi: 10.1016/S1470-2045(12)70109-2
87. Hess JM, Bernards A, Kim J, Miller M, Taylor-Weiner A, Haradhvala NJ, et al. Passenger Hotspot Mutations in Cancer. *Cancer Cell* (2019) 36 (3):675801. doi: 10.1101/675801
88. Tu J, Park S, Yu W, Zhang S, Wu L, Carmon K, et al. The Most Common RNF43 Mutant G659Vfs*41 Is Fully Functional in Inhibiting Wnt Signaling and Unlikely to Play a Role in Tumorigenesis. *Sci Rep* (2019) 9(1):1–12. doi: 10.1038/s41598-019-54931-3
89. Willis JA, Reyes-Uribe L, Chang K, Lipkin SM, Vilar E. Immune Activation in Mismatch Repair–Deficient Carcinogenesis: More Than Just Mutational Rate. *Clin Cancer Res* (2019) 24):11–8. doi: 10.1158/1078-0432.ccr-18-0856
90. Alise AMD, Leoni G, Cotugno G, Troise F, Langone F, Fichera I, et al. Adenoviral Vaccine Targeting Multiple Neoantigens as Strategy to Eradicate Large Tumors Combined With Checkpoint Blockade. *Nat Commun* (2019) 10(2688):1–12. doi: 10.1038/s41467-019-10594-2
91. Gebert J, Gelincik O, Marshall JD, Urban K, Long M, Cortes E, et al. Recurrent Frameshift Neoantigen Vaccine Elicits Protective Immunity With Reduced Tumor Burden and Improved Overall Survival in a Lynch Syndrome Mouse Model. *Gastroenterology* (2021). doi: 10.1053/j.gastro.2021.06.073
92. Abidi A, Gorris MAJ, Brennan E, Jongmans MCJ, Weijers DD, Kuiper RP, et al. Challenges of Neoantigen Targeting in Lynch Syndrome and Constitutional Mismatch Repair Deficiency Syndrome. *Cancers* (2021) 13 (10):2345. doi: 10.3390/cancers13102345
93. Amodio V, Mauri G, Reilly NM, Sartore-bianchi A, Siena S, Bardelli A, et al. Mechanisms of Immune Escape and Resistance to Checkpoint Inhibitor Therapies in Mismatch Repair Deficient Metastatic Colorectal Cancers. *Cancers* (2021) 13:1–33. doi: 10.3390/cancers13112638
94. Montesion M, Murugesan K, Jin DX, Sharaf R, Sanchez N, Guria A, et al. Somatic HLA Class I Loss Is a Widespread Mechanism of Immune Evasion Which Refines the Use of Tumor Mutational Burden as a Biomarker of Checkpoint Inhibitor Response. *Cancer Discovery* (2021) 11:282–92. doi: 10.1158/2159-8290.CD-20-0672
95. Williams DS, Bird MJ, Jorissen RN, Yu YL, Walker F, Hua H, et al. Nonsense Mediated Decay Resistant Mutations Are a Source of Expressed Mutant Proteins in Colon Cancer Cell Lines With Microsatellite Instability. *PloS One* (2010) 5(12). doi: 10.1371/journal.pone.0016012
96. Litchfield K, Reading J, Lim E, Xu H, Liu P, Al-bakir M, et al. Escape From Nonsense Mediated Decay Associates With Anti-Tumor Immunogenicity. *Nat Commun* (2020) 11:3800. doi: 10.1038/s41467-020-17526-5
97. Kwon M, An M, Klempner SJ, Lee H, Kim K, Jason K, et al. Determinants of Response and Intrinsic Resistance to PD-1 Blockade in Microsatellite

Instability-High Gastric Cancer. *Cancer Discovery* (2021) 02:2168–85. doi: 10.1158/2159-8290.CD-21-0219
98. Sahin IH, Akce M, Alese O, Shaib W, Lesinski GB, El-Rayes B, et al. Immune Checkpoint Inhibitors for the Treatment of MSI-H/MMR-D Colorectal Cancer and a Perspective on Resistance Mechanisms. *Br J Cancer* (2019) 121(10):809–18. doi: 10.1038/s41416-019-0599-y
99. Tikidzhieva A, Benner A, Michel S, Formentini A, Link K, Dippold W, et al. Microsatellite Instability and Beta2-Microglobulin Mutations as Prognostic Markers in Colon Cancer: Results of the FOGT-4 Trial. *Br J Cancer* (2012) 106:1239–45. doi: 10.1038/bjc.2012.53
100. Middha S, Yaeger R, Shia J, Stadler K, King S, Guercio S, et al. Majority of B2M-Mutant and -Deficient Colorectal Carcinomas Achieve Clinical Benefit From Immune Checkpoint Inhibitor Therapy and Are Microsatellite Instability-High. *JCO Precis Oncol* (2019) 3:1–14. doi: 10.1200/PO.18.00321
101. Germano G, Lu S, Rospo G, Lamba S, Rousseau B, Fanelli S, et al. CD4 T Cell–Dependent Rejection of Beta-2 Microglobulin Null Mismatch Repair – Deficient Tumors. *Cancer Discovery* (2021) 11(11):1845–59. doi: 10.1158/2159-8290.CD-20-0987
102. Black JRM, Mcgranahan N. Genetic and non-Genetic Clonal Diversity in Cancer Evolution. *Nat Rev Cancer* (2021) 21:379–92. doi: 10.1038/s41568-021-00336-2
103. Nam A, Chaligne R, Landau DA. Integrating Genetic and Non-Genetic Determinants of Cancer Evolution by Single-Cell Multi-Omics. *Nat Rev Genet* (2021) 22:3–18. doi: 10.1038/s41576-020-0265-5

Conflict of Interest: The authors declare that the research was conducted in the absence of any commercial or financial relationships that could be construed as a potential conflict of interest.

Publisher's Note: All claims expressed in this article are solely those of the authors and do not necessarily represent those of their affiliated organizations, or those of the publisher, the editors and the reviewers. Any product that may be evaluated in this article, or claim that may be made by its manufacturer, is not guaranteed or endorsed by the publisher.

frontiers in Oncology

ORIGINAL RESEARCH
published: 28 September 2021
doi: 10.3389/fonc.2021.741013

TNFα Signaling Is Increased in Progressing Oral Potentially Malignant Disorders and Regulates Malignant Transformation in an Oral Carcinogenesis Model

Jeffrey W. Chadwick[1,2], *Rachel Macdonald*[1], *Aiman A. Ali*[1], *Michael Glogauer*[1,2] *and Marco A. Magalhaes*[1,3*]

[1] Faculty of Dentistry, University of Toronto, Toronto, ON, Canada, [2] Department of Dental Oncology and Maxillofacial Prosthetics, Princess Margaret Cancer Centre, University Health Network, Toronto, ON, Canada, [3] Department of Dentistry, Sunnybrook Health Sciences Centre, Toronto, ON, Canada

OPEN ACCESS

Edited by:
Sjoerd H Van Der Burg, Leiden University, Netherlands

Reviewed by:
Tibor Bakacs, Alfred Renyi Institute of Mathematics, Hungary
Amer Najjar, University of Texas MD Anderson Cancer Center, United States

***Correspondence:**
Marco A. Magalhaes
marco.magalhaes@dentistry.utoronto.ca

Specialty section:
This article was submitted to Cancer Immunity and Immunotherapy, a section of the journal Frontiers in Oncology

Received: *14 July 2021*
Accepted: *24 August 2021*
Published: *28 September 2021*

Citation:
Chadwick JW, Macdonald R, Ali AA, Glogauer M and Magalhaes MA (2021) TNFα Signaling Is Increased in Progressing Oral Potentially Malignant Disorders and Regulates Malignant Transformation in an Oral Carcinogenesis Model. Front. Oncol. 11:741013. doi: 10.3389/fonc.2021.741013

Oral carcinogenesis represents a multi-stage process which encompasses several genetic and molecular changes that promote the progression of oral potentially malignant disorders (OPMDs) to oral squamous cell carcinomas (OSCCs). A better understanding of critical pathways governing the progression of OMPDs to OSCCs is critical to improve oncologic outcomes in the future. Previous studies have identified an important role of tumor necrosis factor α (TNFα) and TNF receptor 1 (TNFR1) in the invasiveness of oral cancer cell lines. Here, we investigate the expression of TNFα and TNFR1 in human OPMDs that progress to OSCC compared to non-progressing OPMDs utilizing fluorescent immunohistochemistry (FIHC) to show increased TNFα/TNFR1 expression in progressing OPMDs. In order to interrogate the TNFα/TNFR1 signaling pathway, we utilized a 4-nitroquinoline 1-oxide (4-NQO) mouse model of oral carcinogenesis to demonstrate that TNFα/TNFR1 expression is upregulated in 4-NQO-induced OSCCs. TNFα neutralization decreased serum cytokines, inhibited the development of invasive lesions and reduced tumor-associated neutrophils *in vivo*. Combined, this data supports the role of TNFα in oral malignant transformation, suggesting that critical immunoregulatory events occur downstream of TNFR1 leading to malignant transformation. Our results advance the understanding of the mechanisms governing OSCC invasion and may serve as a basis for alternative diagnostic and therapeutic approaches to OPMDs and OSCC management.

Keywords: carcinogenesis, squamous cell carcinoma, dysplasia, neutrophils, inflammation, TNFa

INTRODUCTION

Cancers affecting the oral cavity represent a heterogeneous group of disorders involving the region which is bounded posteriorly by the plane connecting the circumvallate papillae of the tongue and junction of the hard and soft palate and anteriorly by the mucosal surfaces of the labium superius and inferius oris. Approximately 75-90% of oral malignancies are oral squamous cell carcinomas

(OSCCs) (1, 2). OSCC incidence varies widely depending on geographic region and can be influenced by primary etiological factors which commonly include tobacco, areca nut and alcohol exposure (3). OSCC diagnosis and staging are predicated upon clinical, radiographic and histopathologic evaluation with treatment assuming either single-modality or multi-modal therapy composed of a combination of surgery, external beam radiation and chemotherapy (4–7). Unfortunately, morbidity associated with treatment is considerable and long-term survival associated with advanced OSCC remains low (8, 9).

The development of OSCCs may be preceded by oral potentially malignant disorders (OPMDs) which represent a subset of conditions that possess an increased risk of progression to cancer (10). A 10-year review of the University of Toronto Oral Pathology Service showed that OPMDs are more prevalent than the combination of both benign and malignant tumors of the oral cavity (2). These conditions include, but are not limited to, leukoplakia, erythroplakia, lichen planus and oral submucous fibrosis. Risk assessment and management of OPMDs, despite unfettered access for direct visual examination of the oral cavity, is challenging. While several clinical parameters may increase suspicion of increased cancer risk, the mainstay for diagnosis and monitoring is tissue biopsy and histopathological evaluation to detect features of oral epithelial dysplasia (OED) or OSCC (11). There are many challenges in assessing risk of malignant progression in OPMDs. For example, the selection of biopsy location may not be representative of the entire lesion and histopathological grading of OED is often challenging and may not adequately stratify risk of progression. Other adjunct non-invasive diagnostic tests such as cytology, autofluorescence and spectroscopy have failed to consistently and reliably detect malignant progression (12–14). The need to identify molecular biomarkers capable of stratifying OSCC progression risk are in high demand. As such, unravelling the mechanisms by which OPMDs progress to OSCCs is critical for improving outcomes through the development of innovative diagnostic and treatment modalities.

The mechanisms governing malignant transformation are poorly understood which hamper our ability to provide interceptive therapy in the setting of OPMDs to reduce downstream disease morbidity and mortality. A dysregulated host immune system response within the tumor microenvironment has been identified as a significant factor influencing malignant progression (15, 16). Early work from our laboratory demonstrated a TNFα-dependent increase in OSCC invasiveness, invadopodia formation and matrix degradation (17). More recently, we also showed elevated neutrophil and lymphocyte in OPMDs and OSCCs as well as significantly elevated expression of TNFα in saliva samples of patients diagnosed with OSCC (18). Further, we characterized a phosphoinositide 3-kinase and Src-dependent mechanism for TNFα/TNF receptor 1 (TNFR1) mediated invadopodia formation and OSCC invasion *in vitro* but have not yet addressed this phenomenon *in vivo*.

Animal models of oral cancer have been developed and serve as indispensable tools for the study of the molecular and genetic mechanisms which govern oral carcinogenesis. These models are especially significant as the spontaneous occurrence of OSCCs in laboratory animals is exceptionally rare (19). Experimental induction of OSCCs within the mouse oral cavity through exposure to 4-nitroquinoline 1-oxide (4-NQO) is especially relevant for the study of both malignant and pre-malignant conditions. 4-NQO is a water-soluble quinoline derivative that facilitates DNA adduct formation and strand breaks (20, 21). Protracted administration of 4-NQO to mice via direct topical application or through its addition to drinking water produces a multitude of dysplastic, preneoplastic and neoplastic lesions which recapitulate the temporal, histologic and molecular progression of human OSCC development (22, 23). Other advantages of the use of this model over other popular xenograft and transgenic systems include the maintenance of an intact immune system and predictable progression to OSCC in an orthotopic manner (24, 25).

Here we utilize fluorescent immunohistochemistry (FIHC) and a semi-automated analysis algorithm on human samples of non-progressing and progressing OPMDs and demonstrate increased TNFα/TNFR1 signaling and inflammatory cell recruitment in progressing OPMDs. To determine the role of this pathway in carcinogenesis and progression, we utilize the mouse 4-NQO-induced oral carcinogenesis model and TNFα neutralization. The results show a decreased occurrence of invasive OSCCs in TNFα-neutralized animals. Using a similar FIHC approach, depletion of TNFα was found to reduce both TNFα and TNFR1 expression.

METHODS

Human Study Population

A retrospective analysis was conducted utilizing oral biopsy specimens retrieved from the archives of the Toronto Oral Pathology Service (Faculty of Dentistry, University of Toronto) between December 2005 and January 2014. A total of 20 formalin fixed paraffin embedded (FFPE) samples were selected for analysis (**Supplemental Table 1**). The progressing cohort was comprised of 10 cases of OSCC (any subsite) possessing a previously submitted biopsy specimen demonstrating any grade of epithelial dysplasia from the same anatomic region of interest. The study cohort consisted of 10 progressing cases divided into three groups based on diagnosis: hyperkeratosis without dysplasia (HK; n=2), low-grade dysplasia (LGD; n=3) and high-grade dysplasia (HGD; n=5). The selected cases possessed a minimum of five years of histopathologic follow up, adequate material for analysis and no significant artifacts within the processed sections. The non-progressing cohort was comprised of 10 randomly selected cases of oral epithelial dysplasia which did not demonstrate histopathologic progression to OSCC over a period of nine years: HK (n=3), LGD (n=3) and HGD (n=4). All slides were reviewed by M.A.M. and A.A. The included cases of HK did not possess either the histopathologic or clinical criteria for a diagnosis of proliferative verrucous leukoplakia (PVL). The study was approved by the University of Toronto Research Ethics Board (Protocol 38933).

Animals

A total of 43 six-week-old immunocompetent female C57BL/6 mice (Charles River Laboratories) were acquired and allowed a two-week acclimation period with *ad libitum* access to filtered water and standard chow in a temperature- and humidity-controlled environment with a 12-hour light and 12-hour dark cycle. All mouse studies complied with the relevant ethical regulations and were approved by the University of Toronto Animal Care Committee and the Research Ethics Board (Protocol 20011940).

4-NQO Administration

Animals were maintained on a normal chow. 4-NQO (Sigma) stock solution was prepared weekly in propylene glycol to a final concentration of 5 mg/mL and stored in a light-protected vessel at 4°C. The 4-NQO stock solution was diluted in the drinking water to a final concentration of 100 μg/mL and changed weekly in amber-colored bottles to prevent 4-NQO photodegradation. Mice were divided into an experimental group receiving 4-NQO-containing drinking water (n=33) or a control group (n=10) where drinking water contained propylene glycol (vehicle). Mice in both groups were allowed *ad libitum* access to drinking water. After a 16-week 4-NQO treatment period, mice from both groups were returned to and maintained on standard drinking water until sacrifice, independent of further experimental intervention.

Antibody Administration

Following the 16-week treatment period, 13 mice that had received 4-NQO were randomly selected and divided into groups that received either 0.5 mg of InVivoPlus anti-mouse TNFα antibody (Clone XT3.11, BioXCell, n=6) or 0.5 mg of InVivoPlus rat IgG1 isotype control anti-horseradish peroxidase (HRP) (Clone HRPN, BioXCell, n=7). Both antibodies were diluted into InVivoPure pH 7.0 Dilution Buffer (BioXCell) and injected on a weekly basis for a total of eight weeks via intraperitoneal injection. Blood was collected via the saphenous vein for analysis prior to antibody treatment and at the four-week time point. All animals, including those that only received 4-NQO (n=20), were sacrificed at the eight-week time point. Those animals which did not survive until the experimental endpoint of eight-weeks (n=1, 4-NQO only; n=1, 4-NQO and anti-TNFα treatment) were excluded from the final analysis. Animals demonstrating oral lesions were euthanized prior to the experimental endpoint if lesions became ulcerated or resulted in deteriorating health conditions or pain as per standard operation procedures within the Division of Comparative Medicine including huddled posture, vocalization, hypothermia, or weight loss exceeding 20%. Blood and the entirety of the tongue were retrieved from all animals following humane euthanasia for analysis.

Conventional Histopathology

Resected tongue specimens from experimental animals were immediately placed in 10% buffered formalin following their excision. Clinical photographs of the tongues were acquired prior to excision. Tissue samples were later bisected and one half was embedded in paraffin from which five-micron tissue sections were subsequently prepared and stained with hematoxylin and eosin (H&E). All slides were reviewed by M.A.M. and A.A for histopathologic characterization of oral tongue lesions using a DM2000 light microscope (Leica) at 100X total magnification.

Fluorescent Immunohistochemistry (FIHC)

Five-micron sections were prepared from both human and animal formalin-fixed paraffin-embedded (FFPE) specimen blocks. After heating for 30 minutes at 60°C, slides were immersed in an antigen retrieval buffer (100X Citrate Buffer pH 6.0; Abcam) for one hour at 98°C followed by a wash with 1X Tris-buffered saline with 0.1% Tween® 20 Detergent (TBS-T; Millipore) and permeabilized with 0.5% Triton X-100 (BioShop) for five minutes. The tissue sections were washed with TBS-T and then blocked in Sea Block Serum free -PBS (Abcam) for two hours at room temperature. Human sections were treated by overnight incubation with the following primary antibodies: Rabbit polyclonal anti-TNFR1 (1:200 dilution; Abcam), rabbit polyclonal anti-TNFα (1:250 dilution; Abcam), mouse monoclonal anti-CD45 (1:1000 dilution; Abcam). In the same manner, mouse sections were incubated overnight with the following primary antibodies: Rabbit polyclonal anti-TNFR1 (1:200 dilution; Abcam) and rabbit polyclonal anti-TNFα (1:250 dilution; Abcam). On the following day, slides were washed three times with 1X Tris-buffered saline and 0.1% Tween 20 detergent (TBS-T, Millipore) and incubated for one hour with the following secondary antibodies at room temperature: Anti-rabbit Alexa Fluor® 586 (Abcam), anti-mouse Alexa Fluor® 488 (Abcam). The tissue sections were then rinsed with TBS-T three times for five minutes and 4′,6-diamidino-2-phenylindole (DAPI; Thermo Fisher Scientific) was applied for 30 minutes. After washing with TBS-T three times for five minutes, slides were mounted with ProLong TM Diamond Antifade Mountant (Thermo Fisher Scientific) and imaged the same day. A second set of histology sections were stained using Alexa Fluor® 594 anti-mouse Ly6G (1:500 dilution; BioLegend) which did not require secondary staining.

FIHC Data Analysis

Ten images were acquired from multiple regions of each tissue section using the SP8 confocal microscope (Leica) for human samples and the Quorum Spinning Disk confocal microscope (Quorum Technologies Inc.) for mouse specimens. Data analysis was performed using Volocity Image Analysis Software (PerkinElmer) using a custom protocol that detected positive expression based on fluorescent intensity and area for both human and mouse specimens (26). Identification of morphological features within each tissue section was accomplished using DAPI. For each image, the region of interest (ROI) was manually defined to segment the epithelium and lamina propria (connective tissue) for human specimens and basal/parabasal epithelium and lamina propria for mouse specimens. Where present, the walls and the lumen of medium-sized blood vessels within the lamina propria were removed from the ROI. TNFα and TNFR1 positive cells were identified using an automated protocol based on pixel intensity, selecting those which were greater than or equal to three standard deviations (SD) above the mean intensity of the designated channel. Both the area of the positive pixels

normalized to the area of the ROI as well as the mean fluorescence intensity (MFI) were calculated for each image and averaged from a minimum of five images per specimen. Those images with significant artefactual variations and background autofluorescence were removed from the analysis. Muscular layers and dilated blood vessels were cropped from each image before analysis. Neutrophil quantification from mouse specimens was accomplished by manually counting $Ly6G^+$ cells in 10 high-power fields. The mean number of $Ly6G^+$ cells per field was calculated and considered as the final neutrophil count for analysis.

Flow Cytometry

Whole blood obtained via cardiac puncture at the time of animal sacrifice was fixed with fresh, methanol-free, 1.6% formaldehyde (Thermo Fisher Scientific) for 15 minutes on ice prior to processing. Red blood cell lysis was achieved with two sequential five minute treatments of 1x BD Pharm Lyse (BD Biosciences). Cells (5×10^5) were resuspended in fluorescence-active cell shorting (FACS) buffer composed of 1x Hank's balanced salt solution (HBSS) without calcium and magnesium (Gibco), 1% bovine serum albumin (BioShop) and 2mM EDTA (BioShop). Samples were blocked with 2 μg mouse (Sigma-Aldrich) and 60 μg rat (Sigma-Aldrich) serum for 20 minutes, labeled with anti-mouse Ly6G (1A8, BD Bioscience) and F4/80 (BM8, BioLegend) for 30 minutes on ice in the dark, and washed three times with FACS buffer. Sample acquisition was performed using the BD LSRFortessa X-20 flow cytometer with FACSDiva 8.0.1 (BD Biosciences) and analyzed with FlowJo v10.0.7 (Tree Star). Flow cytometer channel voltages were calibrated manually using Rainbow Calibration Particles (Spherotech) and compensation was performed with single-stained OneComp eBeads Compensation Beads (Invitrogen). Appropriate isotype control antibodies and fluorescence minus one (FMO) samples were prepared to establish negative staining characteristics for each antibody. A minimum of 2×10^5 gated neutrophil events ($Ly6G^+F4/80^-$) were acquired for each sample.

Cytokine Analysis

Serum was prepared from blood samples recovered from experimental animals at 0, 4 and 8 weeks following the termination of 4-NQO or vehicle exposure. Luminex® assays were conducted in 96-well plates according to manufacturer instructions for the Millipore Mouse Cytokine/Chemokine Magnetic Bead Panel (MCYTOMAG-70K, EMD Millipore). Analytes included G-CSF, GM-CSF, M-CSF, IFN-γ, IL-1α, IL-1β, IL-2, IL-3, IL-4, IL-5, IL-6, IL-7, IL-9, IL-10, IL-12 (p40), IL-12 (p70), IL-13, IL-15, IL-17, LIF, LIX, IP-10, KC, MCP-1, MIP-1α, MIP-1β, MIP-2, MIG, TNFα, VEGF, RANTES and Eotaxin/CCL11. Briefly, plates were pre-washed and serum samples were incubated at 4°C overnight with buffer and mixed magnetic beads. Wells were then washed after which detection antibodies were added and allowed to incubate at room temperature for 60 minutes. Streptavidin-phycoerythrin was subsequently added to each well and incubated at room temperature for an additional 30 minutes. A final wash of the plate was then performed and followed by the addition of sheath fluid to each well. The plate was analyzed on the Luminex® MAGPIX® System at the Princess Margaret Genomics Center. The concentrations (pg/L) of cytokines and chemokines were quantified based on a standard curve and normalized to control samples.

Statistical Analysis

One-way or two-way analysis of variance (ANOVA) and Tukey's multiple comparison tests were conducted to assess differences between progressing and non-progressing OPMDs and Fisher's exact test was used to compare 4-NQO-induced tumor outcomes. All statistical analyses were performed using Prism 7.0 (GraphPad). The differences were considered statistically significant if $p<0.05$. Error bars represent standard error of the mean (SEM) unless otherwise indicated.

RESULTS

Increased TNFα and TNFR1 Expression and Immune Cell Recruitment in Progressing OPMDs

TNFα expression was quantified in oral biopsy samples using the MFI of TNFα within the lamina propria. A significant increase in TNFα MFI in progressing OPMDs as compared to non-progressing OPMDs (**Figures 1A, B**) was observed across all histologic diagnoses including progressing hyperkeratosis ($p<0.01$), progressing low-grade dysplasia (mild epithelial dysplasia, $p<0.05$) and progressing high-grade dysplasia (moderate and severe epithelial dysplasia, $p<0.001$). The expression of TNFR1 and OPMD-associated $CD45^+$ immune cells (**Figure 2A**) within the lamina propria and epithelium of non-progressing and progressing lesions was also quantified as the average positive area per field. There was a significant increase in TNFR1 ($p<0.0001$) and CD45 ($p<0.01$) expression within the lamina propria of progressing samples compared to non-progressing samples (**Figure 2B**). Further, a significant increase in $TNFR1^+CD45^+$ immune cells ($p<0.0001$) was also noted in progressing lesions. While no differences were noted in TNFR1 expression within the epithelium, our results demonstrate an increase in intraepithelial $CD45^+$ immune cells ($p<0.0001$) and $TNFR1^+CD45^+$ ($p<0.0001$) expression in progressing samples compared to non-progressing samples (**Figure 2C**).

The 4-NQO Mouse Model of Head and Neck Cancer Produces an Array of OPMDs and Malignant Lesions

At the time of sacrifice, all animals that had received 4-NQO demonstrated mucosal abnormalities involving the tongue. Visual examination of the remainder of the gastrointestinal tract did not demonstrate gross disease in any of the subjects. Animals receiving only vehicle did not demonstrate any mucosal abnormalities along the entire GI tract. For those animals exposed to 4-NQO, tongue lesions were found to be both unifocal and multifocal and demonstrated a variety of gross appearances including hyperkeratotic papules, leukoplakic nodules and exophytic masses (**Supplemental Figure 1A**). It should be noted that regular examination under anesthesia

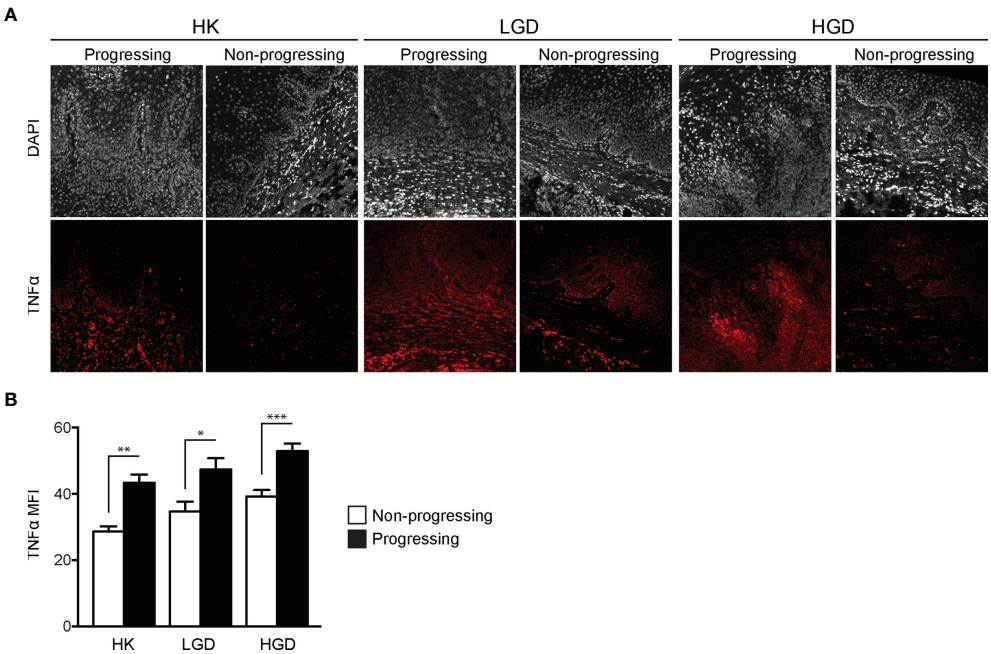

FIGURE 1 | FIHC analysis of TNFα expression in human progressing and non-progressing OPMDs. **(A)** Representative FIHC images of human progressing and non-progressing patient OPMDs consisting of HK, LGD and HGD (white channel – DAPI; red channel – TNFα). **(B)** MFI of TNFα within the lamina propria of human progressing and non-progressing OPMDs. *p < 0.05; **p < 0.01; ***p < 0.001; HK, Hyperkeratosis; LGD, Low-grade dysplasia (mild dysplasia); HGD, High-grade dysplasia (moderate and severe dysplasia); MFI, Mean fluorescence intensity; DAPI, 4′,6-diamidino-2-phenylindole dihydrochloride; FIHC, Fluorescence immunohistochemistry; OPMD, Oral potentially malignant disorderdisorder; TNFα, Tumor necrosis factor α.

following the cessation of 4-NQO exposure and prior to sacrifice was avoided due to the anticipated systemic fragility during carcinogenesis resulting in potential loss of subjects. Expectedly, animals treated with 4-NQO demonstrated significantly decreased body weight relative to controls following the completion of 4-NQO delivery and at the time of sacrifice (**Supplemental Figure 1B**). Microscopic evaluation of H&E stained tissue sections amongst those animals receiving 4-NQO revealed a relatively broad distribution of EH (epithelial hyperplasia), LGD, HGD, carcinoma *in situ* (CIS) and OSCC (**Supplemental Figure 1C**).

Neutralization of TNFα Inhibits OSCC Invasion in Immunocompetent Mice

To study the effect of TNFα blockade in oral carcinogenesis, immunocompetent mice received anti-TNFα antibody injections following the completion of a 16-week exposure to 4-NQO. As expected, control animals (n=6) that received only vehicle and no antibody treatment demonstrated a normal histologic architecture of the tongue (**Figure 3A**). Animals receiving 4-NQO and isotype antibody (n=7) developed lesions that were consistent with either OSCC (n=5, 71.4%) or dysplastic lesions suspicious for invasion (n=2, 28.6%) (**Figure 3B**). Animals receiving 4-NQO and anti-TNFα antibody therapy (n=5) showed dysplastic changes compared to vehicle-treated controls (**Figure 3C**). However, TNFα-neutralized animals did not develop invasive OSCC lesions, demonstrating only those histologic features consistent with high-grade dysplasia (p=0.0278, Fisher's exact test).

To determine TNFα and TNFR1 expression, FIHC analysis was performed on specimens from vehicle, 4-NQO/isotype antibody and 4-NQO/anti-TNFα antibody treated animals (**Figure 4A**). TNFα and TNFR1 expression were quantified in an analogous manner to human samples. A significant decrease in TNFα MFI was noted in 4-NQO/anti-TNFα antibody treated animals compared to 4-NQO/isotype antibody treated animals within the lamina propria (**Figure 4B**) as well as the basal and parabasal layers of the epithelium (**Figure 4C**). There were significant increases in TNFR1 MFI within the lamina propria between control and 4-NQO/anti-TNFα animals relative to 4-NQO/isotype antibody treated animals (**Figure 4B**). No differences were noted in TNFR1 MFI within the epithelial layers between any group (**Figure 4C**).

Chemically-Induced Carcinogenesis Induces Neutrophil Recruitment to Tissues and Neutrophilia in the Peripheral Circulation

To evaluate the recruitment of neutrophils in the setting of 4-NQO-induced carcinogenesis, we utilized FIHC to quantify $Ly6G^+$ cells within the lamina propria (**Figure 5A**). Our results demonstrated a significant increase in $Ly6G^+$ cells after 4-NQO treatment compared to controls (p<0.001). Neutralization of TNFα inhibited the recruitment of neutrophils to the tumor microenvironment induced by 4-NQO treatment (**Figure 5B**) with no significant

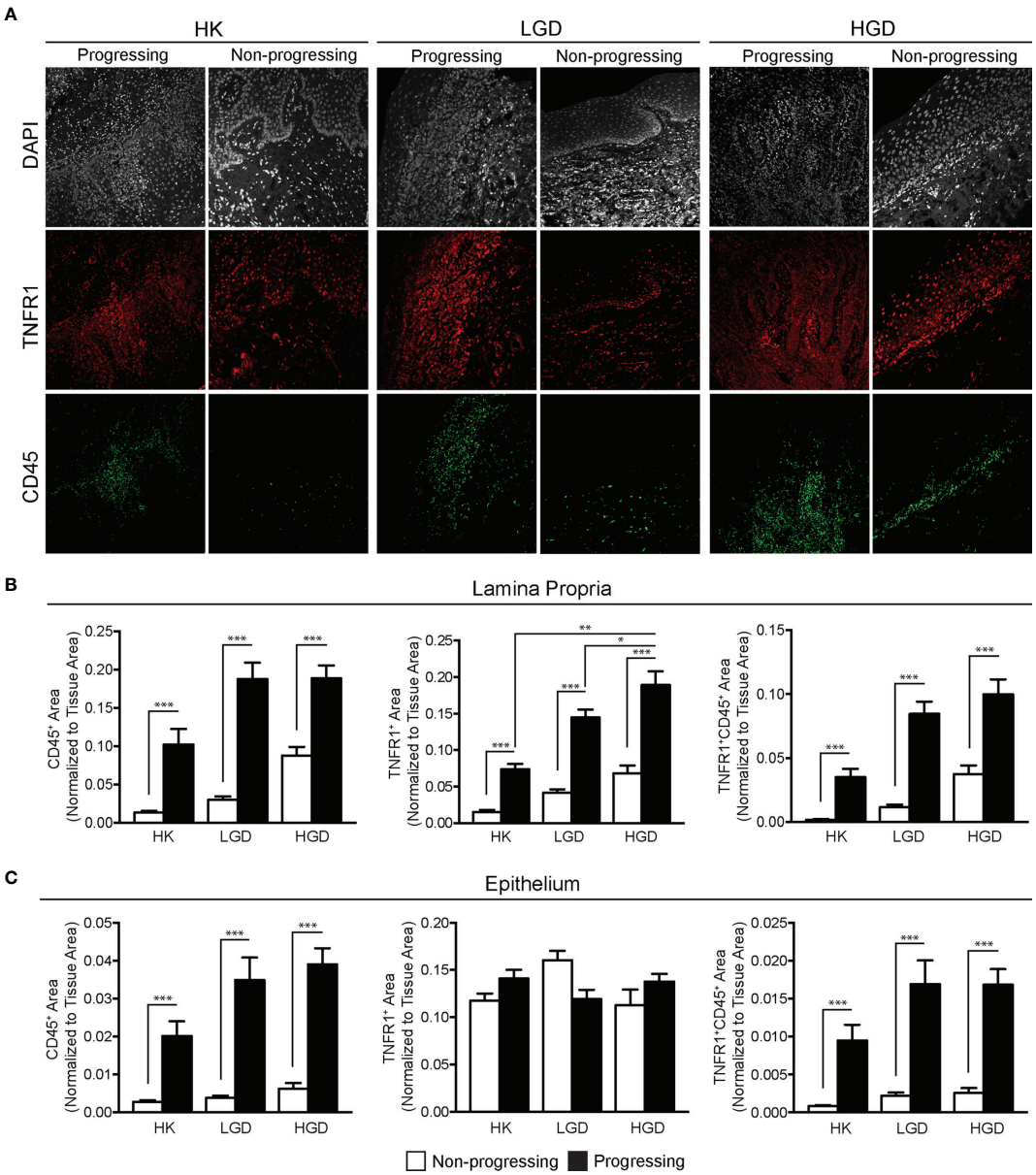

FIGURE 2 | FIHC analysis of TNFR1 and CD45 expression in human progressing and non-progressing OPMDs. **(A)** Representative FIHC images of human progressing and non-progressing OPMDs consisting of HK, LGD and HGD (white channel – DAPI; red channel – TNFR1; green channel: CD45). **(B)** $CD45^+$, $TNFR1^+$ and $CD45^+TNFR1^+$ area within the lamina propria of human progressing and non-progressing OPMDs. **(C)** $CD45^+$, $TNFR1^+$ and $CD45^+/TNFR1^+$ area within the epithelium of human progressing and non-progressing OPMDs. *$p < 0.05$; **$p < 0.01$; ***$p < 0.001$; HK, Hyperkeratosis; LGD, Low-grade dysplasia (mild dysplasia); HGD, High-grade dysplasia (moderate and severe dysplasia; CD, Cluster of differentiation; TNFR1, Tumor necrosis factor receptor 1.

differences between control and TNFα-neutralized animals ($p>0.05$). The increase in neutrophils in 4-NQO-treated animals at the tissue level was also reflected systemically as assessed by flow cytometric analysis of blood specimens collected at both the intermediate timepoint and sacrifice (**Figure 5C**). TNFα neutralization did not abate the systemic neutrophilia.

We also evaluated the inflammatory infiltrates in all treatment groups (**Figure 5D**). Increased severity as characterized by density of the infiltrate, extent as characterized by the depth of the inflammatory cell front relative to the epithelium, lamina propria and muscle as well as intraepithelial recruitment of the inflammatory infiltrate were assessed. There was an increase in the density, extent and presence of intraepithelial inflammation in animals treated with 4-NQO. TNFα neutralization decreased the presence of intraepithelial inflammatory cells. Expectedly, those animals not receiving 4-NQO showed minimal or a complete absence of any underlying inflammation. Further, the general variation in histologic diagnoses as well as inflammatory cell

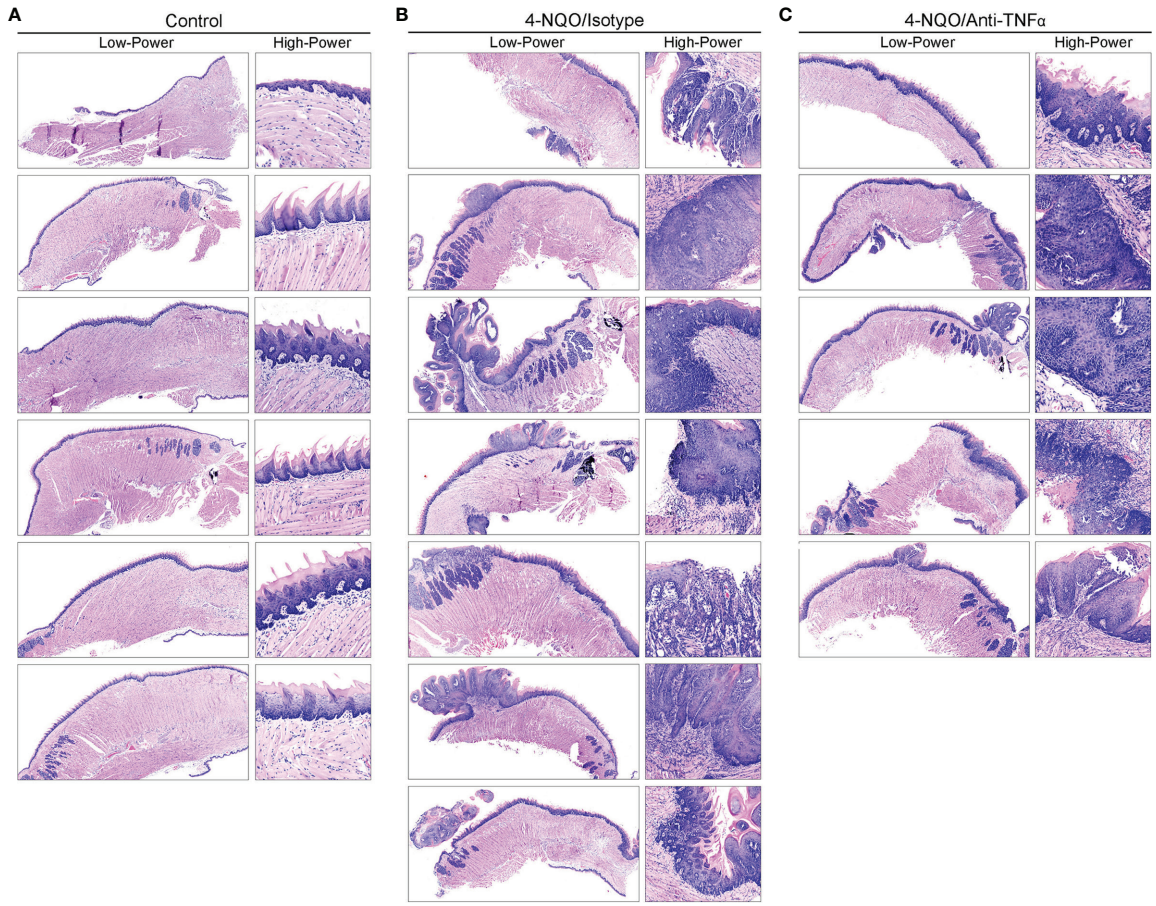

FIGURE 3 | Mouse tongue resection photomicrographs. Representative H&E longitudinal sections (low-power: 10X; high-power: 20X or 60X) of mouse tongue specimens for **(A)** control (vehicle only, n=6) animals demonstrating normal tissue architecture, **(B)** 4-NQO/isotype antibody treated animals (n=7) demonstrating invasive features consistent with OSCC and **(C)** 4-NQO/anti-TNFα antibody treated animals (n=5) demonstrating only dysplastic changes. H&E, Hematoxylin and eosin; 4-NQO, 4-nitroquinoline 1-oxide; TNFα, Tumor necrosis factor α; OSCC, Oral squamous cell carcinoma.

infiltration is reassuring in the use of this model to study malignant transformation as both OPMDs and OSCCs were observed amongst exposed animals.

Cytokine Expression

Multiplex analysis demonstrated the differential expression of multiple cytokines between treatment groups (**Table 1**). Serum samples from animals within each group were combined for analysis at both the initial and four-week timepoints due to limited blood volumes collected by saphenous vein draws and analyzed individually at the time of sacrifice. There was a consistent increase in the concentration of cytokines in 4-NQO-treated animals that received isotype antibody treatment while the vehicle control and TNFα-neutralized animals showed minimal changes in the concentration of the cytokines over the duration of the experiment. At the time of sacrifice, there were significant increases in the concentrations of IL-1α, IL-12 (p40), IL-13, LIX, M-CSF, MIP-2 in 4-NQO/isotype antibody treated animals compared to non-4-NQO treated controls (**Supplemental Figures 2A, B**). These increases were inhibited by TNFα neutralization (**Supplemental Figure 2C**).

DISCUSSION

Due to the poor survival and morbidity associated with late-stage OSCC diagnoses, prevention and early recognition of OPMDs is imperative. As the mechanisms of disease progression from an OPMD to OSCC are not fully understood, the efforts of our work have been focused at characterizing the immunoregulatory and inflammatory events governing this phenomenon.

As the body of oncology literature evolves, both epidemiologic and clinical data continue to support the role of chronic inflammation in carcinogenesis. As a potent regulator of transcription and cell survival, TNFα has been implicated in the progression of multiple human cancers through promotion of tumor growth, angiogenesis, invasion and metastasis. The results from our human biopsy samples demonstrated a progressive increase in TNFα and TNFR1 expression as well as increased recruitment of $CD45^+$ inflammatory cells from non-progressing OPMD samples to progressing OPMD samples, highlighting the crucial role of TNFα in the development of a pro-invasive environment. These results corroborate findings from our previous work which demonstrate that TNFα promotes tumor

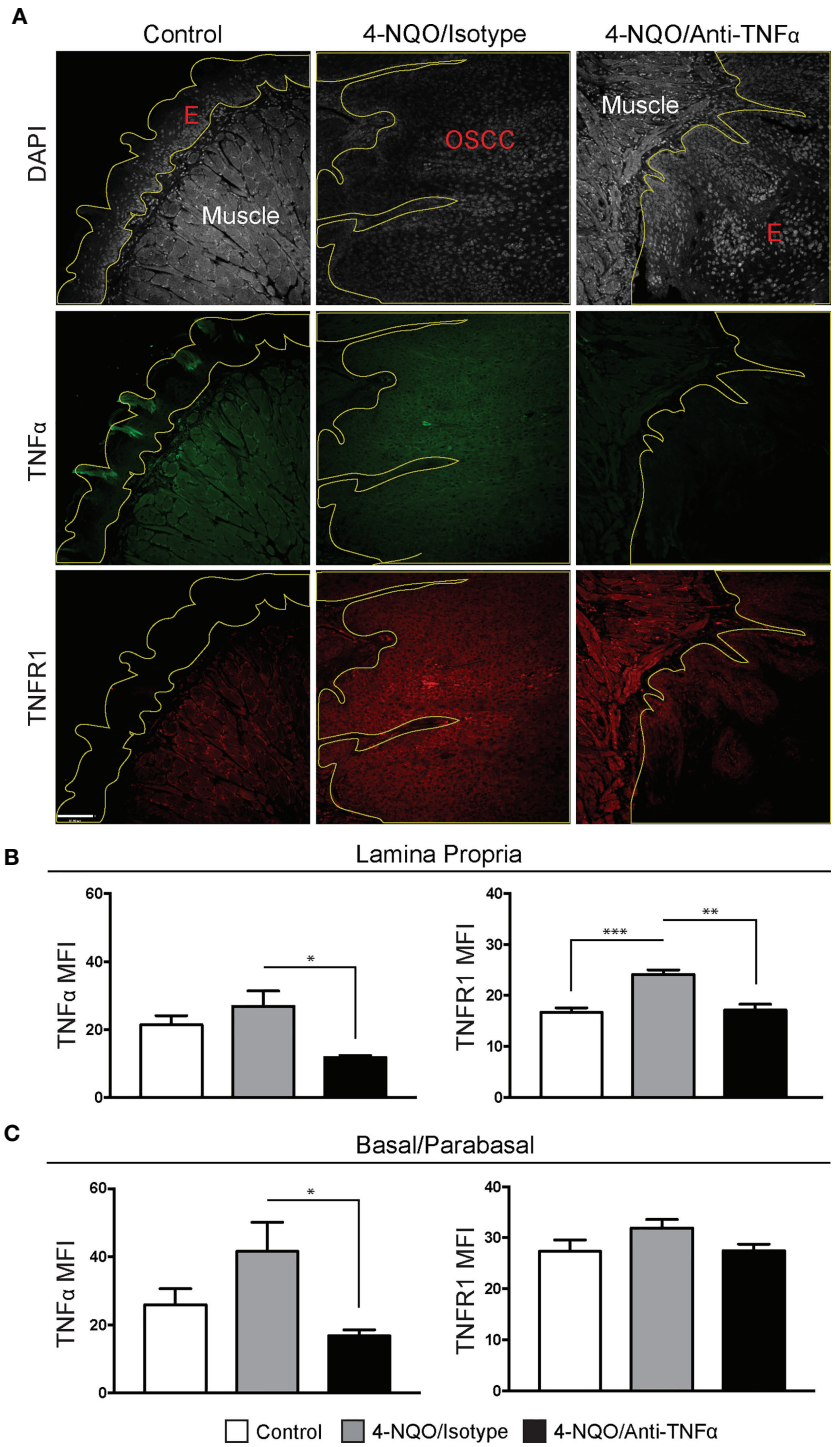

FIGURE 4 | Neutrophil recruitment in the setting of 4-NQO-induced carcinogenesis. **(A)** Representative FIHC images of mouse tongue specimens from control (first column), 4-NQO/isotype antibody treated (second column) and 4-NQO/anti-TNFα antibdody treated (third column) animals (white channel – DAPI; red channel – TNFR1; green channel – TNFα; yellow line – demarcation of epithelium). TNFα and TNFR1 MFI within the **(B)** lamina propria and **(C)** basal/parabasal epithelium for control (n=6), 4-NQO/isotype antibody treated (n=7) and 4-NQO/anti-TNFα antibody treated (n=5) animals. *p < 0.05; **p < 0.001; ***p < 0.0001; E, Epithelium; MFI, Mean fluorescence intensity; 4-NQO, 4-nitroquinoline 1-oxide; FIHC, Fluorescence immunohistochemistry; MFI, Mean fluorescence intensity; DAPI, 4′,6-diamidino-2-phenylindole dihydrochloride; TNFα, Tumor necrosis factor α; TNFR1, Tumor necrosis factor receptor 1.

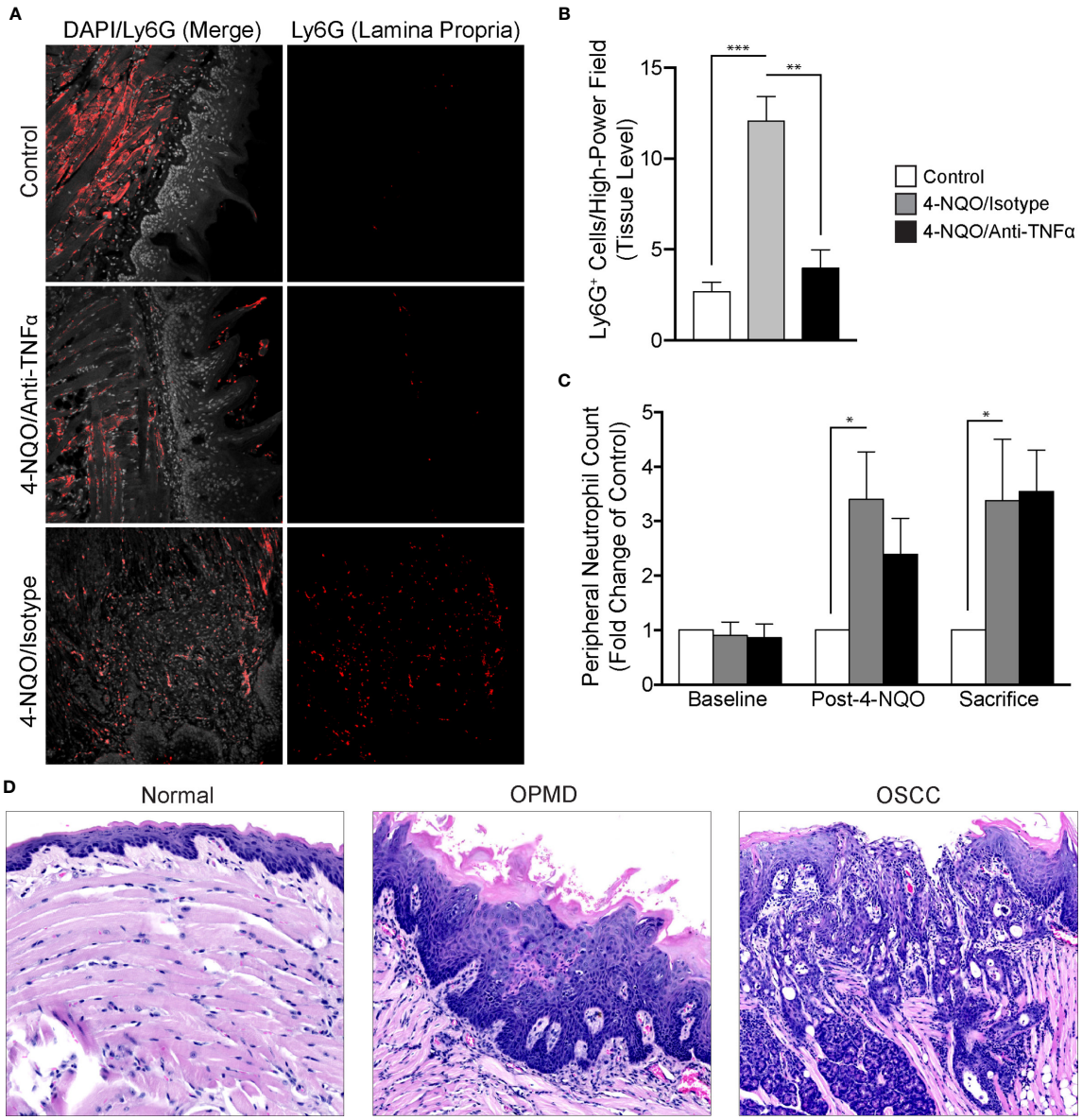

FIGURE 5 | Analysis of neutrophil recruitment in the setting of 4-NQO-induced carcinogenesis. **(A)** Representative FIHC images of mouse tongues from control (first row), 4-NQO/isotype antibody treated (second row) and 4-NQO/anti-TNFα antibody treated (third row) animals (white channel – DAPI; red channel – Ly6G). **(B)** Quantitative analysis of $Ly6G^+$ cells per high-power field for control (n=6), 4-NQO/isotype antibody treated (n=7) and 4-NQO/anti-TNFα antibody treated (n=5) animals at the level of the lamina propria. **(C)** Peripheral blood neutrophil count ($Ly6G^+$ cells per 50 μL of blood) for control (n=6), 4-NQO/isotype antibody treated (n=7) and 4-NQO/anti-TNFα anditbody treated (n=5) animals. **(D)** Selected H&E longitudinal tissue sections demonstrating variations in inflammatory infiltrates between a histologically normal mouse tongue (left panel), mouse tongue afflicted with an OPMD (middle panel) and a mouse tongue demonstrating an OSCC (right panel). *$p < 0.05$; **$p < 0.001$; ***$p < 0.0001$; 4-NQO, 4-nitroquinoline 1-oxide; FIHC, Fluorescence immunohistochemistry; H&E, Hematoxylin and eosin; OSCC, Oral squamous cell carcinoma; OPMD, Oral potentially malignant disorder; DAPI, 4′,6-diamidino-2-phenylindole dihydrochloride; TNFα, Tumor necrosis factor α.

invasion and growth as well as expression of proinflammatory cytokines in an OSCC cell line (17). Further, TNFR1 knockdown has been shown to result in a decrease in oral cancer cell line invasion and inhibition of TNFα-induced invadopodia formation (18). These results in combination with our current findings showing increased TNFR1 expression in progressing OPMD samples is suggestive of a potential therapeutic target and is the first time that TNFα/TNFR1 signaling has been demonstrated to be elevated in progressing OPMDs. As such, we propose a model which suggests that these findings represent a novel mechanism linking oral inflammation and malignant transformation (**Figure 6**).

We studied the TNFα/TNFR1 signaling pathway using a 4-NQO-induced model of head and neck cancer utilizing immunocompetent C57BL/6 mice. While our group has

TABLE 1 | Cytokine Expression.

Cytokine	4-NQO/Isotype			4-NQO/Anti-TNFα			Control		
	Post-4-NQO	Interim	Sacrifice	Post-4-NQO	Interim	Sacrifice	Post-4-NQO	Interim	Sacrifice
	Mean		Mean ± SEM	Mean		Mean ± SEM	Mean		Mean ± SEM
GM-CSF	177.00	91.00	168.00 ± 43.00	223.00	277.00	224.00 ± 58.00	151.00	2216.00	297.00 ± 52.00
Eotaxin	844.93	915.02	1299.87 ± 82.16	1029.99	841.25	1210.81 ± 139.31	972.31	974.90	1489.89 ± 63.40
G-CSF	9.68	202.61	240.60 ± 164.05	0.00	0.00	0.75 ± 0.745	0.00	0.00	0.00 ± 0.00
INF-γ	1.31	138.53	241.40 ± 160.10	0.49	0.00	3.94 ± 2.98	0.00	0.00	0.10 ± 0.10
IL-1α	90.07	2345.41	3672.72 ± 1366.41[a,b]	91.40	136.89	1028.73 ± 841.22[b]	20.39	38.58	15.95 ± 9.11[a]
IL-1β	6.34	5.52	3.59 ± 1.44	6.34	0.76	4.93 ± 2.26	1.72	0.02	0.00 ± 0.00
IL-2	16.23	202.74	330.06 ± 232.37	13.91	11.23	3.70 ± 2.26	10.13	3.61	1.11 ± 0.49
IL-4	1.17	1.38	1.36 ± 0.55	1.35	1.11	1.29 ± 0.54	0.94	0.46	0.58 ± 0.16
IL-3	0.00	0.00	1.32 ± 1.32	0.00	0.00	0.00 ± 0.00	0.00	0.00	0.00 ± 0.00
IL-5	11.02	5.20	3.20 ± 1.06	9.31	10.62	19.20 ± 9.82	14.41	13.38	8.79 ± 1.37
IL-6	4.58	2.70	14.35 ± 6.56	9.81	6.66	5.77 ± 1.59	0.00	7.66	1.57 ± 0.98
IL-7	4.64	14.29	5.34 ± 1.99	12.87	15.96	18.33 ± 9.22	0.00	0.86	36.21 ± 29.83
IL-9	15.10	403.72	1517.34 ± 1220.99	29.64	58.26	76.59 ± 28.39	32.21	7.95	25.41 ± 8.15
IL-10	1.71	8.19	16.22 ± 10.86	8.19	0.00	7.23 ± 4.90	2.33	3.67	2.10 ± 1.34
IL-12 (p40)	12.40	1356.41	2820.61 ± 1103.32[a]	14.83	30.15	724.02 ± 611.51	5.69	1.34	1.28 ± 0.61[a]
IL-12 (p70)	15.11	13.31	26.64 ± 14.91	18.89	1.19	5.74 ± 4.69	9.70	4.38	3.97 ± 2.43
LIF	0.58	1.10	0.87 ± 0.47	0.12	0.03	5.58 ± 3.91	0.03	0.95	20.03 ± 18.17
IL-13	136.70h	4331.21[d,e]	7817.62 ± 5577.97[a,b,c,f,g,h,i]	182.63[g]	105.04[c]	109.67 ± 10.23[b,d]	128.52[i]	110.65[f]	94.93 ± 9.35[a,e]
LIX	1208.43	2191.34	3169.96 ± 1058.76[a]	1147.59	745.36	1557.85 ± 643.45	817.99	1042.73	706.56 ± 416.86[a]
IL-15	24.43	67.93	74.38 ± 23.56	37.23	32.26	78.29 ± 42.94	24.40	92.96	1620.94 ± 1396.70
IL-17	6.94	11.24	10.85 ± 3.49	9.77	5.31	4.92 ± 1.31	2.36	2.95	0.87 ± 0.45
IP10	95.62	84.40	134.71 ± 11.66	103.67	83.76	160.07 ± 24.58	117.21	125.24	172.32 ± 7.09
KC	159.66	500.90	702.91 ± 418.18	198.15	106.48	160.54 ± 24.59	85.45	327.82	267.18 ± 74.71
MCP-1	38.21	34.61	33.99 ± 6.52	120.67	50.04	48.75 ± 10.49	36.43	60.10	40.52 ± 4.49
MIP-1α	72.04	490.44	519.76 ± 272.85	74.42	67.44	45.47 ± 15.42	49.12	29.49	13.14 ± 6.01
MIP-1β	16.04	184.85	242.62 ± 149.55	0.00	0.00	7.18 ± 3.49	4.37	0.00	0.00 ± 0.00
M-CSF	11.59	2001.69	3416.24 ± 1296.99[a,b]	10.08	38.22	788.99 ± 687.76[b]	5.97	3.74	1.99 ± 0.50[a]
MIP-2	104.22	2090.27	2636.20 ± 891.66[a]	104.10	246.02	877.20 ± 596.80	65.87	0.00	27.63 ± 11.68[a]
MIG	106.69	86.96	138.57 ± 26.04	683.41	89.54	187.39 ± 51.26	158.63	147.19	280.49 ± 24.93
RANTES	0.00	14.49	10.21 ± 3.30	10.03	0.00	6.66 ± 2.24	7.30	8.79	5.00 ± 2.69
VEGF	2.59	39.23	119.40 ± 100.54	1.81	1.38	1.34 ± 0.22	1.79	1.17	1.23 ± 0.22
TNFα	5.67	5.86	3.62 ± 1.58	6.53	1.86	4.95 ± 2.62	3.31	2.89	1.35 ± 0.38

Cytokine expression (pg/L) for control (n=6), 4-NQO/anti-TNFα antibody treated (n=5) and 4-NQO/isotype antibody treated (n=7) animals. Note 1: SEMs were omitted for post-4-NQO and interim timepoints as samples were pooled due to insufficient acquired blood volumes for each individual sample. Note 2: Post-4-NQO timepoint follows completion of 16 weeks of 4-NQO or vehicle delivery; Interim and sacrifice timepoints are four- and eight-weeks post-4-NQO delivery cessation, respectively. MFI, Mean florescence intensity; 4-NQO, 4-Nitroquinoline 1-oxide; SEM, Standard error of the mean; GM-CSF, Granulocyte-macrophage colony-stimulating factor; G-CSF, Granulocyte colony-stimulating factor; INF, Interferon; IL, Interleukin; LIF, Leukemia inhibitory factor; LIX, Lipopolysaccharide-induced CXC chemokine; IP, Interferon γ-induced protein; KC, Keratinocytes-derived chemokine; MCP, Monocyte chemoattractant protein; MIP, Macrophage Inflammatory Protein; M-CSF, Macrophage-colony stimulating factor; MIG, Monokine induced by interferon-γ; RANTES, Regulated on activation, normal T cell expressed and secreted; VEGF, Vascular endothelial growth factor; TNF, Tumor necrosis factor; [a,b,c,d,e,f,g,h]$p < 0.05$; [a]Control Sacrifice vs. 4-NQO/Isotype Sacrifice; [b]4-NQO/Isotype Sacrifice vs. 4-NQO/Anti-TNFα Sacrifice; [c]4-NQO/Anti-TNFα Interim vs. 4-NQO/Isotype Sacrifice; [d]4-NQO/Isotype Interim vs. 4-NQO/Anti-TNFα Sacrifice; [e]4-NQO/Isotype Interim vs. Control Sacrifice; [f]Control Interim vs. 4-NQO/Isotype Sacrifice; [g]4-NQO/Anti-TNFα Post-4-NQO vs. 4-NQO/Isotype Sacrifice; [h]4-NQO/Isotype Post-4-NQO vs. 4-NQO/Isotype Sacrifice; [i]Control Post-4-NQO vs. 4-NQO/Isotype Sacrifice.

utilized 3D *in vitro* invasion assays for the study of OSCCs, this model allowed us to evaluate these pathways in an immunocompetent animal model. Our results support the continued use of this model as a wide distribution of dysplastic as well as invasive lesions can be achieved as noted at the time of sacrifice. At this time, however, little is known about the inflammatory response as a result of the development of 4-NQO-induced lesions. Our results support an integral role of tumor-associated inflammation in oral carcinogenesis. As such, the use of ideal models of disease for *in vivo* study cannot be overstated. The application of the 4-NQO-induced model of oral cancer recapitulates dysplastic progression leading to the development of OSCCs in a similar manner to the human condition whilst maintaining an intact immune system. The latter point, in this case, is of critical importance as chronic inflammation associated with malignant progression plays a significant role in disease progression. Further, in the context of tumor evaluation following 4-NQO exposure, it is crucial to report all histopathologic features, as were noted in this study, and ensure that a representative number of sections have been evaluated as OPMDs and OSCCs are not homogenous entities.

Anti-TNFα antibody therapy has been demonstrated to exhibit robust anti-tumor effects in mouse models of pancreatic cancer and achieve disease stabilization in individuals with diagnoses of metastatic breast and recurrent ovarian cancer (27–29). Here, we demonstrate that anti-TNFα antibody treatment following the administration of 4-NQO attenuates or retards malignant transformation during a period where an untreated animal

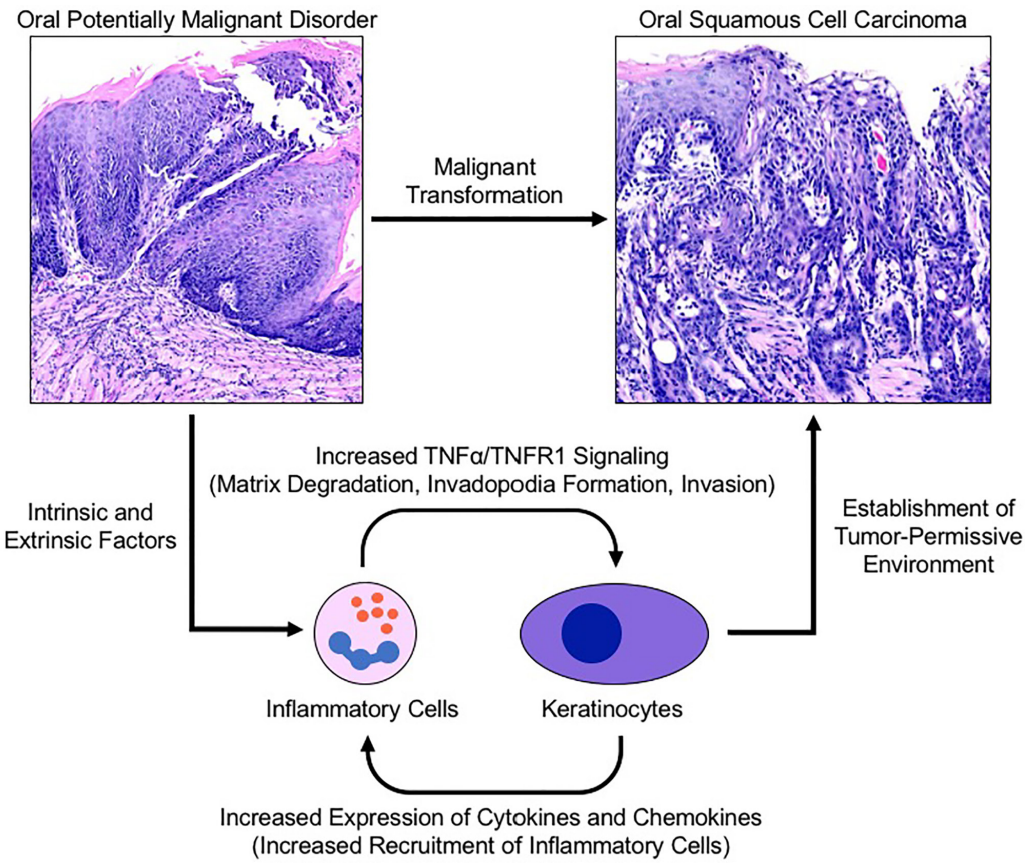

FIGURE 6 | Proposed model for TNFα-induced malignant transformation in the setting of an oral potentially malignant disorder. Intrinsic and extrinsic factors induce oral premalignant disorders resulting in a cyclic signalling process between recruited neutrophils and keratinocytes to establish a tumor-permissive environment via the TNFα/TNFR1 signalling pathway. TNFR1 activation of keratinocytes enhances invadopodia development and matrix degradation thereby facilitating invasion. Pro-inflammatory cytokines released by keratinocytes recruit and activate neutrophils which assist with matrix remodelling and further activation of nearby keratinocytes. TNFR1, Tumor necrosis factor receptor 1; TNFα, Tumor necrosis factor α.

cohort went on to develop invasive lesions. Further studies are needed to determine whether the dysplastic lesions from anti-TNFα antibody treated animals would eventually progress to OSCCs, albeit at a slower pace, or if progression is completely inhibited. Our current findings are suggestive of a potentially critical role for the TNFα/TNFR1 signaling pathway in the context of carcinogenesis and malignant progression through the inhibition of tumor invasion and modulation of the inflammatory response to malignant processes.

We show the differential expression of a number of cytokines in the context of 4-NQO-induced carcinogenesis and TNFα blockade. Previous work from our group has shown a relative increase in salivary expression of proinflammatory cytokines including IL-1β, IL-6 and TNFα in patients with a diagnosis of OSCC compared to control patients with IL-1β and IL-6 demonstrating especially increased expression in advanced disease. In the context of 4-NQO-induced oral cancer, attention should be drawn to several findings at the time of animal sacrifice with respect to cytokine expression. First, there was a reduction in TNFα antibody concentration during anti-TNFα antibody administration as compared to isotype antibody treated controls which was not seen at the time of sacrifice. This suggests that in early stages of carcinogenesis, the aforementioned dosing of anti-TNFα antibody attenuates TNFα expression during treatment but becomes inadequate at later timepoints. While there were no invasive lesions noted on histologic analysis of specimens from the anti-TNFα antibody treated group at the time of sacrifice, it is plausible that with additional time, these lesions may have undergone malignant transformation or, alternatively, new foci of disease may have manifested. Even in the setting of mice deficient in TNFα, carcinogen-induced skin lesions will eventually develop in a significantly delayed fashion relative to control animals of multiple genetic backgrounds (30). Second, as compared to the intermediate time point, there was a significant upregulation of several cytokines which, with the exception of M-CSF, were not significantly different between the isotype and anti-TNFα antibody groups. This suggests that despite persistent TNFα blockade, cytokine expression was normalized to that of those animals treated with isotype antibody. As such, to ascertain the true effect of anti-TNFα antibody treatment in the setting of 4-NQO carcinogenesis, a thorough evaluation of

expression differences at the intermediate timepoint was required which revealed several differences between the groups. As the initial and interim serum cytokine analyses used a pooled sample from all animals within each group, statistical analysis could not be performed at these time points. Despite this limitation, many clear differences could be seen from the dataset with the 4-NQO/isotype antibody treated group showing increases in concentrations of most cytokines including IL-1α, IL-12 (p40), IL-13, LIX, M-CSF, and MIP-2 while IL-1α, IL-12 (p40), IL-13 and M-CSF were significantly reduced in the setting of TNFα blockade. The aforementioned cytokines are all known to participate in immunoregulatory processes of both the innate and adaptive immune system in the setting of malignant processes (31–33). Similarly, the elevated chemokines M-CSF, MIP-2 LIX, have been implicated in specific mechanisms of invasion and metastasis (34–36).

Neutrophils are avid participants in carcinogenesis and metastasis and play an integral role in cancer progression by adopting both tumor-promoting and immunosuppressive functions which facilitate angiogenesis, invasion, migration and metastasis (37, 38). With respect to circulating neutrophils, while variations exist in the degree of association, an elevated neutrophil-to-lymphocyte ratio (NLR) has repeatedly been associated with poor survival outcomes in the context of numerous malignancies (39). In the setting of OSCCs, the NLR has demonstrated some utility as a predictor of survival (40). At the tissue level, it has been suggested that high levels of intratumoral neutrophils are associated with both decreased overall survival as well as diminished periods of recurrence-free, disease free and cancer-specific survival (41). We observed neutrophilia in both isotype and anti-TNFα antibody treatment groups at both the four- and eight-week time points relative to controls. While our results grossly recapitulate the neutrophilia noted with human cancers, there was a decrease in circulating neutrophils at the four-week time-point between the isotype and anti-TNFα treated groups, albeit not statistically significant. While this was likely attributed to the concurrent anti-TNFα antibody administration which was eventually overcome through continued and progressive neutrophil influx up to the point of sacrifice, this finding highlights a potential mechanism by which the inflammatory response significantly alters cancer progression. Recent work from our laboratory has also explored neutrophil influx within the oral cavity in the setting of OSCCs and demonstrated significantly elevated numbers of oral neutrophils relative to control subjects based on $CD45^+CD66^+$ cell counts by flow cytometry. The administration of anti-TNFα antibodies may exploit key immunomodulatory pathways which block or attenuate OSCC invasion through the manipulation of both local and systemic inflammatory mechanisms (**Figure 6**). Further, this response may be quantifiable and allow for disease prognostication and treatment in the setting of OPMDs or OSCCs.

DATA AVAILABILITY STATEMENT

The raw data supporting the conclusions of this article will be made available by the authors, without undue reservation.

ETHICS STATEMENT

The studies involving human participants were reviewed and approved by University of Toronto Research Ethics Board (Protocol 38933). Written informed consent for the use of archived material was not required as per approved ethics protocol. The animal studies were reviewed and approved by University of Toronto Animal Care Committee (Protocol 20011940).

AUTHOR CONTRIBUTIONS

MM conceptualized the research. JC, RM, and AA prepared materials, collected, analyzed and interpreted the data. JC prepared the manuscript. MM supervised RM and MG supervised JC. Editing of the manuscript was performed by JC, AA, MG, and MM. All authors contributed to the article and approved the submitted version.

FUNDING

JC is supported by the Canadian Institutes of Health Research (CIHR). RM is supported by the University of Toronto Faculty of Dentistry Summer Research Program. MM is supported by the Connaught New Researcher Award and a bridge grant (Priority Announcement for Oral Health) provided by the CIHR Institute of Musculoskeletal Health and Arthritis (PJ7-169674).

SUPPLEMENTARY MATERIAL

The Supplementary Material for this article can be found online at: https://www.frontiersin.org/articles/10.3389/fonc.2021.741013/full#supplementary-material

Supplementary Figure 1 | 4-NQO-induced carcinogenesis model characterization. **(A)** Representative oral photographs (left column) and longitudinal H&E low-power (middle column, 10X) and high-power (right column, 20X or 60X) photomicrographs of mouse oral tongue specimens. **(B)** Weight change of control (n=4) and 4-NQO treated (n=19) animals over the course of 4-NQO treatment and post-4-NQO observation. **(C)** Distribution of histologic diagnoses between 4-NQO-treated animals (n=19). *$p < 0.01$; **$p < 0.0001$; EH, Epithelial hyperplasia; LGD, Low-grade dysplasia (mild dysplasia); HGD, High-grade dysplasia (moderate and severe dysplasia); CIS, Carcinoma *in situ*; SCC, Squamous cell carcinoma; H&E, Hematoxylin and eosin.

Supplementary Figure 2 | Cytokine Expression. Comparisons of cytokine concentration (pg/L) between post-4-NQO, interim and sacrifice time points for **(A)** control, **(B)** 4-NQO/isotype antibody treated and **(C)** 4-NQO/anti-TNFα antibody treated groups. MFI, Mean florescence intensity; 4-NQO, 4-Nitroquinoline 1-oxide; SEM, Standard error of the mean; GM-CSF, Granulocyte-macrophage colony-stimulating factor; G-CSF, Granulocyte colony-stimulating factor; INF, Interferon; IL, Interleukin; LIF, Leukemia inhibitory factor; LIX, Lipopolysaccharide-induced CXC chemokine; IP, Interferon γ-induced protein; KC, Keratinocytes-derived chemokine; MCP, Monocyte chemoattractant protein; MIP, Macrophage inflammatory protein; M-CSF, Macrophage-colony stimulating factor; MIG, Monokine induced by interferon-γ; RANTES, Regulated on activation, normal T cell expressed and secreted; VEGF, Vascular endothelial growth factor; TNFα, Tumor necrosis factor α.

REFERENCES

1. Warnakulasuriya S. Global Epidemiology of Oral and Oropharyngeal Cancer. *Oral Oncol* (2009) 45:309–16. doi: 10.1016/j.oraloncology.2008.06.002
2. Abadeh A, Ali AA, Bradley G, Magalhaes MA. Increase in Detection of Oral Cancer and Precursor Lesions by Dentists: Evidence From an Oral and Maxillofacial Pathology Service. *J Am Dent Assoc* (2019) 150:531–9. doi: 10.1016/j.adaj.2019.01.026
3. McDowell JD. An Overview of Epidemiology and Common Risk Factors for Oral Squamous Cell Carcinoma. *Otolaryngol Clin North Am* (2006) 39:277–94. doi: 10.1016/j.otc.2005.11.012
4. Shah JP, Gil Z. Current Concepts in Management of Oral Cancer - Surgery. *Oral Oncol* (2009) 45:394–401. doi: 10.1016/j.oraloncology.2008.05.017
5. Specenier PM, Vermorken JB. Current Concepts for the Management of Head and Neck Cancer: Chemotherapy. *Oral Oncol* (2009) 45:409–15. doi: 10.1016/j.oraloncology.2008.05.014
6. Mazeron R, Tao Y, Lusinchi A, Bourhis J. Current Concepts of Management in Radiotherapy for Head and Neck Squamous-Cell Cancer. *Oral Oncol* (2009) 45:402–8. doi: 10.1016/j.oraloncology.2009.01.010
7. Scully C, Bagan J. Oral Squamous Cell Carcinoma Overview. *Oral Oncol* (2009) 45:301–8. doi: 10.1016/j.oraloncology.2009.01.004
8. Braakhuis BJM, Brakenhoff RH, René Leemans C. Treatment Choice for Locally Advanced Head and Neck Cancers on the Basis of Risk Factors: Biological Risk Factors. *Ann Oncol* (2012) 23:173–7. doi: 10.1093/annonc/mds299
9. Howlader N, Noone A, Krapcho M, Miller D, Brest A, Yu M, et al. *Cancer Statistics Review, 1975-2017*. SEER Statistics, National Cancer Institute. Bethesda, MD. Available at: https://seer.cancer.gov/archive/csr/1975_2017/.
10. Warnakulasuriya S. Oral Potentially Malignant Disorders: A Comprehensive Review on Clinical Aspects and Management. *Oral Oncol* (2020) 102:1–10. doi: 10.1016/j.oraloncology.2019.104550
11. Richards D. Adjunctive Tests Cannot Replace Scalpel Biopsy for Oral Cancer Diagnosis. *Evid Based Dent* (2015) 16:46–7. doi: 10.1038/sj.ebd.6401093
12. Lee JJ, Hung HC, Cheng SJ, Chiang CP, Liu BY, Yu CH, et al. Factors Associated With Underdiagnosis From Incisional Biopsy of Oral Leukoplakic Lesions. *Oral Surgery Oral Med Oral Pathol Oral Radiol Endodontol* (2007) 104:217–25. doi: 10.1016/j.tripleo.2007.02.012
13. Speight PM, Abram TJ, Floriano PN, James R, Vick J, Thornhill MH, et al. Interobserver Agreement in Dysplasia Grading: Toward an Enhanced Gold Standard for Clinical Pathology Trials. *Oral Surg Oral Med Oral Pathol Oral Radiol* (2015) 120:474–82. doi: 10.1016/j.oooo.2015.05.023
14. Lingen MW, Abt E, Agrawal N, Chaturvedi AK, Cohen E, D'Souza G, et al. Evidence-Based Clinical Practice Guideline for the Evaluation of Potentially Malignant Disorders in the Oral Cavity: A Report of the American Dental Association. *J Am Dent Assoc* (2017) 148:712–27. doi: 10.1016/j.adaj.2017.07.032
15. Coussens LM, Werb Z. Inflammation and Cancer. *Nature* (2002) 420:860–7. doi: 10.1038/nature01322
16. Balkwill F, Mantovani A. Inflammation and Cancer: Back to Virchow? *Lancet* (2001) 357:539–45. doi: 10.1016/S0140-6736(00)04046-0
17. Glogauer JE, Sun CX, Bradley G, Magalhaes MAO. Neutrophils Increase Oral Squamous Cell Carcinoma Invasion Through an Invadopodia-Dependent Pathway. *Cancer Immunol Res* (2015) 3:1218–26. doi: 10.1158/2326-6066.CIR-15-0017
18. Goertzen C, Mahdi H, Laliberte C, Meirson T, Eymael D, Gil-Henn H, et al. Oral Inflammation Promotes Oral Squamous Cell Carcinoma Invasion. *Oncotarget* (2018) 9:29047–63. doi: 10.18632/oncotarget.25540
19. Gardner D. Spontaneous Squamous Cell Carcinomas of the Oral Region in Domestic Animals: A Review and Consideration of Their Relevance to Human Research. *Oral Dis* (1996) 2:148–54. doi: 10.1111/j.1601-0825.1996.tb00216.x
20. Bailleul B, Daubersies P, Galiègue-Zouitina S, Loucheux-Lefebvre M -H. Molecular Basis of 4-Nitroquinoline 1-Oxide Carcinogenesis. *Japanese J Cancer Res* (1989) 80:691–7. doi: 10.1111/j.1349-7006.1989.tb01698.x
21. Nagao M, Sugimura T. Molecular Biology of the Carcinogen, 4-Nitroquinoline 1-Oxide. *Adv Cancer Res* (1976) 23:131–69. doi: 10.1016/S0065-230X(08)60545-X
22. Hawkins BL, Heniford BW, Ackermann DM, Leonberger M, Martinez SA, Hendler FJ. 4NQO Carcinogenesis: A Mouse Model of Oral Cavity Squamous Cell Carcinoma. *Head Neck* (1994) 16:424–32. doi: 10.1002/hed.2880160506
23. Kanojia D, Vaidya MM. 4-Nitroquinoline-1-Oxide Induced Experimental Oral Carcinogenesis. *Oral Oncol* (2006) 42:655–67. doi: 10.1016/j.oraloncology.2005.10.013
24. Ishida K, Tomita H, Nakashima T, Hirata A, Tanaka T, Shibata T, et al. Current Mouse Models of Oral Squamous Cell Carcinoma: Genetic and Chemically Induced Models. *Oral Oncol* (2017) 73:16–20. doi: 10.1016/j.oraloncology.2017.07.028
25. Lu SL, Herrington H, Wang XJ. Mouse Models for Human Head and Neck Squamous Cell Carcinomas. *Head Neck* (2006) 28:945–54. doi: 10.1002/hed.20397
26. Ali A, Soares AB, Eymael D, Magalhaes M. Expression of Invadopodia Markers Can Identify Oral Lesions With a High Risk of Malignant Transformation. *J Pathol Clin Res* (2021) 7:61–74. doi: 10.1002/cjp2.182
27. Madhusudan S, Muthuramalingam SR, Braybrooke JP, Wilner S, Kaur K, Han C, et al. Study of Etanercept, a Tumor Necrosis Factor-Alpha Inhibitor, in Recurrent Ovarian Cancer. *J Clin Oncol* (2005) 23:5950–9. doi: 10.1200/JCO.2005.04.127
28. Madhusudan S, Foster M, Mathuramalingam SR, Braybrooke JP, Wilner S, Kaur K, et al. A Phase II Study of Etanercept (Enbrel), a Tumor Necrosis Factor α Inhibitor in Patients With Metastatic Breast Cancer. *Clin Cancer Res* (2004) 10:6528–34. doi: 10.1158/1078-0432.CCR-04-0730
29. Egberts JH, Cloosters V, Noack A, Schniewind B, Thon L, Klose S, et al. Anti-Tumor Necrosis Factor Therapy Inhibits Pancreatic Tumor Growth and Metastasis. *Cancer Res* (2008) 68:1443–50. doi: 10.1158/0008-5472.CAN-07-5704
30. Moore RJ, Owens DM, Stamp G, Arnott C, Burke F, East N, et al. Mice Deficient in Tumor Necrosis Factor-α Are Resistant to Skin Carcinogenesis. *Nat Med* (1999) 5:828–31. doi: 10.1038/10552
31. Baker KJ, Houston A, Brint E. IL-1 Family Members in Cancer; Two Sides to Every Story. *Front Immunol* (2019) 10:1–16. doi: 10.3389/fimmu.2019.01197
32. Lu X. Impact of IL-12 in Cancer. *Curr Cancer Drug Targets* (2017) 17:682–97. doi: 10.2174/1568009617666170427102729
33. Terabe M, Park JM, Berzofsky JA. Role of IL-13 in Regulation of Anti-Tumor Immunity and Tumor Growth. *Cancer Immunol Immunother* (2004) 53:79–85. doi: 10.1007/s00262-003-0445-0
34. Chockalingam S, Ghosh SS. Macrophage Colony-Stimulating Factor and Cancer: A Review. *Tumor Biol* (2014) 35:10635–44. doi: 10.1007/s13277-014-2627-0
35. Kollmar O, Junker B, Rupertus K, Menger MD, Schilling MK. Studies on MIP-2 and CXCR2 Expression in a Mouse Model of Extrahepatic Colorectal Metastasis. *Eur J Surg Oncol* (2007) 33:803–11. doi: 10.1016/j.ejso.2007.01.012
36. Romero-Moreno R, Curtis KJ, Coughlin TR, Cristina Miranda-Vergara M, Dutta S, Natarajan A, et al. The CXCL5/CXCR2 Axis is Sufficient to Promote Breast Cancer Colonization During Bone Metastasis. *Nat Commun* (2019) 10:1–14. doi: 10.1038/s41467-019-12108-6
37. Uribe-Querol E, Rosales C. Neutrophils in Cancer: Two Sides of the Same Coin. *J Immunol Res* (2015) 2015:1–21. doi: 10.1155/2015/983698
38. Powell DR, Huttenlocher A. Neutrophils in the Tumor Microenvironment. *Trends Immunol* (2016) 37:41–52. doi: 10.1016/j.it.2015.11.008
39. Templeton AJ, McNamara MG, Šeruga B, Vera-Badillo FE, Aneja P, Ocaña A, et al. Prognostic Role of Neutrophil-To-Lymphocyte Ratio in Solid Tumors: A Systematic Review and Meta-Analysis. *JNCI J Natl Cancer Inst* (2014) 106:1–11. doi: 10.1093/jnci/dju124
40. Perisanidis C, Kornek G, Pöschl PW, Holzinger D, Pirklbauer K, Schopper C, et al. High Neutrophil-to-Lymphocyte Ratio Is an Independent Marker of Poor Disease-Specific Survival in Patients With Oral Cancer. *Med Oncol* (2013) 30:1–8. doi: 10.1007/s12032-012-0334-5
41. Shen M, Hu P, Donskov F, Wang G, Liu Q, Du J. Tumor-Associated Neutrophils as a New Prognostic Factor in Cancer: A Systematic Review and Meta-Analysis. *PloS One* (2014) 9:1–10. doi: 10.1371/journal.pone.0098259

Conflict of Interest: The authors declare that the research was conducted in the absence of any commercial or financial relationships that could be construed as a potential conflict of interest.

this article, or claim that may be made by its manufacturer, is not guaranteed or endorsed by the publisher.

frontiers in Immunology

ORIGINAL RESEARCH
published: 12 October 2021
doi: 10.3389/fimmu.2021.749597

Identification of Cell Surface Molecules That Determine the Macrophage Activation Threshold Associated With an Early Stage of Malignant Transformation

*Camille Jacqueline[1], Matthew Dracz[1], Sarah Boothman[2], Jonathan S. Minden[2], Rachel A. Gottschalk[1] and Olivera J. Finn[1]**

[1] Department of Immunology, University of Pittsburgh, Pittsburgh, PA, United States, [2] Department of Biological Sciences, Carnegie Mellon University, Pittsburgh, PA, United States

OPEN ACCESS

Edited by:
Sophia N Karagiannis, King's College London, United Kingdom

Reviewed by:
Soldano Ferrone, Massachusetts General Hospital and Harvard Medical School, United States
Markus Biburger, Friedrich-Alexander-University Erlangen-Nürnberg, Germany

***Correspondence:**
Olivera J. Finn
ojfinn@pitt.edu

Specialty section:
This article was submitted to Cancer Immunity and Immunotherapy, a section of the journal Frontiers in Immunology

Received: 29 July 2021
Accepted: 27 September 2021
Published: 12 October 2021

Citation:
Jacqueline C, Dracz M, Boothman S, Minden JS, Gottschalk RA and Finn OJ (2021) Identification of Cell Surface Molecules That Determine the Macrophage Activation Threshold Associated With an Early Stage of Malignant Transformation. Front. Immunol. 12:749597. doi: 10.3389/fimmu.2021.749597

The ability of immune cells to sense changes associated with malignant transformation as early as possible is likely to be important for the successful outcome of cancer immunosurveillance. In this process, the immune system faces a trade-off between elimination of cells harboring premalignant or malignant changes, and autoimmune pathologies. We hypothesized that the immune system has therefore evolved a threshold for the stage of transformation from normal to fully malignant cells that first provides a threat (danger) signal requiring a response. We co-cultured human macrophages with a unique set of genetically related human cell lines that recapitulate successive stages in breast cancer development: MCF10A (immortalized, normal); MCFNeoT (benign hyperplasia); MCFT1 (atypical hyperplasia); MCFCA1 (invasive cancer). Using cytokines-based assays, we found that macrophages were inert towards MCF10A and MCFNeoT but were strongly activated by MCFT1 and MCFCA1 to produce inflammatory cytokines, placing the threshold for recognition between two premalignant stages, the earlier stage MCFNeoT and the more advanced MCFT1. The cytokine activation threshold paralleled the threshold for enhanced phagocytosis. Using proteomic and transcriptomic approaches, we identified surface molecules, some of which are well-known tumor-associated antigens, that were absent or expressed at low levels in MCF10A and MCFNeoT but turned on or over-expressed in MCFT1 and MCFCA1. Adding antibodies specific for two of these molecules, Annexin-A1 and CEACAM1, inhibited macrophage activation, supporting their role as cancer "danger signals" recognized by macrophages.

Keywords: breast cancer, TNF-α, 2D-DIGE, phagocytosis, annexin A1, CEACAM1

INTRODUCTION

Medical and evolutionary sciences have traditionally developed in relative isolation (1). In the 1970s, evolutionary and ecological concepts began to be applied to cancer initiation and progression (2, 3). Since this seminal work, several studies explored the processes of somatic cellular selection and evolution leading to malignant transformation, metastasis or resistance to therapies (4–6). In addition to the evolution of clonal heterogeneity inside the tumor, tumors also evolve in complex and multifaceted ecological contexts. Indeed, tumors are composed of mixtures of cancer cells and non-cancer cells, which compose the tumor microenvironment (TME). Tumor cells vary in their ability to evade the immune system and the "invisible" clones present a selective advantage and proliferate at the expense of others (7). It is now accepted that this co-evolutionary process, called immunoediting, is ongoing in most cancers and involves the immune response as well as immune evasion by some tumor cells (8). Application of evolutionary biology to the understanding of the crosstalk between cancer and immune cells is a promising strategy to better understand the bases of cancer vulnerability. The need for self-tolerance to avoid auto-immunity and the need to eliminate cancer that arises from self, may have exerted a strong selective pressure on the evolution of cancer immunosurveillance (9, 10). Unlike viruses or bacteria, premalignant cells may be particularly challenging for the immune system because they are mostly self with initially only a few characteristics of tumor cells (11).

Macrophages play an important role in the initiation of immune responses that eventually lead to adaptive immunity and immune memory. Their ability to sense "danger signals" on cells undergoing malignant transformation, similarly to how they sense danger signals from pathogens, may determine if and when cancer immunosurveillance is initiated. In the context of microbial stimuli, an evolutionarily conserved threshold for "danger discrimination" controls inflammatory cytokines production (12); MAPK were activated above a certain concentration of microbial products, setting an inflammatory activation threshold in both mouse and human macrophages. Recently, it was shown that in squamous cell carcinoma of the lung, innate inflammatory responses are low in benign lesions but increase with higher grade pre-invasive lesions, suggesting the existence of a threshold of activation of innate immune responses to cancer (13).

We tested this hypothesis in a unique set of human breast cell lines derived on the same genetic background, that recapitulate several steps in breast cancer progression: MCF10A cell line, immortalized but not transformed; MCFNeoT and MCFT1 cell lines, H-ras transformed, corresponding to premalignant hyperplasia and atypical hyperplasia, respectively; and MCFCA1, fully malignant invasive tumor cell line (14, 15). We exposed macrophages to these cells and assessed their activation by the secretion of several cytokines. Macrophages produced IL-10 upon encounter with MCF10A and MCFNeoT but switched to TNF-α and IL-1β when co-incubated with hyperplastic MCFT1 and fully transformed MCFCA1, suggesting an activation threshold at the premalignant stage represented by MCFT1. We also found that increased phagocytic activity followed the same threshold with macrophages forming conjugates with MCF10A and MCFNeoT but fully engulfing MCFT1 and MCFCA1. We measured differences in the transcriptome and the proteome between these cell lines and found several candidate molecules whose expression correlates with the threshold for macrophage activation. We found expression of the same molecules and macrophage infiltration in early stages of malignant transformation in breast tissue samples, recapitulating our findings *in vitro*.

MATERIALS AND METHODS

Antibodies

Mouse monoclonal antibody 4H5, gift from the late Dr. Hilgers (Free University, Amsterdam), was used to stain the hypoglycosylated form of MUC1. Her-2/neu was detected with Herceptin ® (Trastuzumab, Genentech Inc., San Francisco, CA, USA) and CEACAM1 with antibody CEACAM1/CD66a (R&D Systems, Minneapolis, MN, USA). Anti-Serpin B1 (clone 3B4) antibody was obtained from Novus Biologicals (Centennial, CO, USA). Anti-Annexin A1 clone EPR19342 and anti-CD68 (EPR20545) antibodies were purchased from Abcam (Cambridge, UK). Anti-Annexin A1 (74/3) and anti-Calregulin (clone F-4) was purchased from Biolegend (San Diego, CA, USA) and Santa Cruz Biotechnology (Dallas, TX, USA) respectively. Anti-PECAM1 (clone WM59) and FITC-CD47 (clone B6H12) were purchased from BD Biosciences (Franklin Lakes, NJ, USA). APC-conjugated F(ab')2 fragment specific to human IgG (Jackson Immunoresearch, West Grove, PA, USA) and FITC-conjugated goat anti-mouse IgG (Invitrogen, Carlsbad, CA, USA) were used as secondary antibodies. HRP-conjugated goat anti-rabbit (IgG) and goat anti-mouse (IgG) were purchased from Abcam and Jackson ImmunoResearch respectively.

Cell Lines

MCF10A cell line was purchased from ATCC (Manassas, VA, USA). MCFNeoT, MCFT1, and MCFCA1 cells were obtained from the Barbara Ann Karmanos Cancer Institute (Detroit, MI). The four cell lines were maintained as monolayers in Dulbecco's Modified Eagle's Medium-F12 (DMEM/F12) (Gibco, 11320033) supplemented with 5% horse serum (Gibco, 16050122), 1% penicillin/streptomycin (Lonza, 17-602E), 0.5 μg/ml hydrocortisone (StemCell, 37150), 100 ng/ml cholera toxin (Sigma, C-8052), 10 μg/ml insulin (Gibco, 1285014), and 20 ng/ml recombinant human EGF (Invitrogen, PHG0311). THP-1 monocyte cell line was purchased from ATCC (TIB-202, Manassas, VI) and TNF-reporter cell line (THP1-B5) was a gift from Dr. Ian Fraser (NIH/NIAID). Cells were cultured in RPMI-1640 (Life Technologies, Carslbad, CA) supplemented with 10% FBS, 1% Penicillin/Streptomycin and 1% Sodium Pyruvate. MCF cells were trypsinized off the plates. All cell lines were regularly tested for Mycoplasma contamination by PCR.

Macrophage Generation

Human peripheral blood mononuclear cells (PBMCs) were isolated from buffy coats of healthy blood donors (purchased from Vitalant, Pittsburgh, PA) by FicollTM (Sigma-Aldrich) density gradient. Monocytes were sorted by magnetic-activated cell sorting (MACS) using magnetic beads conjugated with anti-human CD14 (CD14 MicroBeads, human, Miltenyi Biotech, Bergish Gladbach, Germany) and cultured for 5 days in RPMI 1640 culture medium and M-CSF (100 ng/mL; R&D systems) to differentiate them into non-polarized (M0) monocyte-derived macrophages. Macrophages were generated from THP-1 and THP1-B5 monocyte cell lines by incubation for 48 hours with 100 nM phorbol 12-myristate 13-acetate (PMA, Sigma, P8139), followed by 48 hours incubation in RPMI medium. 5mM EDTA was used to detach macrophages.

Antibody Blocking of Macrophage Activation and Macrophage Stimulation With Danger Signals

125,000 MCF cell lines were pre-incubated with 1:10 dilution of an mouse IgG1 isotype control antibody (0.5 mg/ml), anti-Serpin B1 (1 mg/ml), anti-Annexin A1 (1 mg/ml) or anti-CEACAM1 (0.5 mg/ml) for 30 min at 4°C before co-incubation with macrophages. Macrophages were stimulated with seven 2-fold serial dilutions of the 50 μg/ml top solution of CEACAM1 and Annexin A1 protein (R&D systems) for 24 hours.

Co-Cultures

Macrophages were always pretreated with 2% FC receptor binding inhibitor (ThermoFisher) for 15 min at 4°C before co-incubation. Co-incubations were carried out in two different step-ups: i) macrophages were plated simultaneously with MCF cells to a ratio macrophages/MCF cells of 1:5 or 1:10. ii) macrophages were plated in the bottom of the plate and MCF cells in a 96-well 0.4 μm transwell (Corning) with the same 1:5 and 1:10 macrophages/MCF cells ratio. All coincubation were carried out in duplicate in 96-well plates, in 150ul of MCF medium and for 24 hours. When indicated in the legend, MCF cells were treated with neuraminidase (1:1000, Sigma-Aldrich) for 2 hours in low-adherent plates before co-incubation.

Cytokine-Based Assays (CBA) and ELISA

At the end of the co-incubation supernatants were collected for the determination of cytokine production and were stored at -80°C until used. Bead-based multiplex cytokine assay was used to measure the following cytokines: IL-1β, IFN-α2, IFN-γ, TNF-α, MCP-1, IL-4, IL-6, IL-8, IL-10, IL-12p70, IL-15, IL-17A, Il-18, IL-23, IL-33 (LEGENDplex™, Biolegend, San Diego, CA, USA). A serial dilution of the inflammatory cytokine panel was run on the same plate according to the manufacturer's instructions and read using a Fortessa flow cytometer. Ten thousand total events were recorded per sample and cytokines were considered undetectable below 2 pg/ml. Alternatively, human TNF-α ELISA Max kit (Biolegend) was used to measure the concentration of TNF-α in the supernatant of stimulated macrophages according to manufacturer's protocol.

Phagocytosis Assay

Macrophages and MCF cells were washed twice in PBS, and labeled with 1 μM CellTrace Yellow, Violet or CSFE (ThermoFisher, Waltham, MA, USA) according to manufacturer's protocol. After 2 hours of co-incubation in 6-well plates, cells were stained with a viability dye (1:1000 dilution in PBS, Ghost Red 780, #13-0865, TONBO Biosciences, San Diego CA, USA) for 15 min at 4°C. Samples were run on a Fortessa flow cytometer and gated based on negative signal for APC-Cy7 (*i.e.*, live cells). AMNIS image cytometry was performed using an Amnis cytometer. Cells were first visualized in a bright field and identified as macrophages (PacBlue) or MCF cells (FITC). The IDEAS software 6.2 was used to evaluate the percentage of doublets using the same gating strategy as for the phagocytosis assay. The images were merged to confirm the uptake of MCF cells by macrophages. The internalization score was measured using the internalization wizard of the IDEAS software.

Flow Cytometry

Cells were trypsinized, washed, collected and then stained with a viability dye (1:1000 dilution in PBS, Ghost Red 780, #13-0865, TONBO Biosciences, San Diego CA, USA) for 15 min at 4°C. Cells were stained with the anti-MUC1 antibody 4H5 (1:100), anti-HER2 antibody trastuzumab (1:2000), anti-CEACAM1 antibody (1:100), anti-Serpin B1 (1:100), anti-Annexin A1 (1:400), anti-CRT (1:100), anti-PECAM1 (1:100) and anti-CD47 (100) diluted in flow cytometry buffer (PBS + 1% BSA), for 30 min at 4°C followed by two washes with FACS buffer. Cells were then stained with secondary goat anti-mouse IgG or F(ab')2 anti-human IgG (1:200 dilution in FACS buffer) for 30 min at 4°C. Samples were run on a Fortessa flow cytometer and gated based on negative signal for APC-Cy7 (*i.e.*, live cells). APC (human) or FITC (mouse) mean fluorescence intensities were measured. 30,000 total events were recorded per sample.

Dual Luciferase Assay of THP1-B5 Cell TNF-α Production

After stimulation, the cells were washed once in PBS and lysed in passive lysis buffer (Promega). Firefly and renilla luciferase activities were determined using SpectraMax i3X and the software Softmax Pro 7.0.3 with an 5s acquisition. The ratio of firefly luminescence to renilla luminescence was used to reflect TNF-α production in response to stimulation.

Microscopy and 3-D Reconstruction

3-D overlay cultures were generated following the published method (16). Briefly, 8-chamber slides (Falcon CultureSlides, #354118) were coated with 40 μl of Matrigel (Corning ® Matrigel ® Matrix, #356234) and 5000 cells/well were seeded in medium containing 2% Matrigel and 5 ng/ml EGF. After 7-9 days, 3-D cultures in Matrigel were washed twice with media before seeding PMA-treated THP-1 (40,000 cells/well). THP-1 were previously labelled with CellTrace CFSE (Carboxyfluorescein

succinimidyl ester) as described above. After 24 hours of incubation, bright-field and fluorescence images were taken using the Z-stack option on an Olympus Fluoview 1000 confocal microscope at the Center for Biologic Imaging, University of Pittsburgh. The pictures were taken under fixed exposure conditions. 3-D reconstruction was performed with NIS-Elements (Nikon Instruments Inc., USA). 3-D cultures were delimited manually on each stack and FITC-positive macrophages were detected using the 3-D spot detection function. The infiltration score was determined as the number of macrophages detected inside the spheroid divided by the total volume of the spheroid, multiplied by 1,000,000.

2D-DIGE and Liquid Chromatography/ Mass Spectrometry (LC/MS) Analysis

Total cell lysates were generated from a confluent 10 cm^2 culture plate by scraping the cells with 100 µl of lysis buffer (7 M Urea, 2 M Thiourea, 10 mM Hepes pH 8.0, 10 mM DTT, 4% CHAPS) followed by 30 min incubation on ice, 7 cycles of 30 s ON/30s OFF sonicator and centrifugation for 15 min at 14,000 rpm. Extracted protein were stored at -70°C. One hundred µg of untreated and treated samples were labelled with Cy3- and Cy5-NHS minimal-labeling DIGE dyes (GE Healthcare, Uppsala, Sweden) diluted in Dimethylformamide (DMF) (Sigma) for 30 min on ice. Labeling of the two samples was reversed (reciprocal labeling) and run concurrently on a second 2D-DIGE gel to eliminate dye-dependent differences, constituting a technical replicate. First-dimension Isoelectric Point Focusing (IEF), and second-dimension SDS-PAGE were conducted as described (17) with the following modifications. Proteins were separated in the first-dimension on 18 cm pH 3-10NL IPG strips on a Protean i12 IEF Cell apparatus (Bio-Rad) for 32,000 Volt-hours. The samples were then separated on the second-dimension SDS-PAGE in 12% polyacrylamide gels in standard Tris-Glycine-SDS running buffer. After electrophoresis, the gels were fixed in a solution of 40% methanol and 10% acetic acid. The gels were imaged on a custom-built, fluorescent gel imager that housed a robotic spot-cutting head. The resultant fluorescent images were analyzed and selected spots that were then cut from the gels and identified *via* Nano LC-ESI-MS/MS, as described (18). We analyzed 2 biological replicates for each cell lines and 2 technical replicates for each biological replicate. After identification, the characteristics of the proteins and their sequences were obtained through the Uniprot database (https://www.uniprot.org). Finally, we applied Source Extractor to quantify the changes in 2D gels. Source extractor is a neural-network based star/galaxy classifier run by Docker. Once the intensity of each spot extracted, we created a cy3/cy5 ratio and normalized it by the mean intensity of 5 guiding spots. Guiding spots were defined as spots equally expressed in both cell lines (appearing yellow in the gel). The ratios were then log transformed to help with visualization.

Gene Expression Profiling

Total RNA was isolated from the four MCF cell lines using microKit (Qiagen). The epithelial cell gene profile was examined using nCounter Human Immunology Panel v2 (NanoString Technologies, Seattle, WA, USA). The protocol was carried out at the Genomics Research Core (University of Pittsburgh) using 100 ng of total RNA from each sample following their commercial protocol. Data were analyzed using the NSolver 4.0 software, following the procedure described in the package instructions (19). Normalization of mRNA content, which adjusts for positive control size factors, background noise and housekeeping genes size factors, as well as differential expression, was performed.

Immunohistochemistry

Human tissue arrays were obtained from BioChain (Newark, CA, USA) and contained 18 cases of normal, premalignant, and malignant breast tissues (#Z7020010). DCIS slides were provided by Dr. Rohit Bhargava (Department of Pathology, UPMC, Pittsburgh). Slides were deparaffinized by baking overnight at 59°C. Endogenous peroxidase activity was eliminated by treatment with 30% H_2O_2 for 15 min at room temperature. Antigen retrieval was performed by microwave heating in 0.1% citrate buffer for 10 min. Non-specific binding sites were blocked with 1% BSA. Reaction with anti-CD68 (1:100), anti-CEACAM1 (1:50) and anti-Annexin A1 (1:100) was performed for 1 hour at room temperature. Secondary antibodies were added at 1:100 dilution for 30 min. Positive signals were visualized by a DAB Substrate Kit (cat. #550880, BD Pharmingen) according to the manufacturer's protocol. Histology sections were viewed on an Olympus BX40 microscope. Images were acquired using Leica DFC420 camera and Leica Application Suite version 2.7.1 R1.

Statistical Analysis

Significance analyses were performed by using GraphPad Prism software version 7.0 (GraphPad Inc. San Diego, CA). Results were represented as means ± standard error of the mean (SEM) as specified in the legend. Statistical means and significance were analyzed using multiple comparison tests (One way ANOVA). Significance for all experiments was defined as follows: * $p<0.05$, ** $p<0.01$, *** $p<0.001$, **** $p<0.0001$.

RESULTS

Macrophages Exhibit an Activation Threshold in Response to Different Stages of Malignant Transformation

We incubated primary human monocyte derived macrophages (hMDM) for 24 hours with the MCF cell lines representing the various stages of malignant transformation, from normal (MCF10A) to premalignant (MCFNeoT and MCFT1) to invasive breast cancer (MCFCA1), and quantified 13 secreted cytokines using a cytometric bead array. We focused on i) cytokines with concentrations above the detection threshold, ii) cytokines secreted at different levels depending on the cancer cell line used in the co-incubation, iii) cytokines secreted in responses to more than one cell line, iv) cytokines for which concentrations were significantly different in co-culture compared to mono-culture. Following this screening method,

we selected three cytokines, TNF-α, IL-1β and IL-10. We found that co-incubation of macrophages with MCF10A induced low levels of TNF-α and IL-1β and high levels of IL-10 (**Figure 1A**). IL-10 levels were lower in co-cultures with MCFNeoT, and there was no detectable TNF-α or IL-1β. TNF-α levels dramatically rose in co-incubation with MCFT1 and decreased but remained high with MCFCA1. While IL-1β paralleled TNF-α, increasing in co-cultures with MCFT1 and reaching even higher levels in response to MCFCA1, IL-10 levels continued to decrease reaching their lowest levels in co-cultures with MCFT1 and MCFCA1.

We repeated these experiments with THP-1 monocyte cell line-derived macrophages that allow high reproducibility and for which a recent study showed that they could be used as a simplified model of human macrophages even though the order of magnitude in cytokine secretion after polarization was lower in hMDM compared to THP-1 (20). We recapitulated the results from primary macrophages: decrease in IL-10 and increase in TNF-α and IL-1β occurred between MCFNeoT and MCFT1 (**Figure 1B**). The result was the same at 1:10 macrophage/MCF cell ratio (**Supplementary Figure S1A**). The production of these three cytokines by the MCF cell lines alone was low and could not account for the difference observed in co-incubation (**Supplementary Figure S1B**). We then tested the importance of cell-cell contact for establishing or maintaining the differences in cytokine patterns of expression between an earlier premalignant stage MCFNeoT and a later premalignant stage MCFT1. We performed the co-incubations in transwell plates where macrophages were seeded in the bottom section of the transwell, separated from the MCF cells that were plated in the top of the transwell (**Figure 1C**). The shift in cytokine expression patterns between MCFNeoT and MCFT1 was diminished in the absence of direct cell-cell contact, with higher TNF-α concentrations in response to MCF10A and MCFNeoT soluble factors and increased IL-10 levels in responses to MCFT1 and MCFCA1. IL-1β levels were not affected and remained higher in response to MCFT1 and MCFCA1 compared to MCF10A.

Compared to unstimulated macrophages, THP-1 in contact with MCF10A showed similar levels of TNF-α and IL-1β but higher levels of IL-10, suggesting that macrophages where inert when sensing MCF10A (**Supplementary Figure S2**). In contrast, when incubated with MCFT1 and MCFCA1, THP-1 macrophages secreted lower levels of IL-10 and a 2-fold increase in TNF-α and IL-1β compared to unstimulated macrophages, suggesting immune activation. In co-incubations with MCFNeoT, macrophages seemed to be in a transitional state with similar levels of IL-10 and TNF-α but higher levels of IL-1β than resting macrophages. Therefore, an activation threshold depending on cell-cell contact and sensing of surface molecules appeared to be between the two premalignant states, MCFNeoT representing benign hyperplasia and atypical hyperplasia represented by MCFT1 in both primary hMDM and THP-1 derived macrophages.

We were also able to identify a similar activation threshold in THP-1-derived dendritic cells (**Supplementary Figure S3**). In co-incubations with MCFT1 and MCFCA1, IL-1β concentration was increased whereas IL-10 concentration was decreased compared to co-incubation with MCF10A, similarly to what was observed in macrophages. TNF-α was however produced at very low levels by dendritic cells and instead IL-18, another proinflammatory cytokine primarily involved in polarized T-helper 1 was increased between MCFNeoT and MCFT1.

Increase in Phagocytic Activity and Tumor Infiltration Coincides With the Macrophage Activation Threshold

We wanted to know if the activation threshold that resulted in increased pro-inflammatory cytokine production extended to other macrophage functions. We used flow cytometry to examine the interaction of labeled macrophages (CellTrace Violet, **Figure 2A**, Q3) with the MCF cell lines (CellTrace Yellow, **Figure 2A**, Q1), and quantified the percentage of the

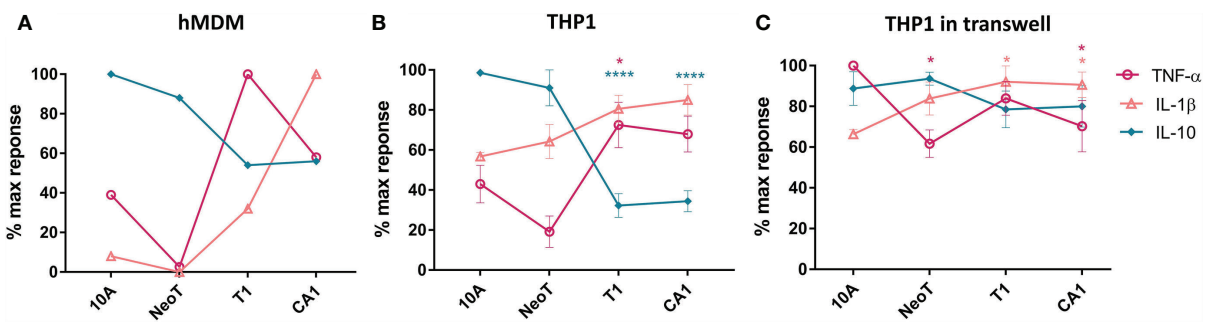

FIGURE 1 | The threshold of macrophage activation occurs between benign hyperplasia and atypical hyperplasia. **(A)** Cytokine production by human monocyte-derived primary macrophages (hMDM) and co-incubated with live cells from the MCF series indicated along the X-axis, at 1:5 macrophages/cell ratio. This result is representative of two experiments with two independent donors. **(B)** THP-1 monocyte cell line-derived macrophages were co-incubated as described in **(A)**. Results are presented as mean values ± SEM of three experiments. **(C)** THP-1 macrophages were co-incubated in a transwell plate with cells plated on top of the transwell. Cytokines were assessed in a bead-based assay and normalized against the highest cytokine concentration observed in responses to one of the cell lines. Results are presented as mean values ± SEM of three experiments. Cytokine concentrations in co-incubations with MCFNeoT (NeoT), MCFT1 (T1) and MCFCA1 (CA1) were compared to MCF10A (10A) using Fisher LSD tests for each cytokine (represented by different color): *p<0.05, ****p<0.0001.

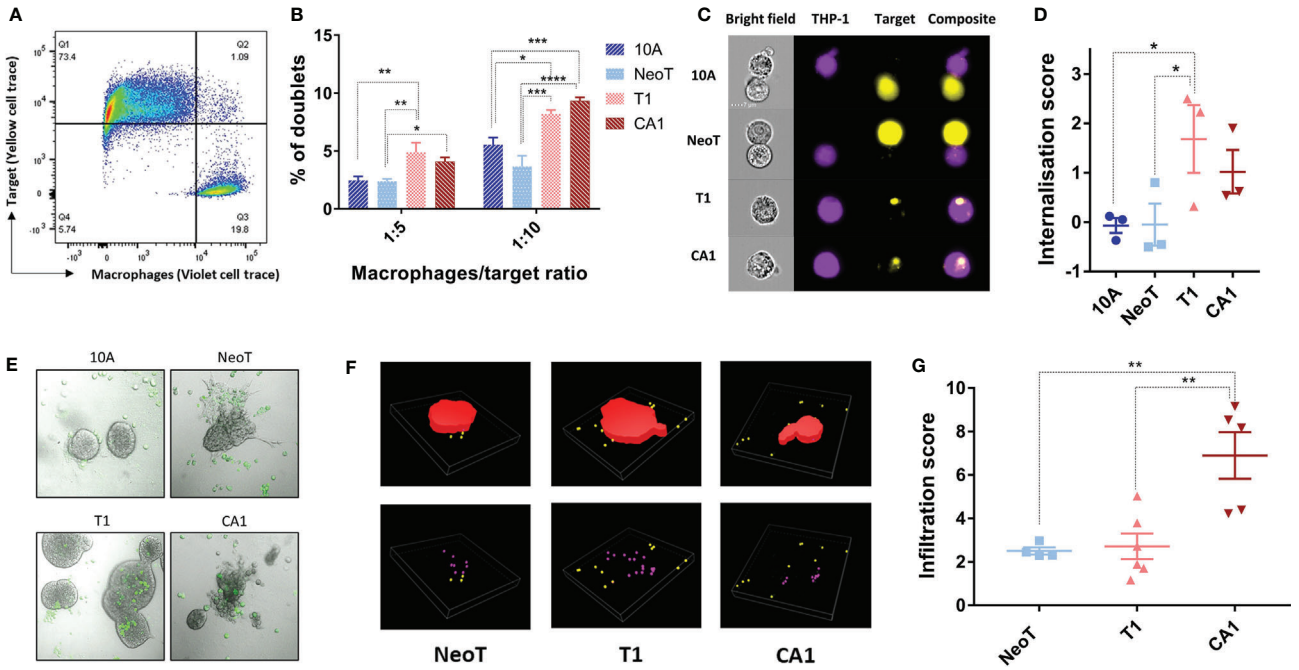

FIGURE 2 | Defining thresholds for macrophage phagocytosis of MCF cell lines in suspension and infiltration into 3-D clusters. **(A)** Example of the gating strategy to identify macrophage-MCF cell doublets. Macrophages and MCFNeoT cells were labeled with Pacific Blue and PE cell tracers, respectively. Doublets (Q2) were identified as PacBlue, PE double positive cells. **(B)** Percentages of doublets in 1:5 and 1:10 macrophage/MCF cell ratio as indicated MCF10A (10A), MCFNeoT (NeoT), MCFT1 (T1) and MCFCA1 (CA1). Results are presented as mean values ± SEM of four experiments. Fisher LSD test: ****p<0.0001, ***p<0.001, **p<0.01, *p<0.05. **(C)** Examples of images taken on the AMNIS 24h after coincubation of macrophages and indicated cells (1:20 ratio). Cells were labeled as in B and gating was on live cells. **(D)** Internalization scores were calculated using the Internalization function in IDEAS 6.2. Results are presented as mean values ± SEM of three experiments. Fisher LSD test: *p<0.05**. (E)** Representative images of macrophages contacting MCF10A (10A) and MCFNeoT (NeoT); infiltrating MCFT1 (T1); destroying MCFCA1 (CA1) cell clusters. Macrophages were labeled with FITC (green) and added on top of cells in 3-D clusters grown in Matrigel. **(F)** Examples of 3-D reconstructions from z-stacked images using the NIS-Element software. 3-D clusters are represented in red, non-infiltrating macrophages in yellow and infiltrating macrophages in pink. **(G)** Infiltration score was calculated as the number of infiltrating macrophages divided by the cluster volume as described in Materials and Methods. Results are presented as mean values ± SEM of 4 clusters for MCFNeoT, 6 for MCFT1 and 5 for MCFCA1. Fisher LSD test: **p<0.01.

total macrophage population that had formed doublets with the MCF cells (**Figure 2A**, Q2). Compared to MCF10A and MCFNeoT, macrophage incubation with MCFT1 and MCFCA1 yielded significantly higher number of doublets, in both 1:5 and 1:10 macrophage/MCF cell ratio (**Figure 2B**). Because these doublets can represent either phagocytosed cells or macrophage-MCF cell conjugates, we used the AMNIS instrument to visualize cell internalization. Indeed, the overlay of the fluorescent cell images allowed visualization of the MCF cells inside the macrophages distinguishing them from cell-cell conjugates (**Figure 2C**). We then used an internalization wizard and found that the doublets were mostly conjugates with MCF10A and MCFNeoT (low internalization score) whereas in the case of MCFT1, whole cells or cell debris were phagocytosed (high internalization score) (**Figure 2D**). Thus, we verified that the phagocytosis threshold was between MCFNeoT and MCFT1, matching the threshold for pro-inflammatory cytokine production.

To represent better the conditions of macrophage interaction with mammary epithelial cells during breast cancer progression *in vivo*, we cultured MCF cell lines in Matrigel for 7-10 days allowing them to form 3-D clusters, followed by the addition of macrophages and incubation for an additional 24h. A substantial number of labeled macrophages (CellTrace CFSE) migrated into the Matrigel and adhered to the 3-D clusters of all four cell lines (**Figure 2E**). MCFCA1 clusters, but not the other cell lines, appeared to be also damaged by macrophages (**Figure 2E**, CA1 panel). We then wanted to determine if the macrophages infiltrated the clusters and if that varied between the cell lines. After 3-D reconstruction (**Figure 2F**), we quantified the number of macrophages inside each cluster and determined an infiltration score normalized by the volume of the cluster. We found that macrophages adhered but did not infiltrate MCF10A. MCFNeoT and MCFT1 clusters were infiltrated similarly by macrophages, however, MCFCA1 clusters showed significantly higher infiltration scores (**Figure 2G**). We therefore observed a two-step infiltration threshold, with the first threshold between MCF10A and MCFNeoT when macrophages start to actively infiltrate the clusters and a second threshold between MCFT1 and MCFCA1 where macrophages infiltrate clusters at greater numbers. While the internationalization score was similar for the two cell lines, the greater infiltration in MCFCA1

clusters could explain the multiple observations of cluster destructions (**Figure 2E**).

Querying Well-Known Molecules Involved in Malignant Transformation, Macrophage Activation and Phagocytosis as Potential Danger Signals at the Macrophage Activation Threshold

As cell-cell contact was necessary to reveal the macrophage activation threshold, we focused our efforts on identifying cell surface molecules that could act as danger signals in malignant transformation. A common mechanism in tumor progression and metastasis is an alteration of glycosylation and sialylation (21). We investigated potential changes in the activation threshold after treating the MCF cells with neuraminidase, a glycoside hydrolase that removes sialic acids from the terminal positions of glycans and exposes the cryptic Tri/m-II, leading to an increased binding of calreticulin (CRT), the "eat me" signal, and phagocytosis (22). We found that neuraminidase treatment increased TNF-α concentration in responses to MCFT1 cells but did not move the threshold to the earlier premalignant stage or impact macrophage TNF-α response to the malignant MCFCA1 cells (**Figure 3A**).

Thus, we focused our next analyses on the expression of well-known tumor-associated antigens and damage-associated molecular patterns (DAMPs) to see which are associated with the transformation stages below *versus* above the macrophage activation threshold. We included in our analysis tumor antigens MUC1 and HER2, which have been reported to be over-expressed in breast cancer and to affect macrophage function (19, 23), and the "eat-me" signal CRT and the "don't eat me" signal CD47 (24). We found that the hypoglycosylated form of MUC1 and Her-2/neu were significantly overexpressed on the surface of MCFCA1 compared to MCFNeoT but not on MCFT1, suggesting that they were not involved in setting the macrophage activation threshold (**Figure 3B**). In contrast, MCFT1 and MCFCA1 expressed significantly higher levels of CRT which may contribute to enhanced phagocytosis of these cells. All three cell lines expressed similar levels of CD47. Finally, we analyzed mRNA expression of a panel of DAMPs such as BCL2, EGR, ICAM-3, IL-1α, IL-6, defensins, fibronectin 1 and the S100 protein (25), and found no correlation of their expression with the macrophage activation threshold (**Figure 3C**). Nevertheless, MCFT1 showed a specific pattern of defensin and EGR gene expression compared to MCFCA1 that could contribute as additional signals for macrophage activation.

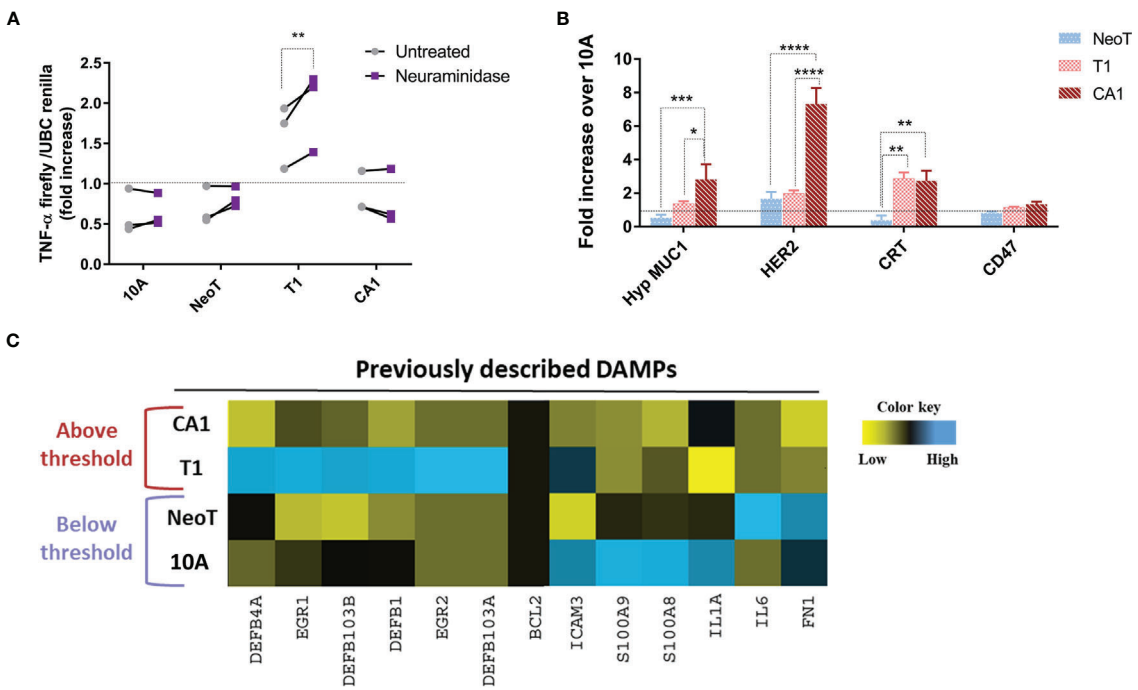

FIGURE 3 | Querying known DAMPs as candidate danger signals for determining macrophage activation threshold in response to transformed cells. **(A)** Sialic acid removal by neuraminidase treatment of MCF cells, indicated along the X-axis, does not affect the threshold. Y-axis shows fold increase of TNF-α in THP-1 B5 macrophages after 24h incubation at 1:5 macrophage/cell ratio. Co-incubation with untreated cells is in gray and with neuraminidase-treated cells in purple. Results are representative of three experiments. Fisher LSD test: **p<0.01. **(B)** Differential expression of well-known tumor-associated molecules in indicated cells compared to MCF10A (10A, dashed line), assessed by flow cytometry. Results are presented as mean values ± SEM of three experiments. Fisher LSD test: ****p<0.0001, ***p<0.001, **p<0.01, *p<0.05. **(C)** Heatmap representation of expression of genes coding for previously described DAMPs. The color key was provided by the software and shows a gradient from low (log2 FC <–1) to high (log2 FC>1) expression.

Unbiased Identification of Potential New Candidates Acting as Danger Signals Associated With the Macrophage Activation Threshold

We next took an unbiased approach to identify candidate danger molecules associated with macrophage activation. We first profiled the four MCF cell lines, quantifying expression of 579 immune response genes using the Nanostring nCounter Human Immunology V2 Panel. We identified 93 genes in MCFNeoT, 192 in MCFT1 and 136 in MCFCA1 that had log2 fold change of expression > 1 over MCF10A. When considering genes with a fold change of expression >5, we could identify four distinct groups of genes associated with various stages of malignant transformation: I) genes overexpressed in both MCFT1 and MCFCA1; II) genes overexpressed in MCFT1 only; III) genes overexpressed in MCFCA1 only; and IV) genes overexpressed in MCFNeoT only (**Figure 4A**). Of greatest interest are the genes in group I because they appear in MCFT1 and persist in MCFCA1, corresponding to the macrophage activation that starts in response to MCFT1 and continues in response to MCFCA1.

Because change in gene expression does not always translate to change in protein expression, we compared the proteome of each transformed cell line with the proteome of MCF10A and identified molecules specifically over-expressed in the premalignant and malignant cells. We extracted proteins from the monolayer cultures and labeled them with two different Cyanine-based, amine-reactive, minimal-labeling dyes and resolved them by 2D-DIGE (17) as described in Materials and Methods. **Figure 4B** is a representative 2D gel where proteins from MCF10A (red) and MCFT1 (green) were resolved and visualized as spots. We quantified the difference in expression of each protein by analyzing the pixel intensity of each spot in the images of 2D gels with Source Extractor across 2 biological and 4 technical replicates (**Supplementary Figure S4A**). After normalization that accounts for differences in dye intensities, we considered that proteins were significantly differentially expressed when they had a log2 fold change of spot intensity > 1 compared to MCF10A (**Supplementary Figure S4B**). Those protein spots were excised from the gel, digested into peptides with trypsin and subjected to mass spectrometry analysis. We found that five proteins were consistently over-expressed in MCFT1 and MCFCA1 but not in MCF10A and MCFNeoT: Tubulin beta, Gelsolin, Annexin A1, Annexin A3 and Serpin B1 (**Figure 4C**).

The Candidate Danger Molecules Annexin A1 and CEACAM1 Participate in the Macrophage Activation Threshold

From the 11 candidate molecules identified with NanoString and 2D-DIGE methods, we decided to focus on 4 of them to further

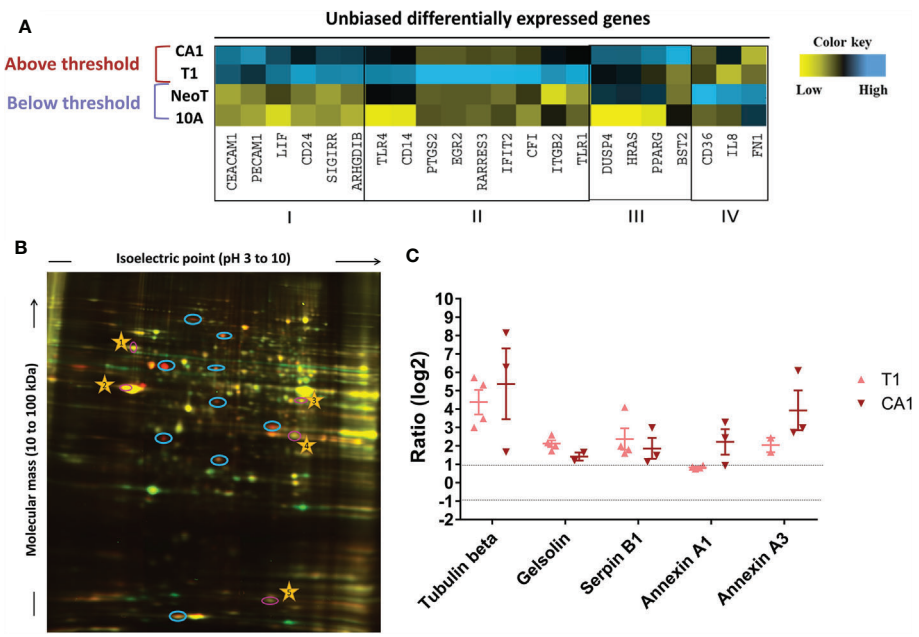

FIGURE 4 | Unbiased identification of genes and proteins associated with the macrophage activation threshold. **(A)** Heatmap representation of expression of genes with a fold increase greater than 5 over MCF10A (10A). The color key was provided by the software and shows an expression gradient from low (log2 FC <–1) to high (log2 FC>1). I, genes upregulated in MCFT1 (T1) and MCFCA1 (CA1); II, genes upregulated in MCFT1(T1) only; III, genes upregulated in MCFCA1 (CA1) only; IV, genes upregulated in MCFNeoT (NeoT) only. **(B)** Differentially expressed proteins between MCF10A labeled with Cy3-NHS (green) and MCFT1 labeled with Cy5-NHS (red); labeled proteins were mixed and resolved on 2D-DIGE as described in Materials and Methods. Shared proteins migrate identically and appear as yellow spots. Blue circles mark spots unique to MCFT1 that were picked for sequencing. Numbered yellow stars were used in the quantification analysis as guiding spots. **(C)** Changes in expression of 2D-DIGE-identified proteins in MCFT1 and MCFCA1 relative to MCF10A. Results are presented as mean values ± SEM of 4 technical replicates.

explore their surface expression and their impact on macrophage activation. We eliminated soluble factors (LIF) and proteins with structural or post-transcriptional changes (Tubulin beta) to focus on proteins for which antibodies were commercially available and their association with epithelial cancer progression had already been documented.

We measured protein expression on the surface of the transformed cell lines by flow cytometry and expressed the results relative to MCF10A (**Figure 5A**). Serpin B1 and PECAM1 were significantly more highly expressed on MCFCA1 compared to MCF10A, while MCFT1 and MCFCA1 both expressed significantly higher levels of CEACAM1 and Annexin A1 (**Figure 5B**). This confirmed that the transcriptomic and proteomic differences observed between the cell lines were associated with differences in surface expression. The only discordance between our 2D-DIGE and flow cytometry analysis was in the case of Serpin B1, which is largely localized to the cytoplasm.

We attempted to interfere with the macrophage threshold by pre-treating MCF cell lines for 30 minutes with antibodies against these three molecules in order to block their recognition by macrophages. **Figure 5C** shows that antibodies against Annexin A1 and CEACAM1, but not against Serpin B1, lowered TNF-α production in response to MCFT1 to levels comparable to what we see in response to MCF10A and MCFNeoT (**Supplementary Figure S5A**). This effect was antibody-dose dependent (**Supplementary Figure S5B**). Finally, we confirmed the potential of our candidates to activate macrophages by stimulating THP-1 macrophages with CEACAM1 and Annexin A1 individually at different concentration (**Figure 5D**). We found that both proteins activate a TNF-α responses in a dose-dependent manner. Activation by Annexin A1 was significant at concentration above 2.5ug/ml and while CEACAM1 followed the same trends it did not reach significance.

Evidence of a Threshold in Annexin A1 and CEACAM1 Expression in Human Breast Cancer Associated With Macrophage Activation

We examined human breast tissue samples of normal breast ducts (MCF10A-like), preneoplastic hyperplasia (MCFNeoT-like), ductal carcinoma *in situ* (DCIS, MCFT1-like) and invasive ductal carcinoma (MCFCA1-like), for evidence of a macrophage infiltration threshold, which we detected by the intensity of staining for the macrophage marker CD68. We saw no macrophages in the normal and in hyperplastic tissue sections (**Figure 6**). The first evidence of macrophage infiltration was found at the DCIS stage and it increased greatly in invasive ductal carcinoma (IDC). We also looked for differential expression of the candidate danger molecules Annexin A1 and CEACAM1 and saw, consistent with our cell line data, increased

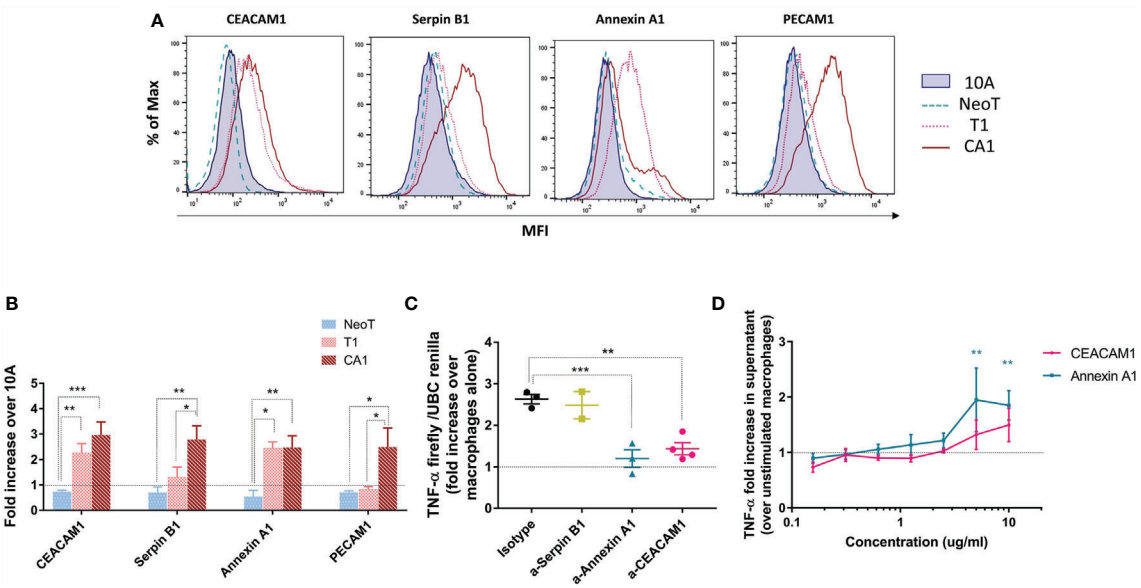

FIGURE 5 | Candidate danger molecules differentially expressed above and below the macrophage activation threshold that promote inflammatory function. **(A)** Representative flow plots of CEACAM1, Serpin B1, Annexin A1 and PECAM1 expression in MCF10A (10A), MCFNeoT (NeoT), MCFT1(T1) and MCFCA1 (CA1). **(B)** Differential expression of selected cell surface proteins by MCFNeoT (NeoT), MCFT1 (T1) and MCFCA1 (CA1) relative to MCF10A (10A, dashed line), assessed by flow cytometry. Results are presented as mean values ± SEM of three experiments. Fisher LSD test: ***p<0.001, **p<0.01. **(C)** Fold increase of TNF-α expression in macrophages co-incubated for 24h at a ratio of 1 macrophage to 5 MCFT1 cells, preincubated for 30 min with either an isotype control antibody or antibodies against Serpin B1 (yellow), Annexin A1 (blue) and CEACAM1 (pink). Results are presented as mean values ± SEM of two to four experiments. Fisher LSD test: **p<0.01, *p<0.05. **(D)** Fold increase in TNF-α production in macrophages stimulated with different concentrations of Annexin A1 and CEA proteins for 24h compared to unstimulated macrophages, as assessed by ELISA. Results are presented as mean values ± SEM of three experiments. Fisher LSD test: **p<0.01.

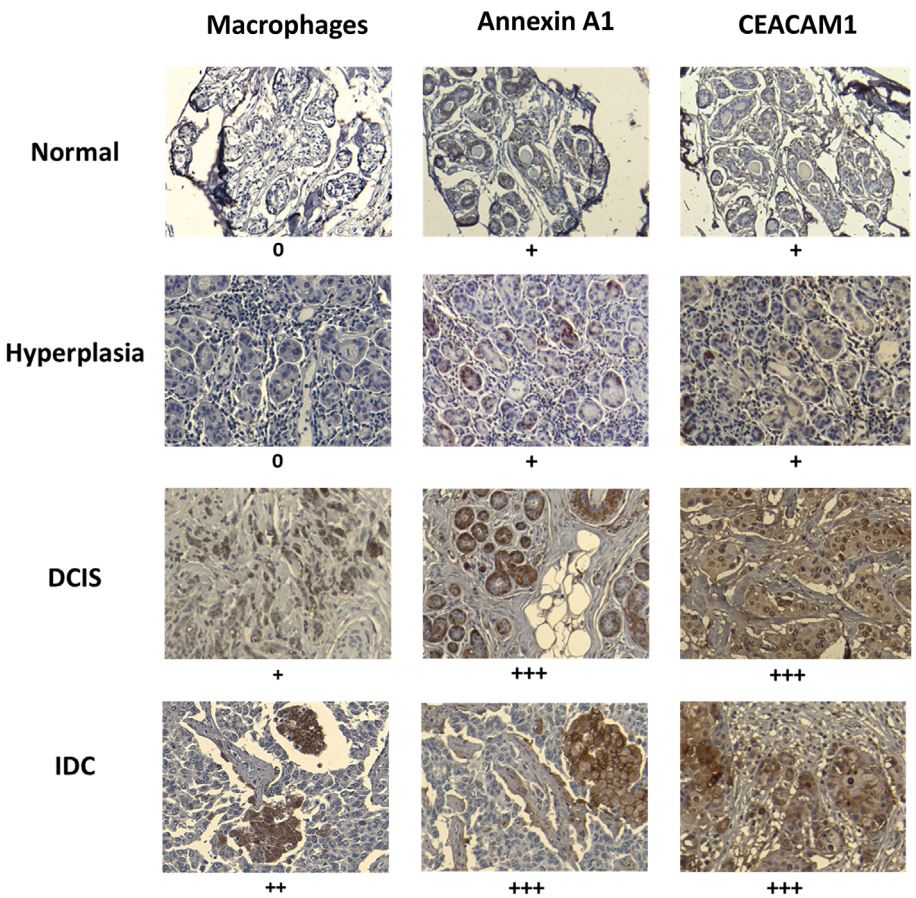

FIGURE 6 | Macrophage infiltration and expression of Annexin A1 and CEACAM1 in human breast tissues at various stages of transformation mirror the *in vitro* observed activation threshold. Example of paraffin-embedded samples of breast tissues, normal (1 of 8 total), hyperplasia (1 of 5 total), ductal carcinoma *in situ* (DCIS) (1 of 8 total) and invasive ductal carcinoma (IDC) (1 of 6 total), sectioned and stained with relevant antibodies (see *Materials and Methods*). Slides were scanned at 10X magnification in order to select for a high-resolution image at 20X. Images were scored by measuring the percentage of IHC positively labeled cells: +, <25%; ++, 25 to 50%; +++, 50 to 75%; and ++++ > 75%. Representative images are shown. The "+" signs refer to results from all analyzed samples in each tissue type.

Annexin A1 and CEACAM1 expression beginning at the DCIS (MCFT1-like) stage and continuing in invasive cancer.

DISCUSSION

Macrophages are known to be important effectors of cancer immunosurveillance (26) through programmed cell removal and activation of TLR pathways (27). However, because cancer cells closely resemble normal cells it is still unknown how early in tumor development can macrophages sense and eliminate abnormal cells or initiate adaptive immunity against them. The results described here give the first evidence in an *in vitro* model system of a threshold of activation and phagocytosis that is observed in macrophages that interact with cells at various stages of malignant transformation. We were able to detect such a threshold by co-culturing macrophages with a series of cell lines that were developed to recapitulate the progression of breast cancer (15). We were able to show a switch from low baseline levels of TNF-α production in response to normal MCF10A to high levels in response to atypical hyperplasia, a premalignant stage of disease. This activation of TNF-α production was dependent on cell-cell contact and was contemporaneous with an increase in phagocytic activity of macrophages against that same premalignant stage. The difference observed between MCFT1 and MCFCA1 in terms of 3-D cluster infiltration could be explained by the difference in "find-me" signal secretion (28). However, we demonstrated that *in vivo*, the threshold for infiltration of macrophages in malignant lesions was similar to the activation threshold, suggesting that our 3-D culture system might not reproduce all the interactions in the tumor microenvironment, especially those with other immune cells. Similarly, our system did not allow to measure the consequences of long-term interactions between tumor cells

and macrophages. Indeed, tumor cells can promote a pro-tumoral phenotype in macrophages, which in turn stimulate angiogenesis and enhance tumor cell invasion and motility. Future studies will explore the long-term interactions between early premalignant lesions and macrophages and how they impact their anti-tumoral activity.

Macrophages have been shown to distinguish cancer cells from normal cells by the DAMPs they express on their surface. DAMPs are recognized by TLR receptors on macrophages and trigger a molecular cascade leading to pro-inflammatory responses. This does not appear to be the main mechanism in the setting of premalignancy. We did not find an association between the expression of previously described DAMPs or known breast tumor-associated antigens with the threshold of activation of premalignant cells. Rather our study showed the importance of other molecules still poorly investigated for their role as "danger signals" or DAMPs, that appear to distinguish "self" from pre-cancer. Among those we found that we could block Annexin A1 and CEACAM1 with antibodies and abrogate the threshold for macrophage activation. They were also individually sufficient to activate TNF-α production by macrophage as previously described for CEA (29). We confirmed that they are overexpressed *in vivo* as early as ductal carcinoma *in situ*, which is represented by the premalignant MCFT1 cell line. In the Human Protein Atlas, expression of Annexin A1 (p=0.025) and CEACAM1 (p=0.007) was associated with an increased survival in breast cancer patients. Annexin A1 is an immune-modulating protein with diverse functions, one of which is an "eat me signal," that plays multiple roles in cancer growth and metastasis (30). Annexin A1 binds to the formyl peptide receptor (FPR) 2, a pathogen recognition receptor that triggers immune responses (31). CEACAM1 is well-known as a tumor-associated antigen over-expressed primarily in colorectal cancers but also in breast cancer (32), and it has been shown to activate inflammatory responses and promote differentiation of human macrophages (29, 33). Macrophages expressed two receptors for CEA molecules, TIM3 that has been identified as a receptor of CEACAM1 on innate cells, and the heterogeneous nuclear ribonucleoprotein M (CEAR) that is involved in immune activation signaling (34, 35).

The origin of ancestral myeloid phagocytes is linked to the appearance of vertebrates 300 million years ago (36) and phagocytic activity was also identified in invertebrate such as starfishes (37). Cancer probably appeared long before that with the transition to multicellularity more than half a billion years ago (38). Therefore, macrophages have been under strong selective pressure to eliminate aberrant cells in the absence of adaptive effectors appearing in mammals. Our study supports that macrophages are involved in the recognition of developing cancer with a threshold of activation with advanced premalignant stages based on highly conserved danger signals. Indeed, Annexin A1 is expressed from mammals to birds with a remarkable conservation of the intron-exon organization (39, 40), while the CEACAM1 gene family is evolving more rapidly but several orthologous genes can be found in distantly related mammals (41). This rather late activation threshold might reflect a trade-off between immunosurveillance and auto-immunity. In fact, because cancer is mainly a post-reproductive disease (42), natural selection is likely to strongly select mechanisms that increase survival in early life such as the ones that are limiting auto-immune responses even at the detriment of letting early premalignant lesions grow. In addition, the evolution of immunosurveillance has probably faced another trade-off related to inflammation associated with cell destruction that can potentially lead to *de novo* damages in surrounding normal cells and tumorigenesis, a situation that has been envisioned in responses to immune-checkpoint inhibitors (43). In light of these constraints, the evolution of inflammatory responses to only fitness-decreasing phenotypes of cancer (i.e., clinically malignant) seems to represent a beneficial equilibrium. However, recent evidence suggests that this equilibrium, and therefore the threshold of activation, might change depending on the importance of particular cells and organs for survival of the individual (44, 45). The eradication of non-essential cells (such as melanocytes) is affordable to the organism and therefore malignant transformation could trigger macrophage activation earlier than what we observed in the breast. Further studies should explore the existence and characteristics of the innate immune activation threshold in different cancer types.

The data emerging from our study suggest significant opportunities to use the "danger signals" on premalignant lesions to develop novel targeted chemoprevention and immunoprophylactic strategies. Drugs could also be developed to lower the discrimination threshold and therefore eliminate more efficiently earlier stages of premalignancy. However, those drugs will have to be carefully assessed for associated side-effects as early premalignant stages still share a lot of similarities with normal cells. Tampering with the immune tolerance trade-off could have dangerous auto-immune consequences and thus identification of markers that are present in premalignant lesions but absent or low in normal cells is crucial for the development of safe drugs. In addition to supporting cancer prevention, a better understanding of mechanisms selected by evolution for a decreased tolerance of the immune system to premalignant cells could have implications for the management of auto-immune disorders.

DATA AVAILABILITY STATEMENT

The datasets presented in this study can be found in online repositories. The names of the repository/repositories and accession number(s) can be found below: The Gene expression data have been deposited and can be found with the accession number GSE181585 at: https://www.ncbi.nlm.nih.gov/geo/query/acc.cgi?acc=GSE181585. Similarly, the mass spectrometry proteomics data have been deposited to the ProteomeXchange Consortium *via* the PRIDE partner repository with the dataset identifier PXD027746.

AUTHOR CONTRIBUTIONS

CJ, RG, and OF contributed to conception and design of the study. CJ and MD conducted the *in vitro* experiments. CJ, SB, and JM performed the 2D DIGE analyses. CJ wrote the first draft of the manuscript. RG, JM, and OF wrote sections of the manuscript. All authors contributed to manuscript revision, read, and approved the submitted version.

FUNDING

This work was supported by NIH grant R35 CA210039 to OJF and Forbeck Foundation grant to CJ.

ACKNOWLEDGMENTS

We are highly appreciative of the help and advice from Dr. Anda Vlad and Ms. Mary Strange, Dr. Simon Watkins and Morgan Jessup, and the Flow Core. This project used the Hillman Center for Biologic Imaging and Genomics Research Core that are supported in part by award P30CA047904.

SUPPLEMENTARY MATERIAL

The Supplementary Material for this article can be found online at: https://www.frontiersin.org/articles/10.3389/fimmu.2021.749597/full#supplementary-material

REFERENCES

1. Williams GC, Nesse RM. The Dawn of Darwinian Medicine. *Q Rev Biol* (1991) 66:1–22. doi: 10.1086/417048
2. Nowell PC. The Clonal Evolution of Tumor Cell Populations. *Science* (1976) 194:23–8. doi: 10.1126/science.959840
3. Cairns J. The Cancer Problem. *Sci Am* (1975) 233:64–72. doi: 10.1038/scientificamerican1175-64
4. Cahill DP, Kinzler KW, Vogelstein B, Lengauer C. Genetic Instability and Darwinian Selection in Tumours. *Trends Cell Biol* (1999) 9:M57–60. doi: 10.1016/S0962-8924(99)01661-X
5. Merlo LMF, Pepper JW, Reid BJ, Maley CC. Cancer as an Evolutionary and Ecological Process. *Nat Rev Cancer* (2006) 6:924–35. doi: 10.1038/nrc2013
6. Greaves M, Maley CC. Clonal Evolution in Cancer. *Nature* (2012) 481:306–13. doi: 10.1038/nature10762
7. Crespi B, Summers K. Evolutionary Biology of Cancer. *Trends Ecol Evol* (2005) 20:545–52. doi: 10.1016/j.tree.2005.07.007
8. Dunn GP, Old LJ, Schreiber RD. The Three Es of Cancer Immunoediting. *Annu Rev Immunol* (2004) 22:329–60. doi: 10.1146/annurev.immunol.22.012703.104803
9. Mapara MY, Sykes M. Tolerance and Cancer: Mechanisms of Tumor Evasion and Strategies for Breaking Tolerance. *J Clin Oncol* (2004) 22:1136–51. doi: 10.1200/JCO.2004.10.041
10. Jacqueline C, Biro PA, Beckmann C, Moller AP, Renaud F, Sorci G, et al. Cancer: A Disease at the Crossroads of Trade-Offs. *Evol Appl* (2017) 10:215–25. doi: 10.1111/eva.12444
11. Hanahan D, Weinberg RA. Review Hallmarks of Cancer: The Next Generation. *Cell* (2011) 144:646–74. doi: 10.1016/j.cell.2011.02.013
12. Gottschalk RA, Martins AJ, Angermann BR, Dutta B, Ng CE, Uderhardt S, et al. Distinct NF-κb and MAPK Activation Thresholds Uncouple Steady-State Microbe Sensing From Anti-Pathogen Inflammatory Responses. *Cell Syst* (2016) 2:378–90. doi: 10.1016/J.CELS.2016.04.016
13. Mascaux C, Angelova M, Vasaturo A, Beane J, Hijazi K, Anthoine G, et al. Immune Evasion Before Tumour Invasion in Early Lung Squamous Carcinogenesis. *Nature* (2019) 571:570–5. doi: 10.1038/s41586-019-1330-0
14. Mullins SR, Sameni M, Blum G, Bogyo M, Sloane BF, Moin K. Three-Dimensional Cultures Modeling Premalignant Progression of Human Breast Epithelial Cells: Role of Cysteine Cathepsins. *Biol Chem* (2012) 1:233–45. doi: 10.1016/j.dcn.2011.01.002.The
15. Santner SJ, Dawson PJ, Tait L, Soule HD, Eliason J, Mohamed AN, et al. Malignant MCF10CA1 Cell Lines Derived From Premalignant Human Breast Epithelial MCF10AT Cells. *Breast Cancer Res Treat* (2001) 65:101–10. doi: 10.1023/A:1006461422273
16. Debnath J, Muthuswamy SK, Brugge JS. Morphogenesis and Oncogenesis of MCF-10A Mammary Epithelial Acini Grown in Three-Dimensional Basement Membrane Cultures. *Methods* (2003) 30:256–68. doi: 10.1016/S1046-2023(03)00032-X
17. Minden JS. Two-Dimensional Difference Gel Electrophoresis. In: *Methods in Molecular Biology (Clifton, N.J.)*. Elsevier (2012). p. 287–304. doi: 10.1007/978-1-61779-821-4_24
18. Balasubramani M, Nakao C, Uechi GT, Cardamone J, Kamath K, Leslie KL, et al. Characterization and Detection of Cellular and Proteomic Alterations in Stable Stathmin-Overexpressing, Taxol-Resistant BT549 Breast Cancer Cells Using Offgel IEF/PAGE Difference Gel Electrophoresis. *Mutat Res* (2011) 722:154–64. doi: 10.1016/j.mrgentox.2010.08.019
19. Cascio S, Finn OJ. Intra-And Extra-Cellular Events Related to Altered Glycosylation of MUC1 Promote Chronic Inflammation, Tumor Progression, Invasion, and Metastasis. *Biomolecules* (2016) 6:1–16. doi: 10.3390/biom6040039
20. Tedesco S, De Majo F, Kim J, Trenti A, Trevisi L, Fadini GP, et al. Convenience *Versus* Biological Significance: Are PMA-Differentiated THP-1 Cells a Reliable Substitute for Blood-Derived Macrophages When Studying *in Vitro* Polarization? *Front Pharmacol* (2018) 0:71. doi: 10.3389/FPHAR.2018.00071
21. Kölbl AC, Andergassen U, Jeschke U. The Role of Glycosylation in Breast Cancer Metastasis and Cancer Control. *Front Oncol* (2015) 5:219. doi: 10.3389/fonc.2015.00219
22. Feng M, Marjon KD, Zhu F, Weissman-Tsukamoto R, Levett A, Sullivan K, et al. Programmed Cell Removal by Calreticulin in Tissue Homeostasis and Cancer. *Nat Commun* (2018) 9:1–15. doi: 10.1038/s41467-018-05211-7
23. Walens A, Dimarco AV, Lupo R, Kroger BR, Damrauer JS, Alvarez JV. CCL5 Promotes Breast Cancer Recurrence Through Macrophage Recruitment in Residual Tumors. *Elife* (2019) 8:e43653. doi: 10.7554/eLife.43653
24. Krysko DV, Ravichandran KS, Vandenabeele P. Macrophages Regulate the Clearance of Living Cells by Calreticulin. *Nat Commun* (2018) 9:1–3. doi: 10.1038/s41467-018-06807-9
25. Roh JS, Sohn DH. Damage-Associated Molecular Patterns in Inflammatory Diseases. *Immune Netw* (2018) 18(4):e27. doi: 10.4110/in.2018.18.e27
26. Chao MP, Majeti R, Weissman IL. Programmed Cell Removal: A New Obstacle in the Road to Developing Cancer. *Nat Rev Cancer* (2012) 12:58–67. doi: 10.1038/nrc3171
27. Feng M, Chen JY, Weissman-Tsukamoto R, Volkmer J-P, Ho PY, McKenna KM, et al. Macrophages Eat Cancer Cells Using Their Own Calreticulin as a Guide: Roles of TLR and Btk. *Proc Natl Acad Sci* (2015) 112:2145–50. doi: 10.1073/pnas.1424907112
28. Ravichandran KS. Find-Me and Eat-Me Signals in Apoptotic Cell Clearance: Progress and Conundrums. *J Exp Med* (2010) 207:1807. doi: 10.1084/JEM.20101157
29. Aarons CB, Bajenova O, Andrews C, Heydrick S, Bushell KN, Reed KL, et al. Carcinoembryonic Antigen-Stimulated THP-1 Macrophages Activate Endothelial Cells and Increase Cell-Cell Adhesion of Colorectal Cancer Cells. *Clin Exp Metastasis* (2007) 24:201–9. doi: 10.1007/s10585-007-9069-7
30. Moraes LA, Ampomah PB, Lim LHK. Annexin A1 in Inflammation and Breast Cancer: A New Axis in the Tumor Microenvironment. *Cell Adh Migr* (2018) 12:1–7. doi: 10.1080/19336918.2018.1486143

31. Schloer S, Hübel N, Masemann D, Pajonczyk D, Brunotte L, Ehrhardt C, et al. The Annexin A1/FPR2 Signaling Axis Expands Alveolar Macrophages, Limits Viral Replication, and Attenuates Pathogenesis in the Murine Influenza A Virus Infection Model. *FASEB J* (2019) 33:12188. doi: 10.1096/FJ.201901265R
32. Shao Y, Sun X, He Y, Liu C, Liu H. Elevated Levels of Serum Tumor Markers CEA and CA15-3 Are Prognostic Parameters for Different Molecular Subtypes of Breast Cancer. *PloS One* (2015) 10:e0133830. doi: 10.1371/journal.pone.0133830
33. Huang EY, Chang JC, Chen HH, Hsu CY, Hsu HC, Wu KL. Carcinoembryonic Antigen as a Marker of Radioresistance in Colorectal Cancer: A Potential Role of Macrophages. *BMC Cancer* (2018) 18(1):321. doi: 10.1186/s12885-018-4254-4
34. Wolf Y, Anderson AC, Kuchroo VK. TIM3 Comes of Age as an Inhibitory Receptor. *Nat Rev Immunol 2019 203* (2019) 20:173–85. doi: 10.1038/s41577-019-0224-6
35. Beauchemin N, Arabzadeh A. Carcinoembryonic Antigen-Related Cell Adhesion Molecules (CEACAMs) in Cancer Progression and Metastasis. *Cancer Metastasis Rev* (2013) 32:643–71. doi: 10.1007/S10555-013-9444-6
36. Barreda DR, Neely HR, Flajnik MF. Evolution of Myeloid Cells. *Microbiol Spectr* (2016) 4(3):10. doi: 10.1128/microbiolspec.mchd-0007-2015
37. Coteur G, DeBecker G, Warnau M, Jangoux M, Dubois P. Differentiation of Immune Cells Challenged by Bacteria in the Common European Starfish, Asterias Rubens (Echinodermata). *Eur J Cell Biol* (2002) 81:413–8. doi: 10.1078/0171-9335-00254
38. Aktipis CA, Nesse RM. Evolutionary Foundations for Cancer Biology. *Evol Appl* (2013) 6:144–59. doi: 10.1111/eva.12034
39. Gao Y, Horseman ND. Structural and Functional Divergences of the Columbid Annexin I-Encoding Cp37 and Cp35 Genes. *Gene* (1994) 143:179–86. doi: 10.1016/0378-1119(94)90094-9
40. Kovacic RT, Tizard R, Cate RL, Frey AZ, Wallner BP. Correlation of Gene and Protein Structure of Rat and Human Lipocortin I. *Biochemistry* (1991) 30:9015–21. doi: 10.1021/bi00101a015
41. Zebhauser R, Kammerer R, Eisenried A, McLellan A, Moore T, Zimmermann W. Identification of a Novel Group of Evolutionarily Conserved Members Within the Rapidly Diverging Murine Cea Family. *Genomics* (2005) 86:566–80. doi: 10.1016/j.ygeno.2005.07.008
42. Rozhok AI, DeGregori J. The Evolution of Lifespan and Age-Dependent Cancer Risk. *Trends Cancer* (2016) 2:552–60. doi: 10.1016/j.trecan.2016.09.004
43. Toomer KH, Chen Z. Autoimmunity as a Double Agent in Tumor Killing and Cancer Promotion. *Front Immunol* (2014) 5:116. doi: 10.3389/fimmu.2014.00116
44. Thomas F, Nesse RM, Gatenby R, Gidoin C, Renaud F, Roche B, et al. Evolutionary Ecology of Organs: A Missing Link in Cancer Development? *Trends Cancer* (2016) 2:409–15. doi: 10.1016/j.trecan.2016.06.009
45. Zitvogel L, Perreault C, Finn OJ, Kroemer G. Beneficial Autoimmunity Improves Cancer Prognosis. *Nat Rev Clin Oncol* (2021) 18(9):591–602. doi: 10.1038/s41571-021-00508-x

Conflict of Interest: OF is on the External Advisory Boards of GeoVax, Biovelocita, Immodulon, IASO and PDS Biotech.

The remaining authors declare that the research was conducted in the absence of any commercial or financial relationships that could be construed as a potential conflict of interest.

Publisher's Note: All claims expressed in this article are solely those of the authors and do not necessarily represent those of their affiliated organizations, or those of the publisher, the editors and the reviewers. Any product that may be evaluated in this article, or claim that may be made by its manufacturer, is not guaranteed or endorsed by the publisher.

frontiers in Immunology

ORIGINAL RESEARCH
published: 28 October 2021
doi: 10.3389/fimmu.2021.761214

Design and Immunological Validation of *Macaca fascicularis* Papillomavirus Type 3 Based Vaccine Candidates in Outbred Mice: Basis for Future Testing of a Therapeutic Papillomavirus Vaccine in NHPs

Patrick Neckermann[1†], Ditte Rahbaek Boilesen[2,3†], Torsten Willert[4], Cordula Pertl[4], Silke Schrödel[4], Christian Thirion[4], Benedikt Asbach[1], Peter Johannes Holst[2,3] and Ralf Wagner[1,5*]*

[1] Institute of Medical Microbiology & Hygiene, Molecular Microbiology (Virology), University of Regensburg, Regensburg, Germany, [2] Centre for Medical Parasitology, the Panum Institute, Department of Immunology and Microbiology, University of Copenhagen, Copenhagen, Denmark, [3] InProTher APS, Copenhagen, Denmark, [4] SIRION Biotech GmbH, Munich, Germany, [5] Institute of Clinical Microbiology and Hygiene, University Hospital Regensburg, Regensburg, Germany

OPEN ACCESS

Edited by:
Nicolas Cuburu,
National Cancer Institute (NCI),
United States

Reviewed by:
Shubhanshi Trivedi,
The University of Utah, United States
Shiwen Peng,
Johns Hopkins University,
United States

***Correspondence:**
Ralf Wagner
ralf.wagner@ur.de
Peter Johannes Holst
pholst@sund.ku.dk

[†]These authors have contributed equally to this work and share first authorship

Specialty section:
This article was submitted to Vaccines and Molecular Therapeutics, a section of the journal Frontiers in Immunology

Received: 19 August 2021
Accepted: 05 October 2021
Published: 28 October 2021

Citation:
Neckermann P, Boilesen DR, Willert T, Pertl C, Schrödel S, Thirion C, Asbach B, Holst PJ and Wagner R (2021) Design and Immunological Validation of Macaca fascicularis Papillomavirus Type 3 Based Vaccine Candidates in Outbred Mice: Basis for Future Testing of a Therapeutic Papillomavirus Vaccine in NHPs. Front. Immunol. 12:761214. doi: 10.3389/fimmu.2021.761214

Persistent human papillomavirus (HPV) infections are causative for cervical neoplasia and carcinomas. Despite the availability of prophylactic vaccines, morbidity and mortality induced by HPV are still too high. Thus, an efficient therapy, such as a therapeutic vaccine, is urgently required. Herein, we describe the development and validation of *Macaca fascicularis* papillomavirus type 3 (MfPV3) antigens delivered *via* nucleic-acid and adenoviral vectors in outbred mouse models. Ten artificially fused polypeptides comprising early viral regulatory proteins were designed and optionally linked to the T cell adjuvant MHC-II-associated invariant chain. Transfected HEK293 cells and A549 cells transduced with recombinant adenoviruses expressing the same panel of artificial antigens proved proper and comparable expression, respectively. Immunization of outbred CD1 and OF1 mice led to $CD8^+$ and $CD4^+$ T cell responses against MfPV3 antigens after DNA- and adenoviral vector delivery. Moreover, *in vivo* cytotoxicity of vaccine-induced $CD8^+$ T cells was demonstrated in BALB/c mice by quantifying specific killing of transferred peptide-pulsed syngeneic target cells. The use of the invariant chain as T cell adjuvant enhanced the T cell responses regarding cytotoxicity and *in vitro* analysis suggested an accelerated turnover of the antigens as causative. Notably, the fusion-polypeptide elicited the same level of T-cell responses as administration of the antigens individually, suggesting no loss of immunogenicity by fusing multiple proteins in one

vaccine construct. These data support further development of the vaccine candidates in a follow up efficacy study in persistently infected *Macaca fascicularis* monkeys to assess their potential to eliminate pre-malignant papillomavirus infections, eventually instructing the design of an analogous therapeutic HPV vaccine.

Keywords: MfPV3, HPV, therapeutic vaccine, adenoviral vector, immunogen design, DNA vaccine, invariant chain

INTRODUCTION

Despite efficient prophylactic vaccines and the possibility to screen for cervical lesions, infection with human papillomavirus (HPV) was still responsible for more than 340.000 cervical cancer-related deaths worldwide in 2020 (1). More than 85% of these cases occurred in middle- and low-income countries (2). Currently, there are three approved prophylactic vaccines providing near complete protection against vaccine-targeted HPV types, yet vaccine uptake is incomplete (3). However, these vaccines do not lead to the eradication of pre-infected cells, since they target the major capsid protein L1, which is not expressed in infected basal layer- and cervical cancer cells (4–7). Thus, novel interventions such as therapeutic vaccines are desirable.

Whereas most HPV infections are spontaneously cleared within months, some persist for years (8). These can progress towards low-grade squamous intraepithelial lesions (LSIL), which can further progress to high-grade squamous intraepithelial lesions (HSIL) and cervical cancer. The expression pattern of viral proteins changes during progression of SILs: in LSIL, mainly the early proteins E1/E2 are expressed, whereas in HSIL and transformed cells, E6/E7 are highly expressed and E2 expression is low or absent (9, 10).

In many cases of SIL, however, natural regression occurs as a result of $CD4^+$ and $CD8^+$ T cell infiltration (11). It has been shown that $CD4^+$ T cells play a major role in lesion regression with increased CD4:CD8 ratios being found in the stroma of LSIL (12). Genetic studies have shown that resistance and susceptibility loci for chronic infections and cancer cluster in the MHC II region. Cellular immune responses against E1 have been detected in some patients with HPV^+ cervical squamous cell carcinoma, mostly at low magnitude, but strikingly correlating with improved clinical outcomes (13). Conversely, $HPV16^+$ cervical cancer patients have impaired memory $CD4^+$ T-helper responses against E2 and E6, which emphasizes the important role of T cell responses in preventing progression and clearing lesions (14–17). It was also reported that HPV-exposed children have E2-specific T cell responses after clearing the infection (18). Current research on therapeutic HPV vaccines is primarily focused on the HSIL and cancer-stage of the disease, and directed toward the oncogenic viral proteins E6 and E7 (7). However, targeting the infection prior to carcinogenesis could be advantageous in terms of reducing morbidity and suffering related to cancer treatment, and might be easier to achieve. Thus, to target pre-malignant infection, other early proteins should be included as antigens.

There is no suitable small animal model to study persistent HPV infections in a preclinical setting, but *Macaca fascicularis* papillomavirus type 3 (MfPV3) has a close phylogenetic and phenotypic relationship to HPV16 (15, 19). Naturally occurring infections with this virus are associated with long-term persistence and at least LSIL-like lesions in the cervix of breeding female cynomolgus macaques (*Macaca fascicularis*), making them an ideal non-human primate (NHP) animal model (20, 21).

In a previous study using recombinant adenovirus-(rAd)-vectored vaccines encoding ancestral E1 and E2 antigens targeting the most conserved N- and C-terminal domains, we observed strong immune responses in mice and in cynomolgus macaques against these proteins, but cross-reactivity against prevalent MfPV types was only observed in a subset of animals. Nevertheless, 3 out of 3 animals with T-cell responses towards MfPV3-E1/E2 ended up clearing the specific MfPV3 infection (22). Furthermore, therapeutic efficacy of both early E1-E2 or E6-E7 antigen DNA vaccines, and synergy from co-administration of both vaccines, was demonstrated in the cottontail rabbit papillomavirus model (23). Combining both approaches by including E1, E2, E6 and E7 in an immunogen to a specific HPV type could potentially target infected cells in all stages of HPV infection and cancer development could be sufficient as therapeutic vaccine. Here, successful stimulation of E1/E2-specific cellular immunity would primarily clear infections in the LSIL-stage (24), whereas E6/E7-specific responses would mainly target the HSIL and cancer stages. As we decided not to attempt a broad ancestral antigen design, we also had the opportunity to include the less conserved parts of full length antigens thereby providing more epitopes for the immune system to act on.

To develop such a therapeutic vaccine, vectors expressing antigen candidates comprising E1, E2, E6 and E7 of MfPV3 were generated and characterized. The antigens are genetically linked to the intrinsic T cell adjuvant MHC-II-associated invariant chain (Ii) that has been shown to increase viral-vector-induced T cell responses in mice, cynomolgus macaques and humans (25–27). The antigens were designed in different configurations as artificial fusion proteins and initially characterized *via* DNA vaccination of outbred CD1 mice. Based on this initial characterization, adenoviral vectors from serotype 19a/64 were generated and characterized *in vitro* as well as *in vivo*.

METHODS

Antigen Sequences

Parts of the sequences encoding E1, E2, E6, and E7 of MfPV3 (EF558839.2) were designed and synthesized at Geneart/Thermo

Fisher (Regensburg, Germany) (28). Mutations were introduced into E6 and E7 to inactivate the oncogenic potential: L110Q and deletion of C-terminal ETEV in E6; E7 was modified by D24G, L71R, C95A; C297A was introduced into E2 to inactivate DNA-binding. Further sequence elements that were optionally used to build the prototype vaccine inserts (**Figure 1**) comprised (i) the human MHC-II-associated Ii invariant chain (25–27) (molecular adjuvant; NM_004355.3), (ii) a 2 amino acid GS-linker connecting E1 and E2 as well as E6 and E7 in the respective fusion proteins as well as (iii) the porcine teschovirus-1 p2A sequence (29) to support co-expression of two fusion proteins, respectively. Vaccine inserts were assembled either with fusion PCR, or using type IIs exocutter sites ("Golden gate" cloning; BsaI-HF v2, New England Biolabs, Ipswich, USA) or the NEBuilder HIFI DNA Assembly Kit (New England Biolabs, Ipswich, USA) according to manufacturer's instructions, and cloned into pURVac, a derivative of a DNA vaccine vector with a proven track record in various NHP and clinical trials (30–33). Vaccine inserts were then subcloned into pO6-19a-HCMV-MCS for subsequent generation of recombinant adenoviruses (34).

Cell Lines, Transfection, and Viral Infection

HEK293T cells and A549 cells were maintained and grown in Dulbecco's MEM (DMEM) supplemented with 10% Fetal Calf Serum (FCS) and 1% Penicillin/Streptomycin (Pen/Strep). 9E10 mycl hybridoma cells were cultivated in RPMI supplemented with 10% FCS, 1% Pen/Strep and 2 mM glutamine (Pan). All cell lines were maintained at 37°C and 5% CO_2 in a non-humidified incubator. HEK293T cells were transfected using the polyethylenimide (PEI) method (35). For PEI transfection, 4×10^5 cells were seeded in 6-well plates one day before transfection. The cells were transfected with 2.5 µg plasmid (equimolar amounts, filled with empty vector) and 7.5 µg PEI in DMEM without any supplements. After 6 h incubation, medium was exchanged to DMEM with 10% FCS and 1% Pen/Strep.

Subconfluent A549 cells were infected with Ad19a/64 vectors at an MOI of 30 in DMEM without any supplements. 2 h post infection, medium was exchanged to DMEM with 10% FCS and 1% Pen/Strep.

Generation and Titration of Adenoviral Vectors

E1/E3 deficient adenoviral vectors of serotype Ad19a/64 (rAd) were generated as previously described (34). Briefly, the vaccine inserts (**Figure 1**) were cloned into the shuttle vector pO6-19a-HCMV-MCS under control of a CMV promoter. The resulting plasmids were then inserted *via* Flp-recombination in *E. coli* into a BAC vector containing the genome of a replication deficient Ad-based vector deleted in E1/E3 genes. Recombinant viral DNA was released from the purified BAC-DNA by restriction digest with PacI. The obtained linear DNA was transfected into HEK293T cells for virus reconstitution and propagation. Recombinant viruses were released from cells *via* sodium deoxycholate treatment. Residual free DNA was digested by DNase I. Afterwards, vectors were purified by CsCl gradient ultracentrifugation followed by a buffer exchange to 10 mM Hepes pH 8.0, 2 mM $MgCl_2$ and 4% Sucrose *via* PD10 columns (GE Healthcare, Chicago, USA). Titration was performed using the RapidTiter method by detection of infected HEK293T cells *via* immunohistochemical staining with anti-hexon antibody (Novus, Adenovirus Antibody (8C4)). Insert integrity was confirmed by PCR amplification from the purified vector DNA followed by DNA sequencing.

Antibodies and Antibody Purification

The antibody against myc (9E10) was obtained from hybridoma cell supernatants. 9E10 mycl hybridoma cells were seeded at 5×10^5 cell per ml in RPMI supplemented with 1% FCS, 1% Pen/Strep and 2 mM glutamine. The supernatant was harvested 5 days after seeding and the antibody was purified *via* a HiTrap Protein G column (GE Healthcare, Chicago, USA). After washing the column with PBS, the antibody was eluted with 0.1 M glycine/HCl (pH 3.2), neutralized with 0.025 volumes of 1 M Tris/HCl (pH 9) and dialyzed against PBS.

Other antibodies used were: mouse anti-p2a peptide (3H4, 1:2000, Merck, Darmstadt, Germany), mouse anti-tubulin (DM1α, 1:1000, Santa Cruz, Heidelberg, Germany), mouse anti-ubiquitin-Biotin (eBioP4D1, 1:1000, Invitrogen, Carlsbad, USA), goat anti-mouse-HRP (115-036-003, 1:5000, Jackson,

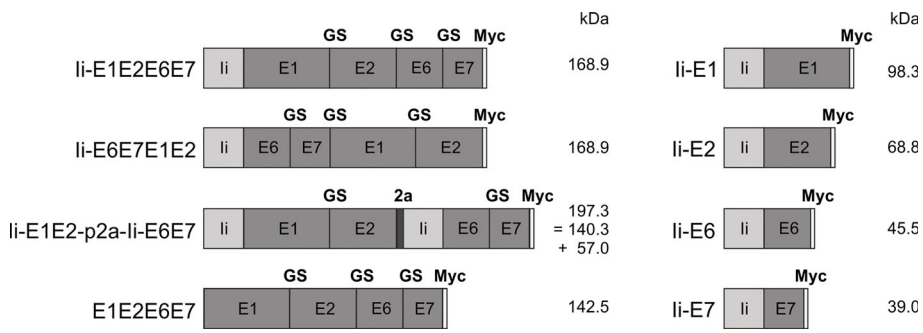

FIGURE 1 | Schematic representation of the conceived MfPV3 antigen variants. MfPV3 antigens were designed as fusion proteins comprising either E1, E2, E6 and E7 altogether, or E1 plus E2 and E6 plus E7 fusion proteins linked by a p2a peptide, and fused to the MHC-II invariant chain (li), respectively. For reference, E1, E2, E6, and E7 were fused as single open reading frames without the li coding sequence. Calculated molecular weights are indicated (kDa). li, MHC-II associated invariant chain; GS, glycine-serine-linker; 2a, p2a peptide for cotranslational separation; Myc, myc-tag sequence for antibody detection; kDa, kilo Dalton.

West Grove, USA), goat anti-rabbit-HRP (P0448, 1:2000, Dako, Santa Clara, USA), Streptavidin-HRP (11089153001, 1:5000, Roche, Basel, Swiss), rat anti-mouse-PE (A85-1, 1:100, BD, Franklin Lakes, USA).

Western Blot Analysis

Western blot analysis was performed as previously described (36). Briefly, cells of interest were lysed in TDLB buffer (50 mM Tris, pH 8.0, 150 mM NaCl, 0.1% SDS, 1% Nonident P-40, 0.5% sodium deoxycholate) supplemented with protease inhibitors (Complete Mini, Roche, Basel, Swiss). Total protein concentration of the supernatants was measured by the Bradford method (Protein Assay, BioRad, Feldkirchen, Germany). The proteins were separated on SDS-PAGE under reducing conditions and blotted on a nitrocellulose membrane for western blot analysis. Targets were probed with primary and secondary antibodies as listed above. HRP-labeled secondary antibodies and enhanced chemiluminescence substrate or Femto ECL (Thermo Fisher, Waltham, USA) were used for detection in a Chemilux Pro device (Intas, Göttingen, Germany).

Analysis of Ubiquitination

To analyze ubiquitinylated proteins, 24 h post transfection, cells were treated with 10 μM MG132 proteasome inhibitor for 6 h. Afterwards, cells were harvested in PBS and washed twice. For inactivation of deubiquitination enzymes, 20 mM N-ethylmaleimide from a freshly prepared stock solution were added to the TDLB lysis buffer. Lysates were generated as described above. Before immunoprecipitation, Protein G dynabeads (Thermo Fisher, Waltham, USA) were loaded with 10 μg of pulldown antibody. Using these beads, target protein was immunoprecipitated out of 500 μg cell lysate over night at 4° C under slow rotation. After washing the beads four times with PBS, SDS-PAGE buffer was added to the beads before heating at 95°C for 10 min. The samples were used for western blot analyses as described above.

Flow Cytometry Analysis of Cell Lines

Intracellular staining of antigens was performed using standard methods (36). Cells were fixed and permeabilized with Cytofix/Cytoperm-Buffer (4% PFA, 1% saponine, in PBS). All washing steps were done with Perm/Wash-Buffer (PBS containing 0.1% saponine). The cells were stained with anti-myc antibody (5 μg/ml, diluted in Perm/Wash-Buffer) and rat anti-mouse-PE (1:100 diluted in Perm/Wash-Buffer) each for 30 min. Flow cytometry was performed using an Attune NxT device (Thermo Fisher, Waltham, USA) with a 488 nm excitation and a 574/26 nm emission filter. Cells were gated on stained, mock-transfected cells. Evaluation of data was performed using Attune NxT software.

Animals and Immunizations

BALB/c and CD1 mice were obtained from Envigo (Horst, The Netherlands) and OF1 mice from Charles River (France). All animals were female, 6-8 weeks old and housed at the Panum Institute, University of Copenhagen. All experiments were initiated after allowing the mice to acclimatize for at least 1 wk. Experiments were approved by the National Animal Experiments Inspectorate (Dyreforsøgstilsynet, license no. 2016-15-0201-01131) and performed according to national guidelines. DNA immunizations were performed intradermal (i.d.) with 0.5 g DNA coated onto 1.6 μm gold microcarriers (BioRad, Feldkirchen, Germany) using the Helios Genegun System (BioRad, Feldkirchen, Germany). The mice received four DNA immunizations at intervals of one week each. One group received a mixture of four plasmids, 0.5 μg each, into one site. Immunizations with adenoviral vectors were performed intramuscular (i.m.) with 2×10^7 IFU rAd diluted in 50 μL PBS. Mice were anesthetized with isofluorane before rAd injections. One group received a mixture of four rAd, 2×10^7 IFU each, into one site.

Flow Cytometry of Splenocytes

Single cell suspensions of splenocytes were obtained by organ harvest in HANKs followed by straining through 70 μm cell strainers. Cells were incubated for 5 hours in 3 μM monensin with or without 1 μg/mL of relevant peptides. The cells were stained against surface markers: APC-Cy7 or BV421 CD8 (53-6.7, 1:200, BioLegend, San Diego, USA), PE-Cy7 CD4 (RM4-5, 1:800, BD), FITC CD44 (IM7, 1:100, BioLegend, San Diego, USA) and PerCP-Cy5.5 B220 (RA3-6B2, 1:200, BioLegend, San Diego, USA). After surface staining, cells were fixed in 1% PFA, permeabilized in 0.5% saponine, and stained intracellularly using APC IFN-γ (XMG1.2, 1:100, BioLegend, San Diego, USA) and PE TNF-α (MP6-XT22, 1:100, BioLegend, San Diego, USA) antibodies. The peptides used were 16-mers overlapping by 11 amino acids covering the entire Ii-E1E2E6E7 antigen. The peptides were pooled in 5 separate pools containing Ii (45 peptides), E1 (123 peptides), E2 (70 peptides, E6 (28 peptides) and E7 (21 peptides) peptides respectively. Peptides were obtained from KareBay, Town, China.

Flow cytometry was performed on the Fortessa 3 (BD Biosciences, Franklin Lakes, USA) flow cytometer and data analysis was performed using FlowJo V10 software. Epitope-specific $CD8^+$ T-cell responses were measured as $B220^-$, $CD8^+$ or $CD4^+$, $CD44^+$, IFN-γ^+ cells and are presented in total number of cells per organ. The quality of the IFN-γ^+ responses were evaluated by MFI of IFN-γ and fraction of double positive cells (expressing both IFN-γ and TNF-α) in the IFN-γ^+ $CD8^+$ or $CD4^+$ populations. The gating strategy is shown in **Supplementary Figure 1**.

In Vivo Cytotoxicity

The assay was performed similarly to what was previously described (37). Briefly, splenocytes from naïve BALB/c mice were incubated with MfPV3 E1, E2, E6 or E7 peptide pools (same as used for immune response analyses, see above) or no peptide for 30 minutes at 37°C, 5% CO_2, 2.5 μg of each peptide/mL, and subsequently stained with combinations of 0.4 or 5 μM CellTrace CFSE and 0.2 and 2.5 μM CellTraceViolet (CTV; ThermoFisher, Waltham, USA) for 10 minutes at 37°C, 5% CO_2. Pulsed and stained splenocytes were mixed at a 1:1:1:1:1 ratio, and a total of 2.5 x10^7 cells were injected intravenously into rAd-vaccinated recipient BALB/c mice. As the assay requires adoptive transfer of syngeneic target cells, it was necessary to use

inbred mice in order to have HLA-matching. 5 hours later, spleens were harvested, and target cells were identified on the Fortessa 3 (BD Biosciences, Franklin Lakes, USA) flow cytometer by CFSE/CTV staining. The percentage of killing was calculated using the following equation:

$$\%\ targeted\ killing = 100 - \left(\frac{\%\ peptide\ pulsed\ cells\ in\ vaccinated\ mice \,/\, \%\ non{-}peptide\ pulsed\ cells\ in\ vaccinated\ mice}{\%\ peptide\ pulsed\ cells\ in\ non{-}vaccinated\ mice \,/\, \%\ non{-}peptide\ pulsed\ cells\ in\ non{-}vaccinated\ mice} \right) * 100$$

Analysis of E1 (SIINFEKL) Presentation on MHC-I

HEK293T cells were transfected with 2.5-3.5 µg of pURVac encoding E1, which was C-terminally extended by the SIINFEKL Ovalbumin derived $CD8^+$ T cell epitope and a myc-tag and optionally fused to the Ii T cell adjuvant (25–27) at its N-terminus together with a pUC57 encoding H2Kb and β-2-microglobulin (β2m). A transfection with H2Kb alone was included as a negative control, and transfection with the H2Kb plasmid and a pUC57 plasmid encoding SIINFEKL fused directly to β2m was included as a technical positive control. 48 hours post transfection, cells were stained with PE anti-H2Kb-SIINFEKL (25-D1.16, 1:160, Invitrogen, Carlsbad, USA) and presence of SIINFEKL-H2Kb presentation on cell surfaces was detected on the LSRII or Fortessa 3 (BD Biosciences, Franklin Lakes, USA) flow cytometers, as a proxy for E1 presentation. All samples were run in biological 6-plicates, and the experiment was repeated at least two times.

Graphical Representation and Statistical Analysis

Non-stimulated samples were used as background controls, and their response values have been subtracted from the peptide-stimulated samples of the corresponding animal before performing statistical analysis and graphical presentation.

In order to aid visual presentation of the results, we applied a threshold for responses based on the average number of $B220^-$, $CD8^+$, $CD44^+$, IFN-γ^+ counts for unstimulated background samples. All samples with less counts than the average + 2 × SD of the background samples, are regarded as non-responding and therefore they have manually been adjusted to a value of 100 for the graphical presentation. All statistical analyses were done on non-adjusted values. The analysis of fraction of double positive (% TNF-α^+ IFN-γ^+ out of all IFN-γ^+) and MFI of IFN-γ^+ was only performed on responders (IFN-γ^+ count > avg + 2 × SD of unstimulated samples).

Statistical analysis was done using GraphPad Prism 8 software (GraphPad Software, San Diego, USA). Values with background subtracted were used to compare the individual groups using the Mann-Whitney test with Bonferroni correction for multiple comparisons. Positive control groups were not included in the multiple comparison analyses. Each symbol represents one mouse. Bars indicate median. Significance levels are marked by * ($p<0.05$), ** ($p<0.01$), *** ($p<0.005$), **** ($p<0.001$).

RESULTS

Design of the Antigens

Aiming towards the generation of a therapeutic vaccine, which is able to eliminate pre-existing papillomavirus-derived premalignant neoplasias, various antigens comprising E1, E2, E6, and E7 were designed. In order to enable future validation of a therapeutic concept in non-human primates, the above antigens were derived from *Macaca fascicularis* papillomavirus type 3 (MfPV3), which was shown to persist and induce LSIL-like lesions in the cervix of breeding female cynomolgus macaques (*Macaca fascicularis*) (20, 21). Herein, we describe the construction and immunological down-selection of eight different antigen designs in an outbred mouse model according to potency and breadth of induced T cell responses as basis for further preclinical validation in non-human primates.

Antigens were conceived as (i) read-through polypeptides with all four MfPV3 early antigens encoded in one open reading frame, (ii) alternatively E1-E2 and E6-E7 fusions were linked *via* a p2A site (38) supporting translational coupling and thus co-expression of the two fusion proteins or (iii) as single expression units. Within fusion proteins, the different MfPV3 early proteins were separated by a GS-linker. With one exception (E1E2E6E7), all polypeptides were NH_2 terminally fused to a the human MHC class II invariant chain (Ii), which has been described earlier to act as a T cell adjuvant (25). Furthermore, all constructs received a C-terminal myc-tag for convenient expression monitoring (**Figure 1**).

Since E6 and E7 are highly potent oncoproteins, only transformation-defective variants should be used in a therapeutic vaccine setting to ensure safety. Based on the homology to HPV16, the oncoprotein E6 was inactivated by introducing a L110Q substitution to prevent binding of E6 to E6BP and subsequent degradation of tumor suppressor p53 (39). Additionally, the C-terminal PDZ-domain was deleted (ΔETEV) to abolish binding of telomerase and other LxxLL proteins (40). E7 was inactivated by introducing the substitutions C24G, L71R, and C95A within the central LxCxE motif inhibit dimerization and reduce binding to pRB as well as Mi2β (40, 41). Furthermore, we changed E2 (C297A) to reduce DNA binding.

For initial biochemical and immunological characterization, the antigen coding sequences (**Figure 1**) were inserted into pURVac, a derivative of a DNA vaccine vector with a proven track record in various NHP and clinical trials (30–33). Transcription of the encoded transgenes is controlled by a human cytomegalovirus (CMV) promoter in combination with a human T-cell leukemia virus-1 (HTLV-1) regulatory element (42) and terminated by a bovine growth hormone poly-A site.

Biochemical and Cell Biological Characterization of MfPV3 Antigens

Following transient transfection of HEK293T cells with the respective DNA vaccine constructs, all antigens were properly expressed yielding proteins chiefly correlating with the calculated

molecular weights (**Figure 2A**). In some cases, especially for proteins with high signal intensities, bands of higher or lower molecular weight than calculated were observed. These might result from incompletely reduced oligomers (43) or N-terminal degradation products, which is expected as Ii transports some of its linked cargo to endosomal compartments where proteolytic degradation naturally occurs.

Since proteins of different sizes behave differently during blotting and signal intensities may not reflect the real expression levels, MfPV3 antigens were quantified by flow cytometry after intracellular staining with the anti-myc-antibody (**Figure 2B** and **Supplementary Figure 1**). Protein levels of the different MfPV3 antigens differed only marginally, except for Ii-E7, which exhibited two- to threefold higher MFI values compared to all other antigens.

MHC Class I-Restricted SIINFEKL Epitope Is Processed From E1 Fusion Protein and Abundantly Presented on MHC-I Molecules *In Vitro*

It has been reported that E1 of bovine papillomavirus type 1 is itself an unstable protein which is ubiquitinylated and rapidly degraded in naturally infected cells (44, 45). This observation together with the reported low prevalence of E1 specific antibodies in women with cervical disease (46) prompted us to assess whether MHC class I-restricted peptides at all can be processed and presented from E1. Therefore, the minimal H2Kb-restricted OVA epitope SIINFEKL (47) was fused to the C-terminus of E1 or, alternatively, to Ii-E1. The SIINFEKL epitope is a high affinity, highly immunodominant epitope, and therefore it is processing and presentation is easy to detect in *in vitro* studies. Following transfection of the respective pURVac expression constructs, MHC class I-restricted presentation of SIINFEKL could be readily detected using an H2Kb-SIINFEKL specific antibody. This supports the choice of E1 as a relevant antigen to be included in the therapeutic vaccine. Noteworthy, presentation was enhanced, when this fusion protein was N-terminally linked to the MHC class II invariant chain (Ii) (**Figure 2C**).

DNA Vaccination of Antigen Constructs Induces CD4$^+$ and CD8$^+$ T Cell Responses Against MfPV3 Early Antigens

Intradermal (i.d.) DNA immunization of outbred CD1 mice confirmed that all pURVac DNA vaccines encoding E1 and/or E2 induced E1- and E2-specific IFN-γ^+ CD8$^+$ and CD4$^+$ T cells (**Figure 3** and **Supplementary Figure 2**). More detailed, all DNA vaccine

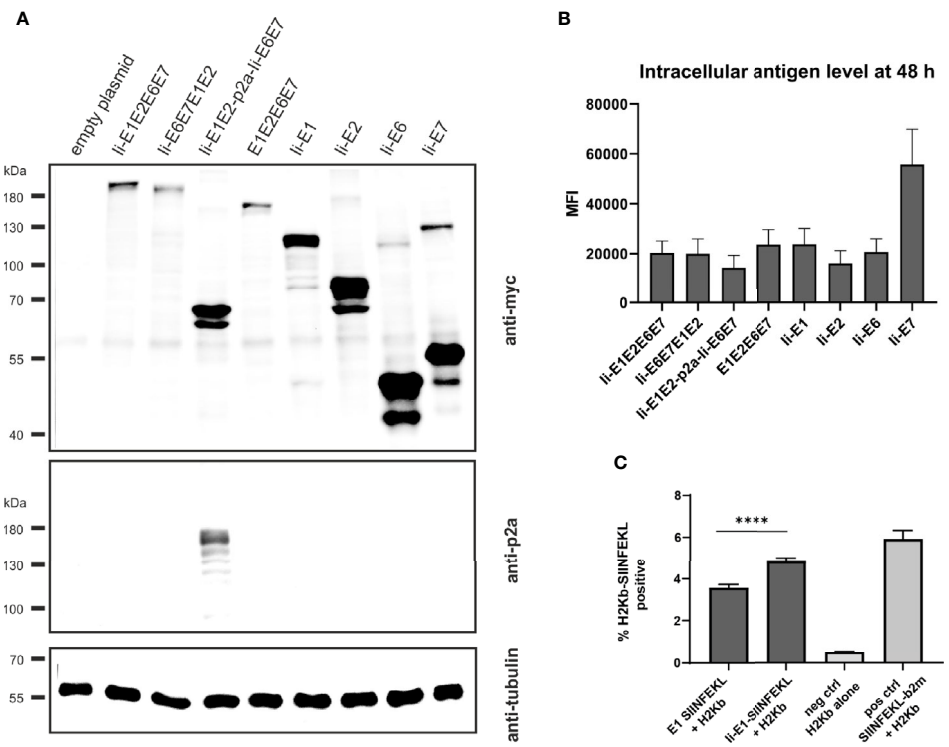

FIGURE 2 | Expression analysis of MfPV3 antigens. **(A)** Western blot analysis of HEK293T cell lysates 48 h following transfection with equimolar amounts of pURVac DNA vaccines expressing the various MfPV3 antigens. Antigens were detected with anti-myc (upper panel) and anti-p2a-peptide (middle panel) antibodies. Tubulin levels were monitored using an anti-tubulin antibody as loading control (lower panel). **(B)** Flow cytometry analysis of HEK293T cells 48 hours following transfection with pURVac DNA vaccines. Intracellular staining was performed with anti-myc antibody. Depicted is the mean fluorescence intensity (MFI) of the average of 3 independent experiments. Error bars indicate standard error of the mean. **(C)** Co-transfection of HEK293T cells with H2Kb alone or together with pURVac E1-SIINFEKL or Ii-E1-SIINFEKL, respectively. The percentage of SIINFEKL-H2Kb positive cells were determined after 48 hours by flow cytometry using an antibody recognizing the SIINFEKL-H2Kb-complex. Error bars indicate standard error of the mean. Light gray bars are negative (no peptide, H2Kb-plasmid only) and positive controls (SIINFEKL-β2m encoding plasmid + H2Kb), respectively. ****$p < 0.001$.

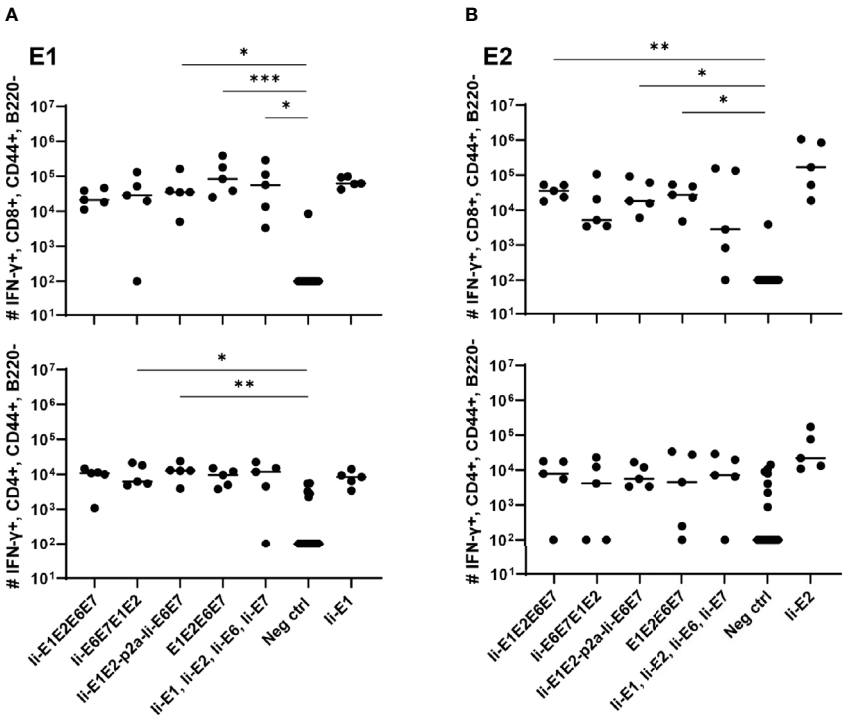

FIGURE 3 | T cell responses induced by the various pURVac DNA vaccines encoding E1, E2, E6 and E7 in outbred CD1 mice. CD1 mice (5 per group) were immunized 4 times in 1 week intervals with 0.5 µg DNA of pURVac DNA encoding the indicated MfPV3 early antigens. Mice were sacrificed 7 days post last immunization, spleens were harvested and $CD8^+$ (top panels) and $CD4^+$ (bottom panels) T-cell immune responses against E1 **(A)**, and E2 **(B)** were measured using ICS and flow cytometry. Negative control groups consist of all mice immunized with a pURVac DNA vaccine encoding antigens not covered by the peptide pools used for *in vitro* restimulation. Asterisks between groups indicate significant differences in response-levels after subtraction of background responses. Each symbol represents one mouse; the horizontal bar represents the median. Reference samples (mice vaccinated with pURVac DNA vaccine containing only the individual antigen linked to Ii, respectively) are not included in the statistical analysis (multiple comparison adjustment). *$p < 0.05$; **$p < 0.01$, ***$p < 0.005$.

candidates had provided an E1 response on par with the positive control (Ii-E1). None of these vaccines induced responses against E6 or E7 in these outbred mice, including the positive controls for these two antigens (Ii-E6; Ii-E7; **Supplementary Figures 3A, B**). Importantly, all vaccines encoding all four antigens as a polyprotein generated responses comparable to those induced by a mix of four vaccines encoding the antigens individually (Ii-E1, Ii-E2, Ii-E6, Ii-E7). This suggests that overall no immunogenicity was lost by delivering the MfPV3 early antigens as polyproteins from a single pURVac DNA vaccine. Regardless of the used pURVac vaccine construct, E1 and E2 specific T cell responses showed no statistical differences regarding the frequencies of E1- and E2-specific IFN-γ^+ $CD8^+$ and $CD4^+$ T cells. This is the case regardless (i) of whether Ii is fused to E1E2E6E7, (ii) of the order of the early antigens in the polyprotein, and (iii) of the use of a p2a site to separate Ii-E1E2 from Ii-E6E7. Only pURVac-Ii-E2, when administered alone, trended to induce slightly higher levels of specific $CD4^+$ and $CD8^+$ positive T cells (although statistically not significant). Contrasting previous findings, N-terminal fusion of the Ii molecular adjuvant did not enhance antigen specific T cell responses when delivered as DNA (48, 49). However, there are much fewer examples of Ii having an adjuvant effect in a DNA context compared to when it is encoded in viral vector transgenes. Additionally, it might be that the lack of Ii-effect is due to the high number of DNA immunizations (four in total), as the continuous boosting may have saturated the immune activation. It is possible that a difference between the Ii and non-Ii vaccines could have been detected after fewer immunizations. We were satisfied to see that all DNA constructs were immunogenic, and to address the Ii effect properly, we decided to create adenoviral vectors of all vaccine designs (see below). The quality of the T-cell responses was comparable across all vaccines (**Supplementary Figures 3C, D**), assessed by MFI of IFN-γ and TNF-α production of IFN-γ^+ T-cells. As expected, we found Ii specific $CD8^+$ T cell responses in most mice, and to $CD4^+$ in some mice (**Supplementary Figures 3A, B**), as the human Ii is allogenic in mice.

Characterization of Adenoviral Vectors

To further increase antigen specific cellular immune responses, viral vectors were subsequently used for antigen delivery. Adenoviral vectors from serotype 19a/64 (rAd) had been shown earlier to be generally suitable to deliver MfPV3 antigens and to efficiently induce $CD8^+$ T cell response in cynomolgus macaques (50). Based on the above DNA vaccination data, a refined panel of rAd vectors was generated comprising a modified set of recombinant MfPV3 antigens. Ii-E6E7E1E2 was excluded because it was not superior to the other polyproteins. However, the trend toward higher E2 specific T cell when administered alone prompted us to generate two additional adenoviruses, one encoding Ii-E1E6E7

linked to E2 *via* a self-separating p2a peptide (Ii-E1E6E7-p2a-Ii-E2) and for control Ii-E1E6E7 lacking E2. In order to confirm proper expression of the encoded antigens, western blot analysis was performed with A549 cells following transduction with the indicated rAds. All vectors readily expressed the antigens with bands resembling the respective fusion proteins at the expected molecular weights (**Figures 1** and **4A**, **B**). As for Ii-E1E2-p2a-Ii-E6E7, no higher than calculated molecular weight fragment could be detected for Ii-E1E6E7-p2a-Ii-E2, revealing that the complete separation at the p2a site also worked upon delivery *via* rAds. Quantitative analysis of transduced A549 cells by flow cytometry yielded comparable expression levels for the different myc-tagged MfPV3 polypeptides with the exception of higher expression of Ii-E7 (**Figure 4C** and **Supplementary Figure 4**). The overall picture was quite similar to the expression efficiencies observed after pURVac mediated antigen delivery in HEK293T cells.

Adenoviral Delivery Induces Potent Cellular Immune Responses Against MfPV3 Early Antigens in Outbred Mice

Intramuscular immunization of outbred CD1 mice confirmed that the rAd-formulation of the vaccines induced both $CD8^+$ and $CD4^+$ T cell responses against E1 and E2 antigens (**Figures 5A, B**). Notably, vaccines including Ii showed a trend towards higher magnitude responses than the vaccine not encoding Ii (**Figures 5A, B**: E1E2E6E7 compared to other vaccines). A tendency of Ii-mediated enhancement of responses was observed for both $CD4^+$ and $CD8^+$ T cell responses for some vaccine configurations, but the difference was only significant for E2-specific $CD8^+$ responses induced by Ii-E1E2-p2a-Ii-E6E7 compared to E1E2E6E7 (**Figure 5B**, upper panel). A direct comparison of the $CD8^+$ T-cell response against E1 from Ii-E1E2E6E7 and E1E2E6E7 (Mann-Whitney rank-sum) revealed a p-value of 0.06, which is not strictly significant, but strongly indicates a tendency of Ii improving the magnitude of $CD8^+$ T-cells against E1. Further, the vaccine without Ii was the only one for which the $CD4^+$ and $CD8^+$ T-cell responses against E1 was not significantly different from the negative control. This may confirm earlier observations suggesting that Ii can boost T cell responses in the context of adenoviral vaccine delivery. No difference in the quality of the T cell responses was detected, assessed by the MFI values of IFN-γ (**Supplementary Figure 5C**). When assessing the quality by the fraction of double-positive T cells capable of secreting both IFN-γ and TNF-α it is seen that E1E2E6E7 without Ii seemed to be inferior to other vaccines containing Ii (**Supplementary Figure 5D**). Based on this, we decided to focus our onwards efforts on antigen-fusion vaccine designs containing the Ii adjuvant.

Even though E6 and E7 represent small proteins as compared to E1 and E2 (11.9%, 8.1%, 50.8% and 29.2%, respectively, of the total antigen size), it was remarkable that no responses against E6 or E7 could be observed in any experiment testing the vaccines in outbred CD1 mice. As the MHC-type of the founders of the CD1 strain is unknown, and has not been controlled for since the

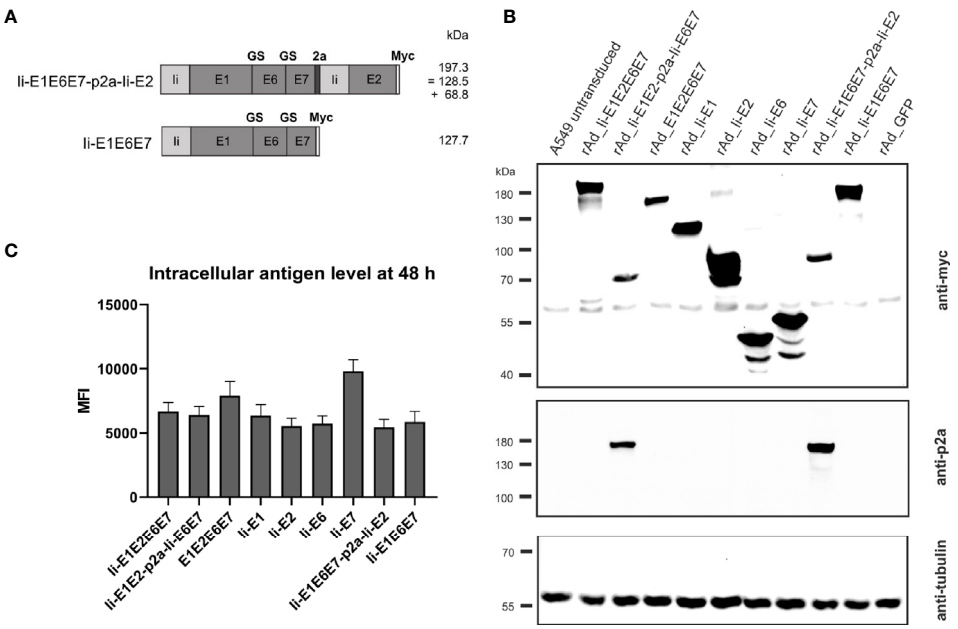

FIGURE 4 | Expression analysis of rAd-shuttled MfPV3 antigen constructs. **(A)** Schematic representation of the MfPV3 antigen variants Ii-E1E6E7-p2a-Ii-E2 and Ii-E1E6E7. Expected molecular weights (kDa) of the resulting polypeptides are shown. **(B)** Western blot analysis of A549 cell lysates 48 h following transduction with rAds encoding the indicated polypeptides at an MOI of 30. Antigens were detected with anti-myc (upper panel) and anti-p2a-peptide (middle panel) antibodies. As loading control, tubulin levels were monitored using an anti-tubulin antibody (lower panel). **(C)** Flow cytometry analysis of A549 cells 48 hours following transduction with rAds expressing the various MfPV3 antigens, at an MOI of 30. Intracellular staining was performed with anti-myc antibody. Depicted is the mean fluorescence intensity (MFI) of the average of 3 independent experiments. Error bars indicate standard error of the mean.

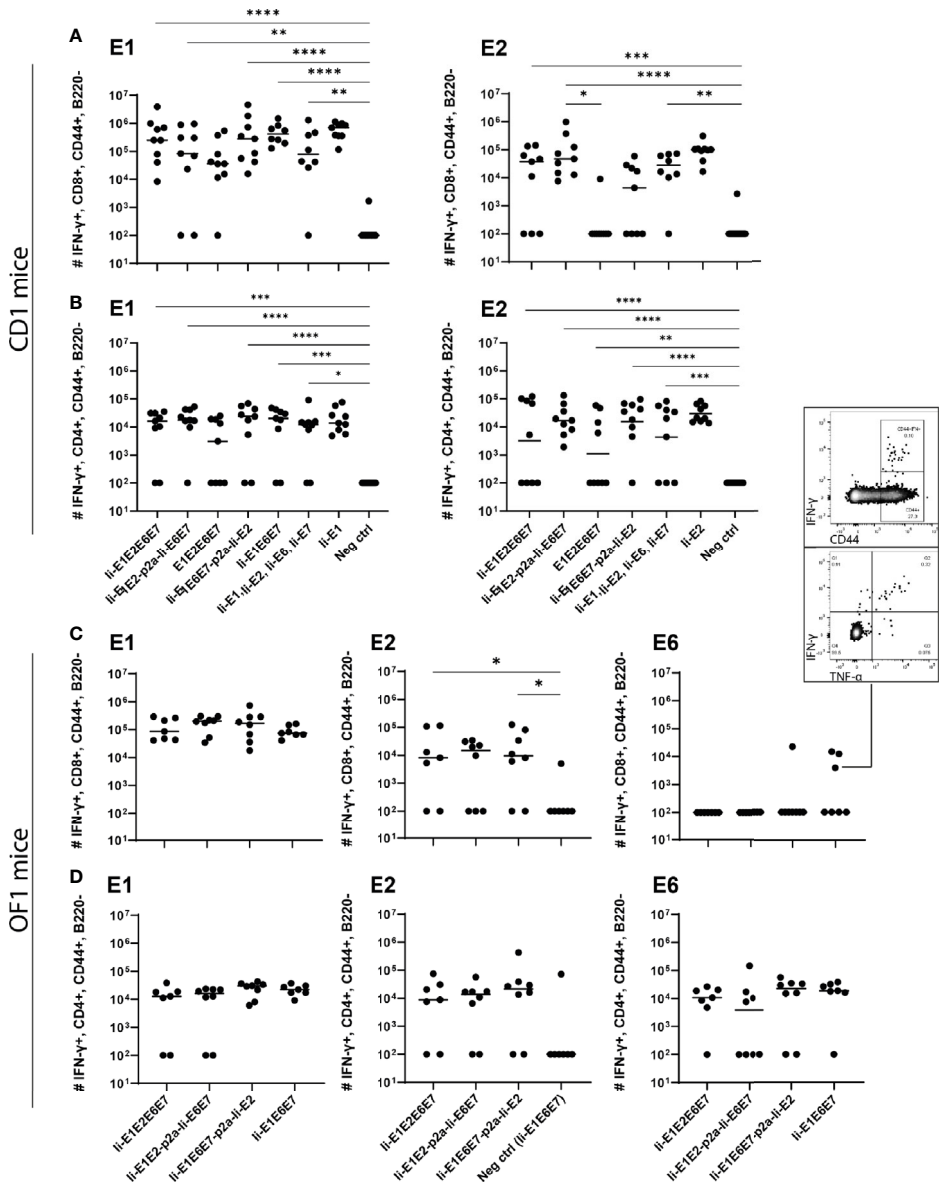

FIGURE 5 | Immunization of mice with adenovirus vectors induces potent cellular immune responses. CD1 mice **(A, B)**, or OF1 mice **(C, D)** were immunized with rAd vaccine (2×10^7 IFU) encoding the various MfPV3 early antigens as indicated. Mice were sacrificed on day 14, spleens were harvested and $CD8^+$ and $CD4^+$ T-cell immune responses against E1, E2, E6, and E7 were measured using ICS and flow cytometry. Negative control groups consist of all mice immunized with rAd encoding antigens not matching the peptide pools used for *in vitro* restimulation, respectively. Each symbol represents one mouse; a representative mouse depicted **(C)**, shows a CD44+IFN-γ+ population. The horizontal bar represents the median. Positive control samples (mice vaccinated with rAd containing only the relevant antigen linked to Ii) are not included in the statistical analysis (multiple comparison adjustment). *p < 0.05; **p < 0.01, ***p < 0.005, ****p < 0.001.

establishment of the strain, we wondered whether there were limitations in terms of MHC-restriction in the CD1 mice we had obtained. Limitations of genetic diversity of outbred mouse models has indeed been described previously and almost all outbred mouse strains except OF1 descent from the same 9 founder mice (51). Hence vaccination of OF1 mice was pursued to possibly detect different and broader immune responses than in CD1 mice. Besides vigorous T-cell responses against E1 and E2 (**Figures 5C, D**), we did indeed see solid $CD4^+$ T-cell responses against E6 (**Figure 5D**). A few mice also had $CD8^+$ T-cells reacting towards E6, confirming correct *in vivo* processing and immunogenicity of our vaccine constructs. Furthermore, the majority of the IFN-γ^+ cells were producing TNF-α as well, confirming the activation phenotype. Overall, the rAd19 delivery of the vaccines efficiently induced T-cells against at least three of the four MfPV3 polyprotein antigens tested, and the immunogenicity of the antigens was enhanced by inclusion of Ii.

Adenoviral Delivery Induces Specific Killing of Target Cells *In Vivo*

To assure that the cellular responses induced by the rAd-delivered antigens had cytotoxic capacity, we immunized inbred BALB/c mice with rAds expressing Ii-E1E2E6E7, Ii-E1E2-p2a-Ii-E6E7 and E1E2E6E7, and 14 days later challenged these mice with peptide-pulsed pre-stained syngeneic target cells. As the assay required adoptive transfer of syngeneic target cells, it was necessary to use inbred mice. The vaccines induced $CD8^+$ responses against E1 in BALB/c mice (**Figure 6A**), but not against the other antigens (data not shown), whereas $CD4^+$ responses were raised against E2 and E6 (**Supplementary Figure 6**). Ii again proved its relevance as molecular adjuvant, as the vaccine without Ii did not give rise to any detectable E1 specific $CD8^+$ responses in this inbred mouse model (**Figure 6A**). Consistent with the above, the *in vivo* cytotoxicity assay showed specific killing of E1 labelled cells (**Figures 6B, C**), and the hierarchy of specific killing capability corresponds to the number of IFN-γ^+ $CD8^+$ E1 specific T cells. We can conclude that the designed rAd vaccines induce potent and cytotoxic responses, which supports our hypothesis that this vaccine design will be capable of removing existing MfPV3 infections.

Ii-Fusion Enhanced Ubiquitination and Proteasomal Degradation

The molecular basis of the T cell adjuvant effect of Ii has not been fully clarified yet (43), but one of the suggested mechanisms of action is Ii mediated ubiquitination leading to proteasomal degradation of the linked antigen and thereby enhanced MHC-I presentation (**Figure 2C**) (27). To investigate if this mechanism could also account for the enhanced $CD8^+$ T-cell responses against the Ii-linked MfPV3 antigens, Ii-E1E2E6E7- and E1E2E6E7-transfected cells were cultivated in absence or presence of the proteasome inhibitor MG132. Anti-ubiquitin western blot analysis of the immunoprecipitated myc-tagged polypeptides revealed stronger ubiquitin-depending signal intensity for Ii-E1E2E6E7 compared to E1E2E6E7 lacking Ii (**Figure 7A**). This effect was even more pronounced when MG132 was present. Myc-specific signals confirmed the fidelity of the immunoprecipitation (IP) procedure, and analysis of the IP supernatants by an anti-tubulin western blot confirmed that comparable amounts of cell lysate were used in the IP procedure (**Figures 7B, C**). A higher level of ubiquitination is commonly associated with faster degradation. This could exemplarily be demonstrated by transiently expressing Ii-E1 and E1, both fused with the C-terminal SIINFEKL peptide, in absence or presence of MG132, respectively (**Figures 7D, E**). Without MG132, Ii-E1-SIINFEKL was hardly detectable whereas a prominent signal could be visualized when MG132 was added. Lower molecular weight signals are indicative of degradation products. This effect was not observed for E1 without Ii, which suggested that Ii induced an accelerated proteasomal degradation, as also reported by Esposito *et al.* (27).

DISCUSSION

Despite the availability of prophylactic vaccines against HPV infections there is an urgent need for an efficient therapeutic

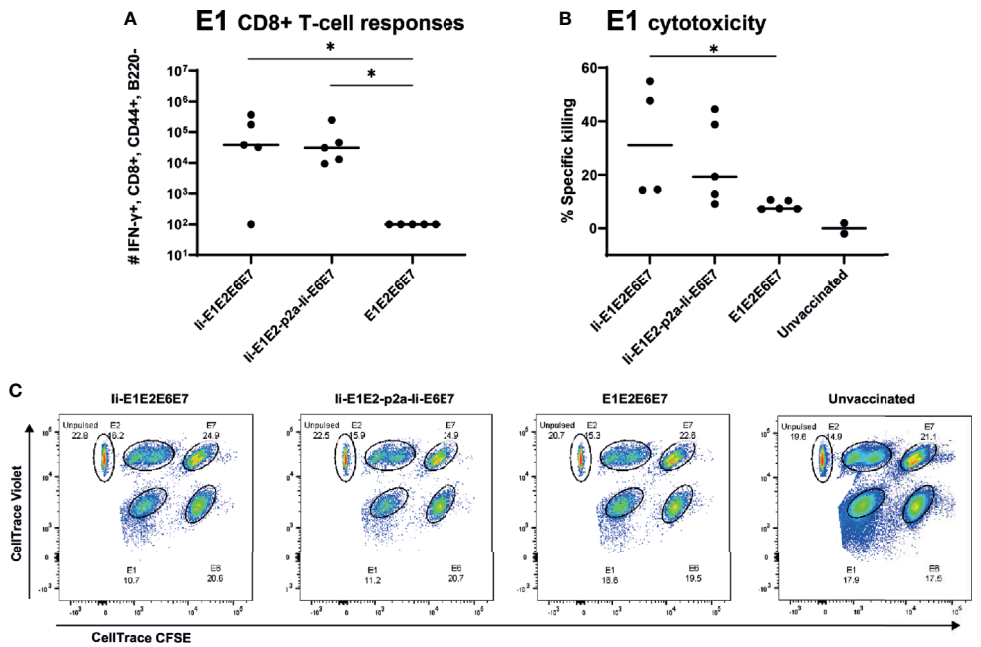

FIGURE 6 | Immune responses in inbred mice and *in vivo* cytotoxicity. Naïve BALB/c mice were immunized with rAd vectored vaccine encoding the indicated MfPV3 early antigens. 14 days post vaccination, immune responses were analyzed by ICS **(A)** or *in vivo* cytotoxicity regarding specific killing of E1-peptide pulsed cells **(B)**. Each symbol represents one mouse. Two unvaccinated mice were included as negative controls. **(C)** Representative plot of *in vivo* cytotoxicity. *$p < 0.05$.

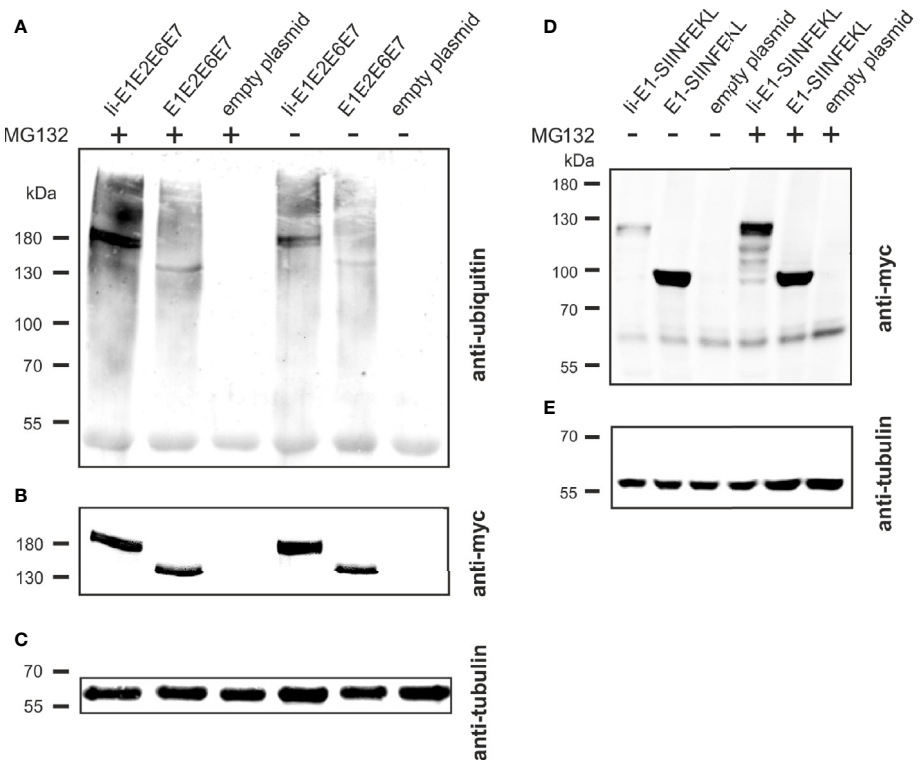

FIGURE 7 | Influence of Ii on ubiquitination and degradation. **(A–C)** pURVac Ii-E1E2E6E7, pURVac E1E2E6E7 or the empty plasmid were transfected into HEK293T cells. 24 h after transfection, cells were treated with MG132 or DMSO as control for 6 h. Myc-tagged proteins were immunoprecipitated and analyzed by western blot using an anti-ubiquitin antibody **(A)** and anti-myc antibody **(B)**. Tubulin levels were monitored using an anti-tubulin antibody as loading control **(C)**. **(D, E)** pURVac Ii-E1-SIINFEKL, pURVac E1-SIINFEKL or empty plasmid were transfected into HEK293T cells. 24 h after transfection, cells were treated with MG132 or DMSO for 6 h. The samples were analysed by western blot using anti-myc antibody **(D)** and anti-tubulin antibody **(E)**.

HPV vaccine. Currently, there are different vaccine development approaches focusing either on early stages (15, 22, 50, 52) of cervical lesions or late stages such as invasive cervical cancer (7, 53–56) or on all stages of pre-malignant cervical lesions (57).

Macaca fascicularis papillomavirus type 3 (MfPV3) infects cynomolgus macaques and infection is associated with persistence and cervical intraepithelial neoplasia (20, 21). Moreover, MfPV3 is phylogenetically closely related to HPV16 deriving from a shared most recent common ancestor and both viruses possess a similar mechanism of oncogenesis (19). The closely related pathogenesis of MfPV3 in *Macaca fascicularis* and the use of MfPV3 as antigen source, opens a perspective towards testing therapeutic vaccination concepts in naturally infected macaques and evaluate the correlates of protection under almost natural conditions (22).

Here, ten different antigens were designed comprising the viral early proteins E1, E2, E6 and E7 of MfPV3 in different configurations. These constructs combine antigens against early and late stages of papillomavirus persistence and should be capable of inducing T cell responses against both asymptomatic infections, LSIL as well as HSIL and cancers. All antigens were properly expressed, and their expression levels were similar, despite being artificially fused polypeptides.

Notwithstanding the limited immunogenicity of DNA vaccines, pURVac plasmid immunization of CD1 mice allowed for fast immunological evaluation in an outbred mouse model. Based on this initial *in vivo* screening, a refined antigen (Ii-E1E6E7-p2a-Ii-E2, and as reference Ii-E1E6E7) was devised in order to separate E2 from the readthrough protein, and Ii-E6E7E1E2 was excluded for further development of rAd-based vaccine prototypes. Antigen delivery with rAds of serotype 19a/64 confirmed that all antigens were immunogenic, with most of them inducing potent $CD4^+$ and/or $CD8^+$ T cell responses (**Figure 5**). In general, adenoviral delivery seemed to be overall more immunogenic than DNA vaccination.

Unexpectedly, no responses against E6 and E7 could be measured in these experiments with CD1 mice. Although fewer mice were expected to respond to E6 and E7 as compared to E2 and E1 due to significant differences in size (factor 5) and thus presumably also number of potential epitopes, it was still surprising that none of the 107 outbred CD1 mice in our experiments that were immunized with E6 and/or E7 harboring vaccines were responding. This might be explained by a yet limited number of MHC alleles in CD1 mice. This hypothesis is supported by the fact that this strain descends from only two male and seven female founder mice

(51). In a different strain, outbred OF1 mice, we could successfully elicit T-cell responses against MfPV3 E6 confirming the general immunogenicity of this antigen.

Coupling of antigens to certain immune regulatory molecules and T cell adjuvants could be beneficial in terms of breaking the immunosuppressive environment of tumors (53, 58). All immunogens expressed *via* rAds contain the T cell adjuvant Ii (except for E1E2E6E7 which serves as reference), which is known to enhance $CD4^+$ and $CD8^+$ T cell responses when delivered by viral vectors (25, 27, 43, 59, 60). A trend towards higher magnitudes of responses against E1 and E2 could be observed in outbred mice when vaccinated with rAd Ii-E1E2E6E7 as compared to E1E2E6E7 (**Figure 5**) and, importantly, a significantly higher level of specific killing in animals vaccinated with Ii-adjuvanted vaccines has been shown (**Figure 6**). Whereas enhancement of $CD4^+$ T cell response is believed to be induced by trafficking to endolysosomal compartments (43), far less is known about the mechanism of enhancing $CD8^+$ T cell response. However, this effect is independent of MHC-II and $CD4^+$ T cell response (59), but possibly depending on enhanced MHC-I loading (43). As shown in **Figure 7**, Ii-fusion leads to more pronounced ubiquitination and faster degradation of Ii-E1E2E6E7 as compared to E1E2E6E7 lacking Ii and therefore might increase the number of peptides that can be loaded on MHC I. Such a mechanism has recently also been reported by Esposito *et al.* (27), as a mode of action for the Ii adjuvant to increase the level of antigen fragments available for MHC presentation.

Considering the protein expression pattern during early stages of HPV infection, it is reasonable to assume that potent $CD4^+$ and $CD8^+$ T cell responses against E1 and E2 should be sufficient to boost naturally raised T cell immunity against PVs in LSIL, especially as E2 responses correlate with absence of lesion progression (14). Noteworthy, E1 is required for successful PV replication in infected cells, and cellular immune responses against E1 have been detected in PBMCs of some patients with HPV^+ cervical squamous cell carcinoma. The presence of E1 responses strikingly correlated in these patients with improved clinical outcomes, but the responses were of low magnitude, suggesting insufficient APC-mediated activation of T-cells (13). An explanation for this could be that E1 during natural infection, is not abundantly expressed and rapidly degraded through the proteasome as shown for bovine PV (44, 45). Therefore, a vaccine delivery format supporting efficient induction of $CD4^+$ and $CD8^+$ specific T cells on the fundament of strong expression and efficient antigen processing and presentation is expected to support elimination of premalignant PV transduced cells - provided that early neoplasias display sufficient amounts of E1/MHC-I complexes on their cell surface. Herein, we demonstrated strong expression of E1 comparable to E2, E6 and also E7, probably attributable to the strong CMV promoter-induced overexpression, and additional Ii-induced accelerated proteasomal degradation (**Figure 7**) and MHC-I presentation (**Figure 2C**). Altogether, our E1 containing vaccine constructs gave rise to solid $CD8^+$ and $CD4^+$ responses, which are cytotoxic to E1-peptide-pulsed target cells (**Figure 6**). This, together with the indication that E1 responses, once induced, are correlated with improved clinical outcome, build a strong case for including E1 in therapeutic HPV vaccine designs.

Our study has limitations regarding weak or absent T-cell responses against E6 and E7 in different mouse strains used in this study. This could potentially be due to immunodominance of E1 and E2 competing with E6 and E7 antigen processing, presentation and induction of specific T-cell responses. Alternatively, we cannot exclude that inactivation of E6- and E7-transforming potential has destroyed relevant epitopes. Ongoing preclinical analysis of viral vector-delivered MfPV3 antigens in macaques and comparable HPV16-derived immunogen designs in selected mouse models will provide further insights regarding the capacity of such immunogens to raise broad T-cell responses to the delivered early antigens including E6 and E7. The latter will also reveal to which extent the antigen design will be transferable to HPV16 and other high-risk HPV types. Given the phylogenetically close relationship and similar mechanisms underlying oncogenesis of the two papillomaviruses (19), similar immunological properties would be assumed.

Taken together, we developed ten immunogens that target the early proteins of MfPV3. These artificially fused polypeptides share similar biochemical and immunological properties without loss of individual antigen responses. Two polypeptides, Ii-E1E2E6E7 and Ii-E1E2-p2a-Ii-E6E7, elicited vigorous T cell responses, in particular, these two antigens were able to induce robust T cell responses against E1, E2 and E6, and to kill peptide-pulsed cells *in vivo*. Due to lower complexity, antigen size and non-inferior immunogenicity, Ii-E1E2E6E7 was chosen for further studies. Ad19a/64 proved to be a suitable vector to deliver Ii-E1E2E6E7 and is currently being validated as a therapeutic vaccine in persistently MfPV3-infected cynomolgus macaques. Moreover, the configuration of this immunogen will serve as template to generate novel vaccine candidates for therapeutic vaccination against high-risk human papillomavirus types.

DATA AVAILABILITY STATEMENT

The original contributions presented in the study are included in the article/**Supplementary Material**. Further inquiries can be directed to the corresponding authors.

ETHICS STATEMENT

The animal study was reviewed and approved by National Animal Experiments Inspectorate (Dyreforsøgstilsynet, license no. 2016-15-0201-01131).

AUTHOR CONTRIBUTIONS

PH, CT and RW designed the study and acquired funding, PN, DB, BA, TW, CP, SS planned and performed the experiments, PN, DB, BA, PH, CT and RW interpreted the data, PN and DB wrote the draft, PN, DB, BA, PH, RW wrote, reviewed and edited

the manuscript. All authors contributed to the article and approved the submitted version.

FUNDING

This project has received funding from the Eurostars-2 joint programme with co-funding from the European Union Horizon 2020 research and innovation programme (E!12151). The project E!12151 was carried out within the framework of the European funding program "Eurostars" and the German partners were funded by the Federal Ministry of Education and Research. The manuscript reflects only the authors' view and the European Commission is not responsible for any use that may be made of the information it contains. The funders had no influence on study design, data collection and analysis, decision to publish, or preparation of the manuscript.

ACKNOWLEDGMENTS

We kindly thank Eurostars-2 joint programme, the European Union Horizon 2020 research and innovation programme and the German Federal Ministry of Education and Research for funding this work. We would like to thank Jan Pravsgaard Christensen, UCPH, for advice on the *in vivo* cytotoxicity experiments, and Anette Stryhn Buus, UCPH, for assistance with peptides for *ex vivo* stimulation.

SUPPLEMENTARY MATERIAL

The Supplementary Material for this article can be found online: https://www.frontiersin.org/articles/10.3389/fimmu.2021.761214/full#supplementary-material

REFERENCES

1. Sung H, Ferlay J, Siegel RL, Laversanne M, Soerjomataram I, Jemal A, et al. Global Cancer Statistics 2020: GLOBOCAN Estimates of Incidence and Mortality Worldwide for 36 Cancers in 185 Countries. *CA Cancer J Clin* (2021) 71:209–49. doi: 10.3322/caac.21660
2. Haghshenas M, Golini-Moghaddam T, Rafiei A, Emadeian O, Shykhpour A, Ashrafi GH. Prevalence and Type Distribution of High-Risk Human Papillomavirus in Patients With Cervical Cancer: A Population-Based Study. *Infect Agent Cancer* (2013) 8:20. doi: 10.1186/1750-9378-8-20
3. Brotherton JML, Zuber PLF, Bloem PJN. Primary Prevention of HPV Through Vaccination: Update on the Current Global Status. *Curr Obstet Gynecol Rep* (2016) 5:210–24. doi: 10.1007/s13669-016-0165-z
4. Lehtinen M, Paavonen J, Wheeler CM, Jaisamrarn U, Garland SM, Castellsague X, et al. Overall Efficacy of HPV-16/18 AS04-Adjuvanted Vaccine Against Grade 3 or Greater Cervical Intraepithelial Neoplasia: 4-Year End-Of-Study Analysis of the Randomised, Double-Blind PATRICIA Trial. *Lancet Oncol* (2012) 13:89–99. doi: 10.1016/S1470-2045(11)70286-8
5. Hildesheim A, Herrero R, Wacholder S, Rodriguez AC, Solomon D, Bratti MC, et al. Effect of Human Papillomavirus 16/18 L1 Viruslike Particle Vaccine Among Young Women With Preexisting Infection: A Randomized Trial. *JAMA* (2007) 298:743–53. doi: 10.1001/jama.298.7.743
6. Schiller JT, Castellsagué X, Garland SM. A Review of Clinical Trials of Human Papillomavirus Prophylactic Vaccines. *Vaccine* (2012) 30(Suppl 5):F123–38. doi: 10.1016/j.vaccine.2012.04.108
7. Hung C-F, Ma B, Monie A, Tsen S-W, Wu T-C. Therapeutic Human Papillomavirus Vaccines: Current Clinical Trials and Future Directions. *Expert Opin Biol Ther* (2008) 8:421–39. doi: 10.1517/14712598.8.4.421
8. Ho GY, Bierman R, Beardsley L, Chang CJ, Burk RD. Natural History of Cervicovaginal Papillomavirus Infection in Young Women. *N Engl J Med* (1998) 338:423–8. doi: 10.1056/NEJM199802123380703
9. Xue Y, Bellanger S, Zhang W, Lim D, Low J, Lunny D, et al. HPV16 E2 is an Immediate Early Marker of Viral Infection, Preceding E7 Expression in Precursor Structures of Cervical Carcinoma. *Cancer Res* (2010) 70:5316–25. doi: 10.1158/0008-5472.CAN-09-3789
10. Chang L, He X, Yu G, Wu Y. Effectiveness of HPV 16 Viral Load and the E2/E6 Ratio for the Prediction of Cervical Cancer Risk Among Chinese Women. *J Med Virol* (2013) 85:646–54. doi: 10.1002/jmv.23490
11. Hibma MH. The Immune Response to Papillomavirus During Infection Persistence and Regression. *Open Virol J* (2012) 6:241–8. doi: 10.2174/1874357901206010241
12. Monnier-Benoit S, Mauny F, Riethmuller D, Guerrini J-S, Capilna M, Felix S, et al. Immunohistochemical Analysis of CD4+ and CD8+ T-Cell Subsets in High Risk Human Papillomavirus-Associated Pre-Malignant and Malignant Lesions of the Uterine Cervix. *Gynecol Oncol* (2006) 102:22–31. doi: 10.1016/j.ygyno.2005.11.039
13. Ma M, Feng Y, Fan P, Yao X, Peng Y, Dong T, et al. Human Papilloma Virus E1-Specific T Cell Immune Response Is Associated With the Prognosis of Cervical Cancer Patients With Squamous Cell Carcinoma. *Infect Agent Cancer* (2018) 13:35. doi: 10.1186/s13027-018-0206-5
14. Woo YL, van den Hende M, Sterling JC, Coleman N, Crawford RAF, Kwappenberg KMC, et al. A Prospective Study on the Natural Course of Low-Grade Squamous Intraepithelial Lesions and the Presence of HPV16 E2-, E6- and E7-Specific T-Cell Responses. *Int J Cancer* (2010) 126:133–41. doi: 10.1002/ijc.24804
15. Ragonnaud E, Pedersen AG, Holst PJ. Breadth of T Cell Responses After Immunization With Adenovirus Vectors Encoding Ancestral Antigens or Polyvalent Papillomavirus Antigens. *Scand J Immunol* (2017) 85:182–90. doi: 10.1111/sji.12522
16. Dillon S, Sasagawa T, Crawford A, Prestidge J, Inder MK, Jerram J, et al. Resolution of Cervical Dysplasia is Associated With T-Cell Proliferative Responses to Human Papillomavirus Type 16 E2. *J Gen Virol* (2007) 88:803–13. doi: 10.1099/vir.0.82678-0
17. de Jong A, van Poelgeest MIE, van der Hulst JM, Drijfhout JW, Fleuren GJ, Melief CJM, et al. Human Papillomavirus Type 16-Positive Cervical Cancer is Associated With Impaired CD4+ T-Cell Immunity Against Early Antigens E2 and E6. *Cancer Res* (2004) 64:5449–55. doi: 10.1158/0008-5472.CAN-04-0831
18. Koskimaa HM, Paaso A, Welters MJP, Grénman S, Syrjänen K, Burg SH, et al. Human Papillomavirus 16-Specific Cell-Mediated Immunity in Children Born to Mothers With Incident Cervical Intraepithelial Neoplasia (CIN) and to Those Constantly HPV Negative. *J Transl Med* (2015) 13:1–11. doi: 10.1186/s12967-015-0733-4
19. Chen Z, Long T, Wong PY, Ho WCS, Burk RD, Chan PKS. Non-Human Primate Papillomaviruses Share Similar Evolutionary Histories and Niche Adaptation as the Human Counterparts. *Front Microbiol* (2019) 10:2093. doi: 10.3389/fmicb.2019.02093
20. Chen Z, van Doorslaer K, DeSalle R, Wood CE, Kaplan JR, Wagner JD, et al. Genomic Diversity and Interspecies Host Infection of Alpha12 Macaca Fascicularis Papillomaviruses (Mfpvs). *Virology* (2009) 393:304–10. doi: 10.1016/j.virol.2009.07.012
21. Wood CE, Chen Z, Cline JM, Miller BE, Burk RD. Characterization and Experimental Transmission of an Oncogenic Papillomavirus in Female Macaques. *J Virol* (2007) 81:6339–45. doi: 10.1128/jvi.00233-07
22. Ragonnaud E, Andersson A-MC, Mariya S, Pedersen AG, Burk RD, Folgori A, et al. Therapeutic Vaccine Against Primate Papillomavirus Infections of the Cervix. *J Immunother* (2017) 40:51–61. doi: 10.1097/CJI.0000000000000153
23. Leachman SA, Shylankevich M, Slade MD, Levine D, Sundaram RK, Xiao W, et al. Ubiquitin-Fused and/or Multiple Early Genes From Cottontail Rabbit Papillomavirus as DNA Vaccines. *J Virol* (2002) 76:7616–24. doi: 10.1128/jvi.76.15.7616-7624.2002

24. Coleman N, Birley HD, Renton AM, Hanna NF, Ryait BK, Byrne M, et al. Immunological Events in Regressing Genital Warts. *Am J Clin Pathol* (1994) 102:768–74. doi: 10.1093/ajcp/102.6.768
25. Holst PJ, Sorensen MR, Mandrup Jensen CM, Orskov C, Thomsen AR, Christensen JP. MHC Class II-Associated Invariant Chain Linkage of Antigen Dramatically Improves Cell-Mediated Immunity Induced by Adenovirus Vaccines. *J Immunol* (2008) 180:3339–46. doi: 10.4049/jimmunol.180.5.3339
26. Capone S, Naddeo M, D'Alise AM, Abbate A, Grazioli F, Del Gaudio A, et al. Fusion of HCV Nonstructural Antigen to MHC Class II-Associated Invariant Chain Enhances T-Cell Responses Induced by Vectored Vaccines in Nonhuman Primates. *Mol Ther* (2014) 22:1039–47. doi: 10.1038/mt.2014.15
27. Esposito I, Cicconi P, D'Alise AM, Brown A, Esposito M, Swadling L, et al. MHC Class II Invariant Chain-Adjuvanted Viral Vectored Vaccines Enhances T Cell Responses in Humans. *Sci Transl Med* (2020) 12:eaaz7715. doi: 10.1126/scitranslmed.aaz7715
28. Raab D, Graf M, Notka F, Schödl T, Wagner R. The Geneoptimizer Algorithm: Using a Sliding Window Approach to Cope With the Vast Sequence Space in Multiparameter DNA Sequence Optimization. *Syst Synth Biol* (2010) 4:215–25. doi: 10.1007/s11693-010-9062-3
29. Liu Z, Chen O, Wall JBJ, Zheng M, Zhou Y, Wang L, et al. Systematic Comparison of 2A Peptides for Cloning Multi-Genes in a Polycistronic Vector. *Sci Rep* (2017) 7:2193. doi: 10.1038/s41598-017-02460-2
30. Asbach B, Kibler KV, Köstler J, Perdiguero B, Yates NL, Stanfield-Oakley S, et al. Priming With a Potent HIV-1 DNA Vaccine Frames the Quality of Immune Responses Prior to a Poxvirus and Protein Boost. *J Virol* (2019) 93: e01529–18. doi: 10.1128/JVI.01529-18
31. Sarwar UN, Costner P, Enama ME, Berkowitz N, Hu Z, Hendel CS, et al. Safety and Immunogenicity of DNA Vaccines Encoding Ebolavirus and Marburgvirus Wild-Type Glycoproteins in a Phase I Clinical Trial. *J Virol* (2015) 211:549–57. doi: 10.1093/infdis/jiu511
32. Joseph S, Quinn K, Greenwood A, Cope AV, McKay PF, Hayes PJ, et al. A Comparative Phase I Study of Combination, Homologous Subtype-C DNA, MVA, and Env Gp140 Protein/Adjuvant HIV Vaccines in Two Immunization Regimes. *Front Immunol* (2017) 8:149. doi: 10.3389/fimmu.2017.00149
33. Pantaleo G, Janes H, Karuna S, Grant S, Ouedraogo GL, Allen M, et al. Safety and Immunogenicity of a Multivalent HIV Vaccine Comprising Envelope Protein With Either DNA or NYVAC Vectors (HVTN 096): A Phase 1b, Double-Blind, Placebo-Controlled Trial. *Lancet HIV* (2019) 6:e737–49. doi: 10.1016/S2352-3018(19)30262-0
34. Ruzsics Z, Lemnitzer F, Thirion C. Engineering Adenovirus Genome by Bacterial Artificial Chromosome (BAC) Technology BT - Adenovirus: Methods and Protocols. In: Chillón M, Bosch A, editors. Totowa, NJ: Humana Press (2014). p. 143–58. doi: 10.1007/978-1-62703-679-5_11
35. Boussif O, Lezoualc'h F, Zanta MA, Mergny MD, Scherman D, Demeneix B, et al. A Versatile Vector for Gene and Oligonucleotide Transfer Into Cells in Culture and *In Vivo*: Polyethylenimine. *Proc Natl Acad Sci* (1995) 92:7297–301. doi: 10.1073/pnas.92.16.7297
36. Kiener R, Fleischmann M, Schwegler C, Ruzsics Z, Thirion C, Schrödel S, et al. Vaccine Vectors Based on Adenovirus 19a/64 Exhibit Broad Cellular Tropism and Potently Restimulate HCMV-Specific T Cell Responses *Ex Vivo*. *Sci Rep* (2018) 8:1474. doi: 10.1038/s41598-018-19874-1
37. Nielsen KN, Steffensen MA, Christensen JP, Thomsen AR. Priming of CD8 T Cells by Adenoviral Vectors is Critically Dependent on B7 and Dendritic Cells But Only Partially Dependent on CD28 Ligation on CD8 T Cells. *J Immunol* (2014) 193:1223–32. doi: 10.4049/jimmunol.1400197
38. Kim JH, Lee SR, Li LH, Park HJ, Park JH, Lee KY, et al. High Cleavage Efficiency of a 2A Peptide Derived From Porcine Teschovirus-1 in Human Cell Lines, Zebrafish and Mice. *PLoS One* (2011) 6:e18556. doi: 10.1371/journal.pone.0018556
39. Liu Y, Chen JJ, Gao Q, Dalal S, Hong Y, Mansur CP, et al. Multiple Functions of Human Papillomavirus Type 16 E6 Contribute to the Immortalization of Mammary Epithelial Cells. *J Virol* (1999) 73:7297–307. doi: 10.1128/JVI.73.9.7297-7307.1999
40. Wieking BG, Vermeer DW, Spanos WC, Kimberly M, Vermeer P, Lee WT, et al. A non-Oncogenic HPV 16 E6/E7 Vaccine Enhances Treatment of HPV Expressing Tumors. *Cancer Gene Ther* (2013) 19:667–74. doi: 10.1038/cgt.2012.55.A
41. Edmonds C, Vousden KH. A Point Mutational Analysis of Human Papillomavirus Type 16 E7 Protein. *J Virol* (1989) 63:2650–6. doi: 10.1128/jvi.63.6.2650-2656.1989
42. Barouch DH, Yang Z, Kong W, Korioth-Schmitz B, Sumida SM, Truitt DM, et al. A Human T-Cell Leukemia Virus Type 1 Regulatory Element Enhances the Immunogenicity of Human Immunodeficiency Virus Type 1 DNA Vaccines in Mice and Nonhuman Primates. *J Virol* (2005) 79:8828–34. doi: 10.1128/JVI.79.14.8828-8834.2005
43. Fougeroux C, Turner L, Bojesen AM, Lavstsen T, Holst PJ. Modified MHC Class II–Associated Invariant Chain Induces Increased Antibody Responses Against Plasmodium Falciparum Antigens After Adenoviral Vaccination. *J Immunol* (2019) 202:2320–31. doi: 10.4049/jimmunol.1801210
44. Malcles M-H, Cueille N, Mechali F, Coux O, Bonne-Andrea C. Regulation of Bovine Papillomavirus Replicative Helicase E1 by the Ubiquitin-Proteasome Pathway. *J Virol* (2002) 76:11350–8. doi: 10.1128/jvi.76.22.11350-11358.2002
45. Mechali F, Hsu C-Y, Castro A, Lorca T, Bonne-Andrea C. Bovine Papillomavirus Replicative Helicase E1 Is a Target of the Ubiquitin Ligase APC. *J Virol* (2004) 78:2615–9. doi: 10.1128/jvi.78.5.2615-2619.2004
46. Ewaisha R, Panicker G, Maranian P, Unger ER, Anderson KS. Serum Immune Profiling for Early Detection of Cervical Disease. *Theranostics* (2017) 7:3814–23. doi: 10.7150/thno.21098
47. Dersh D, Yewdell JW, Wei J. A SIINFEKL-Based System to Measure MHC Class I Antigen Presentation Efficiency and Kinetics. *Methods Mol Biol* (2019) 1988:109–22. doi: 10.1007/978-1-4939-9450-2_9
48. Grujic M, Holst PJ, Christensen JP, Thomsen AR. Fusion of a Viral Antigen to Invariant Chain Leads to Augmented T-Cell Immunity and Improved Protection in Gene-Gun DNA-Vaccinated Mice. *J Gen Virol* (2009) 90:414–22. doi: 10.1099/vir.0.002105-0
49. Brulet J-M, Maudoux F, Thomas S, Thielemans K, Burny A, Leo O, et al. DNA Vaccine Encoding Endosome-Targeted Human Papillomavirus Type 16 E7 Protein Generates CD4+ T Cell-Dependent Protection. *Eur J Immunol* (2007) 37:376–84. doi: 10.1002/eji.200636233
50. Ragonnaud E, Schroedel S, Mariya S, Iskandriati D, Pamungkas J, Fougeroux C, et al. Replication Deficient Human Adenovirus Vector Serotype 19a/64: Immunogenicity in Mice and Female Cynomolgus Macaques. *Vaccine* (2018) 36:6212–22. doi: 10.1016/j.vaccine.2018.07.075
51. Yalcin B, Nicod J, Bhomra A, Davidson S, Cleak J, Farinelli L, et al. Commercially Available Outbred Mice for Genome-Wide Association Studies. *PLoS Genet* (2010) 6:e1001085. doi: 10.1371/journal.pgen.1001085
52. Genticel. *Phase II Study of HPV Therapeutic Vaccine in HPV Infected Women With Normal Cytology or ASCUS/LSIL* (2013). Available at: https://clinicaltrials.gov/show/NCT01957878 (Accessed July 15, 2021).
53. Gan L, Jia R, Zhou L, Guo J, Fan M. Fusion of CTLA-4 With HPV16 E7 and E6 Enhanced the Potency of Therapeutic HPV DNA Vaccine. *PLoS One* (2014) 9:e108892. doi: 10.1371/journal.pone.0108892
54. van de Wall S, Ljungberg K, Ip PP, Boerma A, Knudsen ML, Nijman HW, et al. Potent Therapeutic Efficacy of an Alphavirus Replicon DNA Vaccine Expressing Human Papilloma Virus E6 and E7 Antigens. *Oncoimmunology* (2018) 7:e1487913. doi: 10.1080/2162402X.2018.1487913
55. Choi YJ, Hur SY, Kim T-J, Hong SR, Lee JK, Cho C-H, et al. A Phase II, Prospective, Randomized, Multicenter, Open-Label Study of GX-188E, an HPV DNA Vaccine, in Patients With Cervical Intraepithelial Neoplasia 3. *Clin Cancer Res* (2020) 26:1616–23. doi: 10.1158/1078-0432.CCR-19-1513
56. Turnstone Biologics C. *This is a Trial of MG1-E6E7 With Ad-E6E7 and Atezolizumab in Patients With HPV Associated Cancers (Kingfisher)* (2018). Available at: https://clinicaltrials.gov/ct2/show/NCT03618953 (Accessed July 15, 2021).
57. Hancock G, Blight J, Lopez-Camacho C, Kopycinski J, Pocock M, Byrne W, et al. A Multi-Genotype Therapeutic Human Papillomavirus Vaccine Elicits Potent T Cell Responses to Conserved Regions of Early Proteins. *Sci Rep* (2019) 9:1–12. doi: 10.1038/s41598-019-55014-z
58. Garza-Morales R, Perez-trujillo JJ, Martinez-jaramillo E, Saucedo-cardenas O, Loera-arias MJ, Garcia-garcia A, et al. HPV-16 E7 Antigen has Prophylactic and Therapeutic E Ffi Cacy in a Cervical Cancer Mouse Model. *Cancers (Basel)* (2019) 11:1–12. doi: 10.3390/cancers11010096
59. Holst PJ, Christensen JP, Thomsen AR. Vaccination Against Lymphocytic Choriomeningitis Virus Infection in MHC Class II-Deficient Mice. *J Immunol* (2011) 186:3997–4007. doi: 10.4049/jimmunol.1001251

60. Hobbs SJ, Harbour JC, Yates PA, Ortiz D, Landfear SM, Nolz JC. Vaccinia Virus Vectors Targeting Peptides for MHC Class II Presentation to CD4(+) T Cells. *ImmunoHorizons* (2020) 4:1–13. doi: 10.4049/immunohorizons.1900070

Conflict of Interest: PH is an inventor on a patent detailing the use of the invariant chain as an adjuvant for virally delivered vaccines owned by the University of Copenhagen. The right to use the patent for treating HPV is licensed to InProTher ApS where author PH is the founder, major shareholder, board member and employee. DB is an employed by the company InProTher ApS. TW, CP, and SS are employed by the company SIRION Biotech GmbH. CT is founder and shareholder of SIRION Biotech GmbH and a board member of InProTher ApS. RW is board member of SIRION Biotech GmbH. PN, BA, RW, DB, PH, CP and CT are inventors on a patent application.

Publisher's Note: All claims expressed in this article are solely those of the authors and do not necessarily represent those of their affiliated organizations, or those of the publisher, the editors and the reviewers. Any product that may be evaluated in this article, or claim that may be made by its manufacturer, is not guaranteed or endorsed by the publisher.

frontiers in Immunology

SYSTEMATIC REVIEW
published: 24 November 2021
doi: 10.3389/fimmu.2021.786286

Intercepting Premalignant, Preinvasive Breast Lesions Through Vaccination

*Nadia Nocera Zachariah[1], Amrita Basu[2], Namrata Gautam[2], Ganesan Ramamoorthi[2], Krithika N. Kodumudi[2], Nagi B. Kumar[2], Loretta Loftus[3] and Brian J. Czerniecki[1]**

[1] Department of Breast Surgery, H. Lee Moffitt Cancer Center, Tampa, FL, United States, [2] Clinical Science Division, H. Lee Moffitt Cancer Center, Tampa, FL, United States, [3] Department of Breast Oncology, H. Lee Moffitt Cancer Center, Tampa, FL, United States

Breast cancer (BC) prevention remains the ultimate cost-effective method to reduce the global burden of invasive breast cancer (IBC). To date, surgery and chemoprevention remain the main risk-reducing modalities for those with hereditary cancer syndromes, as well as high-risk non-hereditary breast lesions such as ADH, ALH, or LCIS. Ductal carcinoma *in situ* (DCIS) is a preinvasive malignant lesion of the breast that closely mirrors IBC and, if left untreated, develops into IBC in up to 50% of lesions. Certain high-risk patients with DCIS may have a 25% risk of developing recurrent DCIS or IBC, even after surgical resection. The development of breast cancer elicits a strong immune response, which brings to prominence the numerous advantages associated with immune-based cancer prevention over drug-based chemoprevention, supported by the success of dendritic cell vaccines targeting HER2-expressing BC. Vaccination against BC to prevent or interrupt the process of BC development remains elusive but is a viable option. Vaccination to intercept preinvasive or premalignant breast conditions may be possible by interrupting the expression pattern of various oncodrivers. Growth factors may also function as potential immune targets to prevent breast cancer progression. Furthermore, neoantigens also serve as effective targets for interception by virtue of strong immunogenicity. It is noteworthy that the immune response also needs to be strong enough to result in target lesion elimination to avoid immunoediting as it may occur in IBC arising from DCIS. Overall, if the issue of vaccine targets can be solved by interrupting premalignant lesions, there is a potential to prevent the development of IBC.

Keywords: breast cancer, dendritic cell, vaccine, immunosurveillance, DCIS, ADH, LCIS, tumor-associated antigen

OPEN ACCESS

Edited by:
Sjoerd H. Van Der Burg, Leiden University, Netherlands

Reviewed by:
Mary A. Markiewicz, University of Kansas Medical Center, United States
Behjatolah Monzavi-Karbassi, University of Arkansas for Medical Sciences, United States

****Correspondence:***
Brian J. Czerniecki
Brian.Czerniecki@moffitt.org

Specialty section:
This article was submitted to Cancer Immunity and Immunotherapy, a section of the journal Frontiers in Immunology

Received: *30 September 2021*
Accepted: *01 November 2021*
Published: *24 November 2021*

Citation:
Zachariah NN, Basu A, Gautam N, Ramamoorthi G, Kodumudi KN, Kumar NB, Loftus L and Czerniecki BJ (2021) Intercepting Premalignant, Preinvasive Breast Lesions Through Vaccination. Front. Immunol. 12:786286. doi: 10.3389/fimmu.2021.786286

THE CLINICAL CHALLENGE OF BREAST CANCER PREVENTION

Breast cancer has become the world's most prevalent cancer, with over 7.8 million women alive by the end of 2020 who had been diagnosed with BC in the past 5 years (1). This disease places an immense burden on society in terms of cost of medical care for these patients. As such, there is an intense effort by healthcare professionals to promote BC prevention and risk reduction.

Although clinicians are currently unable to determine which patients will develop breast cancer, they can identify patients who harbor increased risk and offer them risk-reduction options for BC prevention. Several risk calculators are available, such as the Gail Model and Tyrer-Cuzick Model, which are based on several factors within the patient's history and characteristics such as family history, history of breast biopsies, or history of benign proliferative lesions such as atypical ductal hyperplasia (ADH) or lobular carcinoma *in situ* (LCIS). Other high-risk patients are those with hereditary cancer syndromes such as Cowden Syndrome or BRCA1/2 mutations, which are discovered by genetic testing.

Presently, the main forms of BC prevention or risk reduction are lifestyle modifications, surgery, and chemoprevention. Surgical intervention for BC prevention includes risk-reducing prophylactic mastectomy. This tends to be applied to women in whom a contralateral mastectomy is performed synchronous with the treatment of a primary tumor, or as a bilateral procedure in women at high risk of BC. In the average patient, prophylactic mastectomy reduces the risk of contralateral BC by 90–97% (2). Chemoprevention consists of selective estrogen receptor modulators (SERM) or aromatase inhibitors (AI). These are prescribed to women at high risk of BC, and this risk-reducing modality decreases breast cancer development by over 50% (3).

While surgery and chemoprophylaxis remain viable options for BC prevention, these portend high burdens for patients due to side effects of medication, potential complications of surgery, and the additional costs of these treatments. An alternative method of BC prevention that is devoid of these high costs may be vaccination. BC vaccines are an emerging therapy that utilizes the host immune system to provide protection from BC or allow interception of high-risk lesion progression to BC, while sparing patients the high burden of traditional risk-prevention strategies.

This review aims to describe our current understanding of immune response in preinvasive breast lesions and potential targets for developing therapeutic vaccination that can prevent development into invasive disease in breast cancer. For this purpose, we have reviewed the literature including primary research and review articles published in the past 10 years, focusing on the following keywords on PubMed: breast cancer, vaccine, prevention, immunosurveillance, DCIS, dendritic cell, flat epithelial atypia, atypical lobular hyperplasia, atypical ductal hyperplasia, lobular carcinoma *in situ*, and neoantigens.

IMMUNE RESPONSE AND THE DEVELOPMENT OF BREAST CANCER

The breast is a complex organ, which, due to its connection to the outside world, has a multifaceted and complex immune environment. Normal breast tissue contains uniform immune cell infiltrates composed of helper T cells (CD4+), cytotoxic T cells (CD8+), B cells, and natural killer (NK) cells (4). In breast lobules, there are dendritic cells (DCs) as well as cytotoxic T cells that are uniformly present and are in close association with the breast epithelium (4). The presence of CD8+ T cells and DCs suggests a built-in defense system by antigen presentation and immune effector function. These cells within the breast parenchyma also aid in development, lactation, and involution of breast tissue (5). More importantly, they may not only play a role in development of the breast and its microbial defense, but they may also contribute a critical role in cancer immunosurveillance.

Cancer immunosurveillance is a process by which the host's immune cells recognize and eliminate evolving tumor cells. This locally controlled inflammation may control tumor proliferation. A high density of CD8+ T cells in a tumor and nearby stroma has been associated with an improved prognosis in BC, indicating that immune effector cells have effectively identified the malignant cells and have subsequently mounted an immune response (6). A helper T cell response is activated *via* IFN-γ production, or there is direct elimination *via* cytotoxic granules (6).

Supporting cancer immunosurveillance is the observation that immunosuppression increases the risk of cancer, including BC. This has been evidenced in patients on chronic immunosuppressive medication, such as transplant recipients (7). Individuals with severe deficits of immunity have a higher likelihood of developing a variety of cancers (8).

Interestingly, chronic inflammation has been associated with cancer development (9). In chronic inflammation, myeloid suppressor cells, Th2 CD4+ T cells, and regulatory T cells work to repress CD8+ toxicity and induce pro-tumoral polarization of innate immune response *via* cytokine secretion and transforming growth factor beta (TGF-β). These polarized cells then provide a rich pro-tumoral microenvironment (10). Hence, the immune system clearly plays a role in the evolution of cancer by both promoting and preventing it.

PRECURSOR LESIONS TO BREAST CANCER

The favored model of BC evolution includes a stepwise progression of early, definable precursor lesions with cellular atypia to carcinoma *in situ* to invasive breast cancer (IBC) (11). Benign proliferative lesions such as atypical ductal hyperplasia (ADH), atypical lobular hyperplasia (ALH), and flat epithelial atypia (FEA) are all considered non-obligate precursors to BC (12). Genetic studies on these lesions have shown changes in steroid hormone receptor expression levels and epigenetic changes that have been implicated as early carcinogenic events (13). The high expression of hormonal receptors such as estrogen receptors (ER) and progesterone receptors (PR) have been noted in early precursor lesions compared to the normal breast epithelial cells. This change is considered as an important influencer to develop low-grade BC (14). These features of these early precursor lesions fit into the concept of a low-grade cancer pathway, particularly since they also share histological features such as low-grade nuclear atypia (11).

Flat Epithelial Atypia

FEA is identified as a lesion showing architectural features of columnar cell metaplasia and columnar cell changes with low-

grade nuclear atypia. In addition, elongated hyperchromatic nuclei with prominent stratification can also be identified in few groups of patients with FEA (15). FEA is an uncommon premalignant lesion with 2.4% incidence rate and not independently associated with long-term BC risk (16). Studies have observed that FEA is a precursor lesion for the development of low-grade tubular carcinomas and can also upgrade into ductal carcinoma *in situ* (DCIS) (17).

Atypical Lobular Hyperplasia

ALH is categorized as a premalignant lesion and has a high risk for development to BC. Pre- and perimenopausal status among ages 46–55 with ALH is considered as a high risk factor for development of BC compared to a postmenopausal cohort (18). ALH is usually asymptomatic and may be identified by breast imaging or found in association with other features such as radial scars, fibroadenomas, intraductal papillomas, pleomorphic LCIS, or DCIS (11).

ALH and LCIS have similar morphological findings and have been termed as lobular neoplasia. However, ALH primarily differs from LCIS based on the filling of the lobular unit and proliferation degree (19). Lesions such as ALH and LCIS are regarded as both a risk factor as well as a non-obligatory precursor for invasive carcinoma. ALH and LCIS tend to be discovered as incidental findings on core needle biopsy, as they do not have reliable imaging features attributable to them (20). "Upgrade" rate of these lesions is less than 10% (11), and surgical excision is also recommended.

Lobular Carcinoma *In Situ*

LCIS exhibits similar histological features of ALH, but it is more proliferative compared to ALH. LCIS has about 15% risk factor for invasive BC development and may also be affected by menopausal status (21). LCIS can be detected by core needle biopsy, but it is difficult to find using breast imaging. In many cases, careful observation may be recommended to monitor signs of invasive BC progression. This includes breast self-exams, clinical breast exams, mammogram, and MRI (22). Due to the low incidence rate and lack of clear identification by breast imaging, the management of LCIS is a controversial issue (23). Surgical excision may not be required for all LCIS, but bilateral prophylactic mastectomy can be used in some patients with more aggressive form of LCIS in contralateral breast (24). Studies have shown high expressions of hormonal receptors ER and PR in LCIS patients, and these patients may largely benefit by addition of hormonal therapy (25).

Atypical Ductal Hyperplasia

ADH is considered an immediate precursor to DCIS based on clinical and morphologic similarities between the lesions, as well as a high degree of genomic similarity with almost identical kinds of chromosomal imbalances (11). However, the prognostic differences between ADH and DCIS indicate that ADH is not just a low-grade DCIS but is actually a closely related precursor lesion. Clinically, ADH is usually associated with suspicious calcifications found on breast imaging and subsequently recommended for core needle biopsy. Once a lesion is diagnosed as ADH, surgical excision is recommended due to the "upgrade" rate of 10–20% to DCIS or invasive carcinoma (26). Many "upgraded" lesions are actually minimally sampled lesions composed of the upgraded lesion type.

ADH exhibits distinguished features of terminal ductal-lobular partial involvement with architectural disturbances, such as micropapillae and rigid bridges (27). ADH lesions are small and focal with measurement of less than 2–3 mm. With the help of the basal cytokeratin 5/6 expression detection, ADH can be pathologically distinguished from usual ductal hyperplasia (28). The genomic observation studies have supported chromosomal imbalances including deletion of chromosome 16q and 17p and gain on chromosome 1q in patients with ADH. Notably, cancer progresses from premalignant lesion on the same breast that was initially diagnosed for ADH. Menopausal status is also considered as a high-risk factor for progression of invasive BC in patients with ADH (29).

Ductal Carcinoma *In Situ*

DCIS is a preinvasive breast lesion detected with mammography and can either present symptomatically or asymptomatically. It was reported that DCIS accounts for up to 30% of breast lesions detected by breast imaging (30). DCIS is defined as an uncontrolled proliferation of epithelial cells with the breast parenchymal structures and no evidence for the presence of invasion across the basement membrane. With the help of immunohistochemistry, DCIS may be confirmed for basement membrane type IV collagen laminin expression or presence of myoepithelial cells (31). Risk factors for DCIS development include increasing age, postmenopausal status, family history of BC, first pregnancy over 30 years of age, and hormone replacement therapy (32).

Negative ER/PR DCIS with a more aggressive phenotype was found to display increased progression to invasive BC (33). High-grade DCIS has been observed to display different molecular characteristic features compared to low-grade precursor lesions. These changes also include high expression of HER2 gene and various mutations in p53 gene (34). The treatment options for DCIS include mastectomy of the affected breast, breast-conserving surgery with or without adjuvant radiotherapy, and hormonal therapy (SERM or AI). Additionally, patients with HER2-positive DCIS may benefit from HER2-targeted therapies (35, 36).

RATIONALE FOR TARGETING ONCODRIVERS IN BREAST CANCER

The rationale for targeting oncodrivers in developing BC therapy stems from the discovery of oncogene addiction in cancer cells. Oncogene addiction, as defined by Bernard Weinstein, is the dependence of tumor cells on prolonged activity of oncodrivers for their survival and malignant phenotype (37). Such oncogene addiction offers oncodrivers as a promising target for developing cellular immunotherapy that can leverage the overexpression of oncodrivers on tumor cells to educate the immune system to

detect and destroy cancer cells specifically, while avoiding adverse consequences in healthy cells. Genetically engineered mouse models of human cancer, mechanistic studies in human cancer cell lines, and clinical trials involving specific molecular targeted agents have bolstered the benefits of targeting oncodrivers for therapy development (38). While BCR-ABL in chronic myeloid leukemia was the first concrete example of an addictive oncodriver in human cancer, multiple oncodrivers have been identified in various cancers since then. Use of vemurafenib, dabrafenib in BRAF-mutated melanoma; gefitinib, erlotinib in EGFR-mutant NSCLC and crizotinib in ALK-mutated NSCLC; cetuximab, panitumumab in EGFR-amplified colorectal cancer; or tamoxifen, letrozole, and fulvestrant in ER+ BC (38, 39) have revolutionized the therapeutic outcome in patients, consolidating the rationale for oncodriver targeting.

Support for developing oncodriver-targeted therapy in BC comes primarily from the studies on HER2/Erbb2 oncodrivers. HER2 overexpression and constitutive downstream signaling in HER2+ BC cells have been identified as a poor prognostic marker that correlated with enhanced cellular proliferation and therapy resistance, invasiveness, and metastasis, leading to poor survival outcome in BC patients (40–42). Targeted inhibition of HER2 by trastuzumab, pertuzumab, T-DM1 and other strategies have revolutionized the treatment outcome for patients, further highlighting the potential for therapeutic targeting of oncodrivers (36). However, gradual development of therapeutic resistance to HER2-targeted agents in BC suggests the need for developing combinatorial strategies targeting the oncodriver, such as combining antibody-mediated inhibition and stimulation of HER2-specific immune response by DC vaccination.

Multiple models have been proposed to elucidate how targeting oncodriver addiction in cancer cells can be beneficial for targeted therapy development—namely, genetic streamlining (dismissal of non-essential cellular pathways leading to lack of compensatory signals, resulting in collapse of the cellular fitness upon abrogation of dominant signals), oncogenic shock (blockade of addictive oncoproteins subverts the balance of pro-survival and pro-apoptotic signals in favor of cell death), and synthetic lethality (inactivation of two separate pathways result in a synergistic loss of common downstream effector function and subsequent apoptosis or cell cycle arrest) (38). The outcomes of oncodriver targeting in oncogene-addicted cells (apoptosis, senescence, cell cycle arrest) are heavily context-dependent, and the signaling framework underlying such outcomes requires further research for a comprehensive understanding.

TARGETING ONCODRIVERS IN EARLY-STAGE BREAST CANCER

Oncodrivers are proteins overexpressed in tumor cells, essential for proliferation, survival, and malignancy of cancer cells (43). While in healthy breast tissue, oncodriver proteins participate in numerous cellular events during different stages of puberty, pregnancy, lactation, and normal breast development (44), their overexpression and hyperactivity have been linked to progression and poor outcome in BC.

Perhaps the most prominent oncodriver investigated in BC is human epidermal growth factor receptor 2/receptor tyrosine-protein kinase erbB-2 (HER2/Erbb2). DCIS overexpressing HER2 has a higher propensity of progressing into invasive disease than HER2-negative DCIS (45). While HER2 overexpression is noted in more than 50% of DCIS, only 20–30% of IBC overexpress HER2 (45), suggesting a possible emergence of HER2-negative tumor cells due to immunoediting after elimination of HER2-positive cells. Combined HER2+/Ki67+ profile in DCIS has been identified as an independent predictor of local recurrence by multivariate analysis in a cohort of 868 patients (34). Overexpression of HER2 in IBC has been correlated with locally advanced stage disease, early metastasis, chemotherapy resistance, and poor recurrence-free survival in patients (46, 47).

Other members of the ERBB family of growth receptors have also been identified as oncodrivers across BC subtypes. HER3/Erbb3 is the most potent binding partner of HER2 that activates downstream signaling cascades, specifically PI3K/AKT, that contribute to cellular proliferation and survival. Therefore, HER3 hyperactivity has been associated with trastuzumab resistance in HER2-positive BC (48) and tamoxifen resistance in ER-positive BC (49, 50). In TNBC patients, overexpression of HER3 has been identified as a prognostic marker of poor 5-year DFS and 10-year OS (51–53).

EGFR/HER1 is another oncodriver protein overexpressed across BC subtypes, with more frequent appearance in IBC and TNBC subtypes. EGFR overexpression has been associated with larger tumor size and poor clinical outcome (54–56). Combined HER3-EGFR score in a cohort of 510 TNBC patients was a more comprehensive prognostic marker of worse BC-specific and distant metastasis-free survival, than individual oncodriver scores (57). Although EGFR gene amplification is rare in BC, high EGFR gene copy number predicts poor outcome in TNBC (58).

Hepatocyte growth factor receptor/receptor tyrosine kinase MET (HGFR/MET) is another oncodriver known to be overexpressed in TNBC and has been identified as an independent prognostic marker for recurrence and shorter survival (59). We have previously reported expression of HER3 and c-MET in BRCA1- and BRCA2-associated DCIS as well (60). Molecular cross-talk and downstream convergence between MET and ERBB receptor signaling has been predicted to contribute to resistance against HER2- and EGFR-targeted therapies (61).

TARGETING BREAST-SPECIFIC TUMOR-ASSOCIATED ANTIGENS

Tumor-associated antigens (TAAs) are the epitopes displayed on tumor cell surface and also presented by the HLAs on the surface of non-malignant cells that can be identified by comparing

transcriptome of the malignant and healthy tissues and present a promising yet challenging target for therapy development due to immunogenic tolerance and lack of specificity (62, 63). While HER2 is perhaps the most widely investigated TAA identified in BC, other TAAs, e.g., MUC1, mammaglobin-A, lactalbumin, NY-ESO-1, MAGE, and MART-1, have garnered interest as potential therapeutic targets and have been reviewed comprehensively before (Criscitiello, 2012 #12430). Here, we briefly discuss the current status of therapeutic research in BC centered around some of these TAAs.

Mucin-1

Mucin 1 (MUC1) is a transmembrane dimeric mucin, with an aberrant overexpression in over 90% BC compared to normal ductal epithelial cells of the breast tissue. Overexpression of MUC1 results from gene amplification, miRNA regulation, as well as in response to EGF or heregulin stimulation and activation of PI3K/AKT signaling (64). MUC1 has also been identified to complex with HER2, HER3, and HER4 in BC cells and mouse mammary glands. MUC1-based subunit vaccines, DNA vaccines, viral vector vaccines, DC vaccines, and glycopeptide vaccines are currently being tested (65). Subunit vaccine with MUC1 tandem repeats and MBP/BCG adjuvant induced Th1 immune response (66), activation of NK cells, and MUC1-specific CTL in mouse models of melanoma and lung carcinoma (67). In human, adjuvanted MUC1 subunit vaccine was less immunogenic in late-stage cancer patients than in early-stage patients. In metastatic BC patients, 16-amino-acid MUC1 peptide coupled to keyhole limpet hemocyanin plus DETOX adjuvant demonstrated class-I restricted CTL activation (68). Tecemotide, a VNTR MUC1 peptide delivered *via* a liposomal system, showed significantly improved survival after chemoradiation in phase II and III NSCLC trials (69). DC vaccine pulsed with survivin and MUC1 was well tolerated and showed modest antitumor immune response in NSCLC patients (70). However, L-BLP25 (Stimuvax), a liposome-based vaccine with MUC1-N terminal repeats, failed to improve overall survival in phase III trial for unresectable stage III NSCLC (71, 72). PANVAC vaccines containing transgenes for MUC1, CEA, and three T-cell costimulatory molecules (B7.1, LFA-3, and ICAM-1) have also been tested in a clinical trial with metastatic BC patients (73).

Mammaglobin

Mammaglobin-1 (SCGB2A2) is a mammary-specific glycoprotein member of the uteroglobin family and is considered a potential diagnostic and prognostic marker for BC (74, 75). Peripheral blood and tumor tissue from DCIS and IBC patients analyzed by RT-PCR identified mammaglobin expression as the most specific molecular marker for hematological dissemination of BC cells, compared to EGFR and cytokeratin 19 (76). Mammaglobin protein and mRNA expression have been detected in 75–80% of primary and metastatic BC, as well as in bone micrometastases of BC (77). Abundance of this marker in tumor tissue and inherent immunogenicity make mammaglobin a promising target for therapy development.

Lactalbumin

α-lactalbumin is a breast-specific differentiation protein that comprises 25% of total protein found in breast milk, overexpressed in mammary epithelial cells during lactation and in a majority of BCs, specially TNBC. Immunization of female SWXJ mice with recombinant mouse α-lactalbumin has shown dose-dependent proliferation in recall responses in the lymph node, presenting lactalbumin as a targetable TAA. A proinflammatory phenotype involving both CD4+ and CD8+ T cells and high production of IFN-γ and IL-2 was noted (78). Following this, Tuohy et al. showed presence of a proinflammatory T cell repertoire in adult women that can respond to recombinant hα-lactalbumin (79). An open-label, early phase I dose-escalation trial to test α-lactalbumin vaccine in non-metastatic TNBC patients is currently ongoing (NCT04674306).

TARGETING NEOANTIGENS

While TAAs are "self-proteins" shared between malignant and healthy tissues, neoantigens are tumor-specific antigens (TSA), unique non-autologous proteins expressed in tumor, often derived by somatic DNA alterations such as non-synonymous point mutations, insertion/deletion, gene fusion, and frameshift mutations acquired during the tumorigenesis process, due to rapid proliferation and genomic instability (80, 81). Various aspects of neoantigen development and potential as therapeutic target have recently been extensively reviewed by Benvenuto et al. (62). Higher immunogenicity of neoantigens arising from mutations, strong tumor specificity, reduced risk of autoimmunity as foreign antigens, and protection from central immunological tolerance present neoantigens as a more favorable target than TAAs for immunotherapy development (81). Therefore, it is possible that in the TME, lower immunogenicity and weak antigen load of TAAs may require a dramatic shift in up- or downregulation of both anti- and pro-tumorigenic signals, respectively, while higher immunogenicity and abundance of neoantigens may tip the balance in favor of antitumor immune response more comprehensively by modulating only one side of the balance (47).

Multiple preclinical studies of melanoma, lung, breast, and colon cancers have demonstrated tumor rejection by neoantigen-specific vaccination, where most of the epitopes were detected by CD4+ T cells (47, 82). Zhang et al. reported identification of neoantigens from an LL2 murine lung carcinoma model by whole-exon and transcriptome sequencing of the tumor RNA. Vaccination with neoantigen-pulsed DC in mice demonstrated a stronger antigen-specific lymphocyte response, increased number of TILs including CD8+ and CD8+IFN-γ+ T cells, and inhibited tumor growth, compared to the neoantigen-adjuvant vaccination. Combination of local radiotherapy with an RNA-LPX vaccine encoding CD4+ T cell-recognized neoantigens in a CT26 mouse model resulted in activation and long-lasting memory recall response by CD8+ T cells with increased IFN-γ secretion and follow-up with anti-CTLA4 antibody resulted in complete remission of tumors (83). Higher predicted neoantigen

load has been correlated with increased TIL infiltration and improved survival in melanoma, colorectal, and ovarian cancer patients receiving immune checkpoint therapy (84, 85). Immunotherapies targeting neoantigens by synthetic long peptide vaccine, DNA, RNA, and DC vaccines, and adaptive T cell therapy are currently being tested in various preclinical and clinical trials.

Owing to the low mutational burden in BC, TAAs were the primary focus of therapeutic targeting for a long time, and translational research focusing on breast neoantigens has only recently gained traction. BC is known to have a higher proportion of INDEL mutations, and TNBC is characterized by a higher number of neoantigens due to frameshift mutations, with an even higher load in BRCA-1 mutated TNBC. However, no correlation between TNBC and TIL number has been identified in the analysis of a specific cohort of TNBC patients compared with other invasive BC subtypes (86).

Building an array with non-overlapping frameshift neoantigen peptides and vaccination with reactive peptides resulted in slower tumor growth and antibody production that correlated with diminished tumor volume in 4T1 murine model (87). In another study, PALB2, ROBO3, PTPRS, and ZDHHC16 were identified as neoantigens in advanced BC patients. Whole tumor exome analysis from the PDX mouse models generated from those patients identified a large number of non-synonymous single nucleotide variants. Following determination of predicted HLA binding affinity and functional evaluation by ELISPOT, neoantigen-specific T cells were shown to inhibit patient tumor growth implanted in NSG immunodeficient mice (88). Whole exome and RNA sequencing from BC tissues and neoantigen prediction among exonic mutations showed positive correlation between neoantigen load and non-synonymous single-nucleotide variations (nsSNVs). Using primary tumor cells established from pleural fluid of a BC patient, co-culturing neoantigen-pulsed DCs with autologous peripheral lymphocytes resulted in induction of CTLs *ex vivo* (89). Evaluation of the neoepitope burden in BC from TCGA using a predictive algorithm called EpitopeHunter showed that total mutational burden was highest for TNBC, followed by HER2+ BC and lowest for ER+/PR+/HER2− BC and the neoepitope load correlated with such mutational burden (90). Liu et al. have identified >700 non-silent somatic variants in BC patients obtained from the cBioportal dataset and observed higher single-nucleotide variant neoantigens in the elder population (>60 yrs) and identified multiple high-frequency mutations in PIK3CA and AKT that can be recognized by various HLA molecules (91). On the other hand, mutations in the ESR1 gene coding for the ER protein has been identified to be relatively common in metastatic, therapy-resistant cancers and contribute to shorter progression-free survival in endocrine BC (92, 93) and, hence, can be employed for developing neoantigen-pulsed DC vaccination for ER-positive BC.

Identification of neoantigens that are "private" antigens specific for individual patients requires a long and arduous bioinformatic screening followed by experimental validation to verify the epitopes, as well as both quality (specificity and affinity of infiltrating immune cells towards neoantigens) and quantity (number of activated TIL). This can become a limiting factor towards successful development of neoantigen-specific immunotherapy. However, research in the past few years has made remarkable progress towards that direction (94). In patients with NSCLC (95) and melanoma (96), personalized neoantigen-pulsed DC vaccination was found to be safe, reliable, and beneficial to reduce tumor burden and metastatic lesions. Neoantigen targeting with synthetic long peptide or polyepitope DNA vaccines in 4T1 and E0771 murine mammary carcinoma models have led to initiation of two clinical trials (NCT02427581 and NCT02348320) enrolling TNBC patients to test safety of personalized neoantigen vaccines using the same platforms (81). In a recently completed phase I/II clinical trial in TNBC patients, 40% of the patients showed pathologic complete response after receiving cyclin B1/WT-1/CEF tumor antigen-loaded DC vaccination with preoperative chemotherapy (NCT02018458). As summarized by Benvenuto et al. (62) and Han et al. (97), multiple clinical trials are currently testing safety, immunogenicity, effects on pathological complete response, TIL percentage, recurrence rate and survival in TNBC, BRCA-mutated and other subtypes of BC.

DRUG-BASED CHEMOPREVENTION *VS.* IMMUNE-BASED PREVENTION

Patients with a diagnosis of any of the known precursor lesions are considered to be at significantly increased lifetime risk of developing BC, with estimated 10-year cancer risks of 17.3% with ADH, 20.7% with ALH, 23.7% with LCIS, and 26.0% with severe ADH (98). Because of this increased risk, these women are closely surveilled, and chemoprevention is recommended. One major analysis of women with benign proliferative lesions in four chemoprevention trials (NSABP P-1, MAP.3, IBIS-I, and IBIS-II) has demonstrated that chemoprevention with endocrine therapy was associated with 41–79% relative risk reduction of BC (3).

Despite this high rate of risk reduction, there is underutilization and low adherence of chemoprevention by high-risk patients (99). Endocrine therapy places a high burden of side effects on the patient, including major risk of venous thromboembolism, stroke, osteoporosis, and endometrial cancer. More common and noticeable side effects patients may experience include menopause-like symptoms, joint aches, and mental fog. These medications are also recommended to be taken for 5 years for maximum benefit, which, for some patients, may be a significant burden.

Cancer immunoprevention modulates the immune system to recognize aberrant cells and prevent the initiation and progression to malignancy. Potential advantages to immune-based cancer prevention over drug-based chemoprevention include (1) high specificity and adaptability of immune responses (adaptive immunity is specific to a given antigen and can adjust to changes within the antigenic repertoire); (2) favorable toxicity profile (immune strategies—cancer vaccines in particular—appear non-toxic in the majority of cases); (3)

ability to generate immunological memory, providing long-term (potentially lifelong) protection (not achievable with drugs); and (4) ease of administration (i.e., several vaccinations with occasional boosts *versus* daily dosing for many years with chemo preventive agents) (100). Vaccination has been proven to be a proficient and cost-effective means of eradicating many pathogens; hence, it stands to reason that vaccination may be an efficient means for immunoprevention of cancer, especially in high-risk individuals.

Vaccinations for cancers with viral etiologies are widely available and have been shown to be efficacious, such as vaccination against human papilloma virus (HPV) and hepatitis B. Since implementing these vaccination programs, the incidence of cervical and hepatic cancers have been reduced (101). However, unlike cervical and hepatic cancer, BC is a complex and multifactorial disease that does not have a target pathogen for vaccination. A preventative vaccine would rely on targeting normally overexpressed, mutated, or cancer-specific targets (102). Some targets considered in the development of BC vaccines include targeting oncodrivers, i.e., overexpressed proteins, tissue-specific antigens, and targets that are expressed in cancer tissue, but not in normal cells (102).

CD4 T CELL RESPONSE IN CANCER

For a long time, cancer immunotherapies have focused on CD8+ T cells as the principal adaptive immune T cell subset, known for their antitumor cytotoxic response. However, the potential of CD4+ helper T (Th) cells in tumor suppression has recently gained attention in the field of immunotherapy. The overview of various CD4+ T cells (**Figure 1**), its subsets, and their role in mediated tumor immune response has been reviewed by our group previously (https://doi.org/10.3389/fimmu.2021.669474).

IMMUNOEDITING

Since the concept of tumor suppression by immune system introduced by Paul Ehrlich (103) and the hypothesis of cancer immunosurveillance proposed by Burnet and Thomas (104), roles of the immune system in shaping up tumorigenesis and therapeutic response have been established unequivocally. Research by Schreiber and others led to the refinement of the immunosurveillance concept to the hypothesis of cancer immunoediting (105–107) that acknowledges the complexity of tumor immune response in a far more comprehensive manner.

Schreiber et al. envisioned immunoediting in cancer as a three-step process, "the three Es of cancer immunoediting" (108), namely, Elimination, Equilibrium, and Escape. During this final step of immune escape, surviving tumor cells with genetic and epigenetic changes rendered resistant to detection and deletion by the host immune system enter the phase of uncontrolled growth and become clinically observable malignant disease (105, 109–111).

IMMUNE ESCAPE MECHANISMS IN BREAST CANCER

Mechanisms of immune escape in cancer has been reviewed extensively elsewhere (112–114). Loss of immune detection and activation (absence of strong tumor antigen, lack of DC and T cell priming, tumor antigen processing and presentation, reduced MHC class I expression, upregulation of HLA-G to promote tolerogenic phenotype), enhanced resistance to cytotoxicity and apoptosis (constitutive activation of STAT3, oncodriver proteins, e.g., HER2, HER3, EGFR, anti-apoptotic protein Bcl-2), and shaping of an immunosuppressive tumor microenvironment (TME) [secretion of immunosuppressive

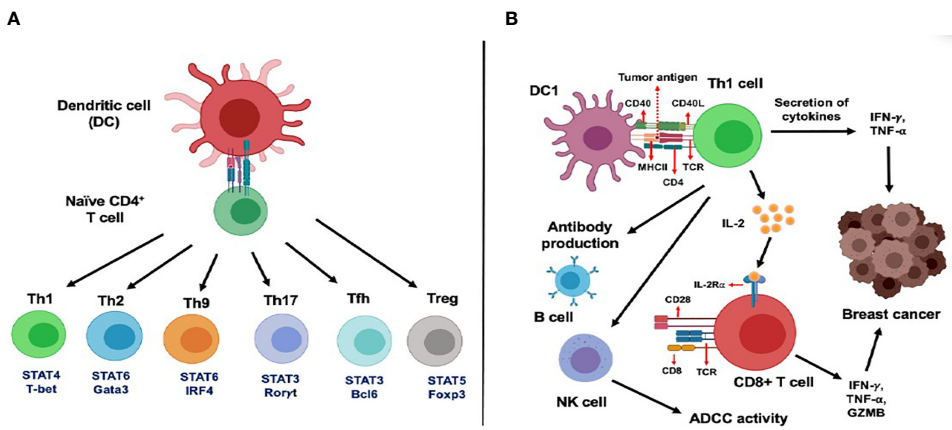

FIGURE 1 | Functional subsets of CD4+ T cells and role of CD4+ T cells in the activation of CD8+ T cells in cancer. **(A)** Dendritic cells (DC) regulate differentiation and polarization of naïve CD4+ T cells into various T helper cells subsets such as Th1, Th2, Th9, Th17, Tfh and Treg cells. **(B)** DCs primed with tumor antigenic peptides can present the antigens to Th1 cells through the MHC class II molecule. Next, these activated Th1 cells secrete two important Th1 cytokines: IFN-γ and TNF-α, leading to direct tumor growth inhibitory effects, mediated by induction of apoptosis, senescence, cell cycle arrest and proliferation arrest. Secretion of IL-2 cytokine from Th1 cells is known to mediate activation and proliferation of IL-2Rα expressing CD8+ T cells which leads to enhanced anti-tumor response. In addition, Th1 cells can regulate B cell-mediated antibody production and NK cell-dependent antibody dependent cellular cytotoxicity (ADCC) in cancer.

cytokines TGF- β, VEGF, and metabolic factors IDO, PGE-2; adaptive immune resistance by upregulation of PD1/PDL-1, LAG3, Tim3; induction of Tregs, tumor-associated macrophages (TAMs), and MDSCs] have been shown to be the potential mechanisms of immune escape in BC and many other subtypes of cancer (110, 114–116).

Inherently low immunogenicity of BC contributes to immune escape, and progression from preinvasive to invasive disease. In residual triple-negative breast cancer (TNBC) after neoadjuvant chemotherapy, Ras-MAPK, PD-L1, and TIL infiltration showed a strong correlation and increased Ras/MAPK activation correlated with a poor TIL phenotype in the residual cancer (117). Expression of PD-L1 has been shown to increase in TNBC after neoadjuvant chemotherapy, while PD-L1 amplification has been detected in triple-negative IDC but not DCIS in a separate study (118). Similarly, HER2 amplification in HER2+ DCIS and IDC has been associated with co-amplification of a nearby cytokine cluster that inversely correlates with intratumoral frequency of granzyme-secreting CD8+ T cells (116). These observations underline the clinical relevance of therapeutic strategies targeting immune escape mechanisms to amplify therapeutic impact on patient outcome.

LOSS OF ANTI-HER2 TH1 RESPONSE DURING BREAST TUMORIGENESIS

While a basal level of anti- HER2 Th1 response is reported in healthy individuals, reflective of immune regulation by HER2, suppression of this Th1 response by malignancy breaks the immune protection, ultimately leading to progressive HER2+ tumor development (44, 119).

We have previously reported an incremental loss of Th1 immunity observed in HER2+ DCIS patients, with negligible responses in HER2+ IBC patients (119). A further sequential loss of HER2-specific Th1 response takes place in advanced IBC patients (120). Our group has also reported that restoration of the anti-HER2 Th1 response culminated in improved survival in HER2+ BC patients (46, 119). The molecular basis of this effect was investigated, and we now know that the Th1 cytokine IFN-γ increased E3 ubiquitin ligase Cullin-5, which led to ubiquitination and degradation of surface HER2 receptors, translating into tumor senescence and diminished tumor growth (121).

To augment expression of MHC-I molecules on tumors and efficient cytotoxic responses by HER2-specific CD8+ T cells, crosstalk between trastuzumab and IFN-γ and TNF is critical (122). Moreover, positive prognosis is anticipated by the presence of infiltrating Th1 IFN-γ-producing cells (123). Not only this, in patient-derived xenograft (PDX) ER– BC model, stimulation of IFN-γ/STAT1 pathway is identified as a prognostic marker of chemotherapy resistance. An ongoing clinical trial (NCT03112590) aims to elucidate how augmenting the Th1 response can be a pivotal immunotherapeutic tool, by testing a combination of IFN-γ with paclitaxel, trastuzumab, and pertuzumab in HER2+ BC. Loss of Th1 responses leading to tumor progression could point towards increase in apoptosis of CD4+ T cells *via* Fas pathway or tolerance to tumor antigens (for instance, CTLA-4 and PD-1) (124, 125). To this end, our group found that improved survival was achieved in TUBO HER2+ murine mammary carcinoma model upon delivering anti-PD1 antibody, post HER2-DC1 vaccination (126).

Similarly, our group has reported a progressive loss of Th1 immunity against HER3 in IBC patients, which was most pronounced in TNBC patients compared to the healthy donors, directing towards a fair chance to boost the Th1 responses to achieve improved survival (127).

ROLE OF DENDRITIC CELLS IN TH CELL DIFFERENTIATION

DCs are considered as master regulators of immune system and play a critical role in activation of adaptive immune cells (128). Three types of DC subsets have been identified, namely, myeloid/conventional DC1 (cDC1), myeloid/conventional DC2 (cDC2), and plasmacytoid DCs (pDC) (129, 130). The functional status of DCs is mainly classified by high expression of MHC class I and class II molecules, and expression of various co-stimulatory receptors including CD80, CD86, CD83, CD40, leucocyte functional antigen (LFA) family of adhesion molecules, and heat stable antigen (131, 132). cDC1s are involved in various antigen presentation to CD8+ T cells and stimulate cytotoxic activity. In addition, DC subsets can also mediate differentiation of CD4+ T cells into Th1, Th2, Th9, Th17, Tfh, and Treg cells (47, 132, 133).

Secretion of IL-12 by cDC1s can mediate Th1 polarization and NK cells infiltration. Stimulation of DCs with lipopolysaccharides has been shown to induce expression of Notch ligand delta, leading to Th1 polarization (134). On the other hand, OX40 ligand activation in myeloid cDC2 can mediate Th2 polarization (135). Preferential MHC II expression and higher IL-12 secretion by cDC2 make them better equipped to contribute to CD4+ Th cell polarization than cDC1 (135). A previous study has shown that calcium signaling activation in human PBMC-derived myeloid DCs can inhibit IL-12 production, which leads to CD83+ DCs activation and regulation of Th2 differentiation (136). Stimulation of DCs by prostaglandin-E2 can facilitate CD4+ T cells into Th2 phenotype polarization (137). Activation of dectin-1 in DCs has been reported to promote Th9 polarization *via* expression of OX40L, TNFSF15, Syk, Raf1, and NF-κB signaling cascades (138, 139). In response to various cytokines such as IL-6, IL-1β, IL-23, and TGF-β, DCs also induce polarization of the Th17 phenotype (140). In addition, stimulation of DCs with prostaglandin-E2 was also identified to control the balance between IL-12 and IL-23 cytokines and promote Th17 differentiation by inhibiting Th1 and Th2 polarization (141).

Cooperation between DCs and B cells has been shown to regulate MHC class II molecule–mediated antigen presentation, which stimulates Tfh cells polarization (142). Another study has

shown that induction of inducible costimulatory (ICOS) ligand expression in plasmacytoid DCs can induce Treg cells polarization (143, 144). IL-10 cytokine can negatively regulate DC functionality, expression status of MHC class II and IL-12 production, which converts DCs to promote Treg polarization (145).

USING DC VACCINATION TO TARGET HER2

DCs are used as a vaccine delivery tool to generate antitumor immune response in BC-targeting tumor antigens (146). Potential of HER2-targeted immunotherapy using the DC platform in BC has been reviewed previously (147, 148). Our group has showed type I polarized DC vaccine pulsed with HER2 peptides (HER2-DC1) generated strong anti-HER2 CD4+ T cell immunity in vaccinated HER2+ BC patients (**Figure 2**), as well in ER+/HER2+ and ER−/HER2+ BC patients, resulting in improved pathologic complete response in HER2+ DCIS and early BC patients (149, 150). In addition, HER2-DC1 vaccination in combination with anti-estrogen therapy enhanced HER2-specific Th1 immunity and reduced disease recurrence, compared to HER2-DC1 monotherapy in ER+/HER2+ patients (151). This study outcome emphasized therapeutic promises of combination therapy approach for HER2/ER-positive BC patients.

CD8α DCs are one of the subtypes of DCs which display high expression of IC-type lectin cell surface receptor DEC205 and are involved in cross antigen presentation and activation of CD4+ and CD8+ T cells (152). DEC205 receptor expressing CD8α DCs pulsed with extracellular domain peptides of the HER2/neu protein was able to generate CD4+ and CD8+ immune response and B cell-mediated antibody production in preclinical model of HER2/neu+ BC. Notably, prolonged antitumor response, rejection of secondary tumor challenge, and improved survival were observed following DC vaccination in HER2/neu+ BC preclinical model (152, 153). GP2 is an MHC class I recognizing immunogenic peptide obtained from the intracellular domain of HER2 protein and has been shown to induce strong CD8+ T cell-mediated antitumor response in HER2+ BC (154). Previously, phase II clinical trial investigating the efficacy of GP2 peptide vaccination in combination with immunoadjuvant GM-CSF treatment showed CD8+ T cells activation with improved 5-year DFS in HER2+ BC patients (155). In addition, GP2 peptide pulsed DC vaccination in transgenic mice induced HER2/neu specific CTL in preclinical BC model (156).

E75 is another immunogenic peptide derived from the extracellular domain of HER2/neu protein that stimulates HER2/neu-specific CTL to cause tumor cell lysis in HER2/neu transgenic mouse model (157). E75 peptide vaccine in combination with immune stimulatory cytokine GM-CSF treatment generated CD8+ T cell immune response and improved DFS in HER2+ BC patients (158). E75 peptide pulsed DC vaccination efficacy has also been tested in clinical trials with early stage and invasive BC patients (159). A phase III clinical trial with E75 peptide vaccine in combination with GM-

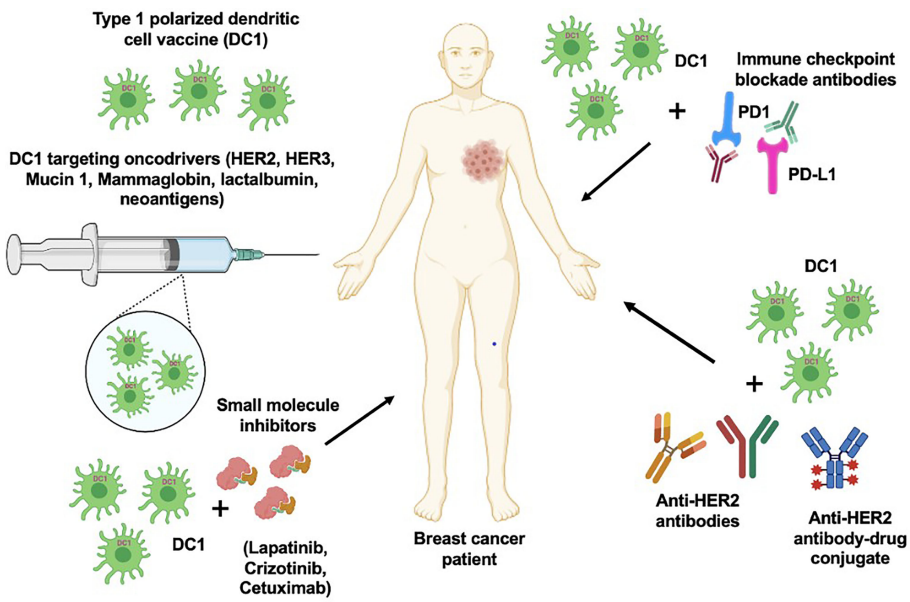

FIGURE 2 | DC1 vaccine with combination therapeutic approach. DC1 vaccination targeting various oncodrivers such as HER2, HER3, mucin 1, lactalbumin and neoantigens can be an effective strategy to improve therapeutic efficacy and survival outcome in breast cancer patients. In addition, combination of DC1 vaccine with clinically available targeted therapies such as anti-HER antibodies, small molecular inhibitors and immune checkpoint blockade antibodies can also enhance the patient outcome.

CSF therapy is currently ongoing in low to intermediate HER2+ BC patients (160).

HER2/neu transgene modified dendritic cell (DCneu) vaccine efficacy has been studied in HER2/neu+ BC mouse model where it suppressed Treg cell activity and enhanced Th1 immune response and HER2/neu specific humoral response. In addition, DCneu vaccination was able to induce strong tumor inhibitory effect and long-lasting antitumor response by protecting from secondary tumor re-challenge in mice (161). The CD4+ T cells recognizing epitope P30 have been reported to enhance CD8+ T cell-mediated immune response. Vaccination with DCs engineered with HER/neu oncogene and P30 epitope eliminated immunological tolerance by self-antigen and induced strong CD4+ and CD8+ T cells immune response in HER2/neu transgenic mouse model (162). Another study showed that treatment of DC vaccine pulsed with truncated neu antigen, interleukin 15 (IL-15), and IL-15Rα reduced mammary carcinoma development and inhibited HER2-dependent Akt signaling pathway in HER2/neu transgenic mice. DC vaccination was able to stimulate CD4+ Th1 immune response and eradicate HER/neu+ tumors in preclinical model (163).

VACCINATION IN ADDITION TO TARGETED THERAPY FOR HER2+ BREAST CANCER

Although HER2-targeted therapies, including anti-HER2 monoclonal antibodies (mAb) such as trastuzumab and pertuzumab, have improved the pathologic complete response (pCR) and DFS, development of resistance, metastasis, and disease recurrence noted in patients remain the main obstacle (164). Notably, combination treatment of DC vaccine with trastuzumab (**Figure 2**) was able to induce strong CTL response and improve anti-HER2 Th1 immune response in HER2+ BC (6). This opened up a new avenue to enhance the efficacy of trastuzumab by combining with HER2-DC1 or immunostimulatory cytokines in HER2+ BC patients. Previous studies have shown that trastuzumab treatment in combination with DCs pulsed with HER2 peptides E75 or GP2 and GM-CSF were able to generate CD8+ T cell immune response in HER2+ BC patients and enhanced DC-mediated presentation of E75 peptides in preclinical model of HER2+ BC (158, 159, 165). In addition, clonal expansion of E75 peptide-specific CD8+ T cells after combination treatment was identified as a key benefit (166). Another study showed HER2/neu oncogene constructed DC vaccine and trastuzumab combination treatment prevented spontaneous mammary carcinoma growth in HER2/neu-overexpressing transgenic mice, as the combination treatment was able to induce strong HER2/neu-specific CD8+ CTL immunity, which prevented tumor growth in mice (126, 167). Recently, it has been observed that HER2-DC1 vaccine, in combination with anti-HER2 antibodies, was able to completely arrest tumor growth in HER2/neu BC preclinical model (121).

Pharmacological inhibition of HER2-dependent PI3K/Akt and MAPK/ERK signaling activation is another attractive therapeutic option in HER2+ BC patients. Dual targeting of HER2 signaling with trastuzumab and tyrosine kinase inhibitor lapatinib is used to treat patients with locally advanced HER2+ BC (168) and has been shown to inhibit HER2 mediated downstream signaling cascades *via* PI3K/Akt and MAPK/ERK activation in HER2+ BC (169). Addition of HER2-targeted therapies such as lapatinib and trastuzumab can further potentiate therapeutic efficacy of DC1 vaccine and overcome therapy resistance in patients. A recent study has observed that combination treatment of class I and class II peptide pulsed HER2-DC1 vaccine with Akt antagonist MK-2206 was able to control the tumor growth in HER2/neu+ BC preclinical model (170). In support of this observation, Th1 cytokine IFN-γ in combination with MK-2206 treatment displayed similar tumor inhibitory effects in HER2/neu+ BC preclinical model and various HER2+ human BC cells (170).

UTILIZING ANTI-HER2 VACCINES AS A PREVENTATIVE STRATEGY

While trastuzumab and pertuzumab are effective adjuvant treatments for HER2+ BC, they are not for use in the preventative setting. Numerous attempts at various modalities for an anti-HER2 BC vaccine have been attempted in order to be used for prevention or in a neoadjuvant setting. Peptides within the HER2 protein can be recognized by CD8+ T cells in MHC class I molecules, and one protein that has been studied for this purpose is the E75 peptide. The E75 vaccine is a peptide vaccine that elicits a CD8+ CTL response. Because it only elicits a CTL response, immunization against this single peptide results in a low-level, short-lived response with paucity of activation of other components of the immune system (171).

Anti-peptide vaccination may be more effective in cancer cells with low HER2 expression because these cells exhibit high MHC class I expression and are more easily recognized by CD8+ T cells, allowing for elimination of tumor cells (46). Peptide vaccination is not likely effective in HER2-high BC due to the downregulation of MHC class I expression, which inhibits CTL recognition (46, 172). Vaccines aimed at targeting HER2-high expressing tumors should elicit activation of CD4+ T helper cells, secrete IFN-γ and TNF-α, which will upregulate expression of MHC class I, increasing sensitivity to CD8+ CTL-mediated lysis. This leads to humoral immunity and long tumor immunologic recognition.

It has been observed that healthy individuals actually harbor anti-HER2 CD4+ Th1 cells that secrete IFN-γ and TNF-α, and in individuals with HER2+ BC, this immune response is diminished (119). DC vaccines have been shown to prime an immune response in vaccinated subjects and, in one study, has achieved pCR in 18% of subjects and eradication of HER2 expression in residual DCIS in 50% of subjects without pCR (173). DCs are efficient in the presentation of antigens and signal activation and polarization of T cells into CTLs and Th cells (174, 175). DCs are also efficient in production of IL-12, which polarizes T cells toward the IFN-γ Th1 phenotype and also has antiangiogenic

capabilities, activates natural killer cells, enhances adaptive immunity, and improves sensitization to tumor antigens (176). Utilizing these properties, DC vaccination against HER2 would provide long-term tumor immunity, even against tumor cells expressing high HER2 levels.

Anti-HER2 DC vaccines have seen more clinical success in early stages of BC—mainly in the DCIS phase (6, 177). This may be due to the fact that in advanced disease, DCs are unable to mount a strong enough immune response to overcome the overwhelming immunosuppressive TMEs that have escaped immunosurveillance (6). During the DCIS phase, tumor cells and the immune system have achieved a state of equilibrium. Tipping the scale in favor of tumor cells results in invasive disease, while moving the scale towards the immune system results in eradication of disease. Anti-HER2 DC vaccination eliminates equilibrium, giving the immune system the boost it needs for elimination of tumor cells.

CONCLUSION

Breast cancer can be a devastating disease; therefore, a great degree of importance is placed on risk reduction and prevention. Identification of which patients would benefit from risk reduction strategies is critical; these patients include genetic mutation carriers, patients with strong family histories, personal history of breast cancer, and/or history of proliferative breast lesions. The current risk reduction and prevention strategies for high-risk patients include prophylactic mastectomy and chemoprevention, which unfortunately are not benign strategies and may pose significant burden to patients. Vaccination against breast cancer-specific oncodrivers or tumor-associated antigens shows promise in intercepting progression to IBC by boosting host immunity to recognize aberrant cells and eradicate them before development of invasive disease. Breast cancer-specific vaccination does not pose significant incumbrance to patients, may be more cost-effective, and may provide long-term protection. However, vaccination against breast cancer is not a one-size-fits-all approach and requires targeting specific antigens that may be present in one type of breast cancer and not another. Targeting benign, premalignant conditions such as ADH, FEA, or LCIS may provide means for risk reduction; however, utilizing vaccines to target a specific antigen in these conditions remains elusive. Certain types of vaccines, such as anti-HER2 DC vaccines given to patients with DCIS, have shown promise, but have yet to be studied in the preventative setting.

The current research in breast cancer vaccination has yet to scratch the surface of potential targets and has mainly focused on oncogenes and peptides such as HER2 and E75 in patients who have already been diagnosed with DCIS or breast cancer. Oncodriver expression may differ according to etiology as non-hereditary DCIS lesions express more HER2 while BRCA mutation carriers express HER3 and C-MET in DCIS, suggesting targeting a single oncodriver may not be sufficient for prevention of all DCIS. Breast-specific tumor-associated antigens such as mammaglobin, MUC1, and lactalbumin may provide a broader range of coverage in a preventative setting, but studies utilizing these proteins in targeted therapies are still in their infancy. The question that remains is, which breast cancer-specific vaccination target will provide the most effective risk reduction with broad coverage for the different subtypes of breast cancer? Moreover, another question still to be addressed is if shared neoantigens such as fusion proteins and frameshift mutations could also be effective targets because of being highly immunogenic in nature. Elucidating a clear target for future successful vaccination strategies to intercept premalignant, preinvasive breast lesions continues to be a difficult task, but eventually will provide a powerful tool for all at-risk patients.

DATA AVAILABILITY STATEMENT

The original contributions presented in the study are included in the article/supplementary material. Further inquiries can be directed to the corresponding author.

AUTHOR CONTRIBUTIONS

NZ, AB, NG, RG, and KK contributed to writing, editing, graphical presentation, and final approval. LL and BC contributed to editing and final approval. All authors contributed to the article and approved the submitted version.

FUNDING

This work was supported by Department of Defense (Award# W81XWH-16-1-0385) and Pennies in action to Dr. Brian Czerniecki.

REFERENCES

1. World Health Organization. *Breast Cancer* (2021). Available at: https://www.who.int/news-room/fact-sheets/detail/breast-cancer.
2. McDonnell SK, Schaid DJ, Myers JL, Grant CS, Donohue JH, et al. Efficacy of Contralateralprophylactic Mastectomy in Women With a Personal and Family History of Breast Cancer. *J Clin Oncol* (2001) 19(19):3938–43. doi: 10.1200/JCO.2001.19.19.3938
3. Hartmann LC, Degnim AC, Santen RJ, Dupont WD, Ghosh K. Atypical Hyperplasia of the Breast–Risk Assessment and Management Options. *N Engl J Med* (2015) 372:78–89. doi: 10.1056/NEJMsr1407164
4. Degnim AC, Brahmbhatt RD, Radisky DC, Hoskin TL, Stallings-Mann M, Laudenschlager M, et al. Immune Cell Quantitation in Normal Breast Tissue Lobules With and Without Lobulitis. *Breast Cancer Res Treat* (2014) 144 (3):539–49. doi: 10.1007/s10549-014-2896-8
5. Hennighausen L, Robinson G. Signaling Pathways in Mammary Gland Development. *Dev Cell* (2001) 1:467–75. doi: 10.1016/S1534-5807(01)00064-8
6. De La Cruz LM, Nocera NF, Czerniecki BJ. Restoring Anti-Oncodriver Th1 Responses With Dendritic Cell Vaccines in HER2/neu-Positive Breast Cancer: Progress and Potential. *Immunotherapy* (2016) 8(10):1219–32. doi: 10.2217/imt-2016-0052

7. Stewart T, Tsai SC, Grayson H, Henderson R, Opelz G. Incidence of De-Novo Breast Cancer in Women Chronically Immunosuppressed After Organ Transplantation. *Lancet* (1995) 346:796–8. doi: 10.1016/S0140-6736(95)91618-0
8. Dunn GP, Bruce A, Ikeda H, Old LJ, Schreiber RD. Cancer Immunoediting: From Immunosurveillance to Tumor Escape. *Nat Immunol* (2002) 3:991–8. doi: 10.1038/ni1102-991
9. Bui JD, Schreiber R. Cancer Immunosurveillance, Immunoediting and Inflammation: Independent or Interdependent Processes? *Curr Opin Immunol* (2007) 19(2):203–8. doi: 10.1016/j.coi.2007.02.001
10. DeNardo DG, Coussens LM. Inflammation and Breast Cancer. Balancing Immune Response: Crosstalk Between Adaptive and Innate Immune Cells During Breast Cancer Progression. *Breast Cancer Res* (2007) 9(4):212. doi: 10.1186/bcr1746
11. Sinn HP, Elsawaf Z, Helmchen B, Aulmann S. Early Breast Cancer Precursor Lesions: Lessons Learned From Molecular and Clinical Studies. *Breast Care (Basel)* (2010) 5(4):218–26. doi: 10.1159/000319624
12. Lakhani SR, Collins N, Stratton MR, Sloane JP. Atypical Ductalhyperplasia of the Breast: Clonal Proliferation With Loss of Het-Erozygosity on Chromosomes 16q and 17p. *J Clin Pathol* (1995) 48(7):611–5. doi: 10.1136/jcp.48.7.611
13. Reis-Filho JS, Simspson P, Gale T, Lakhani SR. The Molecular Genetics of Breast Cancer: The Contribution of Comparative Genomic Hybridization. *Pathol Res Pract* (2005) 201:713–25. doi: 10.1016/j.prp.2005.05.013
14. Allred DC, Brown P, Medina D. The Origins of Estrogen Receptor Alpha-Positive and Estrogen Receptor Alpha-Negative Human Breast Cancer. *Breast Cancer Res* (2004) 6:240–5. doi: 10.1186/bcr938
15. Chivukula M, Bhargava R, Tseng G, et al. Clinicopathologic Implications of "Flat Epithelial Atypia" in Core Needle Biopsy Specimens of the Breast. *Am J Clin Pathol* (2009) 131(6):802–8. doi: 10.1309/AJCPLDG6TT7VAHPH
16. Said SM, Visscher D, Nassar A, Frank RD, Vierkant RA, Frost MH, et al. Flat Epithelial Atypia and Risk of Breast Cancer: A Mayo Cohort Study. *Cancer* (2015) 121(10):1548–55. doi: 10.1002/cncr.29243
17. Pinder SE, Reis-Filho J. Non-Operative Breast Pathology: Columnar Cell Lesions. *J Clin Pathol* (2007) 60(12):1307–12. doi: 10.1136/jcp.2006.040634
18. Page DL, Schuyler P, Dupont WD, Jensen RA, Plummer WD Jr, Simpson JF. Atypical Lobular Hyperplasia as a Unilateral Predictor of Breast Cancer Risk: A Retrospective Cohort Study. *Lancet* (2003) 361(9352):125–9. doi: 10.1016/S0140-6736(03)12230-1
19. Simpson PT, Gale T, Fulford LG, Reis-Filho JS, Lakhani SR. The Diagnosis and Management of Pre-Invasive Breast Disease: Pathology of Atypical Lobular Hyperplasia and Lobular Carcinoma in Situ. *Breast Cancer Res* (2003) 5(5):258–62. doi: 10.1186/bcr624
20. Atkins KC, Cohen MA, Nicholson B, Rao S. Atypical Lobular Hyperplasia and Lobular Carcinoma in Situ at Core Breast Biopsy: Use of Careful Radiologic-Pathologic Correlation to Recommend Excision or Observation. *Radiology* (2013) 269:340–7. doi: 10.1148/radiol.13121730
21. Chuba PJ, Hamre M, Yap J, Severson RK, Lucas D, Shamsa F, et al. Bilateral Risk for Subsequent Breast Cancer After Lobular Carcinoma-in-Situ: Analysis of Surveillance, Epidemiology, and End Results Data. *J Clin Oncol* (2005) 23(24):5534–41. doi: 10.1200/JCO.2005.04.038
22. Andrade VP, Ostrovnaya I, Seshan VE, Morrogh M, Giri D, et al. Clonal Relatedness Between Lobular Carcinoma in Situ and Synchronous Malignant Lesions. *Breast Cancer Res* (2012) 14(4):R103. doi: 10.1186/bcr3222
23. Cutuli B, De Lafontan LB, Kirova Y, Auvray H, Tallet A, Avigdor S, et al. Lobular Carcinoma in Situ (LCIS) of the Breast: Is Long Term Outcome Similar to Ductal Carcinoma in Situ (DCIS)? Analysis of 200 Cases. *Radiat Oncol* (2015) 10(110):1–7. doi: 10.1186/s13014-015-0379-7
24. Oppong BA, King T. Recommendations for Women With Lobular Carcinoma in Situ (LCIS). *Oncology* (2011) 25(11):1051–6.
25. McCart Reed AE, Kalinowski L, Simpson PT, Lakhani SR. Nvasive Lobular Carcinoma of the Breast: The Increasing Importance of This Special Subtype. *Breast Cancer Res* (2021) 23(1):1–16. doi: 10.1186/s13058-020-01384-6
26. Neal L, Sandhu N, Hieken TJ, Glazebrook KN, Mac Bride MB, Dilaveri CA, et al. Diagnosis and Management of Benign, Atypical, and Indeterminate Breast Lesions Detected on Core Needle Biopsy. *Mayo Clin Proc* (2014) 89(4):536–47. doi: 10.1016/j.mayocp.2014.02.004
27. Mesurolle B, Perez J, Azzumea F, Lemercier E, Xie X, Aldis A, et al. Atypical Ductal Hyperplasia Diagnosed at Sonographically Guided Core Needle Biopsy: Frequency, Final Surgical Outcome, and Factors Associated With Underestimation. *AJR Am J Roentgenol* (2014) 202(6):1389–94. doi: 10.2214/AJR.13.10864
28. Nofech-Mozes S, Holloway C, Hanna W. The Role of Cytokeratin 5/6 as an Adjunct Diagnostic Tool in Breast Core Needle Biopsies. *Int J Surg Pathol* (2008) 16(4):399–406. doi: 10.1177/1066896908316901
29. Hartmann LC, Radisky D, Frost MH, Santen RJ, Vierkant RA, Benetti LL, et al. Understanding the Premalignant Potential of Atypical Hyperplasia Through its Natural History: A Longitudinal Cohort Study. *Cancer Prev Res (Phila)* (2014) 7(2):211–7. doi: 10.1158/1940-6207.CAPR-13-0222
30. Yamada T, Mori N, Watanabe M, Kimijima I, Okumoto T, Seiji K, et al. Radiologic-Pathologic Correlation of Ductal Carcinoma in Situ. *Radiographics* (2010) 30(5):1183–98. doi: 10.1148/rg.305095073
31. Zaha DC. Significance of Immunohistochemistry in Breast Cancer. *J Clin Oncol* (2014) 5(3):382–92. doi: 10.5306/wjco.v5.i3.382
32. Virnig BA, Wang S, Shamilyan T, Kane RL, Tuttle TM. Ductal Carcinoma in Situ: Risk Factors and Impact of Screening. *J Natl Cancer Inst Monogr* (2010) 41:113–6. doi: 10.1093/jncimonographs/lgq024
33. Sundara Rajan S, Verma R, Shaaban AM, Sharma N, Dall B, Lansdown M. Palpable Ductal Carcinoma in Situ: Analysis of Radiological and Histological Features of a Large Series With 5-Year Follow-Up. *Clin Breast Cancer* (2013) 13(6):486–91. doi: 10.1016/j.clbc.2013.08.002
34. Miligy IM, Toss MS, Gorringe KL, Lee AHS, Ellis IO, Green AR, et al. The Clinical and Biological Significance of HER2 Over-Expression in Breast Ductal Carcinoma in Situ: A Large Study From a Single Institution. *Br J Cancer* (2019) 120(11):1075–82. doi: 10.1038/s41416-019-0436-3
35. Barrio AV, Van Zee ZK. Controversies in the Treatment of Ductal Carcinoma in Situ. *Annu Rev Med* (2017) 14(68):197–211. doi: 10.1146/annurev-med-050715-104920
36. Wang J, Xu B. Targeted Therapeutic Options and Future Perspectives for HER2-Positive Breast Cancer. *Signal Transduct Target Ther* (2019) 4:34. doi: 10.1038/s41392-019-0069-2
37. Weinstein IB, Joe A. Oncogene Addiction. *Cancer Res* (2008) 68(9):3077–80; discussion 3080. doi: 10.1158/0008-5472.CAN-07-3293
38. Torti D, Trusolino L. Oncogene Addiction as a Foundational Rationale for Targeted Anti-Cancer Therapy: Promises and Perils. *EMBO Mol Med* (2011) 3(11):623–36. doi: 10.1002/emmm.201100176
39. Pagliarini R, Shao W, Sellers WR. Oncogene Addiction: Pathways of Therapeutic Response, Resistance, and Road Maps Toward a Cure. *EMBO Rep* (2015) 16(3):280–96. doi: 10.15252/embr.201439949
40. Tovey SM, Brown S, Doughty JC, Mallon EA, Cooke TG, Edwards J. Poor Survival Outcomes in HER2-Positive Breast Cancer Patients With Low-Grade, Node-Negative Tumours. *Br J Cancer* (2009) 100(5):680–3. doi: 10.1038/sj.bjc.6604940
41. Nikolai BC, Lanz RB, York B, Dasgupta S, Mitsiades N, Creighton CJ, et al. HER2 Signaling Drives DNA Anabolism and Proliferation Through SRC-3 Phosphorylation and E2F1-Regulated Genes. *Cancer Res* (2016) 76(6):1463–75. doi: 10.1158/0008-5472.CAN-15-2383
42. Godoy-Ortiz A, Sanchez-Munoz A, Parrado MRC, Alvarez M, Ribelles N, Dominguez AR, et al. Deciphering HER2 Breast Cancer Disease: Biological and Clinical Implications. *Front Oncol* (2019) 9:1124. doi: 10.3389/fonc.2019.01124
43. Bailey MH, Tokheim C, Porta-Pardo E, Sengupta S, Bertrand D, Weersainghe A, et al. Comprehensive Characterization of Cancer Driver Genes and Mutations. *Cell* (2018) 174(4):1034–5. doi: 10.1016/j.cell.2018.02.060
44. Eccles SA. The Epidermal Growth Factor Receptor/Erb-B/HER Family in Normal and Malignant Breast Biology. *Int J Dev Biol* (2011) 55(7-9):685–96. doi: 10.1387/ijdb.113396se
45. Harada S, Mick R, Roses RE, Graves H, Niu H, Sharma A, et al. The Significance of HER-2/Neu Receptor Positivity and Immunophenotype in Ductal Carcinoma in Situ With Early Invasive Disease. *J Surg Oncol* (2011) 104(5):458–65. doi: 10.1002/jso.21973
46. Nocera NF, Lee MC, de la Cruz LM, Rosemblit C, Czerniecki BJ. Restoring Lost Anti-HER-2 Th1 Immunity in Breast Cancer: A Crucial Role for Th1

Cytokines in Therapy and Prevention. *Front Pharmacol* (2016) 7:356. doi: 10.3389/fphar.2016.00356
47. Basu A, Ramamoorthi G, Albert G, Gallen C, Beyer A, Snyder C, et al. Differentiation and Regulation of TH Cells: A Balancing Act for Cancer Immunotherapy. *Front Immunol* (2021) 12(1577):669474. doi: 10.3389/fimmu.2021.669474
48. Watanabe S, Yonesaka K, Tanisaki J, Nonagase Y, Takegawa N, Haratani K, et al. Targeting of the HER2/HER3 Signaling Axis Overcomes Ligand-Mediated Resistance to Trastuzumab in HER2-Positive Breast Cancer. *Cancer Med* (2019) 8(3):1258–68. doi: 10.1002/cam4.1995
49. Ma J, Lyu H, Huang J, Liu B. Targeting of Erbb3 Receptor to Overcome Resistance in Cancer Treatment. *Mol Cancer* (2014) 13:105. doi: 10.1186/1476-4598-13-105
50. Mishra R, Patel H, Alanazi S, Yuan L, Garrett JT. HER3 Signaling and Targeted Therapy in Cancer. *Oncol Rev* (2018) 12(1):355. doi: 10.4081/oncol.2018.355
51. Bae SY, Choi YL, Kim S, Kim M, Kim J, Jung SP, et al. HER3 Status by Immunohistochemistry is Correlated With Poor Prognosis in Hormone Receptor-Negative Breast Cancer Patients. *Breast Cancer Res Treat* (2013) 139(3):741–50. doi: 10.1007/s10549-013-2570-6
52. Giltnane JM, Moeder CB, Camp RL, Rimm DL. Quantitative Multiplexed Analysis of ErbB Family Coexpression for Primary Breast Cancer Prognosis in a Large Retrospective Cohort. *Cancer* (2009) 115(11):2400–9. doi: 10.1002/cncr.24277
53. Richards L. HER3 Overexpression in Breast Cancer Conveys a Poor Prognosis. *Nat Rev Clin Oncol* (2010) 7(8):423–3. doi: 10.1038/nrclinonc.2010.106
54. Rimawi MF, Shetty PB, Weiss HL, Schiff R, Osborne CK, Chamness GC, et al. Epidermal Growth Factor Receptor Expression in Breast Cancer Association With Biologic Phenotype and Clinical Outcomes. *Cancer* (2010) 116(5):1234–42. doi: 10.1002/cncr.24816
55. Ueno NT, Zhang D. Targeting EGFR in Triple Negative Breast Cancer. *J Cancer* (2011) 2:324–8. doi: 10.7150/jca.2.324
56. Costa R, Shar AN, Santa-Maria CA, Cruz MR, Mahalingam D, Carneiro BA, et al. Targeting Epidermal Growth Factor Receptor in Triple Negative Breast Cancer: New Discoveries and Practical Insights for Drug Development. *Cancer Treat Rev* (2017) 53:111–9. doi: 10.1016/j.ctrv.2016.12.010
57. Ogden A, Bhattarai S, Sahoo B, Mongan NP, Alsaleem M, Green AR, et al. Combined HER3-EGFR Score in Triple-Negative Breast Cancer Provides Prognostic and Predictive Significance Superior to Individual Biomarkers. *Sci Rep* (2020) 10(1):3009. doi: 10.1038/s41598-020-59514-1
58. Park HS, Jang MH, Kim EJ, Kim HJ, Lee HJ, Kim YJ, et al. High EGFR Gene Copy Number Predicts Poor Outcome in Triple-Negative Breast Cancer. *Mod Pathol* (2014) 27(9):1212–22. doi: 10.1038/modpathol.2013.251
59. Zagouri F, Bago-Horvath Z, Rossler F, Branstetter A, Bartsch R, Papadimitriou CA, et al. High MET Expression is an Adverse Prognostic Factor in Patients With Triple-Negative Breast Cancer. *Br J Cancer* (2013) 108(5):1100–5. doi: 10.1038/bjc.2013.31
60. Yang RL, Mick R, Lee K, Graves HL, Nathanson KL, Domchek SM, et al. DCIS in BRCA1 and BRCA2 Mutation Carriers: Prevalence, Phenotype, and Expression of Oncodrivers C-MET and HER3. *J Transl Med* (2015) 13:335. doi: 10.1186/s12967-015-0698-3
61. Minuti G, Landi L. MET Deregulation in Breast Cancer. *Ann Transl Med* (2015) 3(13):181. doi: 10.3978/j.issn.2305-5839.2015.06.22
62. Benvenuto M, Rocaccetti C, Izzi V, Masuelli L, Modesti A, Bei R. Tumor Antigens Heterogeneity and Immune Response-Targeting Neoantigens in Breast Cancer. *Semin Cancer Biol* (2021) 72:65–75. doi: 10.1016/j.semcancer.2019.10.023
63. Ilyas S, Yang JC. Landscape of Tumor Antigens in T Cell Immunotherapy. *J Immunol* (2015) 195(11):5117. doi: 10.4049/jimmunol.1501657
64. Kufe DW. MUC1-C Oncoprotein as a Target in Breast Cancer: Activation of Signaling Pathways and Therapeutic Approaches. *Oncogene* (2013) 32 (9):1073–81. doi: 10.1038/onc.2012.158
65. Gao T, Cen Q, Lei H. A Review on Development of MUC1-Based Cancer Vaccine. *Biomed Pharmacother* (2020) 132:110888. doi: 10.1016/j.biopha.2020.110888
66. Fang F, Ma J, Ni W, Wang F, Sun X, Li Y, et al. MUC1 and Maltose–Binding Protein Recombinant Fusion Protein Combined With Bacillus Calmette –Guerin Induces MUC1–specific and Nonspecific Anti–Tumor Immunity in Mice. *Mol Med Rep* (2014) 10(2):1056–64. doi: 10.3892/mmr.2014.2306
67. Zhang Q, Ni W, Zhao X, Wang F, Gao Z, Tai G. Synergistic Antitumor Effects of Escherichia Coli Maltose Binding Protein and Bacillus Calmette–Guerin in a Mouse Lung Carcinoma Model. *Immunol Lett* (2011) 136 (1):108–13. doi: 10.1016/j.imlet.2010.12.005
68. Reddish MA, MacLean GD, Koganty RR, Kan-Mitchell J, Longenecker BM. Anti-MUC1 Class I Restricted CTLs in Metastatic Breast Cancer Patients Immunized With a Synthetic MUC1 Peptide. *Int J Cancer* (1998) 76(6):817–23. doi: 10.1002/(SICI)1097-0215(19980610)76:6<817::AID-IJC9>3.0.CO;2-0
69. Butts C, Socinski MA, Mitchell PL, Thatcher N, Havel L, Krzakowski M, et al. Tecemotide (L-BLP25) Versus Placebo After Chemoradiotherapy for Stage III Non-Small-Cell Lung Cancer (START): A Randomised, Double-Blind, Phase 3 Trial. *Lancet Oncol* (2014) 15(1):59–68. doi: 10.1016/S1470-2045(13)70510-2
70. Ge C, Li R, Song H, Geng T, Yang J, Tan Q, et al. Phase I Clinical Trial of a Novel Autologous Modified-DC Vaccine in Patients With Resected NSCLC. *BMC Cancer* (2017) 17(1):884. doi: 10.1186/s12885-017-3859-3
71. Decoster L, Wauters I, Vansteenkiste JF. Vaccination Therapy for Non-Small-Cell Lung Cancer: Review of Agents in Phase III Development. *Ann Oncol* (2012) 23(6):1387–93. doi: 10.1093/annonc/mdr564
72. Kroemer G, Zitvogel L, Galluzzi L. Victories and Deceptions in Tumor Immunology: Stimuvax(®). *Oncoimmunology* (2013) 2(1):e23687–7. doi: 10.4161/onci.23687
73. Gatti-Mays ME, Strauss J, Donahue RN, Palena C, Del Rivero J, Redman JM, et al. A Phase I Dose-Escalation Trial of BN-CV301, a Recombinant Poxviral Vaccine Targeting MUC1 and CEA With Costimulatory Molecules. *Clin Cancer Res* (2019) 25(16):4933–44. doi: 10.1158/1078-0432.CCR-19-0183
74. Ghersevich S, Ceballos MP. Mammaglobin A: Review and Clinical Utility. *Adv Clin Chem* (2014) 64:241–68. doi: 10.1016/B978-0-12-800263-6.00006-9
75. Zach O, Kasparu H, Wagner H, Krieger O, Lutz D. Detection of Mammaglobin mRNA as a Marker for Circulating Tumor Cells in Breast Carcinoma. *Acta Med Austriaca Suppl* (2000) 52:13–5.
76. Grünewald K, Haun M, Urbanek M, Riegl M, Muller-Holzner E, Gunsilius E, et al. Mammaglobin Gene Expression: A Superior Marker of Breast Cancer Cells in Peripheral Blood in Comparison to Epidermal-Growth-Factor Receptor and Cytokeratin-19. *Lab Invest* (2000) 80(7):1071–7. doi: 10.1038/labinvest.3780112
77. Talaat IM, Hachim MY, Hachim IY, Ibrahim RAE, Ahmed MAE, Tayel HY. Bone Marrow Mammaglobin-1 (SCGB2A2) Immunohistochemistry Expression as a Breast Cancer Specific Marker for Early Detection of Bone Marrow Micrometastases. *Sci Rep* (2020) 10(1):13061–1. doi: 10.1038/s41598-020-70012-2
78. Jaini R, Kesaraju P, Johnson JM, Altuntas CZ, Jane-Wit D, Tuohy VK. An Autoimmune-Mediated Strategy for Prophylactic Breast Cancer Vaccination. *Nat Med* (2010) 16(7):799–803. doi: 10.1038/nm.2161
79. Tuohy VK, Jaini R, Johnson JM, Loya MG, Wilk D, Downs-Kelly E, et al. Targeted Vaccination Against Human α-Lactalbumin for Immunotherapy and Primary Immunoprevention of Triple Negative Breast Cancer. *Cancers* (2016) 8(6):56. doi: 10.3390/cancers8060056
80. Gubin MM, Artyomov MN, Mardis ER, Schreiber RD. Tumor Neoantigens: Building a Framework for Personalized Cancer Immunotherapy. *J Clin Invest* (2015) 125(9):3413–21. doi: 10.1172/JCI80008
81. Li L, Goedegebuure SP, Gillanders WE. Preclinical and Clinical Development of Neoantigen Vaccines. *Ann Oncol* (2017) 28(suppl_12): xii11–7. doi: 10.1093/annonc/mdx681
82. Schumacher TN, Hacohen N. Neoantigens Encoded in the Cancer Genome. *Curr Opin Immunol* (2016) 41:98–103. doi: 10.1016/j.coi.2016.07.005
83. Salomon N, Vascotto F, Selmi A, Vormehr M, Quinkhardt J, Bukur T, et al. A Liposomal RNA Vaccine Inducing Neoantigen-Specific CD4(+) T Cells Augments the Antitumor Activity of Local Radiotherapy in Mice. *Oncoimmunology* (2020) 9(1):1771925. doi: 10.1080/2162402X.2020.1771925
84. Howitt BE, Shukla SA, Sholl LM, Ritterhouse LL, Watkins JC, Rodig S, et al. Association of Polymerase E-Mutated and Microsatellite-Instable Endometrial Cancers With Neoantigen Load, Number of Tumor-Infiltrating Lymphocytes, and Expression of PD-1 and PD-L1. *JAMA Oncol* (2015) 1(9):1319–23. doi: 10.1001/jamaoncol.2015.2151
85. Strickland KC, Howitt BE, Shukla SA, Rodig S, Ritterhouse LL, Liu JF, et al. Association and Prognostic Significance of BRCA1/2-Mutation Status With

Neoantigen Load, Number of Tumor-Infiltrating Lymphocytes and Expression of PD-1/PD-L1 in High Grade Serous Ovarian Cancer. *Oncotarget* (2016) 7(12):13587–98. doi: 10.18632/oncotarget.7277
86. Turajlic S, Litchfield K, Xu H, Rosenthal R, McGranahan N, Reading JL, et al. Insertion-And-Deletion-Derived Tumour-Specific Neoantigens and the Immunogenic Phenotype: A Pan-Cancer Analysis. *Lancet Oncol* (2017) 18 (8):1009–21. doi: 10.1016/S1470-2045(17)30516-8
87. Zhang J, Shen L, Johnston SA. Using Frameshift Peptide Arrays for Cancer Neo-Antigens Screening. *Sci Rep* (2018) 8(1):17366. doi: 10.1038/s41598-018-35673-0
88. Zhang X, Kim S, Hundal J, Herndon JM, Li S, Petti AA, et al. Breast Cancer Neoantigens Can Induce CD8(+) T-Cell Responses and Antitumor Immunity. *Cancer Immunol Res* (2017) 5(7):516–23. doi: 10.1158/2326-6066.CIR-16-0264
89. Morisaki T, Kubo M, Umebayashi M, Yew PY, Yoshimura S, Park JH, et al. Neoantigens Elicit T Cell Responses in Breast Cancer. *Sci Rep* (2021) 11 (1):13590. doi: 10.1038/s41598-021-91358-1
90. Narang P, C. M, Sharma AA, Anderson KS, Wilson MA. The Neoepitope Landscape of Breast Cancer: Implications for Immunotherapy. *BMC Cancer* (2019) 19(1):1–10. doi: 10.1186/s12885-019-5402-1
91. Chen C, Z. Q, Wu R, Li B, Chen Q, Zhang X, et al. A Comprehensive Survey of Genomic Alterations in Gastric Cancer Reveals Recurrent Neoantigens as Potential Therapeutic Targets. *BioMed Res Int* (2019) 1–10. doi: 10.1155/2019/2183510
92. Zundelevich A, D. M, Kahana-Edwin S, Itay A, Sella T, Gadot M, et al. ESR1 Mutations are Frequent in Newly Diagnosed Metastatic and Loco-Regional Recurrence of Endocrine-Treated Breast Cancer and Carry Worse Prognosis. *Breast Cancer Res* (2020) 22(1):16. doi: 10.1186/s13058-020-1246-5
93. Clatot F, Perdrix A, Beaussire L, Lequesne J, Lévy C, Emile G, et al. Risk of Early Progression According to Circulating ESR1 Mutation, CA-15.3 and cfDNA Increases Under First-Line Anti-Aromatase Treatment in Metastatic Breast Cancer. *Breast Cancer Res* (2020) 22(1):56. doi: 10.1186/s13058-020-01290-x
94. Tang L, Zhang R, Zhang X, Yang L. Personalized Neoantigen-Pulsed DC Vaccines: Advances in Clinical Applications. *Front Oncol* (2021) 11. doi: 10.3389/fonc.2021.701777
95. Ding Z, Li Q, Zhang R, Xie L, Shu Y, Gao S, et al. Personalized Neoantigen Pulsed Dendritic Cell Vaccine for Advanced Lung Cancer. *Signal Transduct Target Ther* (2021) 6(1):1–25. doi: 10.1038/s41392-020-00448-5
96. Carreno BM, Magrini V, Becker-Hapak M, Kaabinejadian S, Hundal J, Petti AA, et al. Cancer Immunotherapy. A Dendritic Cell Vaccine Increases the Breadth and Diversity of Melanoma Neoantigen-Specific T Cells. *Science* (2015) 348(6236):803–8. doi: 10.1126/science.aaa3828
97. Han X-J, Ma X-L, Yang L, Wei Y-Q, Peng Y, Wei X-W. Progress in Neoantigen Targeted Cancer Immunotherapies. *Front Cell Dev Biol* (2020) 8(728). doi: 10.3389/fcell.2020.00728
98. Coopey SB, Mazzola E, Buckley JM, Sharko J, Belli AK, Kim EMH, et al. The Role of Chemoprevention in Modifying the Risk of Breast Cancer in Women With Atypical Breast Lesions. *Breast Cancer Res Treat* (2012) 136(3):627–33. doi: 10.1007/s10549-012-2318-8
99. Banys-Paluchowski M, Gasparri ML, Boniface J, Gentilli O, Stickeler E, Hartmann S, et al. Surgical Management of the Axilla in Clinically Node-Positive Breast Cancer Patients Converting to Clinical Node Negativity Through Neoadjuvant Chemotherapy: Current Status, Knowledge Gaps, and Rationale for the EUBREAST-03 AXSANA Study. *Cancers (Basel)* (2021) 13 (7):1–25. doi: 10.3390/cancers13071565
100. Wojtowicz ME, D. B, Umar A. Immunologic Approaches to Cancer Prevention—Current Status, Challenges, and Future Perspectives. *Semin Oncol* (2016) 43(1):161–72. doi: 10.1053/j.seminoncol.2015.11.001
101. Mbulaiteye SM, Buonaguro FM. Infections and Cancer: Debate About Using Vaccines as a Cancer Control Tool. *Infect Agents Cancer* (2013) 8(16):1–4. doi: 10.1186/1750-9378-8-16
102. Czerniecki BJ, N. N, Lowenfeld L, Showalter L, Koski G. Vaccination Against Breast Cancer and its Role in Prevention. In: R J., editor. *Trends in Breast Cancer Prevention*. Switzerland: Springer (2016).
103. Ehrlich P. Ueber Den Jetzigen Stand Der Karzinomforschung. *Ned Tijdschr Geneeskd* (1909) 5:273–90.
104. Burnet M. Cancer: A Biological Approach. III. Viruses Associated With Neoplastic Conditions. IV. Practical Applications. *Br Med J* (1957) 1 (5023):841–7. doi: 10.1136/bmj.1.5023.841
105. Dunn GP, Bruce AT, Ikeda H, Old LJ, Schreiber RD. Cancer Immunoediting: From Immunosurveillance to Tumor Escape. *Nat Immunol* (2002) 3 (11):991–8. doi: 10.1038/ni1102-991
106. Shankaran V, Ikeda H, Bruce AT, White JM, Swanson PE, Old LJ, et al. IFNgamma and Lymphocytes Prevent Primary Tumour Development and Shape Tumour Immunogenicity. *Nature* (2001) 410(6832):1107–11. doi: 10.1038/35074122
107. Matsushita H, Vesely MD, Koboldt DC, Rickert CG, Uppaluri R, Magrini VJ, et al. Cancer Exome Analysis Reveals a T-Cell-Dependent Mechanism of Cancer Immunoediting. *Nature* (2012) 482(7385):400–4. doi: 10.1038/nature10755
108. Dunn GP, Old LJ, Schreiber RD. The Three Es of Cancer Immunoediting. *Annu Rev Immunol* (2004) 22:329–60. doi: 10.1146/annurev.immunol.22.012703.104803
109. Dunn GP, Old LJ, Schreiber RD. The Immunobiology of Cancer Immunosurveillance and Immunoediting. *Immunity* (2004) 21(2):137–48. doi: 10.1016/j.immuni.2004.07.017
110. O'Donnell JS, Teng MWL, Smyth MJ. Cancer Immunoediting and Resistance to T Cell-Based Immunotherapy. *Nat Rev Clin Oncol* (2019) 16 (3):151–67. doi: 10.1038/s41571-018-0142-8
111. Vesely MD, Kershaw MH, Schreiber RD, Smyth MJ. Natural Innate and Adaptive Immunity to Cancer. *Annu Rev Immunol* (2011) 29:235–71. doi: 10.1146/annurev-immunol-031210-101324
112. Teng MW, Galon J, Fridman WH, Smyth MJ. From Mice to Humans: Developments in Cancer Immunoediting. *J Clin Invest* (2015) 125(9):3338–46. doi: 10.1172/JCI80004
113. Mellman I, Coukos G, Dranoff G. Cancer Immunotherapy Comes of Age. *Nature* (2011) 480(7378):480–9. doi: 10.1038/nature10673
114. Mittal D, Gubin MM, Schreiber RD, Smyth MJ. New Insights Into Cancer Immunoediting and its Three Component Phases–Elimination, Equilibrium and Escape. *Curr Opin Immunol* (2014) 27:16–25. doi: 10.1016/j.coi.2014.01.004
115. Bates JP, Derakhashandeh R, Jones L, Webb TJ. Mechanisms of Immune Evasion in Breast Cancer. *BMC Cancer* (2018) 18(1):556. doi: 10.1186/s12885-018-4441-3
116. Gil Del Alcazar CR, Alečković M, Polyak K. Immune Escape During Breast Tumor Progression. *Cancer Immunol Res* (2020) 8(4):422–7. doi: 10.1158/2326-6066.CIR-19-0786
117. Loi S, Dushyanthen S, Beavis PA, Salgado R, Denkert C, Savas P, et al. RAS/MAPK Activation Is Associated With Reduced Tumor-Infiltrating Lymphocytes in Triple-Negative Breast Cancer: Therapeutic Cooperation Between MEK and PD-1/PD-L1 Immune Checkpoint Inhibitors. *Clin Cancer Res* (2016) 22(6):1499–509. doi: 10.1158/1078-0432.CCR-15-1125
118. Balko JM, Giltnane JM, Wang K, Schwarz LJ, Young CD, Cook RS, et al. Molecular Profiling of the Residual Disease of Triple-Negative Breast Cancers After Neoadjuvant Chemotherapy Identifies Actionable Therapeutic Targets. *Cancer Discov* (2014) 4(2):232–45. doi: 10.1158/2159-8290
119. Datta J, Rosemblit, Berk E, Showalter L, Namjoshi P, Mick R, et al. Progressive Loss of Anti-HER2 CD4(+) T-Helper Type 1 Response in Breast Tumorigenesis and the Potential for Immune Restoration. *Oncoimmunology* (2015) 4(10):e1022301. doi: 10.1080/2162402X.2015.1022301
120. Zhu X, Du L, Feng J, Ling Y, Xu S. Clinicopathological and Prognostic Significance of Serum Cytokine Levels in Breast Cancer. *Clin Lab* (2014) 60 (7):1145–51. doi: 10.7754/Clin.Lab.2013.130738
121. Jia Y, Kodumudi KN, Ramamoorthi G, Basu A, Snyder C, Wiener D, et al. Th1 Cytokine Interferon Gamma Improves Response in HER2 Breast Cancer by Modulating the Ubiquitin Proteasomal Pathway. *Mol Ther* (2021) 29(4):1541–56. doi: 10.1016/j.ymthe.2020.12.037
122. Palucka K, Coussens LM, O'Shaughnessy J. Dendritic Cells, Inflammation, and Breast Cancer. *Cancer J* (2013) 19(6):511–6. doi: 10.1097/PPO.0000000000000007
123. Gu-Trantien C, et al. CD4$^+$ Follicular Helper T Cell Infiltration Predicts Breast Cancer Survival. *J Clin Invest* (2013) 123(7):2873–92. doi: 10.1172/JCI67428

124. Rosenblatt J, et al. PD-1 Blockade by CT-011, Anti-PD-1 Antibody, Enhances Ex Vivo T-Cell Responses to Autologous Dendritic Cell/Myeloma Fusion Vaccine. *J Immunother* (2011) 34(5):409–18. doi: 10.1097/CJI.0b013e31821ca6ce
125. Ge Y, et al. Blockade of PD-1/PD-L1 Immune Checkpoint During DC Vaccination Induces Potent Protective Immunity Against Breast Cancer in Hu-SCID Mice. *Cancer Lett* (2013) 336(2):253–9. doi: 10.1016/j.canlet.2013.03.010
126. Kodumudi KN, et al. Sequential Anti-PD1 Therapy Following Dendritic Cell Vaccination Improves Survival in a HER2 Mammary Carcinoma Model and Identifies a Critical Role for CD4 T Cells in Mediating the Response. *Front Immunol* (2019) 10:1939. doi: 10.3389/fimmu.2019.01939
127. Fracol M, et al. Loss of Anti-HER-3 CD4+ T-Helper Type 1 Immunity Occurs in Breast Tumorigenesis and is Negatively Associated With Outcomes. *Ann Surg Oncol* (2017) 24(2):407–17. doi: 10.1245/s10434-016-5584-6
128. Iwasaki A, Medzhitov R. Control of Adaptive Immunity by the Innate Immune System. *Nat Immunol* (2015) 16(4):343–53. doi: 10.1038/ni.3123
129. Liu J, Zhang X, Chen K, Cheng Y, Liu S, Xia M, et al. Dendritic Cell Migration in Inflammation and Immunity. *Cell Mol Immunol* (2021) 18 (11):2461–71. doi: 10.1038/s41423-021-00726-4
130. Puhr S, Lee J, Zvezdova E, Zhou YJ, Liu K. Dendritic Cell Development-History, Advances, and Open Questions. *Semin Immunol* (2015) 27(6):388–96. doi: 10.1016/j.smim.2016.03.012
131. Anderson DA 3rd, Dutertre CA, Ginhouz F, Murphy KM. Genetic Models of Human and Mouse Dendritic Cell Development and Function. *Nat Rev Immunol* (2021) 21(2):101–15. doi: 10.1038/s41577-020-00413-x
132. Merad M, Sathe P, Helft J, Miller J, Mortha A. The Dendritic Cell Lineage: Ontogeny and Function of Dendritic Cells and Their Subsets in the Steady State and the Inflamed Setting. *Annu Rev Immunol* (2013) 31:563–604. doi: 10.1146/annurev-immunol-020711-074950
133. Zhu J, Yamane H, Paul WE. Differentiation of Effector CD4 T Cell Populations (*). *Annu Rev Immunol* (2010) 28:445–89. doi: 10.1146/annurev-immunol-030409-101212
134. Kadowaki N. Dendritic Cells: A Conductor of T Cell Differentiation. *Allergol Int* (2007) 56(3):193–9. doi: 10.2332/allergolint.R-07-146
135. Lamiable O, Mayer JU, Munoz-Erazo L, Ronchese F. Dendritic Cells in Th2 Immune Responses and Allergic Sensitization. *Immunol Cell Biol* (2020) 98 (10):807–18. doi: 10.1111/imcb.12387
136. Faries MB, Bedrosian I, Xu S, Roros JG, Moise MA, Nguyen HQ. Calcium Signaling Inhibits Interleukin-12 Production and Activates CD83(+) Dendritic Cells That Induce Th2 Cell Development. *Blood* (2001) 98 (8):2489–97. doi: 10.1182/blood.V98.8.2489
137. Kalinski P. Regulation of Immune Responses by Prostaglandin E2. *J Immunol* (2012) 188(1):21–8. doi: 10.4049/jimmunol.1101029
138. Zhao Y, Chu X, Chen J, Wang Y, Gao S, Jiang Y, et al. Dectin-1-Activated Dendritic Cells Trigger Potent Antitumour Immunity Through the Induction of Th9 Cells. *Nat Commun* (2016) 7:12368. doi: 10.1038/ncomms12368
139. Chen J, Zhao Y, Chu X, Lu Y, Wang S, Yi Q. Dectin-1-Activated Dendritic Cells: A Potent Th9 Cell Inducer for Tumor Immunotherapy. *Oncoimmunology* (2016) 5(11):e1238558. doi: 10.1080/2162402X.2016.1238558
140. Agalioti T, Villablanca EJ, Huber S, Gagliani N. TH17cell Plasticity: The Role of Dendritic Cells and Molecular Mechanisms. *J Autoimmun* (2018) 87:50–60. doi: 10.1016/j.jaut.2017.12.003
141. Khayrullina T, Yen JH, Ganea D. *In Vitro* Differentiation of Dendritic Cells in the Presence of Prostaglandin E2 Alters the IL-12/IL-23 Balance and Promotes Differentiation of Th17 Cells. *J Immunol* (2008) 181(1):721–35. doi: 10.4049/jimmunol.181.1.721
142. Krishnaswamy JK, Alsen S, Yrlid U, Eisenbarth SC, Williams A. Determination of T Follicular Helper Cell Fate by Dendritic Cells. *Front Immunol* (2018) 9:2169. doi: 10.3389/fimmu.2018.02169
143. Li DY, Xiong XZ. ICOS(+) Tregs: A Functional Subset of Tregs in Immune Diseases. *Front Immunol* (2020) 11:2104. doi: 10.3389/fimmu.2020.02104
144. Gao X, Zhao L, Wang S, Yang J, Yang X. Enhanced Inducible Costimulator Ligand (ICOS-L) Expression on Dendritic Cells in Interleukin-10 Deficiency and its Impact on T-Cell Subsets in Respiratory Tract Infection. *Mol Med* (2013) 19:346–56. doi: 10.2119/molmed.2013.00035
145. Comi M, Amodio G, Gregori S. Interleukin-10-Producing DC-10 Is a Unique Tool to Promote Tolerance Via Antigen-Specific T Regulatory Type 1 Cells. *Front Immunol* (2018) 9:682. doi: 10.3389/fimmu.2018.00682
146. Palucka K, Banchereau J. Dendritic-Cell-Based Therapeutic Cancer Vaccines. *Immunity* (2013) 39(1):38–48. doi: 10.1016/j.immuni.2013.07.004
147. Basu A, Ramamoorthi G, Jia Y, Faughn J, Wiener D, Swshah S, et al. Immunotherapy in Breast Cancer: Current Status and Future Directions. *Adv Cancer Res* (2019) 143:295–349. doi: 10.1016/bs.acr.2019.03.006
148. Burke EE, Kodumudi K, Gamamoorthi, Czerniecki BJ. Vaccine Therapies for Breast Cancer. *Surg Oncol Clin N Am* (2019) 28(3):353–67. doi: 10.1016/j.soc.2019.02.004
149. Sharma A, Koldovsky U, Xu S, Mick R, Roses R, Fitzpatrick E, et al. HER-2 Pulsed Dendritic Cell Vaccine can Eliminate HER-2 Expression and Impact Ductal Carcinoma in Situ. *Cancer* (2012) 118(17):4354–62. doi: 10.1002/cncr.26734
150. Datta J, Berk E, Xu S, Fitzpatrick E, Rosemblit C, Lowenfeld L, et al. Anti-HER2 CD4(+) T-Helper Type 1 Response is a Novel Immune Correlate to Pathologic Response Following Neoadjuvant Therapy in HER2-Positive Breast Cancer. *Breast Cancer Res* (2015) 17:71. doi: 10.1186/s13058-015-0584-1
151. Lowenfeld L, Zaheer S, Oechsle C, Fracol M, Datta J, Xu S, et al. Addition of Anti-Estrogen Therapy to Anti-HER2 Dendritic Cell Vaccination Improves Regional Nodal Immune Response and Pathologic Complete Response Rate in Patients With ER(pos)/HER2(pos) Early Breast Cancer. *Oncoimmunology* (2017) 6(9):e1207032. doi: 10.1080/2162402X.2016.1207032
152. Wang B, Zaidi N, He L, Zhang L, Kuroiwa JMY, Keler T, et al. Targeting of the Non-Mutated Tumor Antigen HER2/neu to Mature Dendritic Cells Induces an Integrated Immune Response That Protects Against Breast Cancer in Mice. *Breast Cancer Res* (2012) 14(2):R39. doi: 10.1186/bcr3135
153. Armstrong AC, Gilham DE. Targeting Breast Cancer Vaccines to Dendritic Cells: Improved Immunological Responses With Less Protein? *Breast Cancer Res* (2012) 14(3):106. doi: 10.1186/bcr3184
154. Mittendorf EA, Ardavanis A, Litton JK, Shumway NM, Hale DF, Murray JL, et al. Primary Analysis of a Prospective, Randomized, Single-Blinded Phase II Trial Evaluating the HER2 Peptide GP2 Vaccine in Breast Cancer Patients to Prevent Recurrence. *Oncotarget* (2016) 7(40):66192–201. doi: 10.18632/oncotarget.11751
155. Schneble EJ, Berry JS, Trappey FA, Clifton GT, Ponniah S, Mittendorf E, et al. The HER2 Peptide Nelipepimut-S (E75) Vaccine (NeuVax) in Breast Cancer Patients at Risk for Recurrence: Correlation of Immunologic Data With Clinical Response. *Immunotherapy* (2014) 6(5):519–31. doi: 10.2217/imt.14.22
156. Allahverdiyev A, Tari G, Bagirova M, Abamor ES. Current Approaches in Development of Immunotherapeutic Vaccines for Breast Cancer. *J Breast Cancer* (2018) 21(4):343–53. doi: 10.4048/jbc.2018.21.e47
157. Fu Q, Wu Y, Yan F, Wang N, Wang W, Cao X, et al. Efficient Induction of a Her2-Specific Anti-Tumor Response by Dendritic Cells Pulsed With a Hsp70L1-Her2(341-456) Fusion Protein. *Cell Mol Immunol* (2011) 8 (5):424–32. doi: 10.1038/cmi.2011.21
158. Mittendorf EA, Clifton GT, Jolmes JP, Schneble E, van Echo D, Pnniah S, et al. Final Report of the Phase I/II Clinical Trial of the E75 (Nelipepimut-S) Vaccine With Booster Inoculations to Prevent Disease Recurrence in High-Risk Breast Cancer Patients. *Ann Oncol* (2014) 25(9):1735–42. doi: 10.1093/annonc/mdu211
159. Mittendorf EA, Clifton G, Holmes JP, Clive KS, Patil R, Benavides LC, et al. Clinical Trial Results of the HER-2/Neu (E75) Vaccine to Prevent Breast Cancer Recurrence in High-Risk Patients: From US Military Cancer Institute Clinical Trials Group Study I-01 and I-02. *Cancer* (2012) 118(10):2594–602. doi: 10.1002/cncr.26574
160. Benedetti R, Dell'Aversana C, Giorgio C, Astorri R, Altucci L. Breast Cancer Vaccines: New Insights. *Front Endocrinol (Lausanne)* (2017) 8:270. doi: 10.3389/fendo.2017.00270
161. Chan T, Sami A, El-Gayed A, Guo X, Xiang J. HER-2/Neu-Gene Engineered Dendritic Cell Vaccine Stimulates Stronger HER-2/Neu-Specific Immune Responses Compared to DNA Vaccination. *Gene Ther* (2006) 13(19):1391–402. doi: 10.1038/sj.gt.3302797
162. Xie Y, Chen Y, Ahmed KA, Li W, Ahmed S, Sami A, et al. Potent CD4+ T-Cell Epitope P30 Enhances HER2/neu-Engineered Dendritic Cell-Induced Immunity Against Tg1-1 Breast Cancer in Transgenic FVBneuN Mice by Enhanced CD4+ T-Cell-Stimulated CTL Responses. *Cancer Gene Ther* (2013) 20(10):590–8. doi: 10.1038/cgt.2013.60

163. Steel JC, Ramlogan CA, Yu P, Sakai Y, Forni G, Waldmann TA, et al. Interleukin-15 and Its Receptor Augment Dendritic Cell Vaccination Against the Neu Oncogene Through the Induction of Antibodies Partially Independent of CD4 Help. *Cancer Res* (2010) 70(3):1072–81. doi: 10.1158/0008-5472.CAN-09-1301
164. Oh DY, Bang YJ. HER2-Targeted Therapies - A Role Beyond Breast Cancer. *Nat Rev Clin Oncol* (2020) 17(1):33–48. doi: 10.1038/s41571-019-0268-3
165. Clifton GT, Litton JK, Arrington K, Pnniah S, Ibrahim NK, Gall V, et al. Results of a Phase Ib Trial of Combination Immunotherapy With a CD8+ T Cell Eliciting Vaccine and Trastuzumab in Breast Cancer Patients. *Ann Surg Oncol* (2017) 24(8):2161–7. doi: 10.1245/s10434-017-5844-0
166. Gall VA, Philips AV, Qiao N, Clise-Dwyer K, Perakis AA, Zhang M, et al. Trastuzumab Increases HER2 Uptake and Cross-Presentation by Dendritic Cells. *Cancer Res* (2017) 77(19):5374–83. doi: 10.1158/0008-5472.CAN-16-2774
167. Mittendorf EA, Storrer CE, Shriver CD, Ponniah S, Peoples GE. Investigating the Combination of Trastuzumab and HER2/neu Peptide Vaccines for the Treatment of Breast Cancer. *Ann Surg Oncol* (2006) 13(8):1085–98. doi: 10.1245/ASO.2006.03.069
168. Xu ZQ, Zhang Y, Li N, Liu P, Gao L, Gao X, et al. Efficacy and Safety of Lapatinib and Trastuzumab for HER2-Positive Breast Cancer: A Systematic Review and Meta-Analysis of Randomised Controlled Trials. *BMJ Open* (2017) 7(3):e013053. doi: 10.1136/bmjopen-2016-013053
169. Schlam I, Swain SM. HER2-Positive Breast Cancer and Tyrosine Kinase Inhibitors: The Time is Now. *NPJ Breast Cancer* (2021) 7(1):56. doi: 10.1038/s41523-021-00265-1
170. Showalter L, Czerniecki BJ, Koski GK. Th1 Cytokines in Conjunction With Pharmacological Akt Inhibition Potentiate Apoptosis of Breast Cancer Cells *In Vitro* and Suppress Tumor Growth *In Vivo*. *Oncotarget* (2020) 11 (30):2873–88. doi: 10.18632/oncotarget.27556
171. Knutson KL, S. K, Cheever MA, Disis ML. Immunization of Cancer Patients With a HER-2/Neu, HLA-A2 Peptide, P369-377, Results in Short-Lived Peptide-Specific Immunity. *Clin Cancer Res* (2002) 8(5):1014–8.
172. Benavides LC, Gates JD, Carmichael MG, Patil R, Holmes JP, Hueman MT, et al. The Impact of HER2/neu Expression Level on Response to the E75 Vaccine: From U.S. Military Cancer Institute Clinical Trials Group Study I-01 and I-02. *Clin Cancer Res* (2009) 15(8):2895–904. doi: 10.1158/1078-0432.CCR-08-1126
173. Czerniecki BJ, Koski GK, Koldovsky U, Xu S, Cohen PA, Mick R, et al. Targeting HER-2/Neu in Early Breast Cancer Development Using Dendritic Cells With Staged Interleukin-12 Burst Secretion. *Cancer Res* (2007) 67 (4):1842–52. doi: 10.1158/0008-5472.CAN-06-4038
174. Curtsinger JM, J. C, Mescher MF. CD8 T Cell Clonal Expansion and Development of Effector Function Require Prolonged Exposure to Antigen, Costimulation, and Signal 3 Cytokine. *J Immunol* (2003) 171(10):5165–71. doi: 10.4049/jimmunol.171.10.5165
175. Kaiko GE, H. J, Beagley KW, Hansbro PM. Immunological Decision-Making: How Does the Immune System Decide to Mount a Helper T-Cell Response? *Immunology* (2008) 123(3):326–38. doi: 10.1111/j.1365-2567.2007.02719.x
176. Cintolo JA, D. J, Mathew SJ, Czerniecki BJ. Dendritic Cell-Based Vaccines: Barriers and Opportunities. *Future Oncol* (2012) 8(10):1273–99. doi: 10.2217/fon.12.125
177. Disis ML, Calenoff E, McLaughlin G, Murphy AE, Chen W, Groner B, et al. Existent T-Cell and Antibody Immunity to HER-2/Neu Protein in Patients With Breast Cancer. *Cancer Res* (1994) 54:16–20.

Conflict of Interest: BC has a patent application filed for intellectual property on a human version of DC1. LL has stock in Johnson & Johnson, Pfizer, Eli Lilly, Gilead, and Amgen.

The remaining authors declare that the research was conducted in the absence of any commercial or financial relationships that could be construed as a potential conflict of interest.

Publisher's Note: All claims expressed in this article are solely those of the authors and do not necessarily represent those of their affiliated organizations, or those of the publisher, the editors and the reviewers. Any product that may be evaluated in this article, or claim that may be made by its manufacturer, is not guaranteed or endorsed by the publisher.

frontiers in Immunology

REVIEW
published: 27 January 2022
doi: 10.3389/fimmu.2022.840923

Genetic Changes Driving Immunosuppressive Microenvironments in Oral Premalignancy

Roberto Rangel[1], *Curtis R. Pickering*[1], *Andrew G. Sikora*[1] *and Michael T. Spiotto*[2]*

[1] Department of Head and Neck Surgery, The University of Texas M.D. Anderson Cancer Center, Houston, TX, United States,
[2] Department of Radiation Oncology, The University of Texas M.D. Anderson Cancer Center, Houston, TX, United States

Oral premalignant lesions (OPLs) are the precursors to oral cavity cancers, and have variable rates of progression to invasive disease. As an intermediate state, OPLs have acquired a subset of the genomic alterations while arising in an oral inflammatory environment. These specific genomic changes may facilitate the transition to an immune microenvironment that permits malignant transformation. Here, we will discuss mechanisms by which OPLs develop an immunosuppressive microenvironment that facilitates progression to invasive cancer. We will describe how genomic alterations and immune microenvironmental changes co-evolve and cooperate to promote OSCC progression. Finally, we will describe how these immune microenvironmental changes provide specific and unique evolutionary vulnerabilities for targeted therapies. Therefore, understanding the genomic changes that drive immunosuppressive microenvironments may eventually translate into novel biomarker and/or therapeutic approaches to limit the progression of OPLs to potential lethal oral cancers.

Keywords: head and neck cancer, immunosuppression, TP53, CDKN2A, NOTCH1

OPEN ACCESS

Edited by:
Olivera J. Finn,
University of Pittsburgh, United States

Reviewed by:
Paolo Bossi,
University of Brescia, Italy
Patrick Lizotte,
Dana–Farber Cancer Institute, United States

***Correspondence:**
Michael T. Spiotto
MTSpiotto@mdanderson.org

Specialty section:
This article was submitted to Cancer Immunity and Immunotherapy, a section of the journal Frontiers in Immunology

Received: *22 December 2021*
Accepted: *10 January 2022*
Published: *27 January 2022*

Citation:
Rangel R, Pickering CR, Sikora AG and Spiotto MT (2022) Genetic Changes Driving Immunosuppressive Microenvironments in Oral Premalignancy. Front. Immunol. 13:840923. doi: 10.3389/fimmu.2022.840923

INTRODUCTION

Oral squamous cell carcinomas (OSCCs) involving the tongue, cheek, gums, and other sites of the mouth are the most common form of head and neck cancer (HNSCC), responsible for over 377,000 new cases and 177,000 deaths per year worldwide (1). Up to 50% of people developing OSCCs die from this disease. Even with cure, OSCCs are often treated with surgery, chemotherapy and radiation leading to substantial adverse impact on cosmesis, function, and quality of life.

The precursors to OSCC are oral premalignant lesions (OPLs) that affect approximately 4.5% of the world's population (2). Another commonly used term for these lesions is oral potentially malignant disorders (OPMD). Because we are focusing on the progression of these lesions to cancer in both human and mouse systems we will use the term OPL throughout this review. OPLs include a variety of distinct pathological entities including leukoplakia, submucous fibrosis, and lichen planus. OPL remains a diagnostic dilemma with limited preventative and therapeutic options. Even though the majority of OPLs regress, up to 30% of OPL ultimately progress through increasingly severe

grades of dysplasia to oral cancer. The overall annual risk of transformation of leukoplakia (the most common variety in the US) to invasive cancer is 1- 3% per year (3). Since OPLs often present with multifocal lesions across the oral mucosa, patients are subjected to frequent biopsies until a cancer is detected and is surgically removed. At present, diagnosis of OPL requires a physical biopsy in order to distinguish OPL from early OSCC. Consequently, clinicians have few if any noninvasive biomarkers to predict which OPL are at high risk of progression to invasive cancer (4). Furthermore, the only existing treatment for OPL is excision of the lesion with a margin of surrounding healthy tissue. Nevertheless, it is often not practical to remove the entire OPL because OPLs may encompass a large region of the oral cavity while still at variable risk for progressing to invasive disease. Consequently, the diagnostic and therapeutic dilemmas in treating OPLs provide impetus to better understand the biological and immunological underpinnings of this disease.

Representing an intermediate phase during the evolution of normal mucosa into malignant cancer, OPLs have acquired only a subset of the genomic alterations necessary to develop into OSCC. In addition to genomic changes occurring in OPL, OPLs frequently arise in an oral inflammatory environment caused by exogenous factors such tobacco and/or alcohol use, poor dentition and by endogenous factors including auto-immune diseases. It is likely that the genomic alterations cooperate and co-regulate the immune microenvironment in OPLs to facilitate the progression of OPLs to invasive cancer (1, 5). Namely, specific genomic changes may facilitate the transition to an immune microenvironment that permits malignant transformation. Conversely, inflammatory changes in the immune microenvironment may promote genomic instability within OPLs. Here, we will discuss the how OPLs develop an immunosuppressive microenvironment that facilitates progression to invasive cancer. We will then describe how genomic alterations and immune microenvironmental changes co-evolve and cooperate to promote OSCC progression. Finally, we will describe how the genomic context of premalignant lesions may provide specific and unique evolutionary vulnerabilities for targeted therapies. Pursuit of such paradigms may eventually translate into novel biomarker and/or therapeutic use.

THE EVOLUTION OF THE IMMUNOSUPPRESSIVE MICROENVIRONMENT IN OPL

As mutations and other genetic alterations accumulate, OPL become progressively infiltrated with immune suppressive myeloid cells including MDSC, M2 tumor-associated macrophages (TAM) and regulatory T cells (Treg; **Figure 1**). Furthermore, M2 macrophage polarization, Treg infiltration, and expression of the immune checkpoint ligand PD-L1 are associated with increased risk of future malignant transformation (6–9). Despite this progressive accumulation of immune suppressive features, OPL are often strongly infiltrated with $CD8^+$ T lymphocytes (10, 11), suggesting that reversing the immunosuppressive microenvironment of high-risk OPL has the potential to unmask anti-lesion immunity capable of inducing immune regression prior to development of invasive cancer. Here, we will describe the inflammatory and immune changes that occur during OPL progression as well as possible genetic mechanisms drive the cross-talk between the genomic and immune changes.

The transition from OPL to invasive cancer requires that dysplastic lesions escape recognition from infiltrating cytotoxic T lymphocytes (TILs). TILs are increased in OPLs and predict histological grade in dysplastic lesions (12–14). Comparing lichen planus with oral dysplastic lesions, Flores-Hidalgo et al. demonstrated that $CD8^+$ T cells tracked the malignant transformation zones in dysplastic lesions (15). Similarly, Gannot et al. demonstrated increased $CD4^+$, $CD8^+$ and $CD19^+/CD20^+$ lymphocyte infiltration in dysplastic lesions compared to normal epithelium indicating that dysplastic lesions are accompanied by increased cytotoxic and helper T

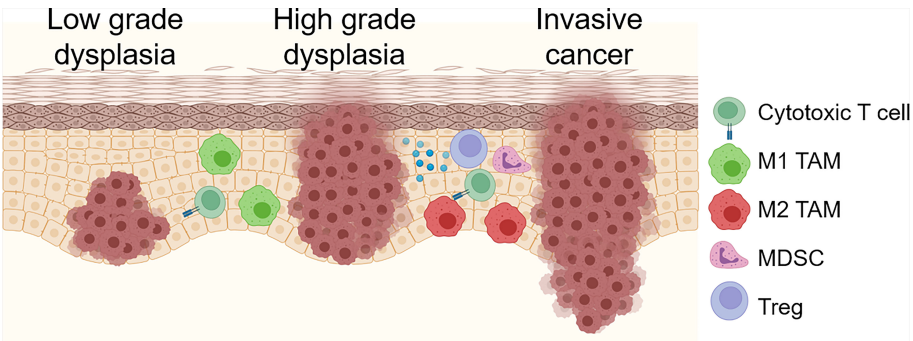

FIGURE 1 | Schema for immune/inflammatory microenvironment evolution during OPL progression. OPL are often strongly infiltrated with $CD8^+$ T cells. Early low grade dysplasias also demonstrate tumoricidal and/or M1 TAMs. As dysplastic lesions progress, increased immunosuppressive M2 TAM, Treg, MDSCs and immunosuppressive molecules including PD-1/PD-L1 and A2AR. Created with BioRender.com.

cells as well as B cells (16). Since these studies only quantified infiltrating lymphocytes, it remains unclear if these TILs are functional and target the dysplastic epithelial cells or more indicative of the general inflammatory microenvironment. However, other reports showed infiltrating plasms cells and other B lymphocytes decreased with high grades of dysplasia and less differentiated OSCCs (17). Similarly, in a 4-nitroquinoline 1-oxide (4-NQO) chemical carcinogenesis mouse model, lymphocytic infiltration was associated with dysplastic and invasive lesions (18).

The role of CD8+ T cell infiltrating OPLs remain unclear. Similar to invasive disease, it remains unclear what antigens these cytotoxic lymphocytes recognize. Over 40% of progressing OPLs expressed at least one of the shared MAGE cancer testis antigens (19). Similarly, common shared antigens such as NY-ESO-1 and MUC1 have been observed in murine OPL (20). Although on average OPL has 167,809 variants per sample, there did not appear to be any differences in mutational burdens between progressing and non-progressing premalignant lesions using a small series of 13 patients (21). Furthermore, the role of neo-antigens form by somatic mutations as targets for infiltrating lymphocytes in OPL remains understudied. Finally, some of these TILs may represent bystander T cells that do not recognize cognate antigens in OPL as seen in other cancers (22). Therefore, OPL does express tumor antigens but the specificities of the TILs remain understudied.

Given the increased lymphocytic infiltration observed in OPLs and OSCCs, immunosuppressive mechanisms are likely required to facilitate the progression of normal epithelium to dysplasia and invasive cancer. To this end, Zhao et al. demonstrated increased regulatory T cells (Tregs), as measured by $CD4^+CD25^+FoxP3^+$ markers, were sequentially increased in the lymph nodes and in the peripheral blood of rats with worsening grades of dysplasia and OSCC (23). Similarly, increased Tregs and decreased IFNγ signaling were observed in the development of oral leukoplakia, oral lichen planus and OSCCs (24). Immunosuppressive molecules may also prevent infiltrating lymphocytes from clearing pre-malignant lesions. A meta-analysis of 9 studies demonstrated that PD-L1 may be enriched in OPL as 48.25% of lesions expressed PD-L1 which was on average 1.65-fold greater than normal mucosa (25). PD-L1 expression in both epithelial cells and tumor associated macrophages (TAMs) was also correlated with malignant transformation (7). In a 4-NQO model of chemical carcinogenesis, Chen et al. observed a nearly 2-fold increase in PD-1 expression on infiltrating $CD8^+$ and $CD4^+$ T cells. PD-1 inhibition reduced MDSCs as well as downregulated PD-1 on TIL that was associated with a 2.27-fold increase in activated TIL (26). Finally, upregulation of the adenosine receptor (A2AR) also likely suppresses anti-tumor lymphocytes as A2AR expression correlated with pathological grade, lymph node status (27). Consequently, OPLs may recruit immunosuppressive Tregs and/or express immunosuppressive checkpoint molecules such as PD-L1 to evade potential rejection by cytotoxic lymphocytes.

Oral dysplastic lesions may also recruit immunosuppressive myeloid cells to evade immune recognition. In many types of solid tumors, TAMs and MDSCs correlated with poor prognosis and progression to invasive cancers (12, 16, 28–31). OPL progression has been associated with increased MDSC and TAM infiltration as well as the polarization of TAM from so-called M1 (tumor-suppressing) to M2 (tumor-promoting) phenotypes in murine models and human cancers. Both pro-tumorigenic M2 tumor associated macrophages (TAM) and myeloid-derived suppressor cells (MDSC) may be a key regulator for governing these pro-tumorigenic and anti-tumorigenic immune responses in OPL by suppressing adaptive T cell immunity and by producing inflammatory cytokines to promote tumor proliferation and angiogenesis (24). Abnormal proliferation of epithelial cells may promote TAM and myeloid cell infiltration. Kawsar et al. demonstrated that human beta-defensin 3 (hBD-3) but not hBD-1 or hBD-2 colocalized to proliferating basal cells in normal epithelium as well as in dysplastic lesions. Furthermore, the increased hBD-3 in dysplastic lesions increased macrophage recruitment in oral dysplastic lesions as well as increased macrophage chemotaxis *in vitro* (32). Consequently, epithelial proliferation that is intrinsic in OPL recruit immunosuppressive myeloid subsets.

Paradoxically, TAMs in OPLs have been shown to display both tumoricidal macrophages and tumorigenic functions. In 58 OPLs and 258 OSCCs, Wang et al. demonstrated that increase $CD163^+$ M2 TAMs were associated with OSCC progression and survival (33). Similarly, Kouketsu et al. found increasing numbers of M2 TAMs, using both the CD163 and CD204 markers for the M2 phenotype, and regulatory T cells with higher grades of OPL (8). Yagyuu et al. demonstrated that dermal M2 macrophages, identified by the CD163 marker, correlated with increased dysplasia (7). However, some groups indicate that TAMs may inhibit OPL regardless of M1 or M2 phenotype. Bouaoud et al. used immune cell deconvolution and enrichment algorithms for RNAseq as well as immunohistochemistry on OPL to observe that M2 macrophages were associated with dysplasia and OSCC even though 3 M2 TAM signatures were associated with better oral cancer-free survival (34). By contrast, Mori et al. demonstrated that the M2 canonical marker CD163 may identify TAMs with an inflammatory rather than immunosuppressive phenotype. $CD163^+$ TAMs in OPLs displayed increased STAT1 and CXCL9 expression suggesting an inflammatory tumoricidal phenotype (31). The authors stipulated that this M1 phenotype was likely driven by TH1 $CD4^+$ T cells producing IFN to drive this anti-tumorigenic phenotype (35). This contrasts with other reports demonstrating that $CD163^+$ TAMs in oral dysplasia expressing immune suppressive cytokines such as IL-10 (36). One possibility to rectify these observations is that the TAM phenotype transitions from a tumoricidal M1-like phenotype to a tumorigenic M2-like phenotype during OPL progression. In 201 OPL specimens, Weber et al. examined both M1 and M2 TAM phenotypes using the canonical markers CD68 and CD163, respectively (37). Increased TAM infiltration, TAM localization to the epithelial compartment and M2 polarization was associated with progression of OPL to invasive cancer. Therefore, TAM phenotypes may represent a dynamic state as OPLs progress to invasive lesions.

Several environmental and/or immune changes may dictate the dynamic changes in TAM phenotype during OPL progression. One potential mediator linking this immune switch during OPL progression is inducible nitric oxide synthase (iNOS), which recruits MDSCs and TAMs as well as polarizes TAMs to the pro-tumorigenic M2 subtype (38–40). iNOS has multiple pleiotropic and contradictory roles in promotion and suppression of cancer development. iNOS is a well-described driver of oncogenic signaling and immune evasion mechanisms in established cancers.

However, iNOS can also act as a mechanism of M1 macrophage anti-tumor activity, and when expressed in $CD4^+$ T cells can inhibit their differentiation to Treg (41) or Th17 cells (42). These contradictory roles for iNOS highlight the importance of assessing iNOS function in a cell type and context specific manner. iNOS expression and immune suppressive myeloid populations (M2 macrophages and MDSC) have both been shown to increase during progressive stages of dysplastic transformation and to be associated with future risk of transition to invasive cancer. iNOS can play different pro-tumor and anti-tumor roles depending on timing of expression and in which cell types. iNOS is known to be expressed by M1 (anti-tumor) TAM where it exerts a tumoricidal function through inducing tumor cytolysis. We have also shown that iNOS expression in myeloid cells acts paradoxically as a negative feedback mechanism to suppresses M1 macrophage polarization (43). However, iNOS (along with Arginase and PD-L1 expression) is a major immune suppressive mechanism of MDSC. We have also shown an important role for tumor-expressed iNOS in orchestrating the induction of tumor-infiltrating myeloid cells and acquisition of MDSC suppressive function in established cancer (39, 44). The apparent paradoxical pleiotropy and cell type specificity of iNOS expression and function highlights the importance of distinguishing between tumor- and myeloid cell-expressed iNOS functions.

In addition, linking environmental risk factors with TAM phenotypes in OPLs, Zhu et al. demonstrated that cigarette smoke extract increased M2 macrophage OPL infiltration and polarization, increased immunosuppressive cytokines including arginase-1 and IL-10 and decreased pro-inflammatory markers TNFα and iNOS (45). Furthermore, this group proposed that smoking activated glutamine transport and metabolism in TAM to promote epithelial proliferation and inhibit apoptosis.

Myeloid derived suppressor cells (MDSCs) which have been shown inhibit anti-tumor immunity also correlate with OPL progression. Both $CD33^+$ tumor infiltrating and circulating MDSC are increased in oral leukoplakia patients with increasingly severe dysplasia (9, 46). In a chemical carcinogenesis model of OPL, P. gingivalis colonization, common in oral cancer patients, further increased MDSC accumulation which was associated with increases in the chemokines CXCL2 and CCL2 as well as the cytokines IL-6 and IL-8 (47). Treating aged mice with 4-NQO increased oral dysplasia that was associate with increased MDSCs and Tregs in tongue lesions that was in part dependent on dectin-1, a surface pattern receptor involved in fungal immunity (48). Although Wen et al. suggested that granulocytic MDSCs mediated local immune suppression, the direct lineage of these MDSCs remains unclear. Therefore, MDSCs represent another immunosuppressive mechanism to facilitate the progression of OPLs.

Other myeloid and/or granulocytic cell types may have lesser appreciated roles for OPL progression. The inflammatory microenvironment evoked by neutrophils may facilitate OPL progression. Elevated neutrophil-to-lymphocyte ratios have been associated with poor survival in multiple head and neck cancer subsites including OSCC conferring a 1.56-fold worse survival (49). Furthermore, OSCCs displayed significantly elevated neutrophil infiltration and TNFα in patients' saliva (50). Chadwick et al. demonstrated that TNFα was necessary for OPL formation and progression in a 4-NQO model of oral carcinogenesis (50). OPLs displayed increased neutrophil infiltration that was lost with TNFα blockade. Furthermore, eosinophils infiltration was elevated in OSCC compared to dysplastic lesions suggesting that eosinophils may be necessary for malignant transformation (51). Similarly, both mast cells and eosinophil infiltration were increasingly elevated during the progression from normal epithelium to dysplasia to invasive cancer (52–55). Currently, it remains unclear how other granulocytic cells alter the tumor microenvironment to facilitate the development pre neoplastic lesions and their transition to invasive cancer. Hydroxy radical species produced by granulocytes and myeloid cells has been shown to cause DNA damage *in vitro*, which may enhance the number of genomic lesions necessary for OPLs to become cancer (56). Furthermore, neutrophils and/or other granulocytic cells can induce immune suppression in various cancers (57, 58). Therefore, the myeloid and granulocytic cell populations may contribute to OPL progression by both promoting the genetic changes necessary for malignant transformation as well as directly suppressing cytotoxic T cells that would otherwise clear abnormal cells.

REGULATION OF THE IMMUNE MICROENVIRONMENT BY GENOMIC CHANGES IN OPLs

OSCC progression model describes the step-wise evolution of normal epithelium to hyperplasia to dysplasia to cancer (**Figure 2**). Large scale profiling has identified the most common genomic alterations that occur in OSCC (59), but modern genomic tools have not been used to understand the detailed evolution of those alterations during OPL progression. Early studies in OPL lesions examined loss of heterozygosity (LOH) at 10 microsatellite markers by PCR analysis and identified 9p (CDKN2A), 3p, and 17p (TP53) loss as the earliest events and 11q, 13q (RB1), 14q loss and others as relatively later events (**Figure 2**) (60). This general order of events was also identified in recent whole genome sequencing analyses of bulk HNSCC tumor samples that mapped the evolutionary history of the tumors (5). These studies identified many of the most common genomic alterations in OSCC (TP53 mutant, CDKN2A mutant/LOH, NOTCH1 mutant) as early events that can be detected in OPL.

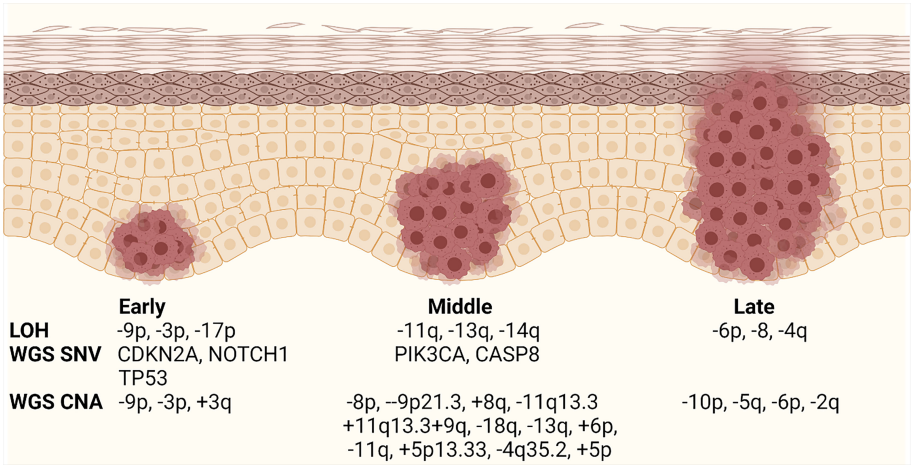

FIGURE 2 | Current OPL progression model. Schematic diagram showing the relative timing of genomic events during OPL progression. The stages are labeled early, middle, and late because the data are not well associated with specific histology. LOH, loss of hetorozygosity; WGS, whole genome sequencing; SNV, single nucleotide variant; CNA, copy number alteration. Modified from Califano and Gerstung. Created with BioRender.com.

Early studies of the genomic landscape of HNSCC led by our group and others and confirmed by The Cancer Genome Atlas (TCGA), demonstrated that mutations and deletions of the *TP53* and *CDKN2A* are the tumor suppressor genes most frequently altered somatically in HNSCC, as *TP53* and *CDKN2A* alterations are seen in up to 85% and 58% respectively of non-human papilloma virus associated (HPV negative) HNSCC (61–63). This highlights the importance of *TP53* and *CDKN2A* alterations are the most frequent genetic events occurring in the early stage of HNSCC development (63).

Another important concept to understand regarding to the early genomic alterations in OPL is field cancerization (64). Field cancerization is where genomic alterations are present throughout regions of histologically normal epithelium. These abnormal epithelial cells may not be macroscopically visible and only detectable under a microscope. In these cases, HNSCC may appear to occur *de novo*. Alternatively, patches of abnormal epithelium, which can occur in individuals with OPL lesions such as leukoplakia or erythroplakia, with macroscopically detectable lesions. The concept of field cancerization also helps describe the multicentric nature of HNSCC that either frequently recur after complete excision or new primaries that arise along the respiratory tract epithelium. may occur over time. as abnormal epithelial cells may not be.

LOH and TP53 mutations have been detected in histologically normal oral epithelium and demonstrate that field cancerization can occur with OPL and OSCC. NOTCH1 mutations are frequently detected in histologically normal sun exposed skin epithelium. Because of the similarities between cutaneous SCC mutation profiles and the biology of squamous epithelium, it is likely NOTCH1 mutations will also be detected in tobacco exposed oral epithelium. The sum total of these mutations is to drive abnormal cellular proliferation and invasion by disarming the self-destruct signals that are activated by uncontrolled proliferation. Unfortunately, there are still many gaps in our knowledge about how these genomic alterations drive OPL progression.

Transcriptomic analysis demonstrated the possibility to select for gene expression profiles of OPL more prone to malignant transformation. Saintigny et al. used gene expression microarrays to identify a 29 gene signature that predicted the progression of OPL to invasive cancer. However, many of these genes were not canonical drivers of carcinogenesis suggesting that this gene signature reflected changes of genes expression that did not likely cause malignant transformation. Sathasivam et al. used a 42 targeted gene Nanostring panel to identify an 11 gene expression signature associated with malignant progression (65). Importantly, this signature employed genes commonly altered during HNSCC carcinogenesis including TP53, NOTCH1 and CDKN2A which increases the likelihood of this signature being robust across multiple cohorts. To this end, this signature was validated using an external OPL dataset with a Hazard Ratio of 2.3. Overall, transcriptomic changes likely reflect the malignant phenotypes that arise in OPLs during malignant progression.

The genetic changes occurring in OPL may also dictate immune microenvironmental changes that promote malignant progression. Using immune cell deconvolution of gene expression datasets from OPL, 2 different OPL subtypes were identified: (1) an immune subtype with increased T cell and immune cell infiltrate and (2) a classical subtype with LOH at 3p14, 17p13 and TP53. However, the progression to invasive cancer was not known in these subtypes (10). One study using multiplex immunofluorescence in 188 OPL patients found that OPL with high risk LOH displayed increase epithelial PD-L1 expression and increased TAM PD-L1 expression. Furthermore, PD-L1 expression was associated with increased cancer progression (66). Therefore, global genomic changes that drive OPL progression also likely dictate immunosuppressive

changes in the microenvironment that are necessary for malignant progression. In addition to chromosomal changes associated with the immune microenvironment, specific genes, which are commonly mutated in OSCCs, have been implicated in dictating immune changes in OPLs and invasive cancers. The major drivers of OSCC and their impact on the immune microenvironment are detailed below (**Figure 3**):

TP53

Studies have shown that *TP53* alterations result in biallelic loss of wild-type *TP53* function. These alterations can include mutations in one or both alleles, mutation of one allele and deletion of the other allele, mutation of one allele conferring a dominant-negative impact on the wild-type allele, or mutations which provide new functions to TP53, termed "gain-of-function" (GOF). The GOF properties impact cellular processes including proliferation, metabolism, invasion, metastasis, inflammation, drug resistance, and survival through transcription-dependent or -independent mechanisms (63, 67–74). Different studies have shown that *TP53* is frequently mutated in oral premalignant lesions and is associated with progression to invasive carcinoma (75–78). Premalignant epithelial cells expressing mutant TP53 increased the production and secretion of inflammatory mediators. Mutant p53 mice exposed to dextran sulfate sodium developed severe chronic inflammation and persistent tissue damage. These mice displayed a rapid onset of dysplastic lesions that progress to invasive carcinoma with an increased NFκB activation compared to wild-type mice, recapitulating features observed in human colitis-associated colorectal cancer (79). Furthermore, TP53 also mediated an immune escape mechanism for dysplastic lesions by recruiting tumor associated macrophages, which maintained the immunosuppressive state within the tumor microenvironment (80). In this model, GOF mutant TP53 correlated with increased iNOS, NF-κB activation leading the increased production of multiple cytokines including IL-6, CXCL5, TNF-α and CCL2. Mutant TP53 also directly interacts with NF-κB to modulate the diverse transcriptional regulators in response to chronic immune signaling (81). These biological mediators generated an inflammatory microenvironment that further increased cell survival of the transformed cells, as well as promoted angiogenesis and evasion of protective immune responses (82).

Other studies have demonstrated that loss of p53 and cooperation of KRAS in cancer cells can modulate the tumor-immune microenvironment to avoid immune destruction. Inactivation of p53 promotes the infiltration of suppressive myeloid CD11b+ cells and Tregs with an increased expression of CCR2-associated chemokines and macrophage colony-stimulating factor (M-CSF), leading to attenuated T cell responses (83). A recent study, demonstrates that TP53 missense mutations generates immune-excluded tumor microenvironments in pancreatic ductal adenocarcinoma (PDCA) mouse model, these findings correlate with clinical

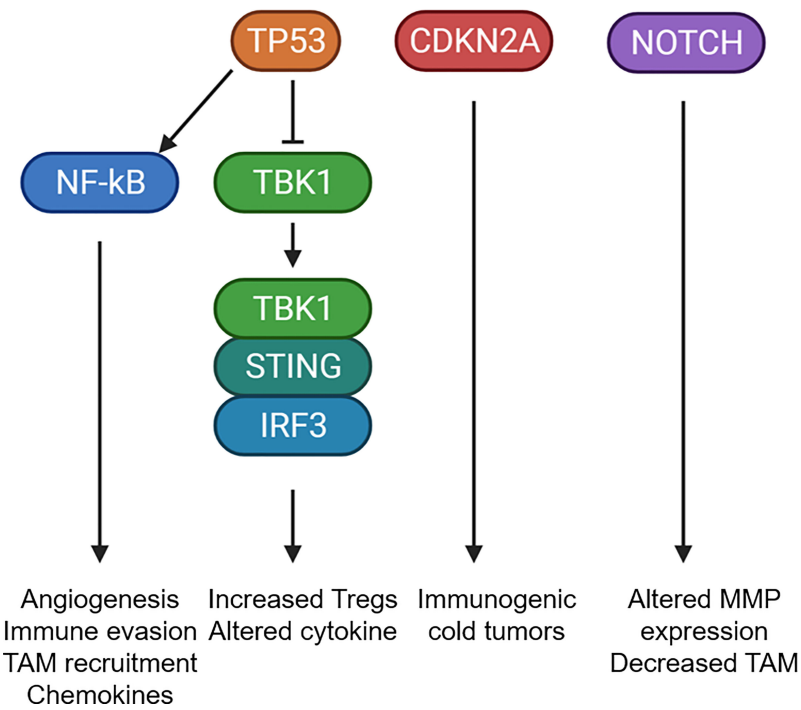

FIGURE 3 | Mutational changes that potentially alter the tumor microenvironment. Schematic diagram showing the common mutational changes in OPL can impact the immune microenvironment. TP53 mutants can activate NF-kB or inhibit the STING pathway to alter cytokine expression, increase TAM recruitment, increate Treg recruitment. CDKN2A mutants has been associated with immunogenic cold tumors through currently unknown mechanisms. NOTCH1 mutants was associated with altered MMP expression and decreased TAM infiltrations. Created with BioRender.com.

data in PDAC patients with a poor survival outcome (84). Since p53 plays an important role in modulating the tumor immune microenvironment, p53 mutations in OPLs suggest an important immunosuppressive role to evade immune rejection.

Recently, it has been reported that mutant p53 interferes with the cGAS-STING signaling pathway a cytoplasmic DNA sensing machinery that activates the innate immune response. Only mutant p53, binds to TANK-binding protein kinase 1 (TBK1) and prevents the protein complex between TBK1, STING, and IRF3, which is required for the transcriptional activation of IRF3. This innate immune signaling alteration by mutant p53 alters cytokine production, resulting in immune evasion (85). We have characterized the 4-Nitroquinoline 1-oxyde (4NQO) oral carcinogenesis in C57BL/6 mouse model to study the role of mutant p53 in the alteration of immune infiltrates at different stages of oral cancer. This carcinogenesis model exhibits similar histological, molecular and chromosomal alterations as observed in human oral carcinogenesis (86, 87). We and others have recently reported that 4NQO induced oral lesions expressing mutant *Trp53*-R172H contain a higher infiltration of FoxP3+ T regulatory cells (Tregs) compared to *Trp53* wild-type mice (88, 89). It is known that Tregs are suppressors of antitumor responses that disrupt the maturation of dendritic cells (DC) and prevent the activation of $CD4^+$ effector and $CD8^+$ cytotoxic cells in the tumor microenvironment (90). This strongly indicates that the oncogenic activity of Trp53 influence the environment to promote a higher infiltration of immune suppressor cells not only at early stages but also are detected in invasive carcinoma. Furthermore, we detected that the protein levels of STING were significantly lower in OPLs expressing mutant Trp53-R172H compared with wild-type Trp53. In addition, we observed a significant reduction of infiltrated DC cells in OPLs expressing mutant p53 (88). While infiltrating immune cells retain wild-type p53 and have normal STING, mutant p53 OPLs have decreased immune cell infiltration and may not compensate for reduced STING expression in lesions with mutant TP53. Thus, OPLs with an altered cGAS-STING signaling will prevent the secretion of type I interferons (IFN), which are induced early during tumor development (91, 92). IFNs activate dendritic cells (DCs) and promote induction of adaptive $CD4^+$ and $CD8^+$ T-cell antitumor immune responses (93).

These studies indicate that early genomic alterations in the *Trp53* gene of oral epithelial cells promote immunosuppressive pathways that disrupt antitumor immunity mechanisms, preventing the activation of innate and adaptive immune response and leading to high-grade lesions promoting oral neoplastic progression.

CDKN2A

CDKN2A controls the cell cycle by inhibiting the ability of cyclin D-CDK 4/6 to phosphorylate the retinoblastoma protein (pRb) (94). pRb phosphorylation by the cyclin-CDK 4/6 leads to the dissociation of the pRb/E2F complex and progression of the cell into S phase (95, 96). The release of E2F activates CDKN2A transcription, as CDKN2A levels increase, its binding to CDK4 and CDK6 increases, inhibiting the kinase activity of cyclin D-CDK 4/6 (97). CDKN2A has been classified as a tumor suppressor, methylation studies have detected promoter hypermethylation of *CDKN2A* in oral and oropharyngeal cancer tissue as well in OPL; therefore *CDKN2A* inactivation is in part due to promoter methylation (98–102). Recently, The Cancer Genome Atlas (TCGA) data shows that 57% of HPV-negative HNSCC contains a mutation or loss of the CDKN2A gene (59), this demonstrates that additional genomic alterations on CDKN2A others than methylation are involved at early events of oral cancer development.

Other studies indicate that loss of *CDKN2A* significantly correlates with immune deserts, defined by a profile of 394 immune transcripts (103). These pieces of evidence suggest that low *CDKN2A* expression both impacts the number and the activity of the intratumoral immune cells. Additionally, some tumors lose *CDKN2A* expression as a result of the deletion of chromosome 9p21 locus. Interestingly, the deletion of adjacent genes including the α and β interferon cluster have been linked with decreased infiltration of immune cells and decreased cGAS-STING signaling in melanoma (104, 105). Recently, immunogenic analysis of clinical specimens from TCGA study and immune checkpoint trials across various cancer types and demonstrates 9p21 loss as a ubiquitous genomic correlate of the "cold" tumor-immune phenotype and primary resistance to immune checkpoint therapy (106, 107). Recently, *Cdkn2a* null mice exposed with 4NQO developed faster and more pronounced oral lesions compared to control mice; and proliferation of tumor cells with *Cdkn2a* gene deletion was associated with the progression of OSCC in mice (108). More studies are necessary in this mouse models to confirm the role of Cdkn2a in the immune surveillance mechanism of OPLs.

Yet, little is known about the interplay of mutant *p53* and inactivation *Cdkn2a* genes in the immune evasion mechanism in OPLs that evolves into tumor progression and invasion. An interesting study involving double mutant mice revealed that a combined *p53* gain of function and *Cdkn2a* inactivation generates a more aggressive skin cancer phenotype with a shorter survival and was associated to metastasis compared to single mutant mice (109). Furthermore, Cdkn2a suppresses the oncogenic activity of mutant p53 that promotes malignant progression in squamous cell carcinoma. In the same study, they analyzed HNSCC HPV-negative patients with co-occurring gain of function p53 mutations and CDKN2A homozygous deletions. Here, the survival of patients was much shorter than that of patients with tumors in which p53 mutations did not contain CDKN2A homozygous deletions, or that of patients with tumors in which homozygous CDKN2A deletions co-existed with loss-of-function mutations in p53 (109). We speculate that co-occurrence of the genomic alterations in *TP53* and *CDKN2A* in OPLs might have a worst outcome and higher probability to develop into invasive carcinoma.

NOTCH

Another potential mutation that also alters the tumor microenvironment is loss or mutation of the NOTCH1 oncogene, which is mutated in 19% of head and neck cancers and regulates macrophage recruitment and M1/M2 macrophage polarization (59). Copy number alterations in NOTCH1 have

been observed during the transition of premalignant lesions to invasive disease (110). Notch1 loss induces the expression of matrix metalloproteinases, cytokines and chemokines to alter the tumor microenvironment (111). In multiple cancers, Notch family member expression was associated increased infiltration of $CD4^+$ T cells, macrophages, neutrophils and dendritic cells (112, 113). Similarly, we have observed that NOTCH1 loss in an autochthonous model of oral pre-malignant lesions alters the cytokines/chemokines driving immune cell infiltrate and correlates with loss of TAM infiltration. By contrast, Notch signaling in immune cells also dictates the extent of tumorigenic versus tumoricidal immune responses. Notch1 signaling promotes M1 TAM differentiation and inhibits MDSCs indicating that Notch1 signaling in immune cells promotes anti-tumor immunity in cancers (114–116). Consequently, global impact of NOTCH activity in OPLs is likely a competition between epithelial expression of NOTCH1 to regulate immune cell trafficking as well as myeloid NOTCH activity which determines TAM, MDSC and other immune cell phenotypes.

REVERSING IMMUNOSUPPRESSION IN OPL

While experimental studies have identified pharmacologic or molecular targeted therapies capable of reducing risk of OPL progression to cancer, there are no preventive therapeutics in routine use. Consequently, there remains an unmet need to better understand the biological and immunological features that can differentiate pre-invasive disease from invasive cancer which can also be exploited to prevent progression to malignancy.

Targeting immunosuppressive molecules may serve as an effective strategy to treat oral dysplasia and prevent malignant progression. Treatment with PD-1 blockade decreased the incidence of dysplastic lesions and invasive OSCC in a carcinogen induced 4-NOQ OPLs model (88). The Heymach group further compared several different checkpoint inhibitors including CD40, PD-1, CTLA04 and OX40, on OPL progression during oral carcinogenesis. Of these inhibitors, CD40 treatment caused the greatest reduction in OPL and OSCC tumor incidence which was associated with increased memory $CD8^+$ T cells and M1 macrophage infiltration (117). Furthermore, inhibition of the adenosine receptor, A2AR, inhibited tumor growth, reduced Treg populations and increased $CD8^+$ T cell infiltration in oral carcinogenesis models (27). Similarly, carotenoid or tocopherol-based treatment was associate with increased in cytotoxic lymphocytes and TAM in murine OPLs (118, 119). Activation of the IFN pathway *via* STING has also shown to inhibit the growth of HNSCC tumor models; however, expression of the STING pathway is not altered in oral dysplasia or pre-malignant lesions (120). Therefore, in pre-clinical models, checkpoint blockade, inhibition of the adenosine receptor and/or activation of the STING pathway reduced OPL incidence.

However, risk of systemic immunotherapies patients may outweigh the benefits in OPL patients that are healthy and may not develop invasive disease. One alternative to this treatment dilemma is local and controlled immunotherapy delivery to prevent oral cancer development. An ideal drug carrier should have satisfactory biocompatibility, biodegradability and controlled drug release at specific oral cavity sites. Furthermore, selecting the correct preclinical model is critical, as is designing delivery technologies that can feasibly be translated to patients. Identification of soluble inflammatory mediators produced by oral epithelial cells undergoing malignant progression which alter myeloid differentiation and/or trafficking can lead to new potential targets for therapeutic interventions.

Lately, multidomain peptide biomaterials have been developed and consist of self-assembled peptides that mimic the extracellular matrix by generating a nanofibrous network to create a hydrogel. The hydrogel can encapsulate drugs, cytokines, and growth factors and control their sustained release to permit a sustained payload release in oral cancer models (121, 122) A recent study by Shi et al. used the hydrogels loaded with PD1 immune checkpoint inhibitor to treat OPLs in p53 mutant and wild-type mice. Mice were expose to the 4NQO carcinogen, a model of carcinogenesis that represents all stages of human oral cancer. Next, hydrogels were implanted in three histological regions of the tongue to increase the ICI biodistribution. Interestingly, OPLs frequency was significantly reduced in p53 wild type mice, however high-risk OPLs were higher in mutant p53 mice (88). This study not only showed the capacity of the hydrogels to control the release of PD-1 antibody and reduce OPL frequency, but also provided evidence of the role of mutant p53 in the mechanism of immunosuppression in OPLs. Other immunoprevention studies using p53 mutant mice have showed similar results but required 8 doses of parental immunotherapy administration (89, 123), compared to a single hydrogel-PD1 dose (88). A recent comprehensive study of patient samples of leukoplakia identified that proliferative leukoplakia predicts a high rate of malignant transformation within 5 years of diagnosis. Interestingly, $CD8^+$ T cell and Treg signatures with PD-L1 overexpression provides a justified approach to use anti-PD1 as immunoprevention approach in oral leukoplakia (124). Since these hydrogels are topically applied similar to TLR agonists used in melanoma, this platform provides an approach to incorporate additional immune agonists alone or to be used to increase the efficacy of checkpoint blockade. Therefore, our studies in selecting the precise preclinical mouse model was critical, and the use of hydrogel loaded with immunotherapeutic antibodies are feasible for translation immunoprevention studies.

Currently, there are only a few ongoing clinical trials studying checkpoint blockade in OPL. All of the studies use agents targeting the PD-1/PD-L1 axis including nivolumab (NCT03692325), sintilimab (NCT04065737) and avelumab (NCT04504552). Of note, these trials use both clinical and/or molecular criteria to select for patients at higher risk for progression. In these trials, clinical features such as multifocality, higher grade and/or size and/or genomic features such as LOH at 3p14 and/or 9p21 are included. Currently, these trials will add value to the role of systemic checkpoint blockade

in OPL and the mechanisms for immune escape. Furthermore, there is a need to address additional immunotherapeutics that alter macrophage and/or Treg function. These studies may discover new agents for a disease with in limited therapeutic options (125).

DISCUSSION

OPL acquire mutations that drive the transformation of normal epithelium to invasive OSCCs, a disease to which patients frequently succumb. These mutations likely alter the immune microenvironment to suppress TILs that would otherwise potentially clear pre-malignant and malignant cells. Mutations in classical HNSCC drivers including TP53, CDKN2A and NOTCH1 have been associated with an altered an immunosuppressive tumor microenvironment. These mutations likely induce Treg and MDSC infiltration as well as the phenotypic switch of M1 TAMs to M2 TAM to suppress cytotoxic T lymphocytes. Modulation of these immunosuppressive signals using checkpoint inhibitors, targeting TAM phagocytosis with CD47 inhibitors and/or altering inflammatory pathways involving adenosine or STING may promote a tumoricidal microenvironment to activate cytotoxic lymphocytes that clear the malignant cells.

AUTHOR CONTRIBUTIONS

All authors contributed to the conception, design, writing and editing of this manuscript. All authors contributed to the article and approved the submitted version.

FUNDING

NIH/NIDCR R01DE027445-01 (MS); NIH/NIDCR/NCI U01DE028233 (AS).

REFERENCES

1. Warnakulasuriya S, Kujan O, Aguirre-Urizar JM, Bagan JV, Gonzalez-Moles MA, Kerr AR, et al. Oral Potentially Malignant Disorders: A Consensus Report From an International Seminar on Nomenclature and Classification, Convened by the WHO Collaborating Centre for Oral Cancer. *Oral Dis* (2021) 27:1862–80. doi: 10.1111/odi.13704
2. Iocca O, Sollecito TP, Alawi F, Weinstein GS, Newman JG, De Virgilio A, et al. Potentially Malignant Disorders of the Oral Cavity and Oral Dysplasia: A Systematic Review and Meta-Analysis of Malignant Transformation Rate by Subtype. *Head Neck* (2020) 42:539–55. doi: 10.1002/hed.26006
3. Petti S. Pooled Estimate of World Leukoplakia Prevalence: A Systematic Review. *Oral Oncol* (2003) 39:770–80. doi: 10.1016/S1368-8375(03)00102-7
4. Monteiro L, Mello FW, Warnakulasuriya S. Tissue Biomarkers for Predicting the Risk of Oral Cancer in Patients Diagnosed With Oral Leukoplakia: A Systematic Review. *Oral Dis* (2021) 27:1977–92. doi: 10.1111/odi.13747
5. Califano J, Westra WH, Meininger G, Corio R, Koch WM, Sidransky D. Genetic Progression and Clonal Relationship of Recurrent Premalignant Head and Neck Lesions. *Clin Cancer Res* (2000) 6:347–52.
6. Silverman S Jr, Gorsky M, Lozada F. Oral Leukoplakia and Malignant Transformation. A Follow-Up Study of 257 Patients. *Cancer* (1984) 53:563–8. doi: 10.1002/1097-0142(19840201)53:3<563::AID-CNCR2820530332>3.0.CO;2-F
7. Yagyuu T, Hatakeyama K, Imada M, Kurihara M, Matsusue Y, Yamamoto K, et al. Programmed Death Ligand 1 (PD-L1) Expression and Tumor Microenvironment: Implications for Patients With Oral Precancerous Lesions. *Oral Oncol* (2017) 68:36–43. doi: 10.1016/j.oraloncology.2017.03.006
8. Kouketsu A, Sato I, Oikawa M, Shimizu Y, Saito H, Tashiro K, et al. Regulatory T Cells and M2-Polarized Tumour-Associated Macrophages are Associated With the Oncogenesis and Progression of Oral Squamous Cell Carcinoma. *Int J Oral Maxillofac Surg* (2019) 48:1279–88. doi: 10.1016/j.ijom.2019.04.004
9. Pang X, Fan HY, Tang YL, Wang SS, Cao MX, Wang HF, et al. Myeloid Derived Suppressor Cells Contribute to the Malignant Progression of Oral Squamous Cell Carcinoma. *PloS One* (2020) 15:e0229089. doi: 10.1371/journal.pone.0229089
10. Foy JP, Bertolus C, Ortiz-Cuaran S, Albaret MA, Williams WN, Lang W, et al. Immunological and Classical Subtypes of Oral Premalignant Lesions. *Oncoimmunology* (2018) 7:e1496880. doi: 10.1080/2162402X.2018.1496880
11. Chen XJ, Tan YQ, Zhang N, He MJ, Zhou G. Expression of Programmed Cell Death-Ligand 1 in Oral Squamous Cell Carcinoma and Oral Leukoplakia is Associated With Disease Progress and CD8+ Tumor-Infiltrating Lymphocytes. *Pathol Res Pract* (2019) 215:152418. doi: 10.1016/j.prp.2019.04.010
12. Migliorati CA, Migliorati EK, Silverman S Jr, Greenspan D, Greenspan JS. Phenotypic Identification of Mononuclear Cells in Oral Premalignant Lesions and Cancer by Monoclonal Antibodies. *J Oral Pathol* (1986) 15:352–8. doi: 10.1111/j.1600-0714.1986.tb00639.x
13. Gannot G, Buchner A, Keisari Y. Interaction Between the Immune System and Tongue Squamous Cell Carcinoma Induced by 4-Nitroquinoline N-Oxide in Mice. *Oral Oncol* (2004) 40:287–97. doi: 10.1016/j.oraloncology.2003.08.008
14. Kujan O, Agag M, Smaga M, Vaishnaw Y, Idrees M, Shearston K, et al. PD-1/PD-L1, Treg-Related Proteins, and Tumour-Infiltrating Lymphocytes are Associated With the Development of Oral Squamous Cell Carcinoma. *Pathology* (2021) S0031-3025(21)00523-7. doi: 10.1016/j.pathol.2021.09.013
15. Flores-Hidalgo A, Murrah V, Fedoriw Y, Padilla RJ. Relationship of Infiltrating Intraepithelial T Lymphocytes in the Diagnosis of Oral Lichen Planus Versus Oral Epithelial Dysplasia: A Pilot Study. *Oral Surg Oral Med Oral Pathol Oral Radiol* (2019) 127:e123–35. doi: 10.1016/j.oooo.2019.02.004
16. Gannot G, Gannot I, Vered H, Buchner A, Keisari Y. Increase in Immune Cell Infiltration With Progression of Oral Epithelium From Hyperkeratosis to Dysplasia and Carcinoma. *Br J Cancer* (2002) 86:1444–8. doi: 10.1038/sj.bjc.6600282
17. Loning T, Burkhardt A. Plasma Cells and Immunoglobulin-Synthesis in Oral Precancer and Cancer. Correlation With Dysplasia, Cancer Differentiation, Radio- and Chemotherapy. *Virchows Arch A Pathol Anat Histol* (1979) 384:109–20. doi: 10.1007/BF00427156
18. Tan MT, Wu JG, Callejas-Valera JL, Schwarz RA, Gillenwater AM, Richards-Kortum RR, et al. A PIK3CA Transgenic Mouse Model With Chemical Carcinogen Exposure Mimics Human Oral Tongue Tumorigenesis. *Int J Exp Pathol* (2020) 101:45–54. doi: 10.1111/iep.12347
19. Ries J, Agaimy A, Vairaktaris E, Kwon Y, Neukam FW, Strassburg LH, et al. Evaluation of MAGE-A Expression and Grade of Dysplasia for Predicting Malignant Progression of Oral Leukoplakia. *Int J Oncol* (2012) 41:1085–93. doi: 10.3892/ijo.2012.1532
20. Young MR, Neville BW, Chi AC, Lathers DM, Boyd Gillespie M, Day TA. Oral Premalignant Lesions Induce Immune Reactivity to Both Premalignant Oral Lesions and Head and Neck Squamous Cell Carcinoma. *Cancer Immunol Immunother* (2007) 56:1077–86. doi: 10.1007/s00262-006-0242-7
21. Farah CS, Jessri M, Bennett NC, Dalley AJ, Shearston KD, Fox SA. Exome Sequencing of Oral Leukoplakia and Oral Squamous Cell Carcinoma Implicates DNA Damage Repair Gene Defects in Malignant

Transformation. *Oral Oncol* (2019) 96:42–50. doi: 10.1016/j.oraloncology.2019.07.005
22. Simoni Y, Becht E, Fehlings M, Loh CY, Koo SL, Teng KWW, et al. Bystander CD8(+) T Cells are Abundant and Phenotypically Distinct in Human Tumour Infiltrates. *Nature* (2018) 557:575–9. doi: 10.1038/s41586-018-0130-2
23. Zhao J, Wang Z, Han J, Qiu X, Pan J, Chen J. Increased Frequency of CD4+ CD25+ FOXP3+ Cells Correlates With the Progression of 4-Nitroquinoline1-Oxide-Induced Rat Tongue Carcinogenesis. *Clin Oral Investig* (2014) 18:1725–30. doi: 10.1007/s00784-013-1146-5
24. Sun Y, Liu N, Guan X, Wu H, Sun Z, Zeng H. Immunosuppression Induced by Chronic Inflammation and the Progression to Oral Squamous Cell Carcinoma. *Mediators Inflammation* (2016) 2016:5715719. doi: 10.1155/2016/5715719
25. Girolami I, Pantanowitz L, Munari E, Martini M, Nocini R, Bisi N, et al. Prevalence of PD-L1 Expression in Head and Neck Squamous Precancerous Lesions: A Systematic Review and Meta-Analysis. *Head Neck* (2020) 42:3018–30. doi: 10.1002/hed.26339
26. Chen Y, Li Q, Li X, Ma D, Fang J, Luo L, et al. Blockade of PD-1 Effectively Inhibits In Vivo Malignant Transformation of Oral Mucosa. *Oncoimmunology* (2018) 7:e1388484. doi: 10.1080/2162402X.2017.1388484
27. Ma SR, Deng WW, Liu JF, Mao L, Yu GT, Bu LL, et al. Blockade of Adenosine A2A Receptor Enhances CD8(+) T Cells Response and Decreases Regulatory T Cells in Head and Neck Squamous Cell Carcinoma. *Mol Cancer* (2017) 16:99. doi: 10.1186/s12943-017-0665-0
28. Eskinazi DP, Perna JJ, Mihail R. Mononuclear Cell Subsets in Patients With Oral Cancer. *Cancer* (1987) 60:376–81. doi: 10.1002/1097-0142(19870801)60:3<376::AID-CNCR2820600315>3.0.CO;2-B
29. Bingle L, Brown NJ, Lewis CE. The Role of Tumour-Associated Macrophages in Tumour Progression: Implications for New Anticancer Therapies. *J Pathol* (2002) 196:254–65. doi: 10.1002/path.1027
30. Pollard JW. Tumour-Educated Macrophages Promote Tumour Progression and Metastasis. *Nat Rev Cancer* (2004) 4:71–8. doi: 10.1038/nrc1256
31. Mori K, Hiroi M, Shimada J, Ohmori Y. Infiltration of M2 Tumor-Associated Macrophages in Oral Squamous Cell Carcinoma Correlates With Tumor Malignancy. *Cancers (Basel)* (2011) 3:3726–39. doi: 10.3390/cancers3043726
32. Kawsar HI, Weinberg A, Hirsch SA, Venizelos A, Howell S, Jiang B, et al. Overexpression of Human Beta-Defensin-3 in Oral Dysplasia: Potential Role in Macrophage Trafficking. *Oral Oncol* (2009) 45:696–702. doi: 10.1016/j.oraloncology.2008.10.016
33. Wang S, Sun M, Gu C, Wang X, Chen D, Zhao E, et al. Expression of CD163, Interleukin-10, and Interferon-Gamma in Oral Squamous Cell Carcinoma: Mutual Relationships and Prognostic Implications. *Eur J Oral Sci* (2014) 122:202–9. doi: 10.1111/eos.12131
34. Bouaoud J, Foy JP, Tortereau A, Michon L, Lavergne V, Gadot N, et al. Early Changes in the Immune Microenvironment of Oral Potentially Malignant Disorders Reveal an Unexpected Association of M2 Macrophages With Oral Cancer Free Survival. *Oncoimmunology* (2021) 10:1944554. doi: 10.1080/2162402X.2021.1944554
35. Mori K, Haraguchi S, Hiori M, Shimada J, Ohmori Y. Tumor-Associated Macrophages in Oral Premalignant Lesions Coexpress CD163 and STAT1 in a Th1-Dominated Microenvironment. *BMC Cancer* (2015) 15:573. doi: 10.1186/s12885-015-1587-0
36. Shigeoka M, Koma YI, Nishio M, Komori T, Yokozaki H. CD163(+) Macrophages Infiltration Correlates With the Immunosuppressive Cytokine Interleukin 10 Expression in Tongue Leukoplakia. *Clin Exp Dent Res* (2019) 5:627–37. doi: 10.1002/cre2.228
37. Weber M, Wehrhan F, Baran C, Agaimy A, Buttner-Herold M, Ozturk H, et al. Malignant Transformation of Oral Leukoplakia is Associated With Macrophage Polarization. *J Transl Med* (2020) 18:11. doi: 10.1186/s12967-019-02191-0
38. Nagaraj S, Schrum AG, Cho HI, Celis E, Gabrilovich ,DI. Mechanism of T Cell Tolerance Induced by Myeloid-Derived Suppressor Cells. *J Immunol* (2010) 184:3106–16. doi: 10.4049/jimmunol.0902661
39. Jayaraman P, Parikh F, Lopez-Rivera E, Hailemichael Y, Clark A, Ma G, et al. Tumor-Expressed Inducible Nitric Oxide Synthase Controls Induction of Functional Myeloid-Derived Suppressor Cells Through Modulation of Vascular Endothelial Growth Factor Release. *J Immunol* (2012) 188:5365–76. doi: 10.4049/jimmunol.1103553
40. Grimm EA, Sikora AG, Ekmekcioglu S. Molecular Pathways: Inflammation-Associated Nitric-Oxide Production as a Cancer-Supporting Redox Mechanism and a Potential Therapeutic Target. *Clin Cancer Res* (2013) 19:5557–63. doi: 10.1158/1078-0432.CCR-12-1554
41. Jayaraman P, Alfarano MG, Svider PF, Parikh F, Lu G, Kidwai S, et al. iNOS Expression in CD4+ T Cells Limits Treg Induction by Repressing TGFbeta1: Combined iNOS Inhibition and Treg Depletion Unmask Endogenous Antitumor Immunity. *Clin Cancer Res* (2014) 20:6439–51. doi: 10.1158/1078-0432.CCR-13-3409
42. Jianjun Y, Zhang R, Lu G, Shen Y, Peng L, Zhu C, et al. T Cell-Derived Inducible Nitric Oxide Synthase Switches Off Th17 Cell Differentiation. *J Exp Med* (2013) 210:1447–62. doi: 10.1084/jem.20122494
43. Lu G, Zhang R, Geng S, Peng L, Jayaraman P, Chen C, et al. Myeloid Cell-Derived Inducible Nitric Oxide Synthase Suppresses M1 Macrophage Polarization. *Nat Commun* (2015) 6:6676. doi: 10.1038/ncomms7676
44. Varghese SS, Sunil PM, Madhavan RN. Expression of Inducible Nitric Oxide Synthase (iNOS) in Oral Precancer and Oral Squamous Cell Carcinoma: An Immunohistochemical Study. *Cancer biomark* (2010) 8:155–60. doi: 10.3233/CBM-2011-0207
45. Zhu Y, Zhang S, Sun J, Wang T, Liu Q, Wu G, et al. Cigarette Smoke Promotes Oral Leukoplakia via Regulating Glutamine Metabolism and M2 Polarization of Macrophage. *Int J Oral Sci* (2021) 13:25. doi: 10.1038/s41368-021-00128-2
46. Chen WC, Lai CH, Chuang HC, Lin PY, Chen MF. Inflammation-Induced Myeloid-Derived Suppressor Cells Associated With Squamous Cell Carcinoma of the Head and Neck. *Head Neck* (2017) 39:347–55. doi: 10.1002/hed.24595
47. Wen L, Mu W, Lu H, Wang X, Fang J, Jia Y, et al. Porphyromonas Gingivalis Promotes Oral Squamous Cell Carcinoma Progression in an Immune Microenvironment. *J Dent Res* (2020) 99:666–75. doi: 10.1177/0022034520909312
48. Bhaskaran N, Jayaraman S, Quigley C, Mamileti P, Ghannoum M, Weinberg A, et al. The Role of Dectin-1 Signaling in Altering Tumor Immune Microenvironment in the Context of Aging. *Front Oncol* (2021) 11:669066. doi: 10.3389/fonc.2021.669066
49. Mascarella MA, Mannard E, Silva SD, Zeitouni A. Neutrophil-To-Lymphocyte Ratio in Head and Neck Cancer Prognosis: A Systematic Review and Meta-Analysis. *Head Neck* (2018) 40:1091–100. doi: 10.1002/hed.25075
50. Goertzen C, Mahdi H, Laliberte C, Meirson T, Eymael D, Gil-Henn H, et al. Oral Inflammation Promotes Oral Squamous Cell Carcinoma Invasion. *Oncotarget* (2018) 9:29047–63. doi: 10.18632/oncotarget.25540
51. Deepthi G, Kulkarni PG, Sr KN. Eosinophils: An Imperative Histopathological Prognostic Indicator for Oral Squamous Cell Carcinoma. *J Oral Maxillofac Pathol* (2019) 23:307. doi: 10.4103/jomfp.JOMFP_111_19
52. Flynn EA, Schwartz JL, Shklar G. Sequential Mast Cell Infiltration and Degranulation During Experimental Carcinogenesis. *J Cancer Res Clin Oncol* (1991) 117:115–22. doi: 10.1007/BF01613134
53. Madhura MG, Gajalakshmi S, Kumar BV, Suma S, Sarita Y, Shweta RD. Role of Tissue Eosinophils in Oral Leukoplakia: A Pilot Study. *J Oral Maxillofac Pathol* (2015) 19:286–90. doi: 10.4103/0973-029X.174647
54. Saxena S, Singh A, Singh P, Sundaragiri KS, Sankhla B, Bhargava A. Evaluating the Role of Immunological Cells (Tissue Eosinophils and Mast Cells) in Progression of Oral Squamous Cell Carcinoma. *Mymensingh Med J* (2018) 27:382–8.
55. Pereira NDS, Pinheiro TN. Histomorphometric Comparative Analysis Between Oral Dysplastic Potentially Malignant Disorders and Oral Squamous Cell Carcinoma. *Eur J Dent* (2019) 13:1–4. doi: 10.1055/s-0039-1688734
56. Shen Z, Wu W, Hazen SL. Activated Leukocytes Oxidatively Damage DNA, RNA, and the Nucleotide Pool Through Halide-Dependent Formation of Hydroxyl Radical. *Biochemistry* (2000) 39:5474–82. doi: 10.1021/bi992809y
57. Cheng Y, Li H, Deng Y, Tai Y, Zeng K, Zhang Y, et al. Cancer-Associated Fibroblasts Induce PDL1+ Neutrophils Through the IL6-STAT3 Pathway

That Foster Immune Suppression in Hepatocellular Carcinoma. *Cell Death Dis* (2018) 9:422. doi: 10.1038/s41419-018-0458-4
58. Gomez-Aleza C, Nguyen B, Yoldi G, Ciscar M, Barranco A, Hernandez-Jimenez E, et al. Inhibition of RANK Signaling in Breast Cancer Induces an Anti-Tumor Immune Response Orchestrated by CD8+ T Cells. *Nat Commun* (2020) 11:6335. doi: 10.1038/s41467-020-20138-8
59. Cancer Genome Atlas, N. Comprehensive Genomic Characterization of Head and Neck Squamous Cell Carcinomas. *Nature* (2015) 517:576–82. doi: 10.1038/nature14129
60. Gerstung M, Jolly C, Leshchiner I, Dentro SC, Gonzalez S, Rosebrock D, et al. The Evolutionary History of 2,658 Cancers. *Nature* (2020) 578:122–8. doi: 10.1038/s41586-019-1907-7
61. Agrawal N, Frederick MJ, Pickering CR, Bettegowda C, Chang K, Li RJ, et al. Exome Sequencing of Head and Neck Squamous Cell Carcinoma Reveals Inactivating Mutations in NOTCH1. *Science* (2011) 333:1154–7. doi: 10.1126/science.1206923
62. Pickering CR, Zhang J, Yoo SY, Bengtsson L, Moorthy S, Neskey DM, et al. Integrative Genomic Characterization of Oral Squamous Cell Carcinoma Identifies Frequent Somatic Drivers. *Cancer Discov* (2013) 3:770–81. doi: 10.1158/2159-8290.CD-12-0537
63. Zhou G, Liu Z, Myers JN. TP53 Mutations in Head and Neck Squamous Cell Carcinoma and Their Impact on Disease Progression and Treatment Response. *J Cell Biochem* (2016) 117:2682–92. doi: 10.1002/jcb.25592
64. Leemans CR, Snijders PJF, Brakenhoff RH. The Molecular Landscape of Head and Neck Cancer. *Nat Rev Cancer* (2018) 18:269–82. doi: 10.1038/nrc.2018.11
65. Sathasivam HP, Kist R, Sloan P, Thomson P, Nugent M, Alexander J, et al. Predicting the Clinical Outcome of Oral Potentially Malignant Disorders Using Transcriptomic-Based Molecular Pathology. *Br J Cancer* (2021) 125:413–21. doi: 10.1038/s41416-021-01411-z
66. William WN, Uraoka N, Peng SA, Lee JJ, El-Naggar AK, Cuentas ERP, et al. Immune Profiling of Oral Pre-Malignant Lesions (OPLs): An Erlotinib Prevention of Oral Cancer (EPOC) Study Biobank Analysis. *J Clin Oncol* (2017) 35(15_suppl):1545. doi: 10.1200/JCO.2017.35.15_suppl.1545
67. Oren M, Rotter V. Mutant P53 Gain-of-Function in Cancer. *Cold Spring Harb Perspect Biol* (2010) 2:a001107. doi: 10.1101/cshperspect.a001107
68. Freed-Pastor WA, Prives C. Mutant P53: One Name, Many Proteins. *Genes Dev* (2012) 26:1268–86. doi: 10.1101/gad.190678.112
69. Di Minin G, Bellazzo A, Dal Ferro M, Chiaruttini G, Nuzzo S, Bicciato S, et al. Mutant P53 Reprograms TNF Signaling in Cancer Cells Through Interaction With the Tumor Suppressor DAB2IP. *Mol Cell* (2014) 56:617–29. doi: 10.1016/j.molcel.2014.10.013
70. Muller PA, Vousden KH. Mutant P53 in Cancer: New Functions and Therapeutic Opportunities. *Cancer Cell* (2014) 25:304–17. doi: 10.1016/j.ccr.2014.01.021
71. Zhou G, Myers JN. Mutant P53 Exerts Oncogenic Functions by Modulating Cancer Cell Metabolism. *Mol Cell Oncol* (2014) 1:e963441. doi: 10.4161/23723548.2014.963441
72. Pfister NT, Fomin V, Regunath K, Zhou JY, Zhou W, Silwal-Pandit L, et al. Mutant P53 Cooperates With the SWI/SNF Chromatin Remodeling Complex to Regulate VEGFR2 in Breast Cancer Cells. *Genes Dev* (2015) 29:1298–315. doi: 10.1101/gad.263202.115
73. Zhu J, Sammons MA, Donahue G, Dou Z, Vedadi M, Getlik M, et al. Gain-Of-Function P53 Mutants Co-Opt Chromatin Pathways to Drive Cancer Growth. *Nature* (2015) 525:206–11. doi: 10.1038/nature15251
74. Tanaka N, Zhao M, Tang L, Patel AA, Xi Q, Van HT, et al. Gain-Of-Function Mutant P53 Promotes the Oncogenic Potential of Head and Neck Squamous Cell Carcinoma Cells by Targeting the Transcription Factors FOXO3a and FOXM1. *Oncogene* (2018) 37:1279–92. doi: 10.1038/s41388-017-0032-z
75. Shahnavaz SA, Regezi JA, Bradley G, Dube ID, Jordan RC. P53 Gene Mutations in Sequential Oral Epithelial Dysplasias and Squamous Cell Carcinomas. *J Pathol* (2000) 190:417–22. doi: 10.1002/(SICI)1096-9896(200003)190:4<417::AID-PATH544>3.0.CO;2-G
76. Cruz I, Napier SS, van der Waal I, Snijders PJ, Walboomers JM, Lamey PJ, et al. Suprabasal P53 Immunoexpression is Strongly Associated With High Grade Dysplasia and Risk for Malignant Transformation in Potentially Malignant Oral Lesions From Northern Ireland. *J Clin Pathol* (2002) 55:98–104. doi: 10.1136/jcp.55.2.98
77. Ogmundsdottir HM, Bjornsson J, Holbrook WP. Role of TP53 in the Progression of Pre-Malignant and Malignant Oral Mucosal Lesions. A Follow-Up Study of 144 Patients. *J Oral Pathol Med* (2009) 38:565–71. doi: 10.1111/j.1600-0714.2009.00766.x
78. Sawada K, Momose S, Kawano R, Kohda M, Irie T, Mishima K, et al. Immunohistochemical Staining Patterns of P53 Predict the Mutational Status of TP53 in Oral Epithelial Dysplasia. *Mod Pathol* (2021). doi: 10.1038/s41379-021-00893-9
79. Cooks T, Pateras IS, Tarcic O, Solomon H, Schetter AJ, Wilder S, et al. Mutant P53 Prolongs NF-kappaB Activation and Promotes Chronic Inflammation and Inflammation-Associated Colorectal Cancer. *Cancer Cell* (2013) 23:634–46. doi: 10.1016/j.ccr.2013.03.022
80. Cooks T, Pateras IS, Jenkins LM, Patel KM, Robles AI, Morris J, et al. Mutant P53 Cancers Reprogram Macrophages to Tumor Supporting Macrophages via Exosomal miR-1246. *Nat Commun* (2018) 9:771. doi: 10.1038/s41467-018-03224-w
81. Rahnamoun H, Lu H, Duttke SH, Benner C, Glass CK, Lauberth SM. Mutant P53 Shapes the Enhancer Landscape of Cancer Cells in Response to Chronic Immune Signaling. *Nat Commun* (2017) 8:754. doi: 10.1038/s41467-017-01117-y
82. Hanahan D, Weinberg RA. Hallmarks of Cancer: The Next Generation. *Cell* (2011) 144:646–74. doi: 10.1016/j.cell.2011.02.013
83. Blagih J, Zani F, Chakravarty P, Hennequart M, Pilley S, Hobor S, et al. Cancer-Specific Loss of P53 Leads to a Modulation of Myeloid and T Cell Responses. *Cell Rep* (2020) 30:481–496 e486. doi: 10.1016/j.celrep.2019.12.028
84. Maddalena M, Mallel G, Nataraj NB, Shreberk-Shaked M, Hassin O, Mukherjee S, et al. TP53 Missense Mutations in PDAC are Associated With Enhanced Fibrosis and an Immunosuppressive Microenvironment. *Proc Natl Acad Sci USA* (2021) 118:e2025631118. doi: 10.1073/pnas.2025631118
85. Ghosh M, Saha S, Bettke J, Nagar R, Parrales A, Iwakuma T, et al. Mutant P53 Suppresses Innate Immune Signaling to Promote Tumorigenesis. *Cancer Cell* (2021) 39:494–508.e495. doi: 10.1016/j.ccell.2021.01.003
86. Yuan B, Oechsli MN, Hendler FJ. A Region Within Murine Chromosome 7F4, Syntenic to the Human 11q13 Amplicon, is Frequently Amplified in 4NQO-Induced Oral Cavity Tumors. *Oncogene* (1997) 15:1161–70. doi: 10.1038/sj.onc.1201269
87. Tang XH, Knudsen B, Bemis D, Tickoo S, Gudas LJ. Oral Cavity and Esophageal Carcinogenesis Modeled in Carcinogen-Treated Mice. *Clin Cancer Res* (2004) 10:301–13. doi: 10.1158/1078-0432.CCR-0999-3
88. Shi Y, Xie TX, Leach DG, Wang B, Young S, Osman AA, et al. Local Anti-PD-1 Delivery Prevents Progression of Premalignant Lesions in a 4NQO-Oral Carcinogenesis Mouse Model. *Cancer Prev Res (Phila)* (2021) 14:767–78. doi: 10.1158/1940-6207.CAPR-20-0607
89. Wang J, Hu Y, Escamilla-Rivera V, Gonzalez CL, Tang L, Wang B, et al. Epithelial Mutant P53 Promotes Resistance to Anti-PD-1-Mediated Oral Cancer Immunoprevention in Carcinogen-Induced Mouse Models. *Cancers (Basel)* (2021) 13:1471. doi: 10.3390/cancers13061471
90. Ohue Y, Nishikawa H. Regulatory T (Treg) Cells in Cancer: Can Treg Cells be a New Therapeutic Target? *Cancer Sci* (2019) 110:2080–9. doi: 10.1111/cas.14069
91. Woo SR, Fuertes MB, Corrales L, Spranger S, Furdyna MJ, Leung MY, et al. STING-Dependent Cytosolic DNA Sensing Mediates Innate Immune Recognition of Immunogenic Tumors. *Immunity* (2014) 41:830–42. doi: 10.1016/j.immuni.2014.10.017
92. Khoo LT, Chen LY. Role of the cGAS-STING Pathway in Cancer Development and Oncotherapeutic Approaches. *EMBO Rep* (2018) 19:e46935. doi: 10.15252/embr.201846935
93. Diamond MS, Kinder M, Matsushita H, Mashayekhi M, Dunn GP, Archambault JM, et al. Type I Interferon is Selectively Required by Dendritic Cells for Immune Rejection of Tumors. *J Exp Med* (2011) 208:1989–2003. doi: 10.1084/jem.20101158
94. Serrano M, Hannon GJ, Beach D. A New Regulatory Motif in Cell-Cycle Control Causing Specific Inhibition of Cyclin D/CDK4. *Nature* (1993) 366:704–7. doi: 10.1038/366704a0

95. Sherr CJ. G1 Phase Progression: Cycling on Cue. *Cell* (1994) 79:551–5. doi: 10.1016/0092-8674(94)90540-1
96. Morgan DO. Principles of CDK Regulation. *Nature* (1995) 374:131–4. doi: 10.1038/374131a0
97. Li Y, Nichols MA, Shay JW, Xiong Y. Transcriptional Repression of the D-Type Cyclin-Dependent Kinase Inhibitor P16 by the Retinoblastoma Susceptibility Gene Product pRb. *Cancer Res* (1994) 54:6078–82.
98. Loughran O, Malliri A, Owens D, Gallimore PH, Stanley MA, Ozanne B, et al. Association of CDKN2A/p16INK4A With Human Head and Neck Keratinocyte Replicative Senescence: Relationship of Dysfunction to Immortality and Neoplasia. *Oncogene* (1996) 13:561–8.
99. Papadimitrakopoulou V, Izzo J, Lippman SM, Lee JS, Fan YH, Clayman G, et al. Frequent Inactivation of P16ink4a in Oral Premalignant Lesions. *Oncogene* (1997) 14:1799–803. doi: 10.1038/sj.onc.1201010
100. Rocco JW, Li D, Liggett WH Jr, Duan L, Saunders JK Jr, Sidransky D, et al. P16ink4a Adenovirus-Mediated Gene Therapy for Human Head and Neck Squamous Cell Cancer. *Clin Cancer Res* (1998) 4:1697–704.
101. Chen Q, Luo G, Li B, Samaranayake LP. Expression of P16 and CDK4 in Oral Premalignant Lesions and Oral Squamous Cell Carcinomas: A Semi-Quantitative Immunohistochemical Study. *J Oral Pathol Med* (1999) 28:158–64. doi: 10.1111/j.1600-0714.1999.tb02016.x
102. Kresty LA, Mallery SR, Knobloch TJ, Song H, Lloyd M, Casto BC, et al. Alterations of P16(INK4a) and P14(ARF) in Patients With Severe Oral Epithelial Dysplasia. *Cancer Res* (2002) 62:5295–300.
103. Morrison C, Pabla S, Conroy JM, Nesline MK, Glenn ST, Dressman D, et al. Predicting Response to Checkpoint Inhibitors in Melanoma Beyond PD-L1 and Mutational Burden. *J Immunother Cancer* (2018) 6:32. doi: 10.1186/s40425-018-0344-8
104. Linsley PS, Speake C, Whalen E, Chaussabel D. Copy Number Loss of the Interferon Gene Cluster in Melanomas is Linked to Reduced T Cell Infiltrate and Poor Patient Prognosis. *PloS One* (2014) 9:e109760. doi: 10.1371/journal.pone.0109760
105. Kim H, Kim H, Feng Y, Li Y, Tamiya H, Tocci S, et al. PRMT5 Control of cGAS/STING and NLRC5 Pathways Defines Melanoma Response to Antitumor Immunity. *Sci Transl Med* (2020) 12:eaaz5683. doi: 10.1126/scitranslmed.aaz5683
106. Han G, Yang G, Hao D, Lu Y, Thein K, Simpson BS, et al. 9p21 Loss Confers a Cold Tumor Immune Microenvironment and Primary Resistance to Immune Checkpoint Therapy. *Nat Commun* (2021) 12:5606. doi: 10.1038/s41467-021-25894-9
107. William WN Jr, Zhao X, Bianchi JJ, Lin HY, Cheng P, Lee JJ, et al. Immune Evasion in HPV(-) Head and Neck Precancer-Cancer Transition is Driven by an Aneuploid Switch Involving Chromosome 9p Loss. *Proc Natl Acad Sci USA* (2021) 118. doi: 10.1073/pnas.2022655118
108. Ishida K, Tomita H, Kanayama T, Noguchi K, Niwa A, Kawaguchi M, et al. Specific Deletion of P16(INK4a) With Retention of P19(ARF) Enhances the Development of Invasive Oral Squamous Cell Carcinoma. *Am J Pathol* (2020) 190:1332–42. doi: 10.1016/j.ajpath.2020.01.017
109. Li Z, Gonzalez CL, Wang B, Zhang Y, Mejia O, Katsonis P, et al. Cdkn2a Suppresses Metastasis in Squamous Cell Carcinomas Induced by the Gain-of-Function Mutant P53(R172H). *J Pathol* (2016) 240:224–34. doi: 10.1002/path.4770
110. Veeramachaneni R, Walker T, Revil T, Weck A, Badescu D, O'sullivan J, et al. Analysis of Head and Neck Carcinoma Progression Reveals Novel and Relevant Stage-Specific Changes Associated With Immortalisation and Malignancy. *Sci Rep* (2019) 9:11992. doi: 10.1038/s41598-019-48229-7
111. Zhong R, Bao R, Faber PW, Bindokas VP, Bechill J, Lingen MW, et al. Notch1 Activation or Loss Promotes HPV-Induced Oral Tumorigenesis. *Cancer Res* (2015) 75:3958–69. doi: 10.1158/0008-5472.CAN-15-0199
112. Hu J, Yu J, Gan J, Song N, Shi L, Liu J, et al. Notch1/2/3/4 are Prognostic Biomarker and Correlated With Immune Infiltrates in Gastric Cancer. *Aging (Albany NY)* (2020) 12:2595–609. doi: 10.18632/aging.102764
113. Geng Y, Fan J, Chen L, Zhang C, Qu C, Qian L, et al. A Notch-Dependent Inflammatory Feedback Circuit Between Macrophages and Cancer Cells Regulates Pancreatic Cancer Metastasis. *Cancer Res* (2021) 81:64–76. doi: 10.1158/0008-5472.CAN-20-0256
114. Wang YC, He F, Feng F, Liu XW, Dong GY, Qin HY, et al. Notch Signaling Determines the M1 Versus M2 Polarization of Macrophages in Antitumor Immune Responses. *Cancer Res* (2010) 70:4840–9. doi: 10.1158/0008-5472.CAN-10-0269
115. Cheng P, Kumar V, Liu H, Youn JI, Fishman M, Sherman S, et al. Effects of Notch Signaling on Regulation of Myeloid Cell Differentiation in Cancer. *Cancer Res* (2014) 74:141–52. doi: 10.1158/0008-5472.CAN-13-1686
116. Wang SH, Lu QY, Guo YH, Song YY, Liu PJ, Wang YC. The Blockage of Notch Signalling Promoted the Generation of Polymorphonuclear Myeloid-Derived Suppressor Cells With Lower Immunosuppression. *Eur J Cancer* (2016) 68:90–105. doi: 10.1016/j.ejca.2016.08.019
117. Monteiro De Oliveira Novaes JA, Hirz T, Guijarro I, Nilsson M, Pisegna MA, Poteete A, et al. Targeting of CD40 and PD-L1 Pathways Inhibits Progression of Oral Premalignant Lesions in a Carcinogen-Induced Model of Oral Squamous Cell Carcinoma. *Cancer Prev Res (Phila)* (2021) 14:313–24. doi: 10.1158/1940-6207.CAPR-20-0418
118. Schwartz JL, Sloane D, Shklar G. Prevention and Inhibition of Oral Cancer in the Hamster Buccal Pouch Model Associated With Carotenoid Immune Enhancement. *Tumour Biol* (1989) 10:297–309. doi: 10.1159/000217629
119. Shklar G, Schwartz JL, Trickler DP, Reid S. Prevention of Experimental Cancer and Immunostimulation by Vitamin E (Immunosurveillance). *J Oral Pathol Med* (1990) 19:60–4. doi: 10.1111/j.1600-0714.1990.tb00797.x
120. Baird JR, Feng Z, Xiao HD, Friedman D, Cottam B, Fox BA, et al. Correction: STING Expression and Response to Treatment With STING Ligands in Premalignant and Malignant Disease. *PloS One* (2018) 13:e0192988. doi: 10.1371/journal.pone.0192988
121. Leach DG, Newton JM, Florez MA, Lopez-Silva TL, Jones AA, Young S, et al. Drug-Mimicking Nanofibrous Peptide Hydrogel for Inhibition of Inducible Nitric Oxide Synthase. *ACS Biomater Sci Eng* (2019) 5:6755–65. doi: 10.1021/acsbiomaterials.9b01447
122. Leach DG, Young S, Hartgerink JD. Advances in Immunotherapy Delivery From Implantable and Injectable Biomaterials. *Acta Biomater* (2019) 88:15–31. doi: 10.1016/j.actbio.2019.02.016
123. Wang J, Xie T, Wang B, William WN Jr, Heymach JV, El-Naggar AK, et al. PD-1 Blockade Prevents the Development and Progression of Carcinogen-Induced Oral Premalignant Lesions. *Cancer Prev Res (Phila)* (2017) 10:684–93. doi: 10.1158/1940-6207.CAPR-17-0108
124. Hanna GJ, Villa A, Mistry N, Jia Y, Quinn CT, Turner MM, et al. Comprehensive Immunoprofiling of High-Risk Oral Proliferative and Localized Leukoplakia. *Cancer Res Commun* (2021) 1:30–40. doi: 10.1158/2767-9764.CRC-21-0060
125. Lodi G, Franchini R, Warnakulasuriya S, Varoni EM, Sardella A, Kerr AR, et al. Interventions for Treating Oral Leukoplakia to Prevent Oral Cancer. *Cochrane Database Syst Rev* (2016) 7:CD001829. doi: 10.1002/14651858.CD001829.pub4

Conflict of Interest: The authors declare that the research was conducted in the absence of any commercial or financial relationships that could be construed as a potential conflict of interest.

Advantages of publishing in Frontiers

OPEN ACCESS
Articles are free to read for greatest visibility and readership

FAST PUBLICATION
Around 90 days from submission to decision

HIGH QUALITY PEER-REVIEW
Rigorous, collaborative, and constructive peer-review

TRANSPARENT PEER-REVIEW
Editors and reviewers acknowledged by name on published articles

Frontiers
Avenue du Tribunal-Fédéral 34
1005 Lausanne | Switzerland

Visit us: www.frontiersin.org
Contact us: frontiersin.org/about/contact

REPRODUCIBILITY OF RESEARCH
Support open data and methods to enhance research reproducibility

DIGITAL PUBLISHING
Articles designed for optimal readership across devices

FOLLOW US
@frontiersin

IMPACT METRICS
Advanced article metrics track visibility across digital media

EXTENSIVE PROMOTION
Marketing and promotion of impactful research

LOOP RESEARCH NETWORK
Our network increases your article's readership